

## PROJECT ADMINISTRATION DATA SHEET



ORIGINAL



REVISION NO. \_\_\_\_\_

Contract No. A-3509GTRI/~~GTR~~DATE 4/5/83Contract Director: Dr. B. R. Livesay~~SCRS~~/Lab EMLContractor: Semiconductor Research CorporationAgreement: Contract No. 83-01-004Contract Period: From 4/1/83 To 3/31/84 (Performance) 6/30/84 (Reports)Contract Amount: Total Estimated: \$ 99,974 ~~6-30-84~~ 9-30-85 Funded: \$ 99,974Sharing Amount: \$ --- Cost Sharing No: ---Investigations of Mechanical-Environmental Interactions in VLSI Bond Interfaces

## ADMINISTRATIVE DATA

OCA Contact Frank Huff x4820

Sponsor Technical Contact:

2) Sponsor Admin/Contractual Matters:

Mr. Richard D. AlbertsSame as 1Semi-conductor Research Corporation300 Park Drive, P.O. Box 12053Research Triangle Park, NC 27709(919) 549-9333Sponsor Priority Rating: ---

Military Security Classification: \_\_\_\_\_

(or) Company/Industrial Proprietary: \_\_\_\_\_

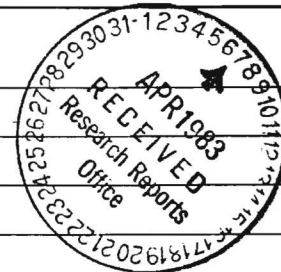
## RESTRICTIONS

Attached ---- Supplemental Information Sheet for Additional Requirements.

Level: Foreign travel must have prior approval - Contact OCA in each case. Domestic travel requires sponsor approval where total will exceed greater of \$500 or 125% of approved proposal budget category.

Equipment: Title vests with sponsor; see Article 7.

## REMARKS:



## COPIES TO:

Research Administrative Network

Research Property Management

Accounting

Procurement/EES Supply Services

RM OCA 4.7B1 (Rev 982)

Research Security Services

Reports Coordinator (OCA)

GTRI

Library

Research Communications (2)

Project File

Other \_\_\_\_\_

Other \_\_\_\_\_

Livesay

SPONSORED PROJECT TERMINATION/CLOSEOUT SHEET

Date 7/24/85

Project No. A-3509

XXXXXX School/Lab EML

Subproject No.(s) \_\_\_\_\_

Project Director(s) Dr. B. R. Livesay

GTRC / ~~GIT~~

Sponsor Semiconductor Research Corporation

Investigations of Mechanical - Environmental Interactions in VLSI Bond Interfaces

TRY CO.  
GEORGIA 300

Effective Completion Date: 7/22/85\*

(Performance) 7/22/85 (Reports)

Contract Closeout Actions Remaining:

☐ None

☒ Final Invoice or Final Fiscal Report

☐ Closing Documents

☒ Final Report of Inventions

☒ Govt. Property Inventory & Related Certificate

☐ Classified Material Certificate

☐ Other \_\_\_\_\_

\*Sponsor has terminated project pursuant to paragraph B.14.1 of the contract.

Continues Project No. \_\_\_\_\_

Continued by Project No. \_\_\_\_\_

COPIES TO:

Project Director  
Research Administrative Network  
Research Property Management  
Accounting  
Procurement/GTRI Supply Services  
Research Security Services  
Reports Coordinator (OCA)  
Legal Services

Library  
GTRC  
Research Communications (2)  
Project File  
Other A. Jones; M. Heyser



QUARTERLY TECHNICAL REPORT

July 1 - September 30, 1983

INVESTIGATIONS OF MECHANICAL-ENVIRONMENTAL  
INTERACTIONS IN VLSI BOND INTERFACES

A-3509

PREPARED FOR  
THE SEMICONDUCTOR RESEARCH CORPORATION  
300 PARK DRIVE, P.O. BOX 12053  
RESEARCH TRIANGLE PARK  
NORTH CAROLINA 27709

BY  
B. R. LIVESAY  
GEORGIA INSTITUTE OF TECHNOLOGY  
MICROELECTRONICS RESEARCH CENTER  
ATLANTA, GEORGIA 30332

## INTRODUCTION

A research program is being conducted to investigate effects of several environmental stress factors on the mechanical performance of wire bond interfaces. The initial phases of this work were described in the first quarterly report. Micromechanical testing instrumentation was adapted to carry out low cycle fatigue experiments on bond wire systems. Two new wire bonders were also received and installed during that period, a K&S ultrasonic wedge bonder and a thermosonic ball bonder. These bonders thus provide an in-house capability for producing bond systems equivalent to industrial standards. Low cycle fatigue measurements were conducted at room temperature and in air on Al-Al and Au-Au wire bond interfaces. The initial specimens provide base-line data for the subsequent environmental fatigue studies. In addition, test fixtures and an environmental test chamber were fabricated and adapted for these types of investigations.

## EXPERIMENTAL INVESTIGATIONS

The environmental fatigue studies were initiated during the second period. The specimens have involved Al-Al (1% Si) wires bonded to chip pads. The environmental conditions were maintained in a small chamber mounted on one of the micromechanics instruments. The conditions employed during this quarter were dry air, water saturated air and a NaCl-water vapor environment.

A number of specimens prepared under identical bonding conditions were fatigued in each of the three environments for comparison. Stress-strain hysteresis loops were recorded at convenient intervals during the fatigue life of each specimen in order to correlate energy dissipation and work hardening behavior with cyclical history and environmental conditions.

The room temperature fatigue characteristics of the Al wire bonds stressed under these three environments were not significantly different from each other. Some bonds fatigued within the water-NaCl vapor appeared to fail a little prematurely due to corrosion fatigue mechanisms. SEM micographs of these fracture surfaces

indicated some attack as the fatigue crack progressed through the fracture interface. These observations supported the measurement of sharp decreases in hysteresis loop amplitudes relative to dry bonds near fracture. However, the 1% Al wire bonds had only a slightly reduced fatigue life under the salt-vapor conditions relative to that of the dry wires.

In order to facilitate the fatigue measurements, modifications were made on two other micromechanics devices. The electromagnetic driven microtensile apparatus has been equipped so that fatigue profiles, frequencies, cyclical durations, etc. can be driven by programs using an Apple computer. In addition, a cam-driven fatigue device was modified to include the amplitudes and frequencies appropriate to bond wires so that multiple specimens can be fatigue-cycled at one time. Mechanical fatigue measurements, by their nature, are time consuming. These instrumentation improvements will therefore multiply the rate at which specimens can be investigated.

Dr. Livesay was away (at RADC) for about two months during the three months of this report period. His

research at RADC concerned investigations of fundamental mechanisms involved in electromigration degradation within metal film conductors. We expect his experiences during that visit to be particularly valuable in future phases of the current investigations.

#### **PLANS FOR THE NEXT PERIOD**

The investigations will be extended to include elevated temperatures and electrical stress during the next period. As mentioned previously, the fatigue durability of bond interfaces in the salt-vapor and water vapor environments was not significantly reduced compared to that in a dry environment. However, the mechanical cycling within circuits is normally induced by, or associated with, elevated temperatures and electrical current through the bond interface. These conditions will be imposed while mechanically cycling wire bonds in a dry environment.

We have been introduced to our industrial mentor, Mr. Charlie Hewitt of the Harris Corporation, and plan a visit to his plant. He is willing to provide us with VLSI circuits fabricated in their normal lines which we

can employ as test specimens. His technical input is considered particularly valuable here because of his extensive experience with these systems.

#### COST REPORT

The expenditures during the second quarter were \$20,206.72. The balance from the contract is \$72,820.75.

**QUARTERLY TECHNICAL REPORT**  
**For The Period**  
**October 1 - December 31, 1983**

**INVESTIGATIONS OF MECHANICAL-ENVIRONMENTAL  
INTERACTIONS IN VLSI BOND INTERFACES**

**A-3509**

**PREPARED FOR**  
**THE SEMICONDUCTOR RESEARCH CORPORATION**  
**300 PARK DRIVE, P.O. BOX 12053**  
**RESEARCH TRIANGLE PARK**  
**NORTH CAROLINA 27709**

**By**  
**B. R. LIVESAY**  
**GEORGIA INSTITUTE OF TECHNOLOGY**  
**MICROELECTRONICS RESEARCH CENTER**  
**ATLANTA, GEORGIA 30332**

## INTRODUCTION

Investigations are being conducted at the Georgia Institute of Technology to provide quantitative measurements of the mechanical behavior of wire bond systems under conditions appropriate to VLSI packaging stresses. The increased demands on performance dictated by current and emerging VLSI chip and package technologies has enhanced our need to understand the fundamental characteristics and limits of the materials employed for chip to package interconnections. The intermetallic interface introduced at each bond includes impurities such as oxides or other surface contaminants which always occur to some extent on wire and pad surfaces. Bonds between different metals, primarily aluminum and gold, introduce metallurgical gradients. The important considerations for microcircuits concern how the very small dimensions, high current densities, the proximity and character of surface films and interfaces, and particular metallurgical factors associated with alloy composition influence mechanical performance in the package environment.

Low cycle fatigue investigations were reported last quarter on aluminum-aluminum wire bond systems in air and in an environmental chamber to exercise control on humidity and temperature. These measurements provided new data on some critical parameters such as work hardening coefficients and hysteresis energies to characterize differences in the behavior of bond systems due to environmental stresses. Instrumentation of the Micromechanics Laboratory is being employed to make these types of measurements possible. Special fixtures were designed and



fabricated to apply loads and to measure the response of wire bond systems. Methods were also investigated for sectioning the tiny specimens for microstructural studies to correlate structure-property relationships. Various arrangements with packages and bond pads were explored to provide the most suitable specimen configurations to both accommodate the micromechanics experiments and to have realistic correlations with VLSI wire interconnect wire bonds and geometries.

The mechanical measurements on wire bond systems have provided relationships between fatigue life and strain levels which can be correlated with the published behavior of bulk aluminum fatigue specimen behavior in plastic deformation modes. The measured cycles-to-failure values for the specimens fatigued in air vary inversely with strain amplitude similar to the behavior of bulk specimens. Micrographs of fracture surfaces on the wires show striations as commonly noted for many bulk fatigue specimens. The results from simple aluminum wire specimens exposed only to air or moisture have provided a level of confidence in the basic techniques being employed for these investigations. The fundamental mechanisms responsible for fatigue degradation in microcircuit materials correspond closely with those for bulk specimens of the same metal. The work of the current reporting period has been extended to experiments involving the synergism of electrical and thermal stresses imposed with mechanical cycling and to more detailed considerations of microstructural degradation mechanisms.

## EXPERIMENTAL INVESTIGATIONS

The experiments of the current period were extended to include investigations of the effects of electrical current on the mechanical fatigue characteristics of wire bond systems. Other studies involve investigations of thermal induced modifications of bond wire microstructures and an analysis of dislocation processes occurring within the wire and at bond interfaces. The bond wires in operating devices have long been known to experience thermal-mechanical cycling as power levels change resulting, ultimately, in failures related to mechanical fatigue mechanisms. The data for these thermally induced fatigue failures are not quantitative due to the the lack of stress and strain definition.

The fatigue studies being conducted here employ experimental configurations which permit the definition of mechanical and electrical parameters. The electrical current values employed range from 5 ma to 100 ma for 1 mil, 1% Si aluminum wires bonded to aluminum pads. The methods for preparing reproducible test specimens with good control on bonding parameters and with close tolerances on the bond wire loop configuration and the validation experiments have been described previously. There was a problem for the fatigue experiments involving elevated temperatures and current carrying wires in that adhesives such as Eastman 910 were no longer suitable for attaching the mechanical stress probe. Several techniques were explored to grasp the bond wire with stainless steel loops and clasps in a manner which would securely hold the wire without introducing mechanical damage to the wire.

A successful technique was developed for milling a slot the precise width of the bond wire being tested into the side of and at the tip of an 0.008 inch section of stainless steel wire. This technique has provided highly satisfactory precision "hooks" for both positive and negative load applications to carry out mechanical cycling over the entire range of electrical, thermal and chemical environments of importance to microcircuit materials. A sketch showing this simple but effective arrangement is shown in Figure 1.

The cyclical measurements are providing data for the effects of strain amplitude and current levels on details of cyclical mechanical hysteresis loops and the cyclical durability of the bond wire interconnection. The initial quarter cycle of a hysteresis loop is equivalent to a simple stress-strain curve. Plastic deformation always appears to occur in this initial quarter cycle for aluminum bond wire measurements even for very small strains. Typical mechanical behavior through the first several quarter cycles for a 1% Si Al alloy wire bond is illustrated in Figure 2. The asymmetry of this curve is due to the geometry of the bond wire loop. The first few cycles exhibit measurable work-hardening during each quarter cycle, indicating a large increase in dislocation density within the metals.

Several levels of strain amplitude have been employed during the cyclical measurements with current. As expected, the number of cycles to fracture decreases rapidly as the strain amplitude is increased. The magnitude of the effect of electrical current on fatigue durability is much smaller for the large strain

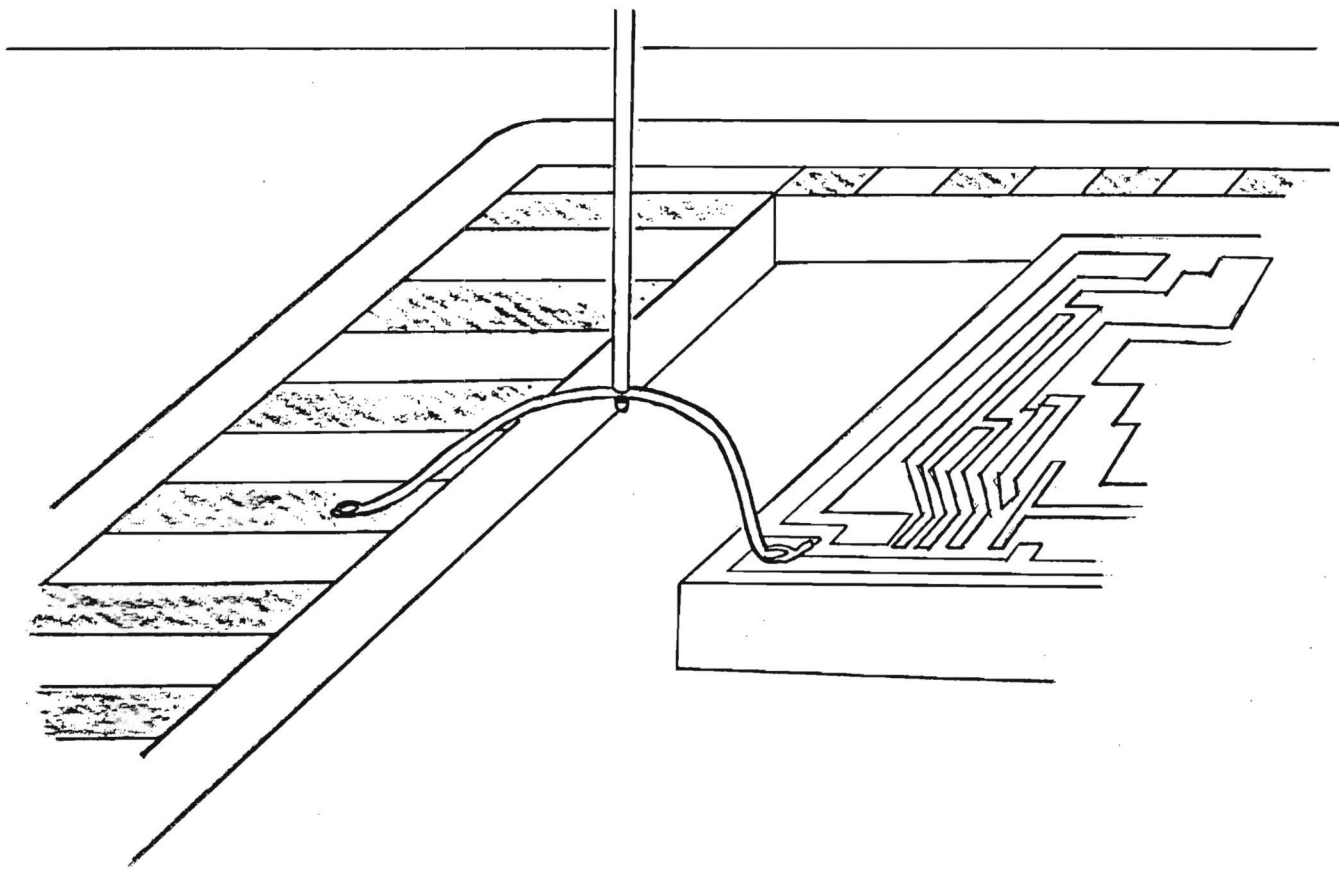


Figure 1. Hook for fatigue of wire interconnection. The hook is a 0.0015 inch slot milled into side of 0.008 inch stainless steel wire. This arrangement provides both positive and negative displacements with minimum backlash in all relevant environmental conditions.

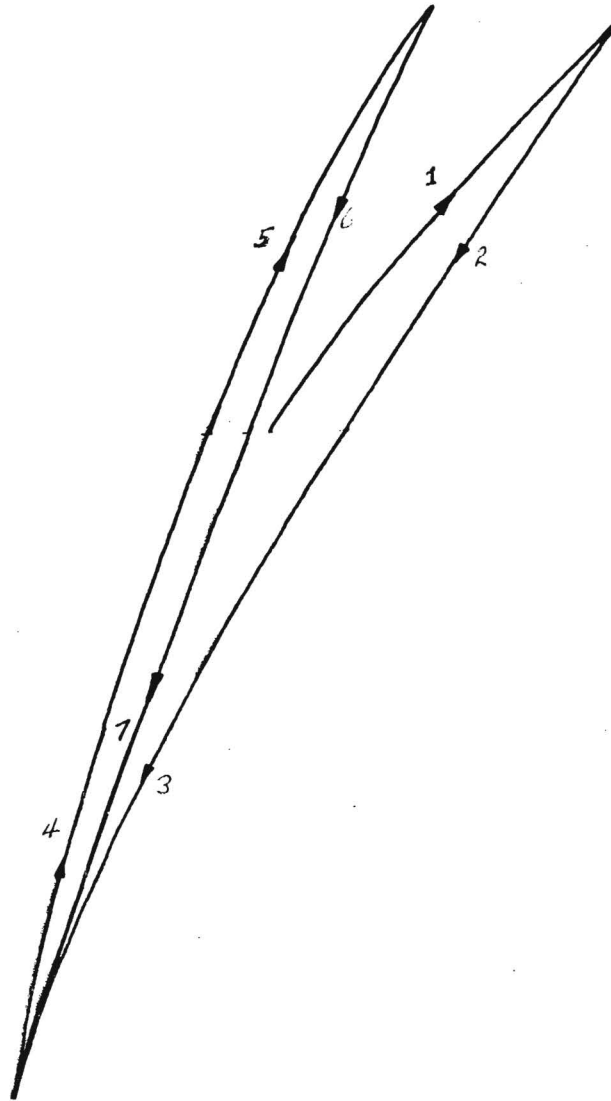


Figure 2. Stress-strain behavior of wire interconnect during first seven quarter fatigue cycles. After several cycles the curve becomes a closed mechanical hysteresis loop. The area, force amplitude and slope of these loops provide parameters indicating stages of fatigue degradation in interconnect materials.

amplitudes than is observed for the low strain amplitude cycling. Microstructural characteristics of the wire interconnections are significantly altered while mechanical cycled at the higher currents. Grain boundary sliding within the wire is clearly more prevalent at the combination of higher current and strain amplitude. Faceting of the wire surfaces is also noted, apparently associated with thermal-mechanical induced mechanisms. The electrical current also modifies characteristics of the bond fractures. Details of correlations between cyclical mechanical behavior and microstructural degradation mechanisms are currently being pursued.

Elevated temperatures modify metallurgical details of both the wire and the bond interface during normal operating conditions. In order to separate out some of these effects on bond wires alone, a simple series of measurements was outlined. Wire specimens were obtained from several suppliers of bond wires used by VLSI manufacturers. Sections of the different wires were placed in an oven for different times and temperatures to simulate the purely thermal environment of a microcircuit. For example, the silicon doped aluminum wires are a precipitation hardened alloy. The mechanical strengths of bulk structural alloys based on silicon precipitates are very sensitive to time-temperature relationships. On the other hand, the strengthening of magnesium doped aluminum is based on solution hardening mechanisms. In addition, grain size and surface interactions are influenced by time-temperature and gas exposure. These factors are critical to the reliability or durability of

the interconnections.

Pure Al, 1% Si-Al and 1% Mg-Al wires are oven annealed for specific times in both dry air and in containers providing moist environments prior to the mechanical testing. An electromagnetically loaded microtensile apparatus was adapted to measure the mechanical behavior of the wires as tensile specimens. This apparatus provides response and other characteristics which are particularly useful for precision stress-strain measurements at very low strain levels. The load control basis of this device is specially designed to separate out interface strengthening mechanisms. The apparatus has recently been modified to further improve the response characteristics and is now programmed for operational control and data collection with a small computer.

A series of over two hundred wires from the different suppliers has been heat treated and the mechanical data are being accumulated for the different conditions. The effect on tensile behavior of simple annealing in air for increasing times at the same temperature is illustrated in Figure 3 for three Al-Si wires. The elongation has increased with time at temperature, as expected for an over-aging situation. In addition, the yield point initially decreases with annealing time. However, the yield point begins to increase after extended heating in air as seen in the 5 hour curve. This apparently contradictory behavior is attributed to the growth of a thicker thermal oxide film on the surface of the aluminum wire. The aluminum oxide coating contributes interface strengthening mechanisms which are partially associated with the elastic modulus discontinuity at

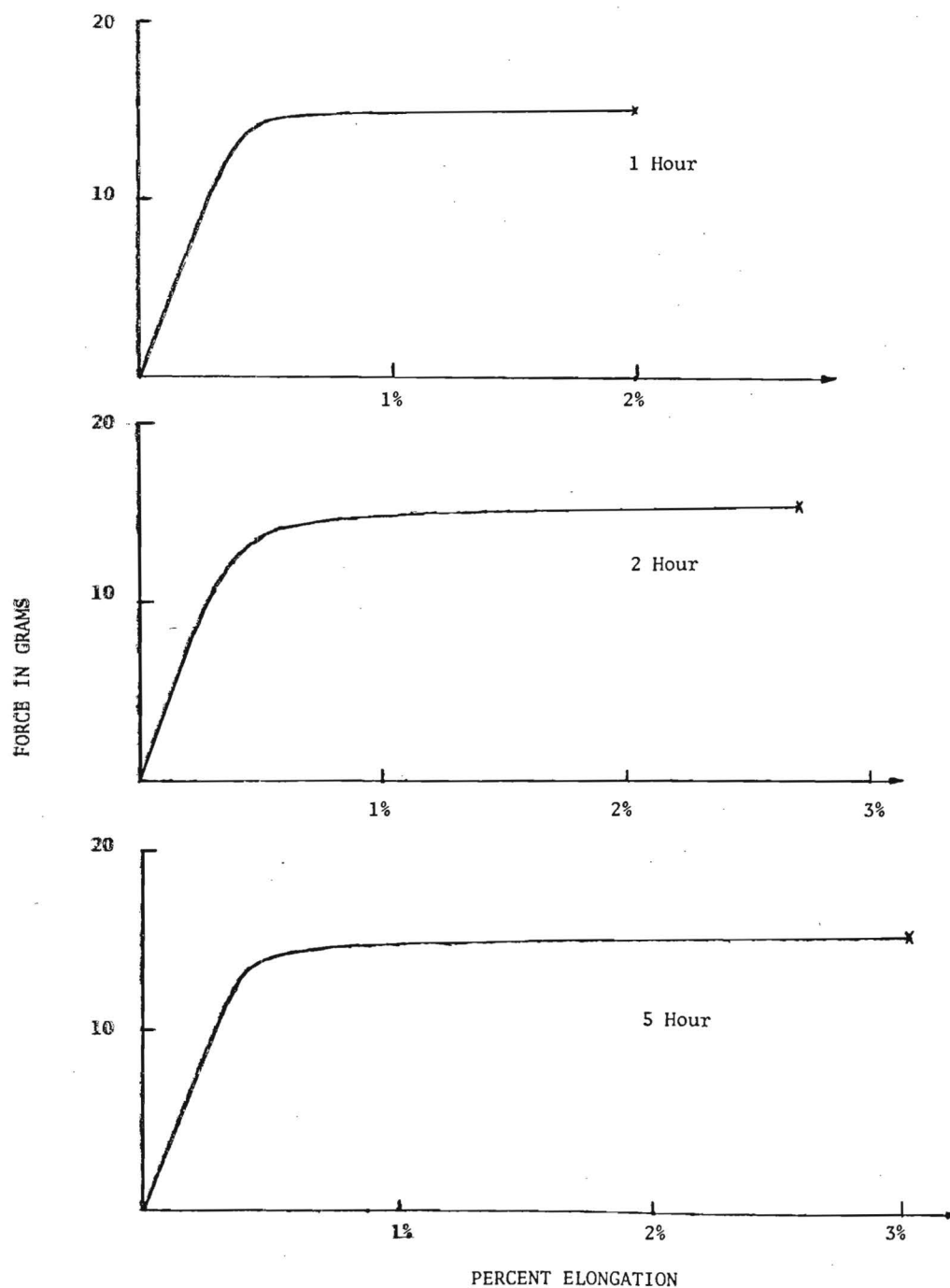


Figure 3. Three tensile stress-strain curves for a particular silicon doped aluminum bond wire annealed in air at 62°C for the indicated periods. Note the increased yield point after 5 hours which is due to a surface strengthening effect associated with the dislocation barrier at the metal-oxide interface.



the metal-coating interface. These interface strengthening mechanisms have proved to be critical to the performance of many high strength bulk structural alloys. Due to the close proximity of all surfaces and interfaces in the very small dimensions of microcircuits the importance of these interface factors on the strength and durability of interface materials is greatly enhanced. The oxide coating can serve as a barrier to inhibit the generation and transmission of dislocations. Once significant plastic deformation occurs, the slip bands have fractured the oxide barrier to allow subsequently created dislocations to exit from the surface.

Theoretical modeling is being carried out for the geometries involved with the wire interconnect structures. As mentioned above, the high elastic modulus attributed to aluminum oxide coatings provides strong image repulsion forces on dislocations near the interface. Far from the interface, there is an attractive interaction. In the case for the small dimensions involved here, a major fraction of the entire structure is in, what is normally considered, the surface or interface region. This should be reflected by an enhanced tensile strength of the bond wires relative to that for bulk materials of the same alloy. Indeed, we have observed precisely this effect in our tensile measurements. However, aluminum oxide coatings as grown here have been shown to have highly variable mechanical characteristics which depend upon many factors, including a strong moisture effect. For example, the elastic modulus of the oxide ranges from high values for the dry environments of a high

vacuum to quite low values with exposure to high humidity levels. The image calculations for dislocation-interface models show that the interface can therefore range from serving as a repulsive barrier for a dry oxide to, possibly, an attractive force with high humidity.

Cyclical deformation leads to the creation of dislocation debris layers near the surfaces and at intermetallic interfaces which exist in bulk materials. The thicknesses of debris layers in the bulk metals are generally estimated to be comparable to the dimensions of our bond wires. We also have what is effectively a dense debris layer at the wire-pad interface which can inject dislocations into the wire. The multiple interactions between dislocations which occurs with increased mechanical deformation forms dislocation dipoles, complex dislocation arrays and microcracks. The surface damage introduced mechanically during wire drawing and in the bonding machine also contributes to the dislocation content of the surface region. Most fractures are initiated in bulk materials at surfaces of weldments or other features where a large debris layer and microcracks are likely to accumulate. Details of the metallurgical composition strongly effect these processes. The bond interface with multiple inclusions and a high dislocation density represents a strong source for dislocation generation.

The theoretical approaches previously developed to model bulk metal behavior are providing a useful theoretical apparatus to support the modeling work being done here on the interconnection materials. Close coordination with both the mechanical property

measurements and the microstructural studies is critical to the model configurations employed. The presence of surface coatings results in a series of dislocation images from which the net interactions with real dislocations are best handled with computer methods.

An electrical current in the interconnection has both positive and detrimental effects on the durability of the metals. The increased temperature supports the reduction of the debris layer by aiding dislocation movement through barriers and other dislocations. There is evidence that electrons actually interact directly with dislocations resulting in an electro-mechanical effect in metals. We have planned an experiment associated with the current tensile measurements which we hope will shed light on the magnitude of this mechanism. On the other hand, observations of significant grain boundary sliding and with phenomena associated with thermal faceting and the growth of hillocks with current and heat are not favorable for mechanical durability. A reduction in strength and brittleness also occurs with thermal and electrical current induced segregation of doping and impurity atoms in the interconnection metals.

Material is being assembled for two papers, one describing results from the fatigue experiments and the other concerning the bond wire modifications with exposure to temperature and moist or dry gas environments.

## **COST REPORT**

The expenditures during this quarter were \$12,701.97. The balance from the contract is \$60,118.78

**TECHNICAL REPORT**

**For Period**

**January 1, 1984 - June 30, 1984**

**INVESTIGATIONS OF MECHANICAL-ENVIRONMENTAL  
INTERACTIONS IN VLSI BOND INTERFACES**

**A-3509**

**PREPARED FOR**

**THE SEMICONDUCTOR RESEARCH CORPORATION**

**300 PARK DRIVE, P.O. BOX 12053**

**RESEARCH TRIANGLE PARK**

**NORTH CAROLINA 27709**

**BY**

**B. R. LIVESAY**

**GEORGIA INSTITUTE OF TECHNOLOGY**

**MICROELECTRONICS RESEARCH CENTER**

**ATLANTA, GEORGIA 30332**

## INTRODUCTION

This report outlines the work accomplished during the period of 1 January to 30 June, 1984. The objective of these investigations is to establish quantitative measures of the mechanical behavior of VLSI wire bond interface systems under appropriate operational and environmental stress levels. The increasing demands on performance levels dictated by VLSI chip and package configurations have enhanced our need to understand the performance characteristics and limits of materials used for chip-to-package interconnections. VLSI devices involving over 300 interconnects clearly require a high level of precision for establishing strong bonds in order to have an acceptable production yield. These bonds must also remain stable under operational and environmental stresses to provide long term device durability.

The critical interfaces formed at intermetallic bonds actually are not uniform pure metal-metal interfaces but normally consist of numerous interfacial combinations based on initial surface oxides, impurities, metal phases and the intermetallic compounds which may form with dissimilar metals. As a point of fact, the materials geometries employed in typical VLSI device structures result in extraordinarily complex composite interface systems. The ratios of interface area to the volume of features in these devices greatly surpass that of any other precision structures fabricated by man. Specific characteristics of these interfaces in terms of material parameters they bridge are controlling factors in the ability of these devices to be manufactured in the first place and then to remain mechanically, electrically and chemically stable during their functional lives.

It is clearly important to establish threshold levels at which various operational and environmental stresses activate particular failure mechanisms in these complex electronic

devices. Quantitative data are crucial for establishing performance specifications for quality control during manufacturing, for evaluating the effects of defects on device reliability, for setting intelligent stress screening levels and for evaluating the long term durability under appropriate operating stresses for particular device materials geometries.

The investigations underway in this program are focused on acquiring quantitative engineering data on a range of factors affecting the mechanical strength of wire bond interface systems. Mechanical studies are being conducted on wire bond systems while exposed to conditions which include both electrical and chemical environments. Both low-cycle and high-cycle fatigue measurements are made on individual wire bonds using instrumentation of the Micromechanics Laboratory. These measurements have provided, for the first time, data showing details of mechanical hysteresis loops in these small structures, providing new insights about the mechanisms operating in the bond interface region. Distinct behavior differences have been measured for loop characteristics as a function of electrical current through the interface and also for chemical interactions resulting from the superposition of either pure moisture or sodium ions within the gas environment. Scanning electron microscopy conducted on both fractured surfaces and on sectioned interface specimens has provided essential information about metallographic microstructural characteristics for the interpretation of operating mechanisms. The effects of thermal history on the bond wire materials, alone, were measured by exposing a large number of bond wires to successive heat treatments and measuring their stress-strain behavior. Variations of plastic yield points, elongation and fracture stresses were determined as a function of thermal treatment for bond wires which have been provided for these studies by several leading sources of these wires for VLSI fabrication. These data are particularly relevant for

characterizing metallurgical modifications which occur in the interconnecting wires over time at moderately elevated operating temperatures.

Extension of the bond wire measurements to examine elevated temperature aluminum wire creep behavior led to the very recent discovery of a surprising room temperature creep failure mechanism. We had anticipated that mechanical creep in the bond interface might be important at the elevated operating temperatures, but only near the normal yield point (as is the case for corresponding bulk structural alloys), and were intending to simply measure the limits of mechanical creep as an aid in interpreting our other measurements. However, we have measured room temperature creep as a function of time on wire bonds at loads as small as  $1/3$  the "fast" fracture stress for identical bonds. Times to creep fracture are about two hours at the low stress levels. There is clearly a need to explore the implications of these observations for such procedures as "nondestructive" bond pull tests and for long term device durability.

Models of the probable dislocation mechanisms appropriate to the fatigue, creep and thermal history studies are being pursued along with the experimental work. Computer calculations of interface strengthening processes due to dislocation interactions with material property discontinuities at planar interfaces are being made. High current density induced dislocation mobility is clearly evident in the low-cycle fatigue measurements with electrical currents applied to the bond interface. The current induced dislocation dynamics have extraordinary implications for both bond interface integrity and other very important VLSI circuit considerations. The electrical current induced dislocation dynamics have been postulated here to be a critical factor accounting for observed electromigration processes.



## WIRE BOND FATIGUE INVESTIGATIONS

The environmental fatigue investigations have been providing a significant body of data describing progressive details about the fatigue damage mechanisms occurring in the neighborhood of mechanically cycled wire bond interfaces. Mechanical hysteresis loops are recorded at selected intervals (as described earlier) as fatigue cycles are accumulated. A long series of measurements is being carried out in which aluminum-aluminum wire bonds are mechanically cycled while a d.c. current passes through the interface. The current levels have involved steps between 0 and 350 mamp. The cycle rates and the mechanical and electrical stress levels employed here provide accelerated fatigue test conditions so that data can be accumulated in reasonable time periods. However, the rates and stress levels were carefully selected to insure that only relevant degradation mechanisms would be activated so that meaningful correlations can be made in order to approximate real operational conditions.

Some of the observations include the following:

1. The maximum mechanical stress at the set strain limit generally decreases with the number of mechanical cycles for all current levels.
2. The work-hardening coefficients tend to decrease with increasing current levels.
3. Work-hardening coefficients increase by small amounts as a function of the number of accumulated cycles for some current levels. However, it decreases for others.
4. The cycles-to-failure data do not exhibit a distinct relationship with current levels.
5. The mechanical hysteresis loop energies of specimens uniformly decrease as a function of accumulated cycles for the lower current levels. However, the hysteresis

loop energy increased with accumulated cycles for some of the specimens stressed at the highest current densities.

6. The mechanical hysteresis energy tends to increase with current.
7. Most fractures appear to grow from incipient surface cracks.
8. High angle bonds tend to have shorter life-times than do low angle bonds.
9. Micrographs of fracture surfaces show striations over much of the surface for low currents but tend to exhibit dimples as the crack grows at higher current levels.

Specimens are sectioned for microstructure studies using the TEM where one can study dislocation networks. Micrographs are examined of partially cycled as well as fractured bond specimens. For a number of the bond fatigue experiments, the electrical resistance of the bond has been monitored continuously as the number of mechanical cycles accumulated.

#### **TENSILE STRENGTH STUDIES OF BOND WIRES**

The properties of bond wires alone are critical to their performance in circuits. Bond wires experience a range of thermal-mechanical treatments during the course of their manufacture, during their application to a circuit and during normal testing and operational sequences. A simple series of measurements was carried out on wire specimens obtained from several cooperative bond wire suppliers. The stress-strain characteristics of a large number of segments from five different 1% Al-Al production wire specimens were investigated as a function of temperature and time at temperature. The maximum

temperature employed to date is 150°C.

The characterization of these wires has shown that the 1% silicon-aluminum alloy wire specimens apparently are normally supplied with somewhat varied thermal histories. While some wire samples become stronger with low temperature heat treatments and then softened for higher temperature and longer times, others only age-soften. In a number of cases, wire tensile samples were quite brittle, perhaps indicative of the growth of large silicon-rich precipitates. Other samples from the same lot may have a fairly large elongation after long heat treatment. Microstructural studies (using thinned specimens in the TEM) are being made to correlate microstructural characteristics with performance in an effort to determine why specimens from the same lot sometimes behave so differently. The point is that, these wire segments might all make satisfactory bonds in a circuit based on an "nondestructive" pull test but could be expected to exhibit a very different long term operational durability performance where the circuits normally experience a wide range of thermal histories. The distribution of silicon-rich particles which precipitate from the alloy is a major factor determining how the bond wire handles cyclical deformation as well as tensile stresses.

#### **MECHANICAL CREEP**

The tensile tests on the bond wire segments are being conducted using an electromagnetically actuated stress-controlled microtensile apparatus in the Micromechanics Laboratory. Due to the measured variability of the simple tensile stress-strain measurements discussed above, both high temperature stress-strain measurements and some mechanical creep studies were indicated to better identify the deformation mechanism. The simple creep measurements were also intended as a critical first step for

definitive current induced plastic flow experiments planned next. The microtensile apparatus used here happens to be uniquely suited for the bond wire creep studies.

For the creep studies, each end of the bond wire segments were bonded to pads on chips, which in turn were cemented to tabs for attachment to the microtensile apparatus. It was noted that wire segments loaded to 80% of their expected bond break strengths exhibited mechanical creep of very small magnitude but easily measured with the sensitivity of the apparatus. After a few minutes, there was failure. This surprising behavior was initially thought to simply be the result of a bad bond. However, measurements on additional wire segments demonstrated that this room temperature mechanical creep was characteristic of the bond rather than a freak situation. A more detailed series of experiments was accordingly organized to determine the stress threshold for this behavior and to identify the operating microstructural mechanisms.

The subsequent experiments have shown that mechanical creep can be measured in bonds stressed to only about 35% of the fast fracture stress, and that bonds fracture at these low stresses after about two hours. A threshold value for no fracture has yet to be measured. The disturbing point is that the force levels where these creep failures are now being observed are only a gram or so greater than the test forces normally recommended for 100% "nondestructive" bond pull.

#### **DISLOCATION BARRIER CALCULATIONS**

Computer calculations have been initiated to evaluate the magnitude of strengthening which is provided by some of the more prominent interfaces in a microcircuit. Coatings such as aluminum oxide grown on the aluminum metallization actually introduce long ranged stress fields which affect dislocation dynamics throughout

typical VLSI conductors. The elastic modulus discontinuity existing at the metal-oxide interface provides a barrier inhibiting both the motion of dislocations and the operation of dislocation sources within the aluminum. These are the interfaces for which the calculations are now being made. However, one expects similar strengthening associated with metal interfaces with other dissimilar materials, including nitride layers, silicon oxides, certain other metals and the silicon of the chip itself. It is suspected here that these interface strengthening mechanisms may account for a large part of the fact that the tiny features of VLSI devices mechanically survive normal operational environmental stresses. The current calculations are being limited to evaluating relevant strengthening in the aluminum wire bonds and in the wire itself.

## DISCUSSION

The studies outlined above are yielding valuable information concerning the degradation mechanisms which ultimately determine the reliability of wire interconnection systems. The low stress creep phenomena observed in the aluminum wire bonds may be due to the discontinuous nature of all such bonds. The actual metal to metal fusion is seen to actually involve numerous small areas over the surface of a bond. The actual mechanical stress in these regions might thus be much higher than supposed assuming a uniform bond. However, this does not explain the three to one differences measured between fast and creep fractures. The answer may lie in the dispersed oxide particles within the bond interface region. These particles could provide pinning points for dislocation sources which could support Nabarro creep mechanisms. Careful microstructural studies are clearly needed here.

The fatigue data for high current densities show significant

energy loss occurring within the bond region compared to data for no current. This indicates enhanced activation of dislocation dynamics. The constricted area for electrical conduction results in localized high current densities. The high local currents thus would cause corresponding local heating resulting in enhanced dislocation motion (i.e. increased temperature softens the metal). In addition, current assisted dislocation motion may be sufficient here to make a contribution to the energy losses observed.

The results outlined above are currently being prepared for publication.

## EXPENDITURES

The expenditures for the investigation during the previous two quarters are as follows:

Jan 1 - March 31, 1984	\$18,609.25
April 1 - June 30, 1984	\$21,247.74
Balance as of June 30, 1984	\$20,402.84

**ANNUAL REPORT**

**INVESTIGATIONS OF MECHANICAL-ENVIRONMENTAL  
INTERACTIONS IN VLSI BOND INTERFACES**

**A-3509**

**PREPARED FOR**

**THE SEMICONDUCTOR RESEARCH CORPORATION  
300 PARK DRIVE, P.O. BOX 12053  
RESEARCH TRIANGLE PARK  
NORTH CAROLINA 27709**

**By**

**B. R. LIVESAY  
GEORGIA INSTITUTE OF TECHNOLOGY  
MICROELECTRONICS RESEARCH CENTER  
ATLANTA, GEORGIA 30332**

**June 1985**



**ANNUAL REPORT**

**INVESTIGATIONS OF MECHANICAL-ENVIRONMENTAL  
INTERACTIONS IN VLSI BOND INTERFACES**

**A-3509**

**PREPARED FOR**

**THE SEMICONDUCTOR RESEARCH CORPORATION  
300 PARK DRIVE, P.O. BOX 12053  
RESEARCH TRIANGLE PARK  
NORTH CAROLINA 27709**

**By**

**B. R. LIVESAY  
GEORGIA INSTITUTE OF TECHNOLOGY  
MICROELECTRONICS RESEARCH CENTER  
ATLANTA, GEORGIA 30332**

**June 1985**

## TABLE OF CONTENTS

	Page
List of Illustrations.....	ii
I. Introduction.....	1
II. Nature of Microcircuit Wire Bonds.....	4
III. Interface Mechanics.....	12
IV. Environmental Fatigue Investigations.....	26
V. Bond Fatigue.....	35
VI. Mechanical and Metallurgical Factors Affecting Wire Bond Behavior.....	69
VII. Creep Experiments.....	76
VIII. Technical Discussion.....	84

## LIST OF FIGURES

Figure	Page
1. Interface Dislocation Network.....	16
2. Array of Misfit Accommodating Dislocations at Interface.....	17
3. Dislocation and Image Near Interface.....	19
4. Dislocation Pile-Ups at Barrier Interface.....	20
5. Dislocation Near Interface of Surface Coating.....	21
6. Force On A Dislocation As A Function of Distance From Interface.....	24
7. Hook Attachment To Bond Wire For Fatigue Test.....	27
8. Fatigue Apparatus.....	28
9. Series Of Low Cycle Fatigue Hysteresis Loops.....	31
10. Measurement of Hysteresis Loop.....	36
11. Response Curves For Al-1% Si Bonds Fatigue In Lab Air.....	38
12. Work Hardening In Al Bond Fatigued In Lab Air...	39
13. Work Softening In Al Bond Fatigued in Lab Air....	40
14. Response Curves For Al - 1% Si Bonds Fatigued In Humidity.....	41
15. Response Curves for Al - 1% Si Bonds Fatigued While Conducting d.c. Current.....	43
16. Work Softening In Al Bond Fatigued While Conducting 200 mA.....	44
17. Peak Stress Behavior For Cyclic Fatigue Of Al Bond Conducting 300 mA.....	45
18. Peak Stress Behavior For Cyclic Fatigue of Al Bond Conducting 350 mA.....	46
19. Hysteresis Loop Energy versus Fatigue Cycle For Al Bond Conducting 50 mA.....	48

Figure	Page
20. Hysteresis Loop Energy versus Fatigue Cycle For Al Bonds Conducting d.c. Current.....	49
21. Peak Stress Behavior For Cyclic Fatigue Of A Gold Ball Bond.....	50
22. Hysteresis Loop Energy versus Cycle For The Gold Ball Bond.....	51
23. SEM Fractographs of Al Bond Fatigued While Conducting 10 mA.....	53
24. SEM Fractographs of Al Bond Fatigued While Conducting 50 mA.....	54
25. SEM Fractographs of Al Bond Fatigued While Conducting 75 mA.....	55
26. Deformation Induced During Ultrasonic Bonding....	57
27. SEM Fractograph of Al Bond Fatigued While Conducting 100 mA.....	59
28. SEM Fractographs of Al Bond Fatigued While Conducting 150 mA.....	61
29. SEM Fractographs of Al Bond Fatigued While Conducting 200 mA.....	62
30. SEM Fractographs of Al Bond Fatigued in Humid Environment.....	64
31. SEM Fractographs of Al Bond Fatigued In Humid Environment.....	65
32. SEM Fractographs of Al Bond Fatigued in Humid Environment.....	66
33. SEM Fractograph Showing Features of Bond-Pad Interface.....	67
34. Deformation Induced During Bonding Process.....	68
35. Load To Fracture versus Annealing Time For Al - 1% Si Bond Wires.....	71
36. Yield Strength versus Annealing Time For Al - 1% Si Bond Wires.....	72

<u>Figure</u>	<u>Page</u>
37. Percent Elongation versus Annealing Time For Al - 1% Si Bond Wires.....	73
38. Stress Controlled Micromechanics Apparatus.....	77
39. Mechanical Creep of Al-Al Bond.....	80
40. Mechanical Creep of Al-Al Bond.....	81
41. Intersecting Slip Bands.....	88
42. Dislocation Pile-Ups Due to Cycle Straining.....	90
43. Environmentally Assisted Cyclic Slip Band Cracking.....	92
44. Model of Fatigue Crack Growth by Shear Sliding...	93

## ACKNOWLEDGMENTS

The following individuals have been contributing their efforts to the various aspects of these investigations:

### Students

Elaine A. Webb, now with Intel Corporation

Dawn L. Maguire

John W. Vidic

### Postdoctoral Fellow

Dr. Srivatsan S. Tirumalai

### Professional Staff

J. L. Larsen

H. M. Harris

Dr. John T. Sparrow

In addition, Mr. Charles Hewitt of the Harris Corporation, the industrial mentor, has visited with us and provided a number of specimen packages which have greatly aided these investigations.

## Introduction

Investigations are being conducted at the Georgia Institute of Technology to study fatigue degradation mechanisms operating in microcircuit wire bonds. The wire bonding techniques developed by the microelectronics industry account for approximately  $10^9$  chip-to-package interconnections each year. To perform their electrical interconnection function, the bond metals must remain structurally sound over the desired lifetime of the device. Mechanical, chemical and electrical stresses associated with the storage and operating environments of a microcircuit can induce degradation processes in the wire bond metals.

The pure and lightly doped aluminum and pure gold wires normally employed for bond wires and pads definitely are not to be considered as high tensile or fatigue strength metals. In addition, structural modifications made to the wire and pad metals during the bonding processes introduce microstructural features which normally accelerate fatigue damage. However, use of these metals is highly preferred because of factors associated with their electrical conductivity and mechanical ductility, as discussed later.

This report describes investigations in progress concerned with gaining a deeper understanding of the degradation mechanisms operating in the bonded interconnections of microcircuits. Experimental methods were developed for the cyclical stressing of wire bond specimens using micromechanics instrumentation which makes it possible to continuously record details of the stress-

strain characteristics of tiny wire bond specimens. Suitable stress-strain parameters were worked out for these studies so that the fatigue degradation mechanisms induced in the wire bond specimens would correlate with those activated in microcircuit materials during normal operations. Low cycle mechanical hysteresis loop data is being recorded for a number of wire bond specimens under a range of environmental stresses which included laboratory air, pure humidity, NaCl moisture and a range of electrical currents through the bonds. The hysteresis data from these experiments are analyzed and correlated with SEM microstructural examinations of bonds to aid the interpretation of degradation mechanisms.

Related studies have also shed considerable light on the mechanical degradation mechanisms in the wire bonds. Calculations were made of interface strengthening effects based on dislocation image force interactions for the aluminum-aluminum oxide film interface at the surfaces of both wires and thin film conductors. The effects of various time-temperature exposures on the mechanical behavior of bond wires obtained from a number of standard suppliers of these materials were also experimentally evaluated.

Tensile measurements at constant loads, with and without, electrical currents showed that microcircuit wire bonds exhibit mechanical creep phenomena, even at room temperature. The discovery of this effect demonstrated that an important mechanism of viscous plastic flow could affect the cyclical degradation of



wire bond specimens.

The following sections of this report discuss the important aspects of microcircuit wire bonds that make them a special class of materials for performing low cycle fatigue investigation. Interface strengthening processes are then described in terms of their importance concerning the small dimensions involved with both the wire interconnections and with metallization layers on the chips of microcircuits. Results from the several types of mechanical investigations are presented and interpretations of the operating degradation mechanisms in the bond metals are discussed.

## THE NATURE OF MICROCIRCUIT WIRE BONDS

The standard wire bonding processes employed by the microelectronics industry are extraordinary in that both identical and dissimilar metal pairs are reliably joined without their surfaces being made molten, without a flux and without an interconnecting solder or weld alloy. The techniques for both thermocompression and ultrasonic wire bonding of microcircuits are well documented in the technical literature. Our principal concern here is with the effects these bonding techniques have on bonded metal members and with the interface(s) created by the bond. The mechanisms required to make intermetallic joints result in highly altered microstructures in the metal pairs in the immediate neighborhood of the bond. The resulting physical state of the deformed bonded metals and the geometrical aspects of the bond shape are critical to the performance and ultimate durability of the bond interconnection under operational and other stresses imposed on the circuit.

The wire and pad of either a thermocompression or an ultrasonic bond are highly deformed during bonding, but by very different mechanisms. Aluminum, gold and other proposed metals for bond wires have the face centered cubic structure with twelve slip systems, which promotes easy deformation within randomly oriented individual grains. Purely thermocompression bonds are heated to facilitate plastic flow under mechanical pressure. The plastic flow creates new, atomically clean, metal surfaces of the

wire and pad materials at their interface as they are compressed together. Creation of the new surfaces at the wire-pad interface enhances interfacial diffusion and thus establishes the intimate metallic contact essential for making the conducting bond. In the case of thermocompression bonding, thermally activated mechanisms greatly enhance dislocation dynamics to provide for extensive plastic deformation under moderately applied mechanical pressure. It is crucial for making conducting wire bonds that the wire and pad metals have high ductility in order to facilitate the necessary plastic flow required to create the new surfaces, as mentioned above. The ductility of the bond wire metal also disperses the mechanical forces of bonding which minimizes stress concentration, and potential damage, to the brittle chip material.

In contrast, ultrasonic bonding processes employ intense ultrasonic energy to facilitate easy dislocation glide without appreciably increasing the temperature of the bonding members. The intense ultrasonic energy is absorbed by the crystal lattice and is concentrated on lattice defects in a manner which enhances dislocation glide past normal pinning features without appreciably raising temperatures of the bonding metals. One can make correspondence between the experimental tensile curves for pure aluminum stressed at various elevated temperatures and similar curves of aluminum exposed to progressively elevated ultrasonic energy densities, but with the aluminum held at a low temperature. The yield point of aluminum is decreased

significantly as the temperature is raised and, correspondingly, as the ultrasonic energy density is increased. The extensive plastic flow with coincidental exposure to intense ultrasonic energy and mechanical pressure brings freshly created metal surfaces into immediate contact. Intermetallic bonding at the interface requires sufficient interatomic diffusion between the wire and pad metals to establish the bond interface. During the last few years, thermosonic ball bonders have been available which simultaneously take advantage of both thermal and ultrasonic enhancement of plastic flow.

A microcircuit wire bond is normally a complex metallurgical structure. The bonding mechanisms involve extensive deformation of the wire and pad, as mentioned above. In addition, surface oxides and other surface impurities remain in the resulting bond interface. The fact that gold does not form a surface oxide at room temperature has been a characteristic of immense value for making electrical contacts, including microcircuit wire bonds. However, even gold-to-gold bonds are found to have interface impurities due to residual processing materials, improper handling and atmospheric impurities, including moisture, which may exist in process areas.

A gold-aluminum bond thus has the potential for establishing an array of intermetallic compounds with consequent multiple interfaces. The formation of these intermetallic compounds is critically sensitive to the combination of time and temperature exposure, either during the bonding process or with subsequent

exposure to elevated temperatures. Certain of the interfaces which develop in the Al-Au system after elevated temperature exposure are so brittle that bonds lift at zero force levels from the bond pads. Bond failures involving Al-Au intermetallic compound interfaces have resulted in some well known catastrophic system failures. There have been a number of investigations concerning the materials and processing parameters which lead to the excessive growth of the Au-Al intermetallic compounds and their effects on the mechanical behavior of wire bond systems. The gold-aluminum phase diagram has five intermetallic compounds,  $\text{Au}_4\text{Al}$ ,  $\text{Au}_5\text{Al}_2$ ,  $\text{Au}_2\text{Al}$ ,  $\text{AuAl}$  and  $\text{AuAl}_2$ . The important point is that an aluminum-gold bond is metallurgically unstable. Either mistakes during manufacture or subsequent exposure to elevated temperatures during testing, storage or operation can provide the thermal environment which supports the growth of one or more of the intermetallic compounds in the bond interface. The electronics industry has carefully learned to handle the Au-Al intermetallic compound problem by essentially trying to avoid the relevant circumstances.

The Al-Al ultrasonic bond has become increasingly more important in recent years for microcircuit interconnections for several reasons. Aluminum metallization is now used in most microcircuits and it is therefore advantageous to use aluminum wires in order to avoid the intermetallic compounds discussed above. In addition, gold wires have significantly greater mass and are subject to correspondingly greater mechanical

acceleration problems. Radiation damage is also a major problem with gold. The technology for making aluminum ball bonds has been developed during the last several years and should have a favorable impact for greater aluminum wire usage in the future.

Fragments from the natural oxide of aluminum remain conspicuously within the interface of all aluminum wire bonds. Sectioned Al-Al wire bonds clearly show that patches of aluminum oxide are distributed throughout the central plane of the bond interface. During the ultrasonic bonding process, the oxide is fractured into many tiny segments as the bonding surface effectively expands during compressive deformation. The effective electrical and mechanical bond is provided by numerous tiny intermetallic bonds made by atomic contact between the newly created, and protected, surfaces.

Ultrasonic bonds are employed in enormous quantities to provide interconnections between chip and package terminals and also between adjacent chips within a package. Early generations of monolithic devices generally required 10-30 wire interconnections from chip pads to package posts. Complex hybrid microcircuits have long involved hundreds of wire bonds. During the last few years the development of high density VLSI chips has greatly multiplied the number of chip-to-package interconnections in monolithic circuits. Some VLSI devices now require over 300 I/O terminals and the numbers are increasing.

The large numbers of bonds involved with individual microcircuits has greatly emphasized the importance of the

reliability statistics for making good wire bonds. In addition, the bond structure must be durable under the operational and environmental stresses it is required to handle within a microcircuit package. If the statistical reliability for making good bonds were 99%, there clearly would be a major concern with production yields for microcircuits having a hundred or more bonds. This concern led to the early development of "non-destructive" bond pull tests for hybrids where large bond counts made it statistically probable to have one or more bad bonds within each package. Hybrids with an investment of a number of chips and an expensive package cannot be simply discarded because of a single bad bond, as is the case for simpler ICs. A "non-destructive" bond pull test consisting of a low force tug on each bond essentially determines that the bond adheres to the pad. The magnitude of this low force tug introduces mechanical deformation within the bond wire material which may, or may not, be of truly non-destructive nature.

The wire bond is subject to mechanical, chemical and electrical stresses in testing, storage and operation of the circuit. The response of the wire bond material structure to these stresses will be an important factor in the overall durability of the microcircuit. Mechanical stresses are generated within the wire bond during thermal excursions due to differential thermal expansion coefficients of circuit materials and due to thermal gradients associated with rapid thermal excursions. Temperature cycling occurs during normal operation,

in various environments while the circuit may even be electrically dormant and during environmental stress screening. In addition, microcircuit fabrication processes always leave residual mechanical stresses within the wire bond materials. The chemical stresses are associated with tiny quantities of residual process chemicals, moisture, impurities introduced during fabrication and packaging and chemical agents which come out of packaging materials such as epoxies used for die bonding, etc. All of these chemical agents make up the microenvironment of a package cavity. Electrical stress occurs with high currents in certain bond wires to a circuit.

The metal in the bond region is highly deformed and contains a high density of defects as well as trapped debris consisting of oxides and other impurities originally on the wire and pad surfaces. The highly deformed region where the wire is flattened against the bond pad to form the bond is mechanically supported by the bond interface. The geometrical configuration of the heel region, which bridges the flattened wire with the undeformed wire, serves as a microscopic stress concentration factor. Movement of the wire loop due to thermal expansion and contraction or to mechanical vibrations will accordingly introduce the greatest mechanical stress in the metal of the heel region of the bond. Mechanically induced bond failures of "good" bonds generally occur at the heel.

The heel region of the wire contains a high defect density from the bonding deformation and generally has a roughened



surface from abrasive interactions with the bonding tool. The defects include an extensive dislocation debris and voids. The nature of the deformation also leaves residual mechanical stresses in the bond metals. The high dislocation density at the heel effectively work hardens the metal. The dislocation networks will concentrate voiding leading to the formation of incipient microcracks in the aluminum with mechanical cycling. These and other factors emphasize the susceptibility of the heel region of a wire bond to mechanical fatigue damage.

## INTERFACE MECHANICS

The close proximity of surfaces and other interfaces profoundly affect the mechanical behavior of metal structures. The thin planar configuration of microcircuits makes all metal features on a chip subject to strong interface interactions. For example, yield strength measurements for bulk aluminum single crystals are normally on the order of  $5 \times 10^6$  dyne/cm<sup>2</sup>, or less. According to this value, an aluminum crystal only one micron thick by ten microns wide would thus yield with a tensile load of about 0.5 dyne. If the aluminum interfaces of this thin strip were only with vacuum (i.e. an unsupported aluminum film with no oxide or other coating), then the surface energy of aluminum, 860 dyne/cm, would itself support a load of about 1.7 dynes.

The real situation for the metals in a microcircuit is much more complex. There are no pure aluminum-vacuum interfaces but rather interfaces between aluminum and its oxide, another metal, the silicon chip or a dielectric. A similar statement can be made for gold metallization as well, except that gold does not have a stable oxide under these conditions. Pure gold and pure aluminum are face-centered-cubic metals whose mechanical properties are very well characterized from large numbers of investigations on bulk specimens. The mechanical durability exhibited by thin film structures of these metals deposited on chips with respect to the stresses to which they are exposed in normal operational cycles definitely cannot be attributed to the basic strength intrinsic

to these metals alone.

In order to account for the structural integrity of a microcircuit, one must examine other factors. The critically important mechanical strengthening factors for a microcircuit structure are associated with the discontinuities bridged by the interfaces between the metal film and neighboring layers.

A deposited fcc film is normally polycrystalline with columnar grains having a close-packed plane parallel to the substrate. Developing a fine grain structure in bulk metals is important for mechanical strengthening. However, the dimensions of strip lines and other metal features in VLSI devices are comparable with the grain sizes. This results in a "bamboo" appearance in etched thin circuit conductors demonstrating that the conductor becomes like a string of tiny single crystals connected together in a line. Similarly, one also sees a bamboo structure in bond wires exposed to elevated temperatures for sufficient time to grow large grains.

The annealing which takes place in a microcircuit during either the high temperature bake, burn-in or with time in normal operation would result in very weak mechanical structures based on the intrinsic lattice strengths of gold and aluminum. If only lattice strengthening processes were available in these thin structures, one reasonably would expect the gold or aluminum films to be catastrophically distorted under the imposed thermal mechanical stresses during operation of microcircuit. The complex interface structures created in microcircuit designs in order to

accomplish their electronic functions turn out to be critically important for mechanical durability as well.

The deformation characteristics of all fcc metals, including gold and aluminum, is associated with dislocation mechanics. The strength of these metals is thus determined by the effectiveness of barriers to dislocation motion within the metal lattice. High strength is achieved in structural alloys through careful alloying and heat treatment schedules to control grain structures. Only limited alloying is used in microcircuit metallic conductors and the thermal treatments normally involved here lead to mechanical softening rather than strengthening.

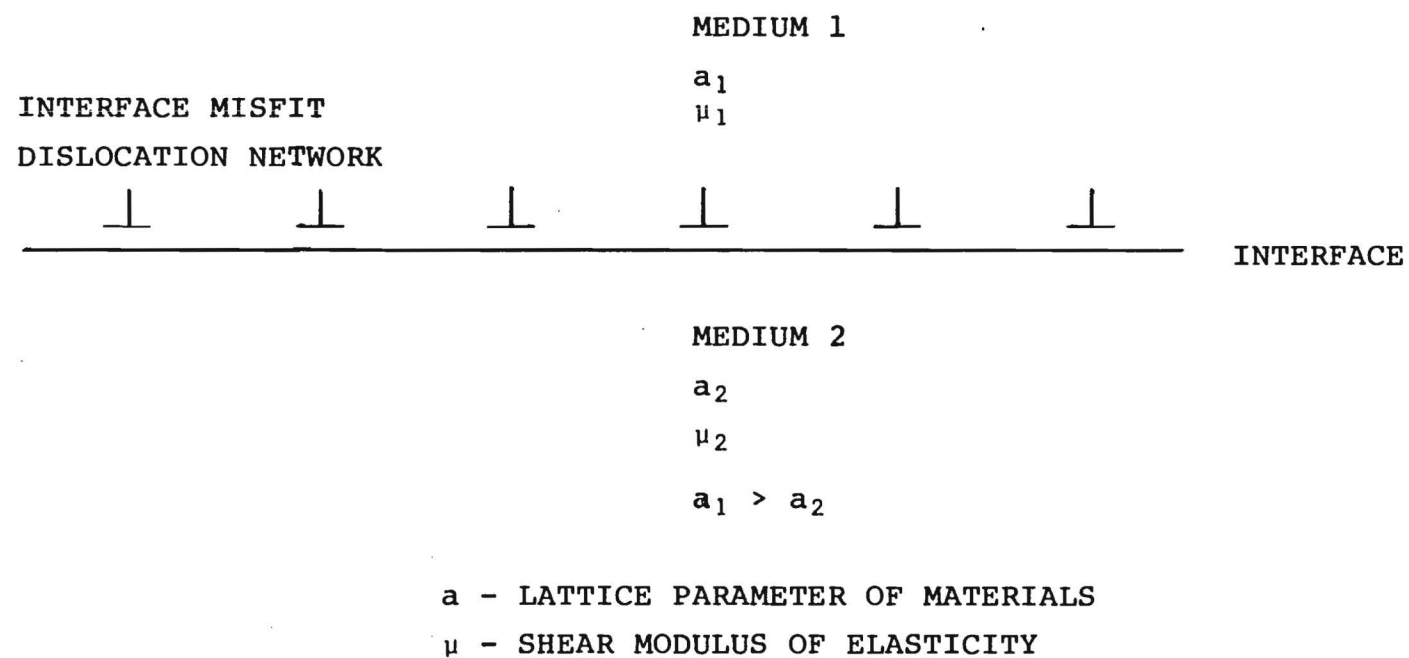
Dislocation stress fields extend over distances comparable to one or more dimensions of microcircuit features. Interfaces may present material discontinuities which distort dislocation stress fields effectively to either attract or repel the dislocation from the interface. For example, an aluminum-vacuum interface energetically favors dislocations moving to the surface and out of the metal, or a softening effect. However, an aluminum interface with either its own oxide, with silicon or with most dielectric materials will provide a barrier to the egress of dislocations, and thus strengthen the metal layer.

The barrier effects created by dislocation interactions with normal microcircuit interfaces are primary strengthening mechanisms in microcircuit metals. In general, interface strengthening factors are important for metal members having dimensions typical of microcircuit bond wires as well as the thin

metallization layers mentioned above. Microcircuit interfaces bridge differences in such parameters as elastic modulus, lattice constants, crystal structures, crystallographic orientation and chemical properties. In addition to the surface tension effects mentioned earlier, interfacial energies play an important role in the formation and strength of an interface. A detailed analysis is necessary to evaluate the effect of particular interface configurations on the strength and durability of a metallic structure.

The following describes several of the interface strengthening mechanisms of importance to VLSI materials.

Differences in lattice constants across an interface introduce large elastic strain components in a coherent interface. The lattice misfit would thus generate local mechanical stresses well beyond the strength of the material extended over a few lattice spacings. In order to successfully accommodate this misfit, metals are found to generate arrays of dislocations which essentially serve to relax the accumulated stress built up after several lattice spacings. These periodic arrays of dislocations, shown schematically in Figures 1 and 2, are called accommodating dislocation networks and they are critically important for being able to produce a good interface between two materials. The creation of this network depends upon the existence of a suitable dislocation generation and glide mechanism within the crystal structure of the metal. If the crystallographic natures of a particular pair of materials is



$a$  - LATTICE PARAMETER OF MATERIALS

$\mu$  - SHEAR MODULUS OF ELASTICITY

Figure 1. INTERFACE DISLOCATION NETWORK

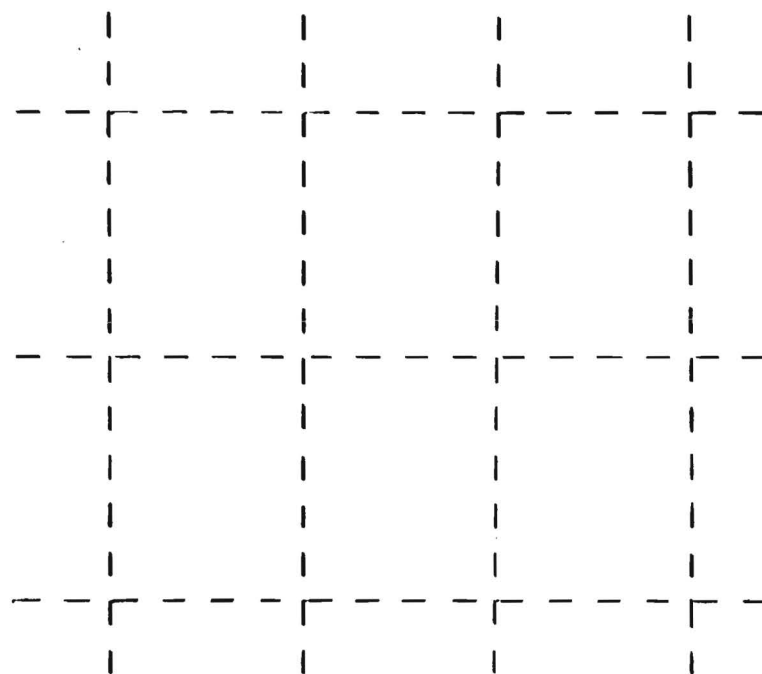


Figure 2. ARRAY OF MISFIT ACCOMMODATING DISLOCATIONS AT INTERFACE

such that they cannot generate a suitable accommodating dislocation network, one usually finds extensive cracking or separation in the surface coating.

The important point concerning these accommodating networks here is that glide dislocations must traverse the network in the interface during plastic deformation. The stress field of the fixed accommodating network inhibits the dislocation glide towards and through the interface, with a net strengthening contribution. Another factor associated with the lattice misfit is that the Burgers vectors are different in the two materials bridged by the interface. The forced (under mechanical stress) transmission of dislocations through the interface thus generates a lattice displacement debris corresponding to the Burgers vector difference and the accumulated number of transmitted dislocations. This interface displacement debris is accompanied by a lattice stress field effectively repelling successive glide dislocations.

The effect of elastic modulus difference on dislocation glide towards an interface is briefly outlined in the following model.

The stress field of a dislocation in a solid is long ranged, having an inverse distance dependence. A dislocation located at distance,  $a$ , from an interface (see Figure 3) thus experiences an effective force of interaction,  $F_x$ , due to the interface according to expressions of the form



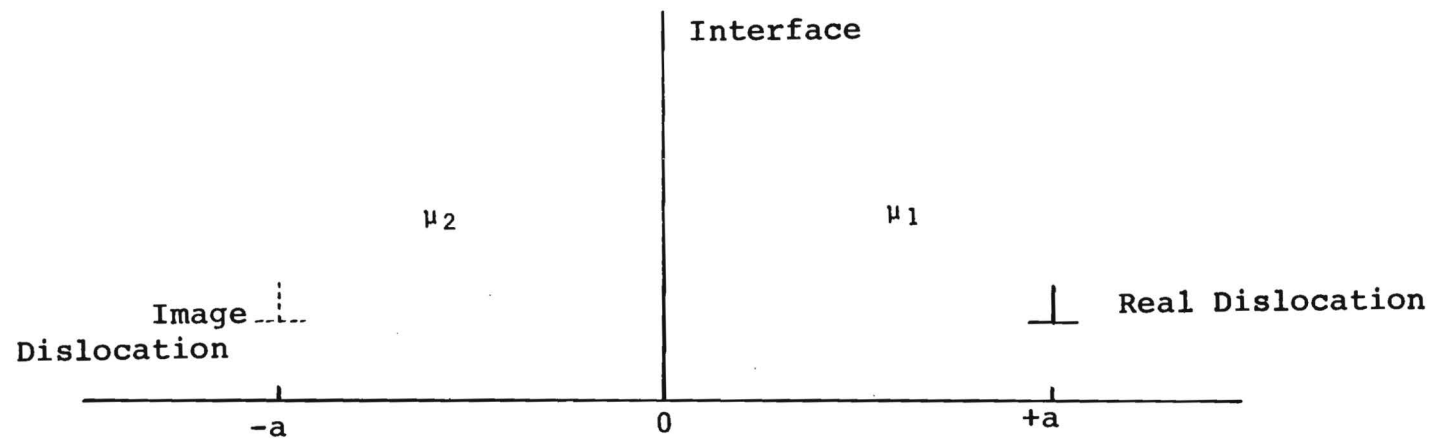


Figure 3. Dislocation and Image Near Interface  
of Two Semi-Infinite Solids

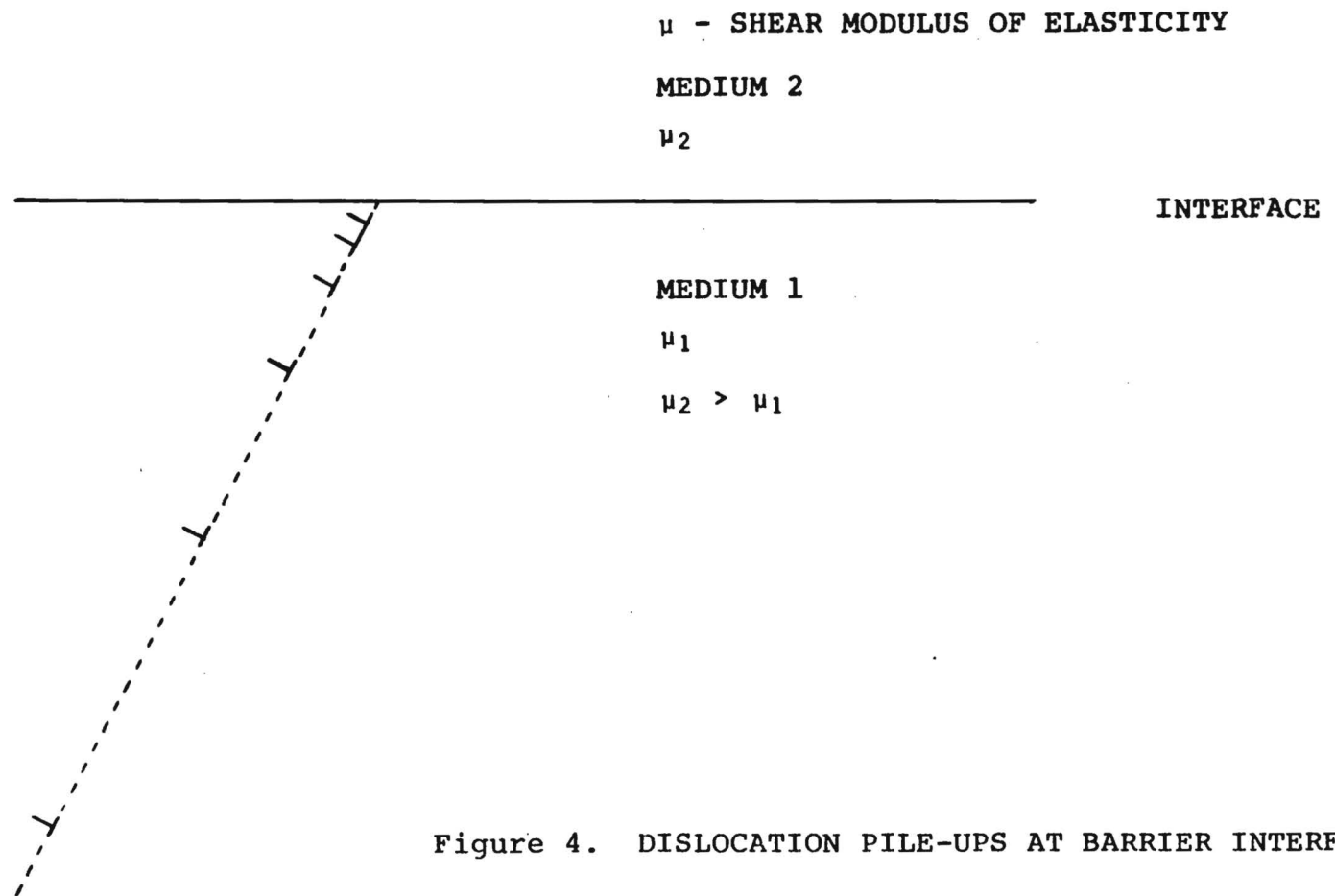


Figure 4. DISLOCATION PILE-UPS AT BARRIER INTERFACE

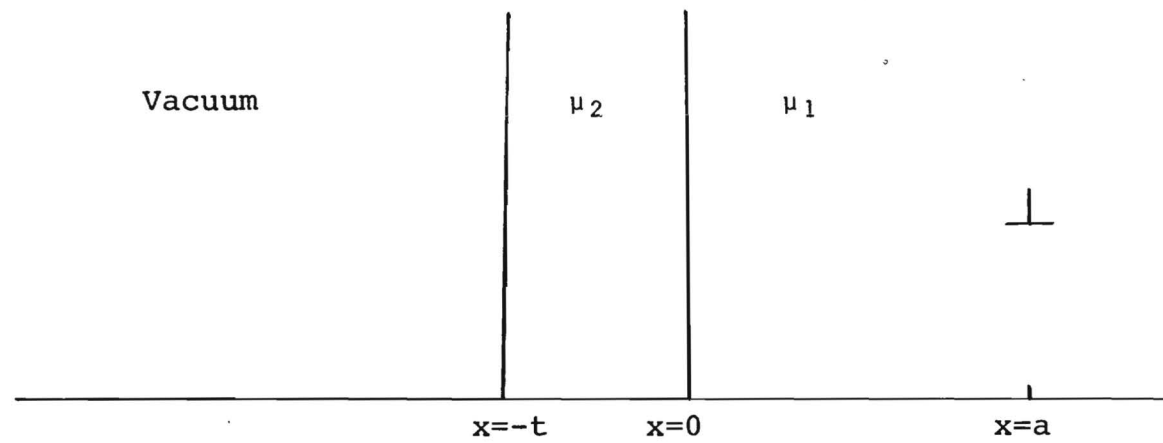


Figure 5. Schematic of Dislocation Near Interface of Surface Coating

$$F_x = \left( \frac{\mu_2 - \mu_1}{\mu_2 + \mu_1} \right) \mu_1 \frac{b^2}{4\pi a} \quad (1)$$

where  $\mu_1$  and  $\mu_2$  are the elastic moduli of the two materials and  $b$  is the Burgers vector of the dislocation.

One can see from equation 1 that for a metal-vacuum interface, i.e.  $\mu_2 = 0$ , the elastic stress field in the medium exerts a force on the dislocation towards the interface. Thus dislocations energetically are prone to exit at free surfaces of crystals where they have sufficient mobility. However, if  $\mu_2 > \mu_1$ , then the image dislocation effectively repels the real dislocation. One has an effective barrier to dislocation transport across the interface. This situation is shown in Figure 4 where a dislocation pile-up is indicated schematically on a slip plane oriented at an angle to the interface. Such dislocation pile-ups are routinely observed in transmission electron microscopy investigations of dislocations.

The interface configuration relevant to a surface coating (which may be a thin deposited film, a thermal oxide, etc.) of thickness,  $t$ , is shown schematically in Figure 5. The theoretical calculations for this configuration are made by considering individual interactions of the single real dislocation with an infinite series of image dislocations. The expression used to carry out computer calculations for the net force acting on a

dislocation at any site due to the proximity of a surface having a finite coating is

$$F = \frac{\mu_1 b^2}{4\pi a} \left[ \kappa - (1 - \kappa^2) \sum_{n=1}^{\infty} \frac{\kappa^{n-1}}{1 + nr} \right] \quad (2)$$

where  $r = t/a$ , and  $k = (\mu_2 - \mu_1)/(\mu_2 + \mu_1)$ .

Assuming an aluminum-aluminum oxide interface, interaction forces were calculated for dislocations approaching the oxide from within the metal and are shown in Figure 6. At large distances from the interface, the dislocation is attracted towards the interface as it would be if the interface were a free surface. As a dislocation approaches the interface, the attractive force decreases, which is the opposite situation to that for a free surface. At a particular distance from the surface, based on substrate and coating material characteristics, the dislocation is in equilibrium and the force on the dislocation then becomes repulsive as the dislocation approaches the interface from that point. Calculations for smaller coating

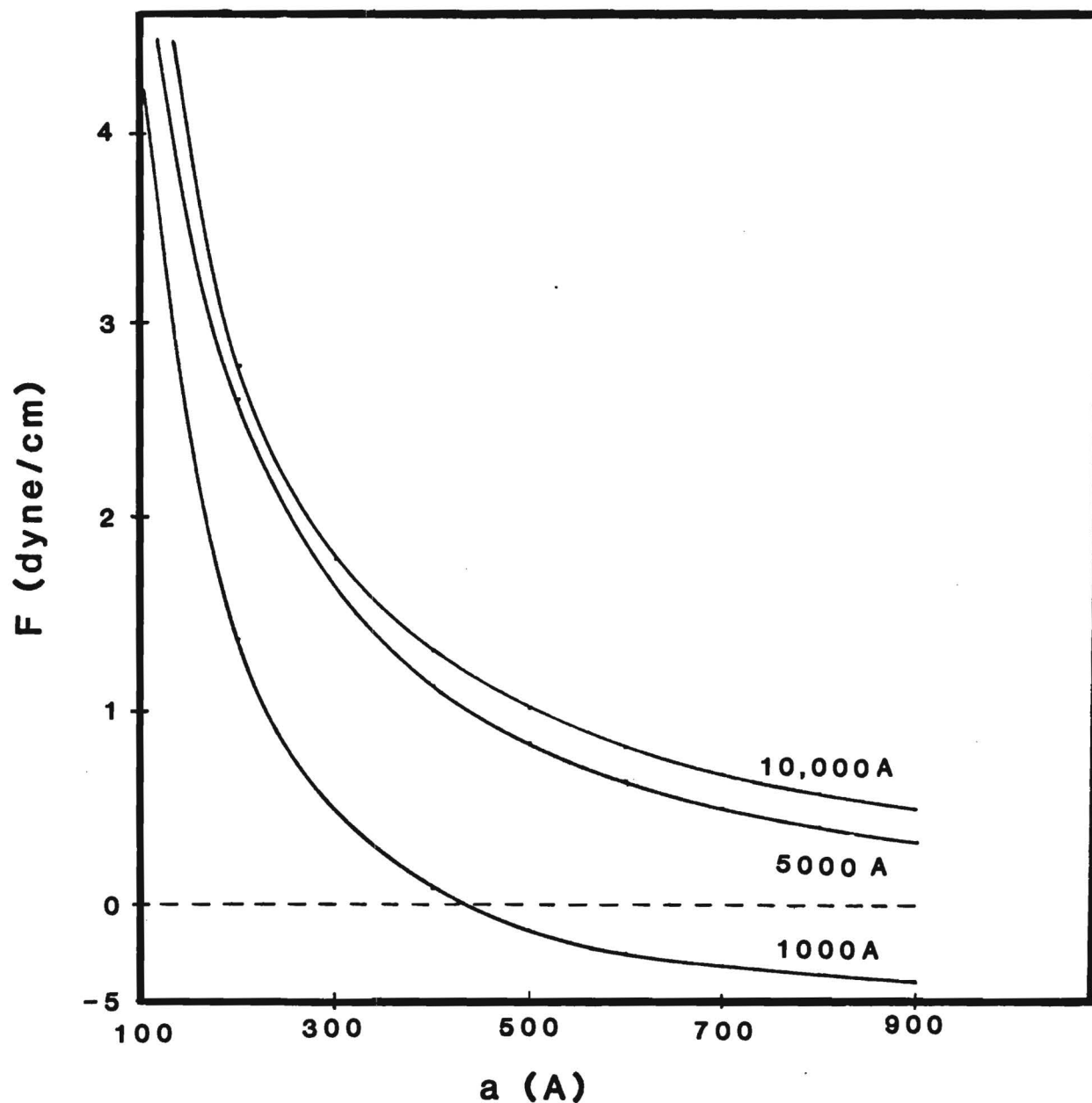


Figure 6. Curves of calculated forces acting on a dislocation in aluminum as a function of the dislocation distance,  $a$ , from the metal-oxide interface. Curves for several oxide thicknesses are shown here. Note the force equilibrium at about 450 Å for the 1000 Å film thickness curve. Similar calculations for thinner oxides show that the equilibrium distance decreases linearly with the film thickness below 1000 Å.

thicknesses indicate that the equilibrium distance decreases linearly with film thickness. The maximum repulsive force is determined by factors associated with the region of highly displaced crystal within the dislocation core. The effective shear stress,  $\tau$  , imposed by the interface is given by the expression

$$\tau = F/b \quad (3)$$

The real metal members actually involve multiple dislocation interactions occurring simultaneously. In addition, brittle metal oxide layers at the surfaces bond wires fracture with the egress of slip bonds, and thereby modify the interfacial configuration. The new surfaces created by the egress of slip bands provide significant interfacial energy changes which also account for mechanical strengthening in these thin members. Certainly it is not possible to represent a bond or a strip line with a single dislocation model, any more than one represents electrical conductivity with single electron transport models. However, the dislocation interface interaction calculations do provide order of magnitude estimates of these effects. Further, a more detailed representation of the microcircuit interface configurations will increase the precision of theoretical results. The mechanisms considered here, indeed, do control the strengthening processes in the various thin metal features involved in microelectronic device structures.

## ENVIRONMENTAL FATIGUE INVESTIGATIONS

The loops of bonded wire interconnects are cyclically stressed under selected environmental conditions. The primary emphasis has been to apply strain-controlled flexures of bond wire loops to accelerate the stresses typically experienced by microcircuit wire bonds during temperature cycling associated with operating or other temperature variations. A major concern in the design of these experiments has been to represent the physical stress configurations generated with wire loop flexures while employing a fatigue test geometry which can be applied as consistently as possible with successive wire bond specimens.

The experimental arrangement sketched in Figure 7 was adapted to the strain-controlled microtensile apparatus shown in Figure 8. The microcircuit package is cyclically displaced via a micrometer screw drive mechanism. The fixture used to clasp the bond wire consists of a slot with an opening slightly larger than the diameter of the bond wire which had been machined into the side of a stainless steel wire. This slot clasps the bond wire in order to apply and measure both compressive and tensile flexure forces at the apex of the wire loop. Small wire hooks with various adhesives were employed for a number of the early bond fatigue measurements. However, the adhesives were sometimes found to degrade with either the environment or the mechanical cycling. An arrangement was needed for making a precise attachment to the



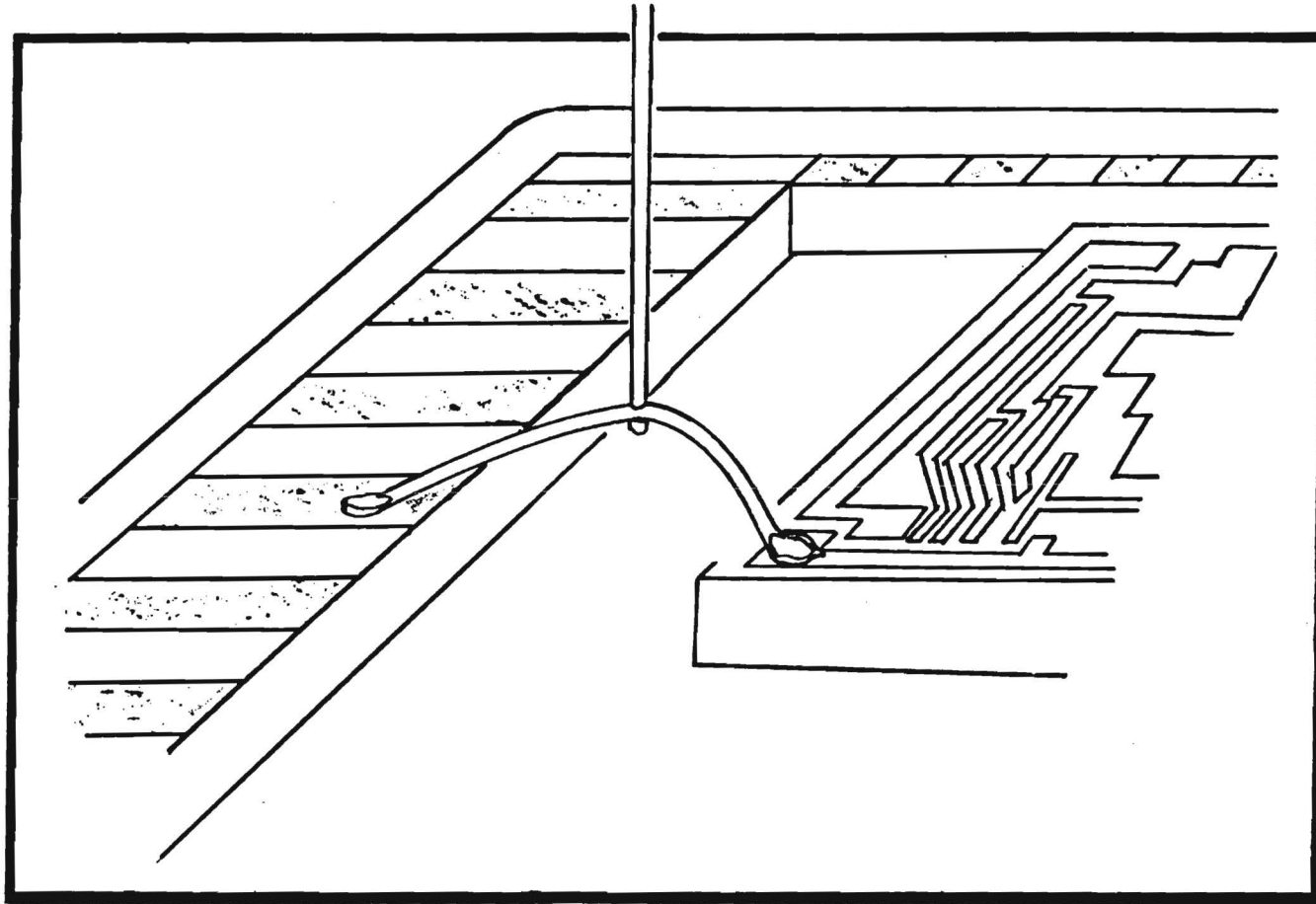


Figure 7. Schematic of the notched hook as it grasps the aluminum wire during a low cycle fatigue experiment. The wire is bonded in a standard DIP package.

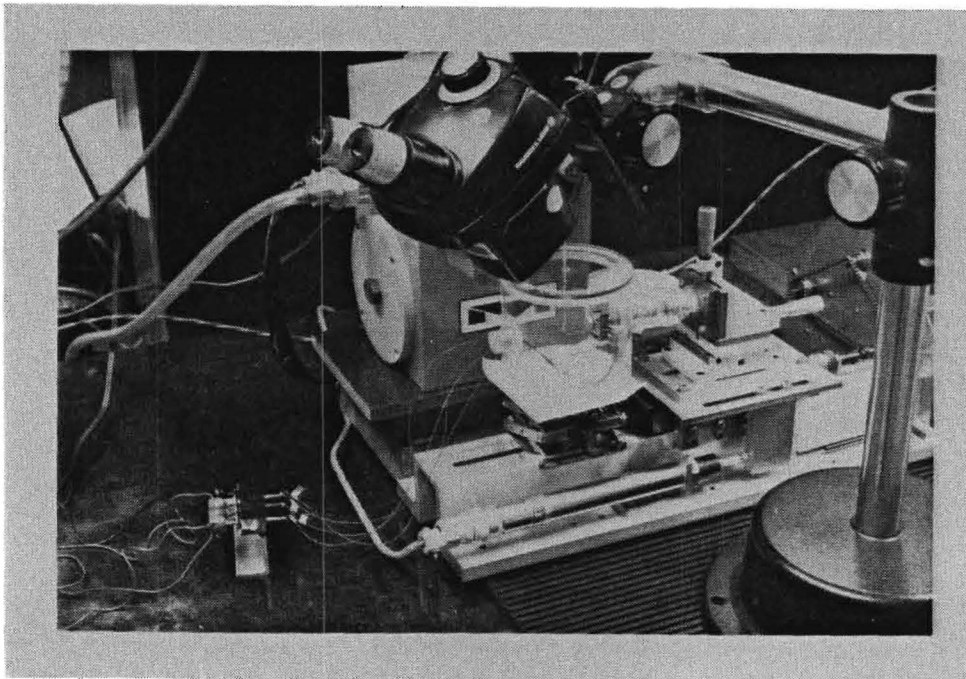
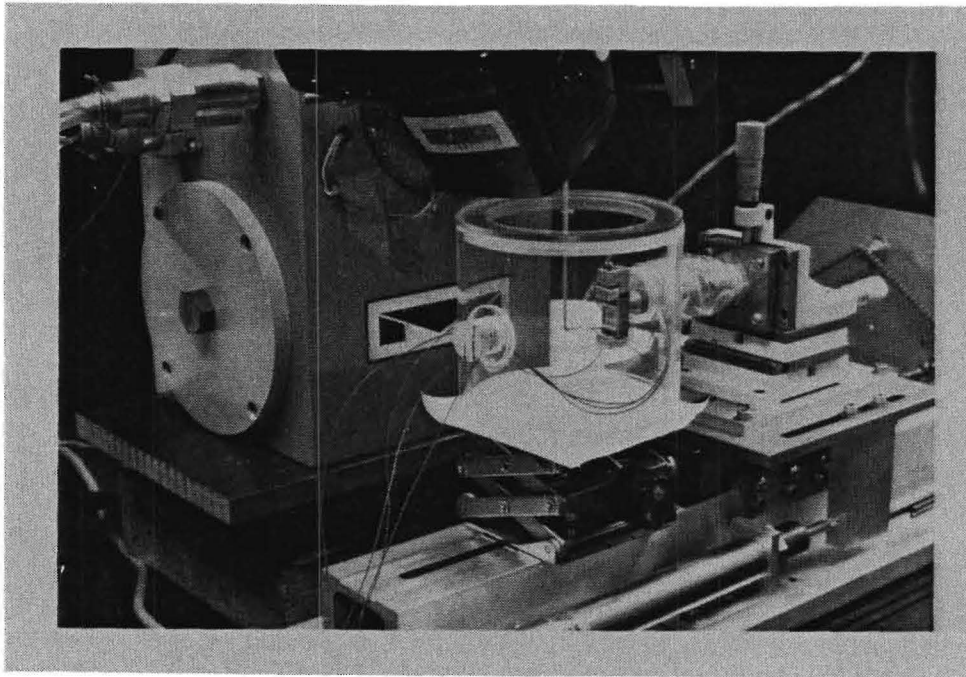


Figure 8. Strain controlled micromechanics apparatus shown in configuration for low cycle fatigue measurements on microcircuit wire bonds.

wire without causing any metallurgical damage to the soft metal of the wire and which could handle the temperature excursions associated with current conduction through the wire bond. A method was subsequently developed for the precision machining of the slots to the dimensions of the wire bond which have proved convenient for clasping the wire and have made it possible to cycle over a wide temperature range.

An automatic mechanism drives the package with a preselected cycling amplitude and strain rate. The flexure force is measured using a torque dynamometer having an air bearing to which a fine tube is attached as a lever arm. At the other end of this lever arm, attachment is made to a fine wire or tube having either a hook or the above described slot to clasp the bond wire. The package is supported by a mounting fixture attached to a three stage micropositioner. The micropositioner is used to bring the wire viewed through a microscope precisely to the location of the hook or slot without introducing any mechanical deformation to the very soft bond wire metal. The three dimension micropositioner is mounted on the micrometer screw driven slide stage of the micromechanics apparatus. Loop displacements are measured with a differential transformer transducer. Analog outputs for the flexure force and displacement are supplied to an x-y recorder to display and record low-cycle mechanical hysteresis loops. A special chamber was designed for the apparatus which allows the necessary attachments to the wire and package while providing a means to expose specimens to a range of

gases and vapors at atmospheric pressure. The chamber is transparent since the ability to continuously observe specimens through a microscope is important. Arrangements are also made for bringing electrical conductors into the chamber for applying current to the bond wire and for resistance measurements.

The number of cycles to failure for microcircuit wire bonds varies according to stress amplitudes, and is sometimes in the thousands of cycles. This can result in large numbers of hysteresis loops recorded for each specimen. Procedures were therefore evolved for selecting particular cycles for recording hysteresis loops.

Selected mechanical hysteresis curves taken in sequence while cyclically stressing an aluminum ultrasonic wedge wire bond are shown in Figure 9. These curves, which are reduced from 11x14 inch x-y recorder plots, illustrate the typical recorded stress vs. strain behavior of the asymmetrical configuration where a bond wire loop is stressed in compression and tension with the attachment made at the apex of the wire loop and with the line of displacement approximately perpendicular to the wire.

A central problem with conducting any experimental fatigue investigation is in selecting appropriate stress (or strain) amplitudes and cyclical rates such that the experiments can be conducted in reasonable time periods. The cyclical stress and time rate values normally associated with actual microcircuit environments, of course, involve fatigue time-to-failure periods which would be entirely impractical for experimental

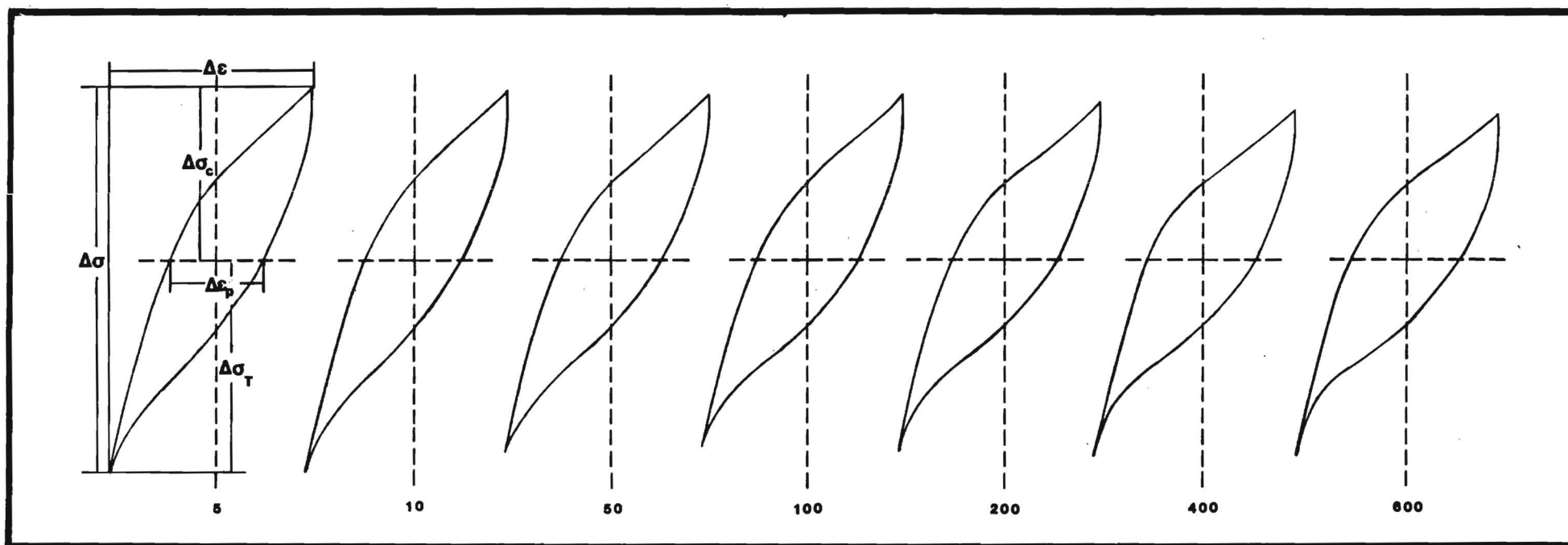


Figure 9. Reduced graphs of mechanical hysteresis loops for an aluminum wire bond recorded at indicated cyclical intervals in the fatigue life of the bond. The vertical axis is mechanical stress and the horizontal axis is strain. The stress and strain amplitudes, the instantaneous slopes of stress-strain behavior and the loop areas (hysteresis energy) are valuable parameters for interpreting damage mechanisms.

investigations. The purpose of these investigations is to increase the understanding of the degradation mechanisms involved in mechanical fatigue processes in the wire bonds of microelectronic devices. One therefore wishes to accelerate the mechanical damage processes in a manner which does not appreciably alter the operation of the basic mechanisms within the materials. When the concern is with environmental fatigue mechanisms, as is the case here, there clearly are important time dependent environmental interactions acting in synergism with the mechanical stress fields. The accelerated fatigue cycling rates therefore should be as slow as practical for accumulating experimental data.

There have been a few experimental investigations reported in the literature for mechanical and thermal mechanical fatigue in microcircuit bond wires. However, none of the previous experiments have involved the necessary instrumentation to provide quantitative stress-strain data, as needed for evaluating low-cycle fatigue mechanisms. The earlier work thus provided little in terms of quantitative data to design the experiments necessary to achieve the goals of the program. It therefore was required for us to empirically determine optimum stress and strain amplitudes and cyclical rates which would be most appropriate for the environmental fatigue investigations on VLSI wire bond interconnections.

Thermal cycling studies conducted by Fitch on large numbers of packaged ICs showed significant wire bond fatigue failures

occurring after 1,000 to 4,000 temperature cycles. He noted that microstructural damage occurred in wire bonds after only a few cycles. Fitch also found that the circuits having longer bond wires experienced greater failure rates.

The bond wires involved with VLSI devices are generally longer than those in the LSI circuits studied by Fitch. The temperature coefficient of expansion for aluminum,  $25 \times 10^{-6}/\text{C}$  degree, is considerably larger than that of most of the other materials used in the fabrication of microcircuits. For example, the thermal expansion coefficient of aluminum is about ten times the value of  $3 \times 10^{-6}/\text{C}$  degree for silicon. Thermal excursions in wire interconnects of over 100 C are quite common. Depending upon details of particular VLSI loop geometries, the thermal expansion induced deflection of a bond wire loop normal to and at the apex of the loop would be 50 to 300 microns. Our empirical fatigue tests on wire bonds at various strain levels in normal laboratory air also indicated that this amplitude range provided mechanical cycled fatigue lives ranging from a few hundred to several thousand cycles, depending upon bonding parameters. These values correspond well with the IC wire bond wear-out temperature cycling data of Fitch. Our calculations of thermal mechanical induced stresses based on his temperature excursions and assumed bond wire geometries also are in reasonable agreement with our conditions. It was accordingly concluded that the bond stress and strain levels which result from the direct mechanical displacement of the wire apex in this range would be appropriate

for the quantitative wire bond fatigue studies. Most of our environmental wire bond fatigue life experiments are therefore being conducted employing strain amplitudes of between 50-150 microns and with 50 second cycle durations.



## BOND FATIGUE

A typical mechanical hysteresis loop measured for an aluminum wedge bond is shown in Figure 10 with the stress and strain amplitudes for compression and tension modes as indicated. This particular curve is an actual loop taken for the 5th cycle of an Al-Al wedge bond. The area of the curve represents the mechanical energy absorbed by the wire interconnection during a single complete cycle. The absorbed energy is dissipated in plastic deformation processes occurring within the overall bond wire loop material. However, close microscopic observations of the flexure motions in different regions of a wire loop and studies of fatigue degradation in numerous wire bonds indicate that most of this energy is absorbed either within or in the neighborhood of the heel region of the bonds located at the two ends of the wire loop. In contrast, the corresponding stress-strain behavior for a similar wire loop of a material stressed only in the elastic region, (perhaps a hardened steel wire) would appear as a closed hysteresis loop, or roughly as a single sloped curve on the plot.

The cyclical stress-strain data from aluminum and gold wire bond materials clearly demonstrate that significant plastic deformation is occurring with the strain amplitudes discussed above and that finite hysteresis occurs even with considerably smaller strain amplitudes. Low cycle fatigue damage mechanisms are thus operating in wire bonds during each power (temperature)

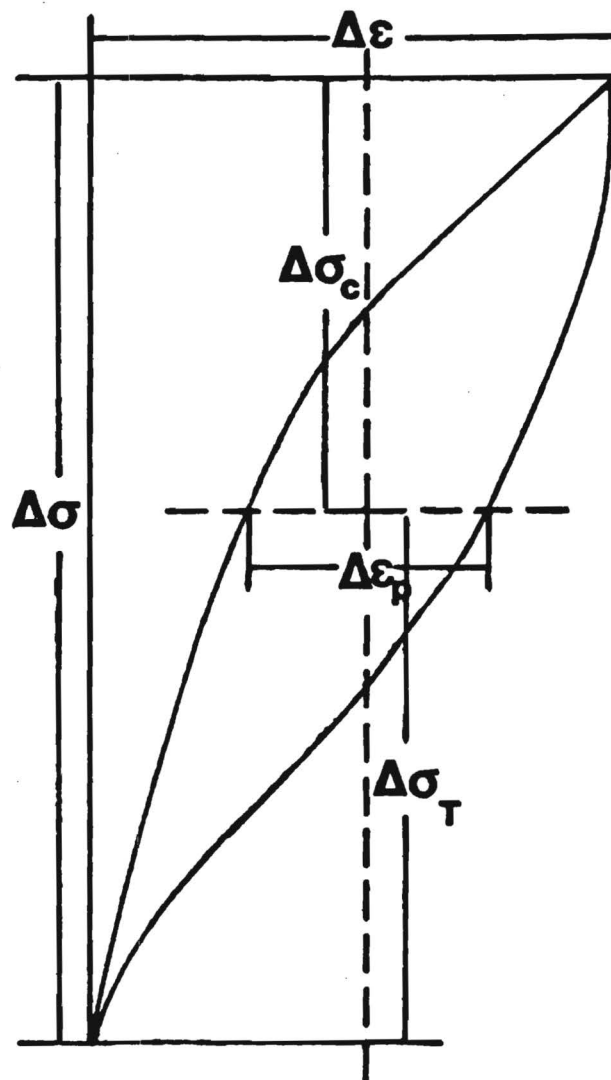


Figure 10. Shows a hysteresis loop as it is measured for plastic strain and peak tensile and compressive stresses.

excursion greater than some small increment. In addition to the loop parameters mentioned above, the slopes of the individual stress-strain characteristics provide data which are useful for evaluating the work-hardening, or softening, occurring in the bond regions during the course of a cycle.

Cyclical response curves for three bond wires mechanically cycled in the normal laboratory environment are shown in Figure 11. The stress amplitudes taken from hysteresis curves during the fatigue life of a bond are plotted as a function of the cycle number. The plastic strain amplitude reflects cyclical "strengthening" or "weakening" effects which occur in the heel region of the bond as cycling progresses. Figures 12 and 13 show the manner in which the measured peak stresses vary as a function of the cycle number over the fatigue lives in air of two supposedly identical aluminum-aluminum ultrasonically bonded wires. In each figure, the upper curves are the maximum stress on the hysteresis loop in the tension (pulling) mode where the lower curves are for the compression mode (actually, a negative force). The mechanisms responsible for this behavior are discussed in greater detail later, but are determined by microstructural modifications induced in the bonded metals by the mechanical cycling.

Cyclical response curves taken for a set of similar aluminum wire bonds cycled at the same rate and wire loop displacement in an environment very close to 100% relative humidity are shown in Figure 14. The bonds cycled in high humidity have generally

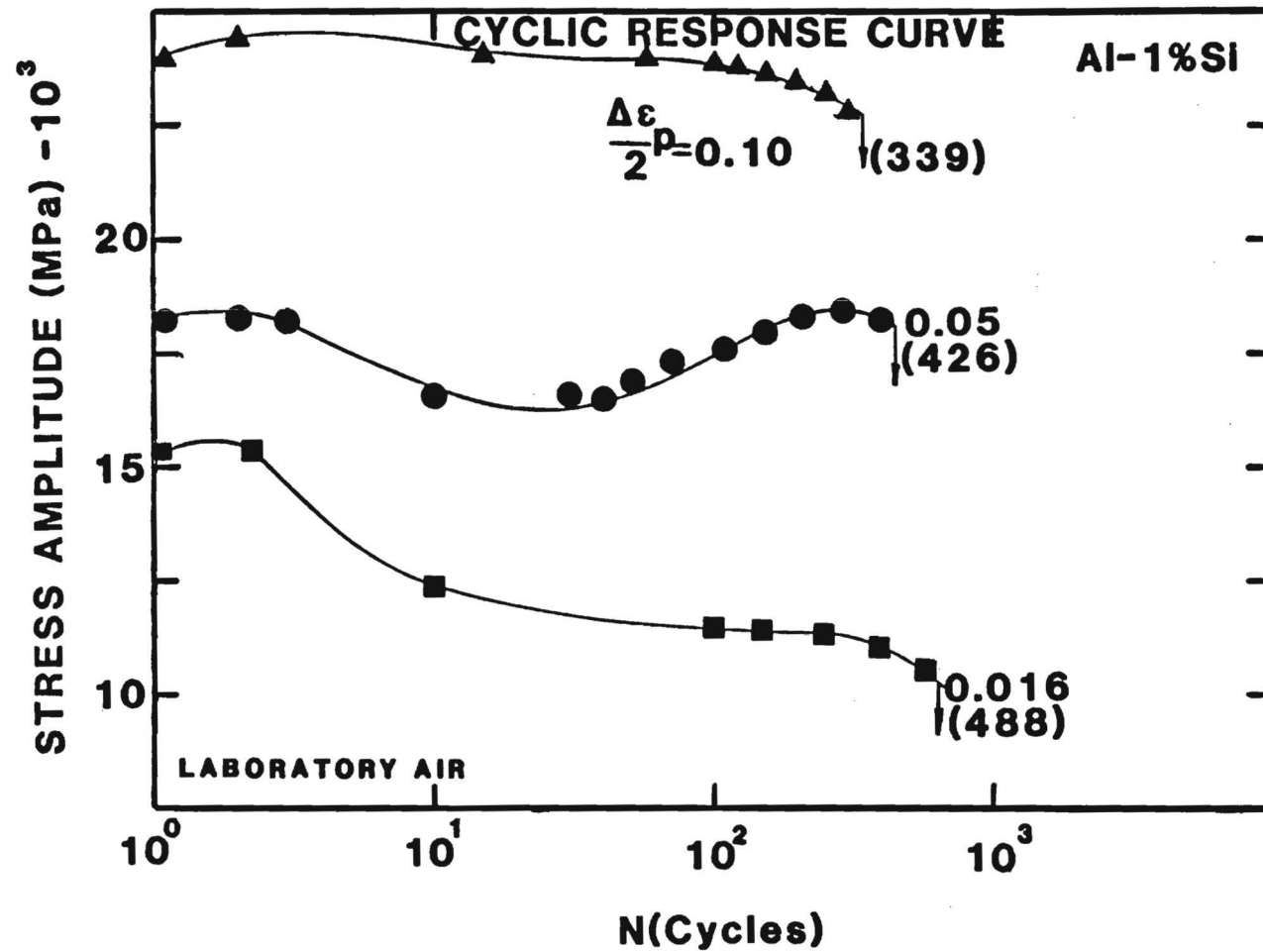


Figure 11. Cyclic response curve for the Al-1%Si bond wire fatigued in laboratory air at different plastic strain amplitudes. Number in parenthesis denotes cycles to failure ( $N_f$ ).

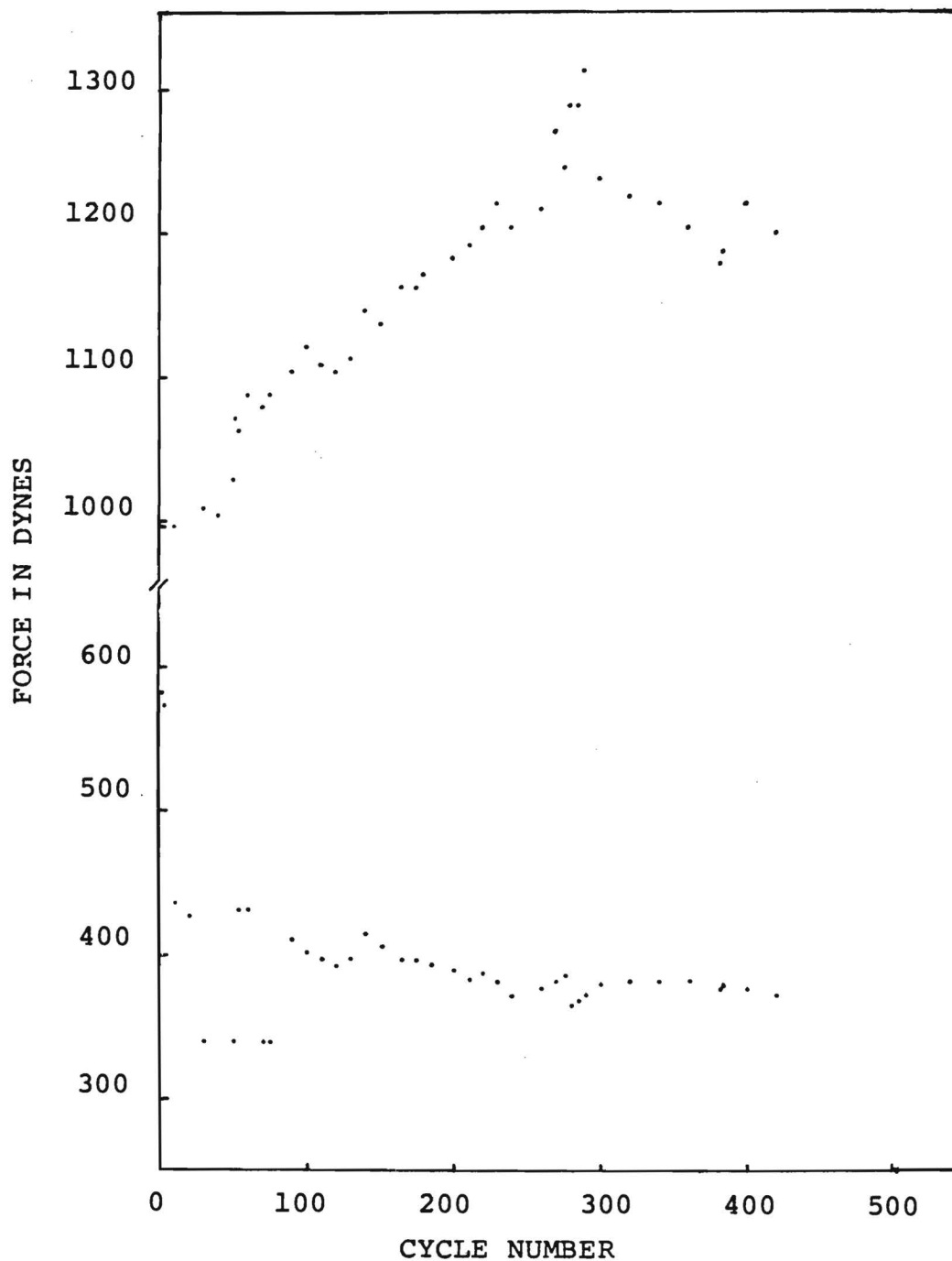


Figure 12. Peak stresses measured as a function of the cycle number of an Al-Al wire bond specimen fatigued in air. The upper curve is for tension (pulling) and the lower curve compression. The bond is found to cyclically work-harden in the tension mode for the first 300 cycles, followed by gradual work softening to failure at about 400 cycles. The compression mode shows only work softening.

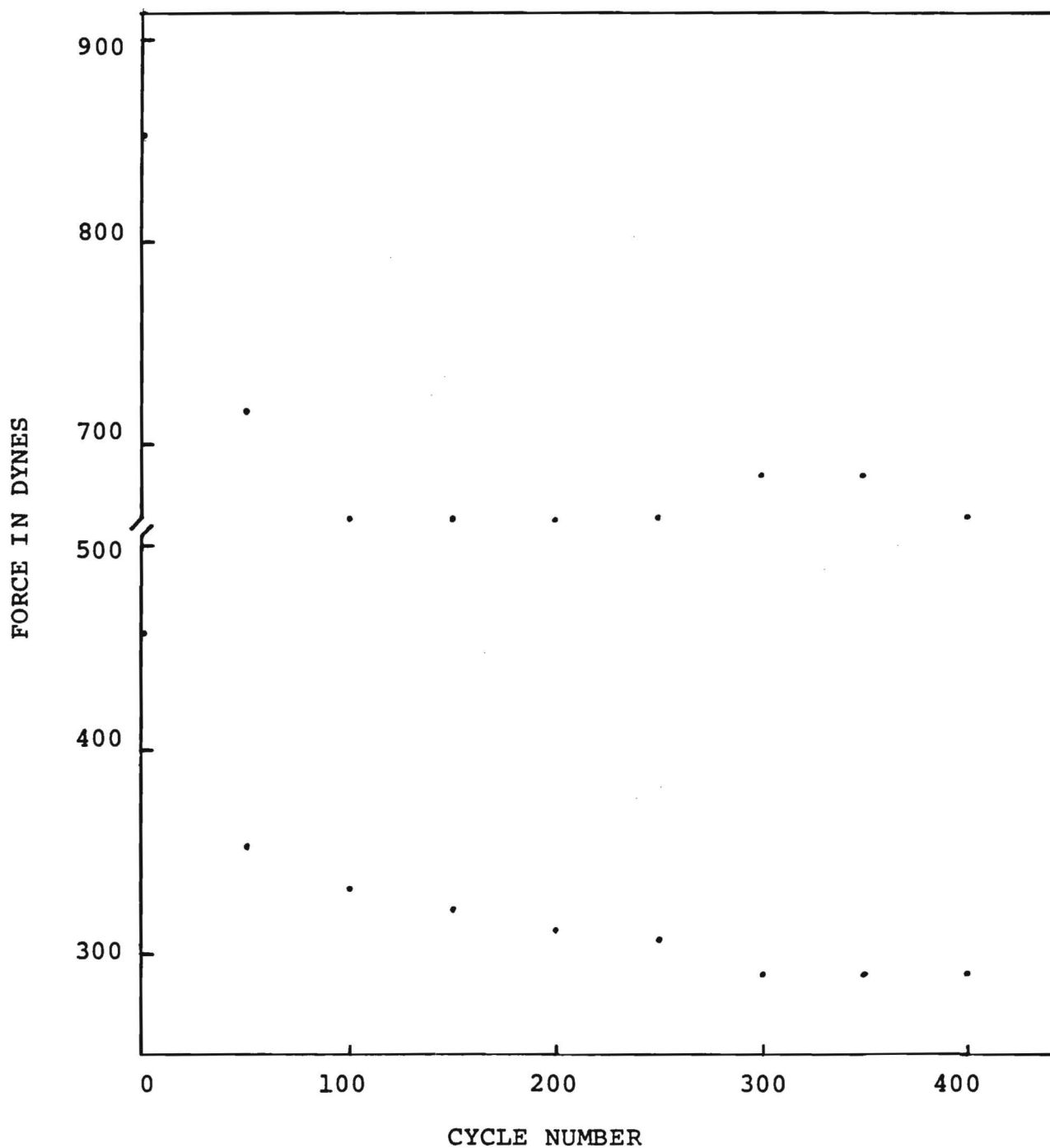


Figure 13. Peak stresses measured as a function of the cycle number of an Al-Al wire bond specimen fatigued in air. The upper curve is from the tension (pulling) mode and the lower curve is from the compression mode. The measurements show significant cyclical work softening occurring during the first 100 cycles in both the tension and compression modes. The bond subsequently hardens in tension until just prior to fracture.

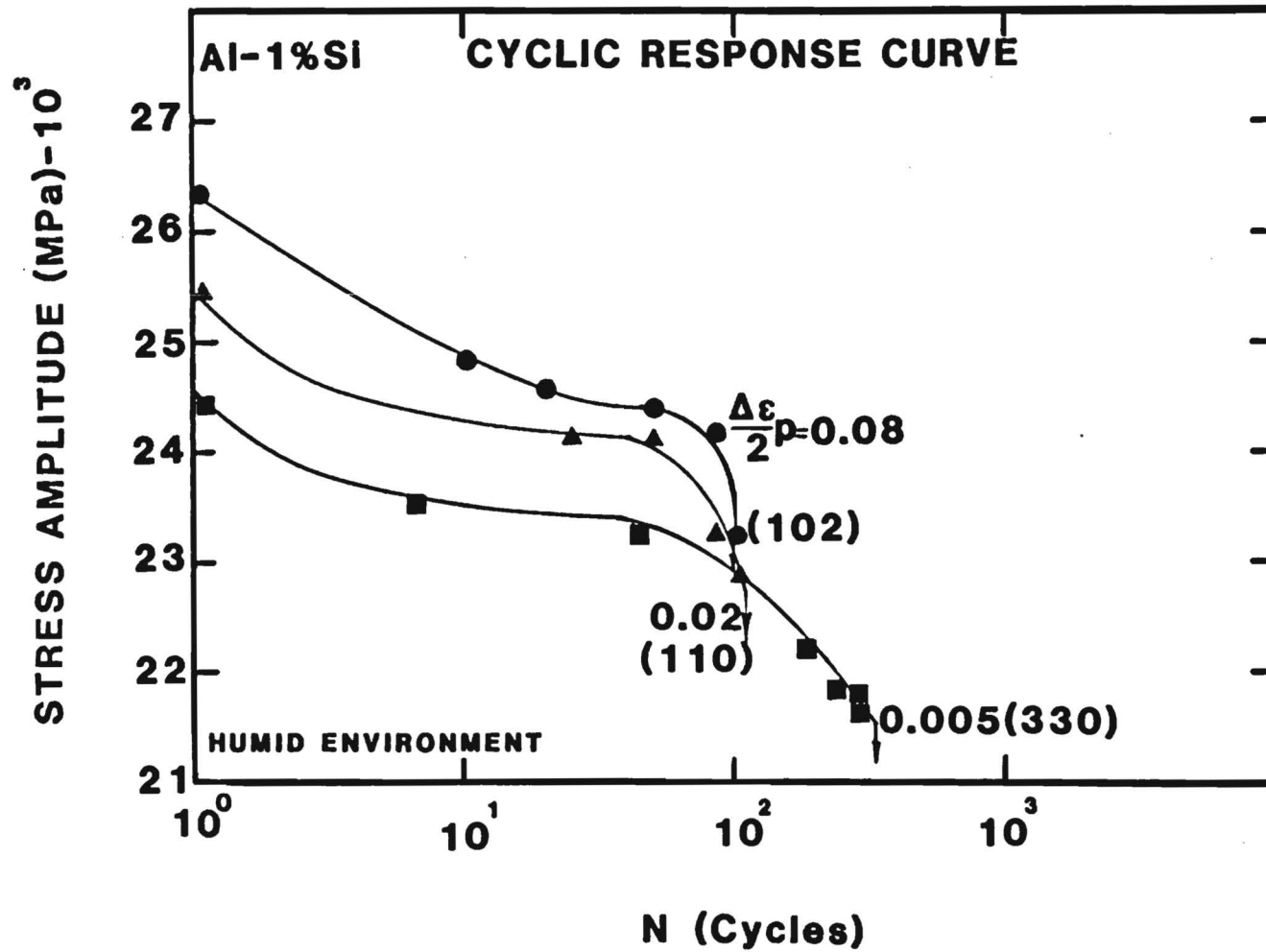


Figure 14. Cyclic response curve for the Al-1%Si bond wire showing progressive softening to failure at all plastic strain amplitudes in the humid environment. Number in parenthesis denotes cycles to failure ( $N_f$ ).

failed earlier than those under otherwise identical circumstances but in ambient room air. It should be pointed out here that a lot of scatter is found in the fatigue data for different bonds such that some wire bonds cycled in a high humidity have had lives somewhat longer (over 400 cycles) than those indicated above. However, the comparative data for the two sets of wire bonds shown above are representative of the overall trends found for for these environments at various strain levels. The more rapid rate of cyclical softening is characteristic of the aluminum bonds fatigued in high humidity. The mechanical hysteresis loop areas for bonds cycled in humid environments are generally smaller than those for bonds cycled in dry air.

A third set of cyclical response curves is shown in Figure 15 for wires fatigued under mechanical conditions identical to those previously shown except that d.c. currents at the indicated levels were conducted through the bonds as they were mechanically cycled. Cyclical softening appears consistently with the cycle number to failure. Once again, there is scatter in the performance of bonds with current. Bonds cycled at higher current levels tend towards more rapid cyclical degradation, as anticipated. However, significant variations in behavior are noted. One bond survived 1300 cycles at 50 ma. Figures 16-18 provide comparisons for peak stresses taken for the low-cycle hysteresis data for three aluminum-aluminum wire bond specimens fatigued, respectively, with bond currents of 20 ma, 300 ma and 350 ma. The particular bond cycled with a current of 200 ma



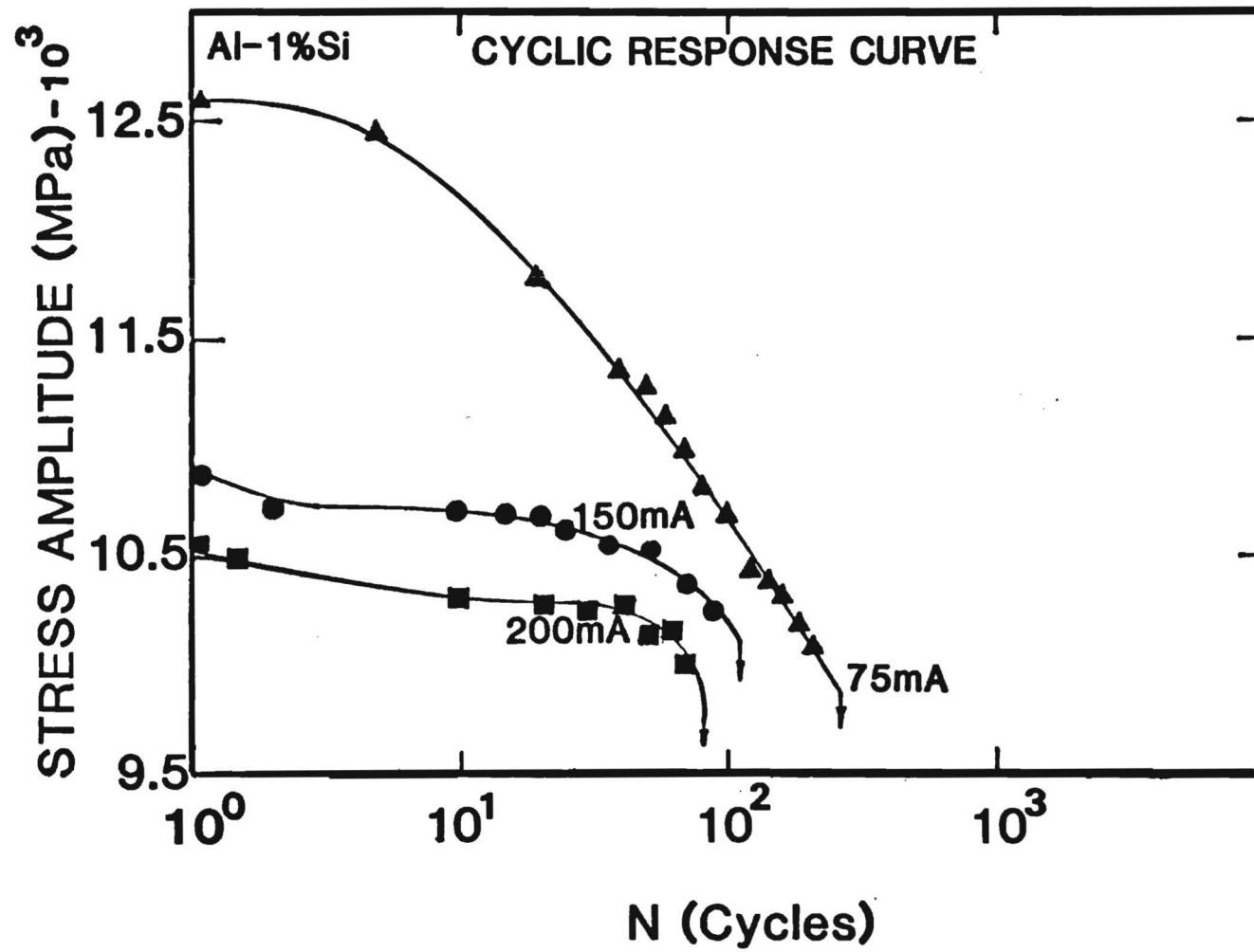


Figure 15. Cyclic response curve for the Al-1%Si bond wire showing cyclic softening to failure for the different values of electric current.

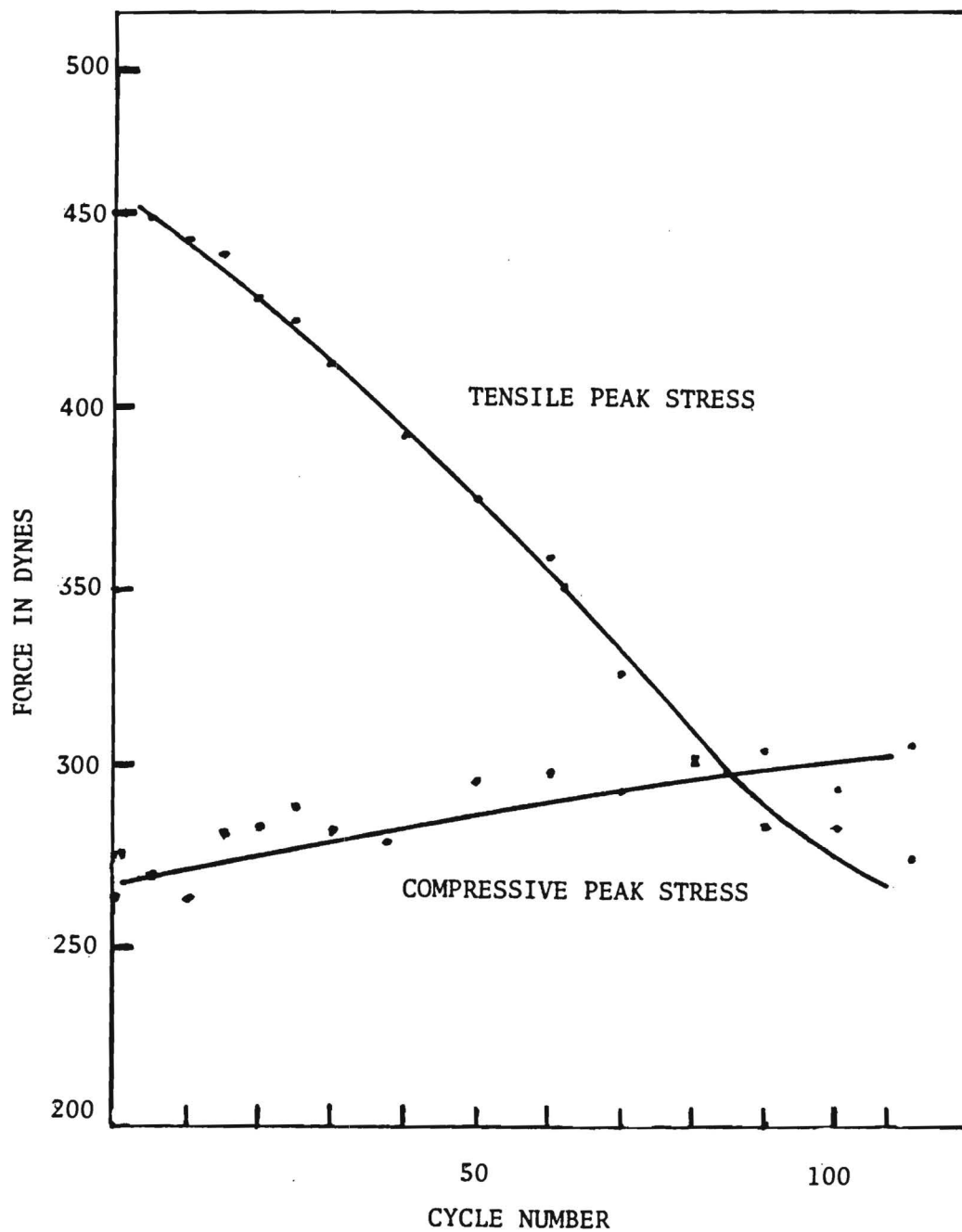


Figure 16. Peak cyclical force values measured versus cycle number for an aluminum-aluminum bond conducting 200mA current. The tensile peak rapidly softens to early failure.

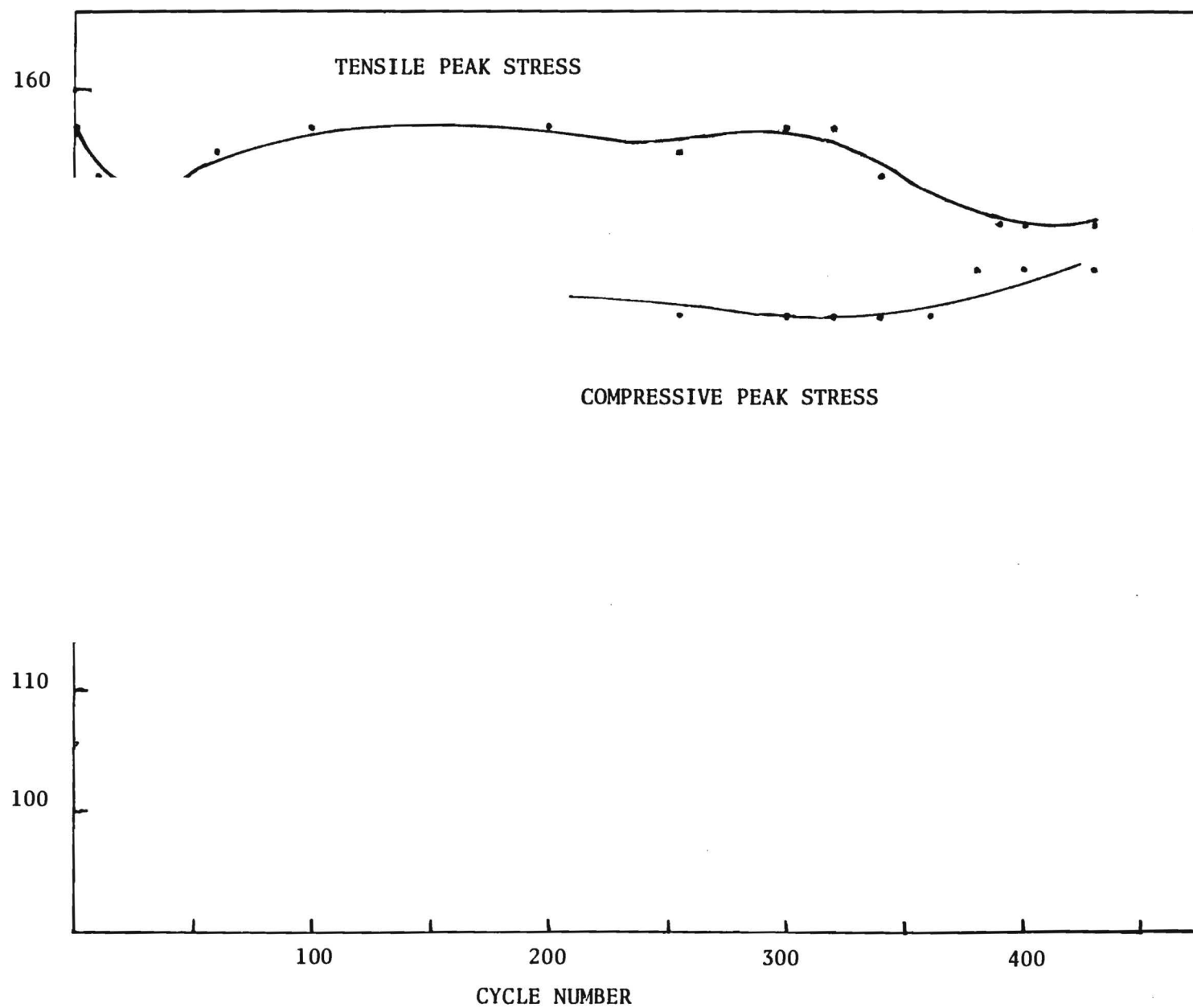


Figure 17. Plots of tensile and compressive peak stresses as a function of cycle number for an aluminum bond conducting 300mA current.

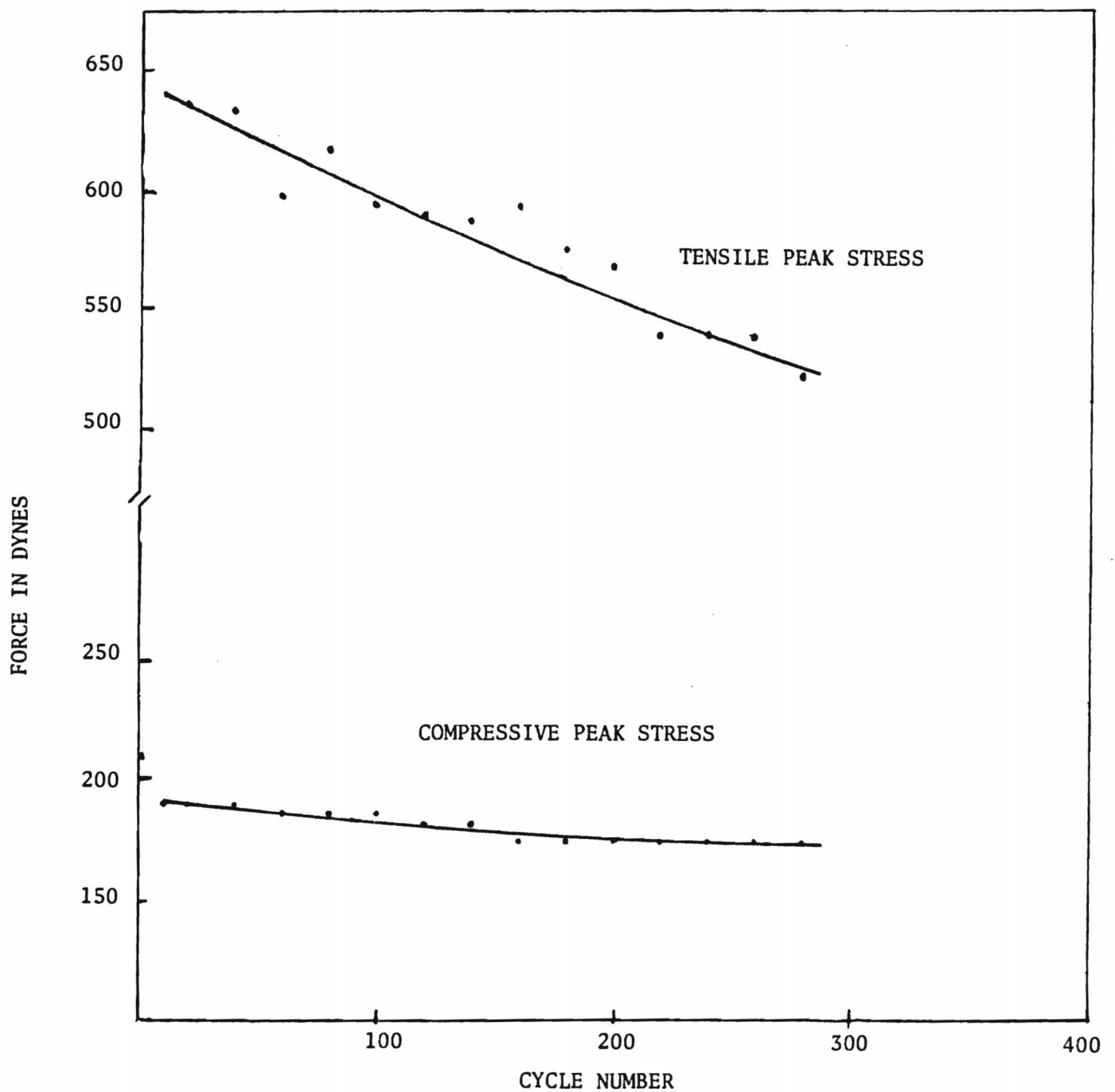


Figure 18. Tensile and compressive peak stresses plotted as a function of cycle number for an aluminum-aluminum bond conducting a 350mA current.

demonstrated rapid tensile work softening from the first cycle on and resulted in early failure. The specimen of Figure 18 cycled with a current of 350 ma uniformly work softened in both compressive and tensile modes with a long fatigue life at this current level. Figure 18 is included because it shows an aluminum-aluminum bond at 300 ma having regions of both work hardening and softening in compression and tension, but the force levels are much smaller than normal. However, the bond remained "good" for over 400 cycles. A plot of the hysteresis loop energy per cycle is shown in Figure 19 as a function of the cycle number for an aluminum wedge bond fatigued with 50 ma. The loop energy is seen to decrease during the early phases of the bond life, but then increase to an elevated value just prior to the final sharp decrease typical of crack propagation to failure. Hysteresis loop energies measured for three specimens cycled at currents of 300 ma and greater are shown in Figure 20. The small differences seen between successive loops taken every 20-30 cycles have been noted repeatedly in wire bond data and appear to be in response to microstructural modifications proceeding in the bond regions. Corresponding peak stresses and hysteresis energies for a thermosonically ball bonded gold (to aluminum) wire are shown for comparison in Figures 21 and 22. The gold wire was not conducting a current.

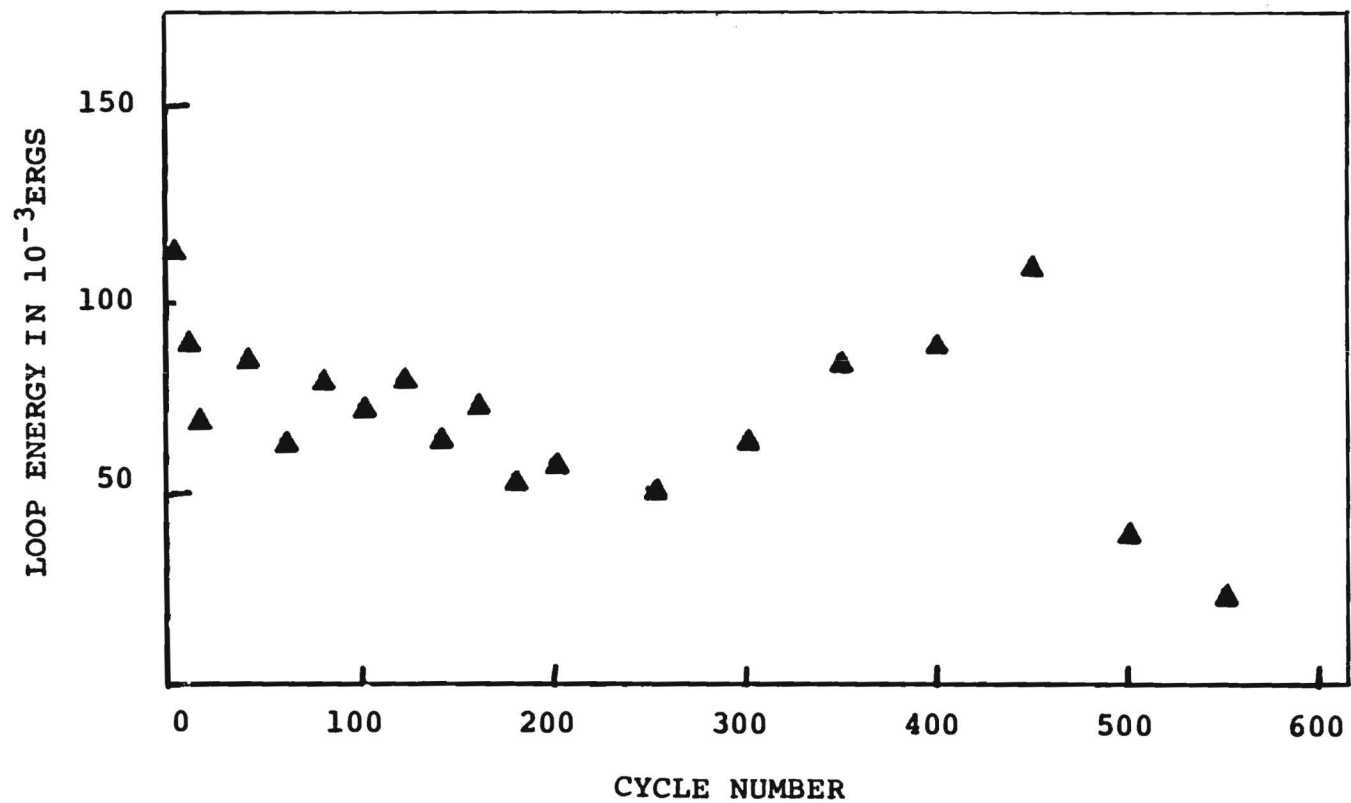


Figure 19. Hysteresis loop energy for an aluminum-aluminum wire bond cycled with 50mA d.c. current.

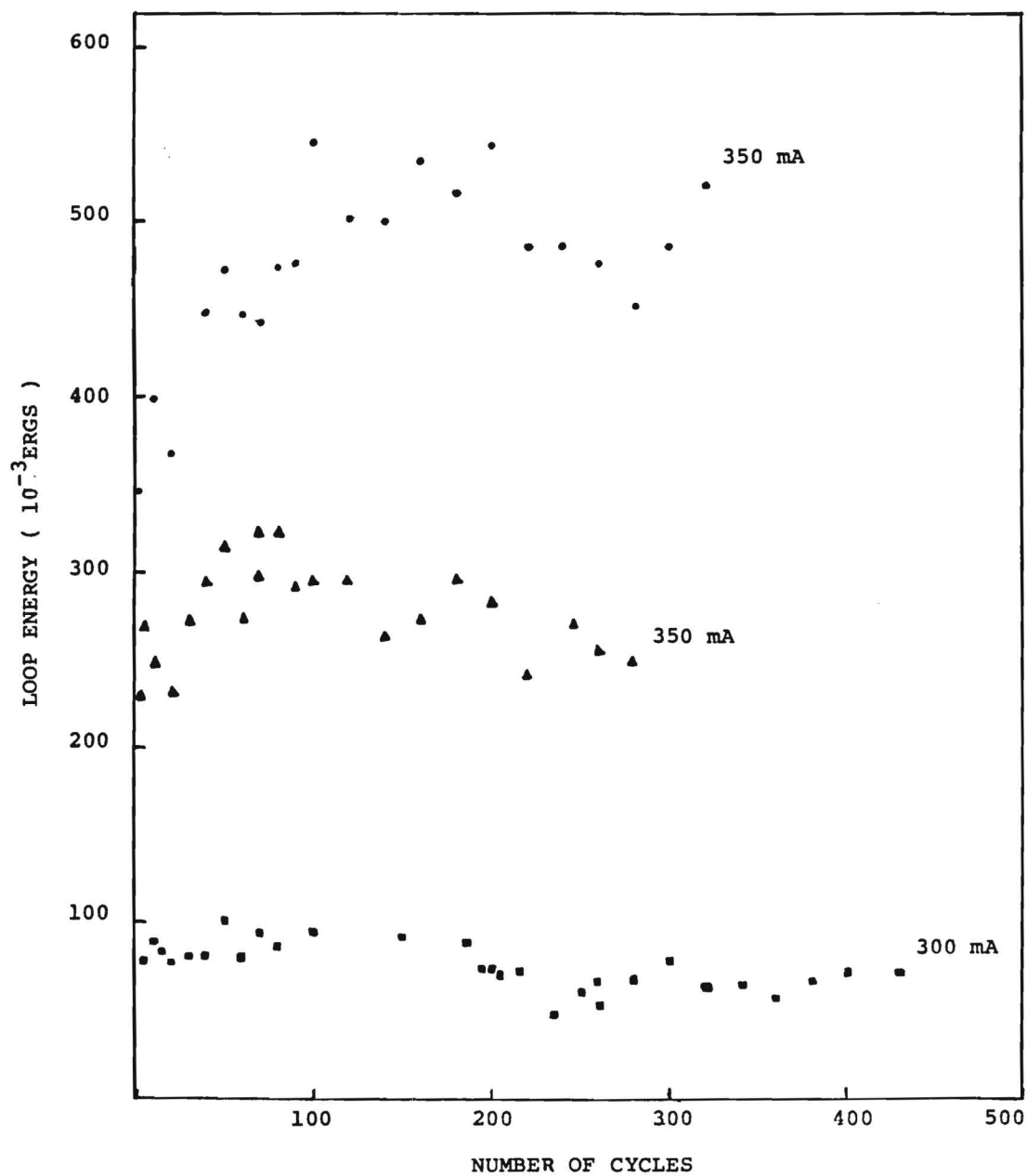


Figure 20. Low cycle fatigue hysteresis loop energies measured as a function of cycle number for three aluminum-aluminum wire bonds mechanically cycled while conducting currents at the indicated level.

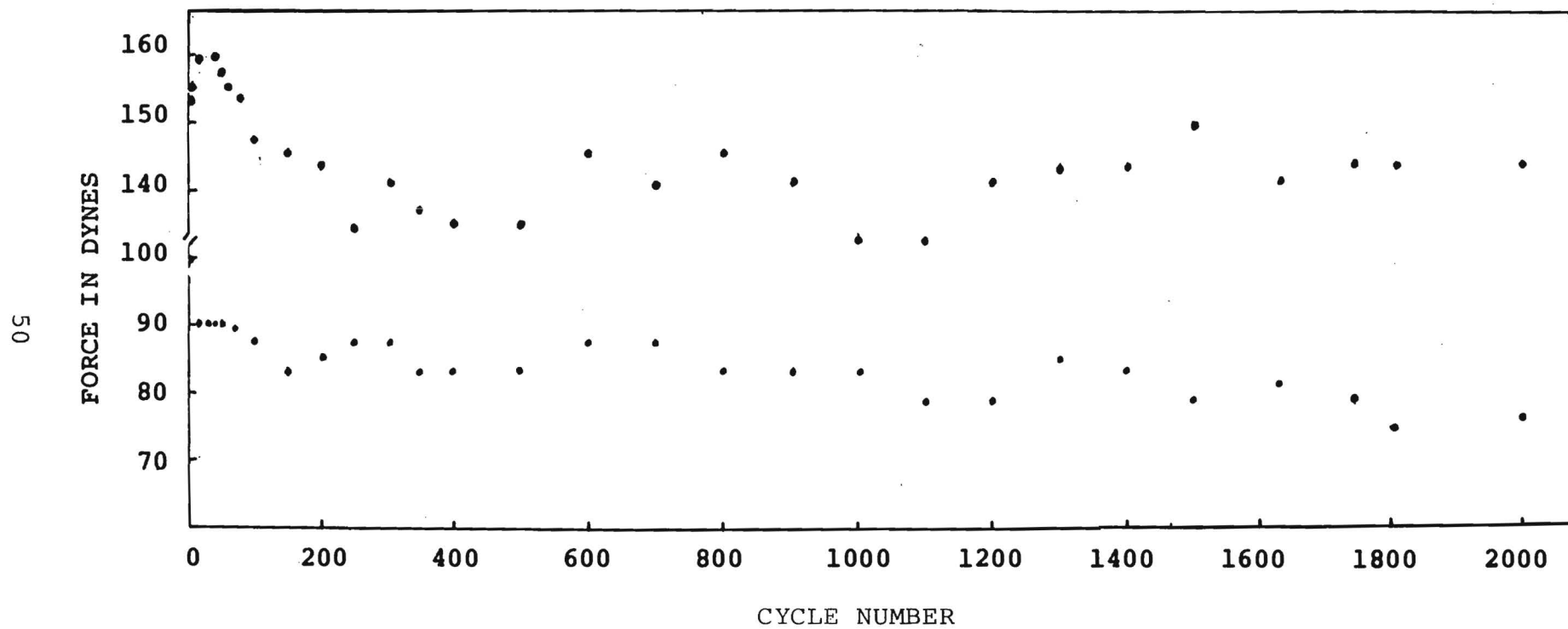


Figure 21. Peak force values measured for a gold ball bond (to aluminum.)



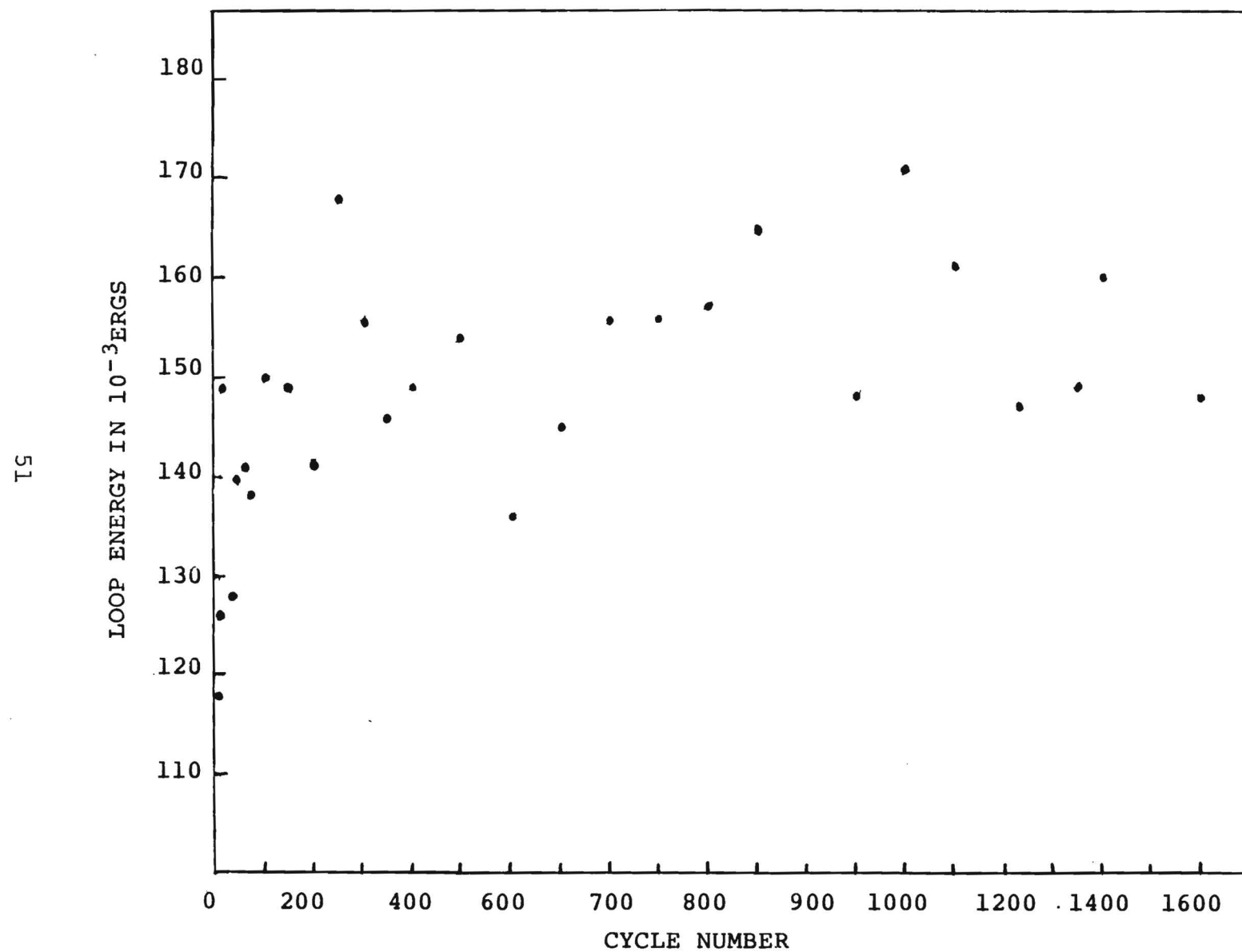


Figure 22. Hysteresis loop energies measured for a gold ball bond that was mechanically cycled in air.

The SEM micrographs in Figure 23 show the fracture surface of an aluminum wire bond mechanically cycled to failure while conducting a small current. The fracture occurred at the thin heel region of the bond. The 10 ma. current in the bond during cycling probably did not appreciably affect the fatigue degradation. The current was used here to monitor the changes in electrical resistance of the bond via a four point probe arrangement as the cyclical degradation progressed. Intergranular crack propagation is evident in the fracture surfaces. In addition, there are regions indicating a viscous flow behavior in the aluminum. The crack producing the failure appears to have been initiated at the surface with the crack propagated intergranular. In the latter stages, the central region of the wire undergoes a highly ductile type of fracture, having a viscous flow appearance. The initial surface oxides appear as debris at the wire-pad bond interface.

Figure 24 shows the heel of an aluminum bond following 1350 cycles, but prior to complete fracture. The upper left micrograph shows the surface configuration of the bond prior to the specimen being installed on the micromechanics testing machine. By carefully monitoring the mechanical hysteresis loops, the specimen was removed from the testing apparatus in a late stage of its fatigue life, but before failure and placed in an SEM for structural studies. The remaining two micrographs in Figure 24 show the arrested growth of a crack from the upper surface of the heel into the central region of the bond wire.

Figure 25 contains micrographs showing fracture surfaces of

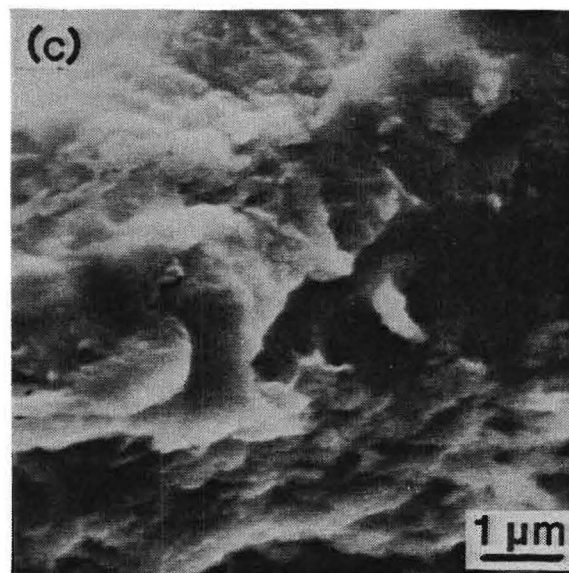
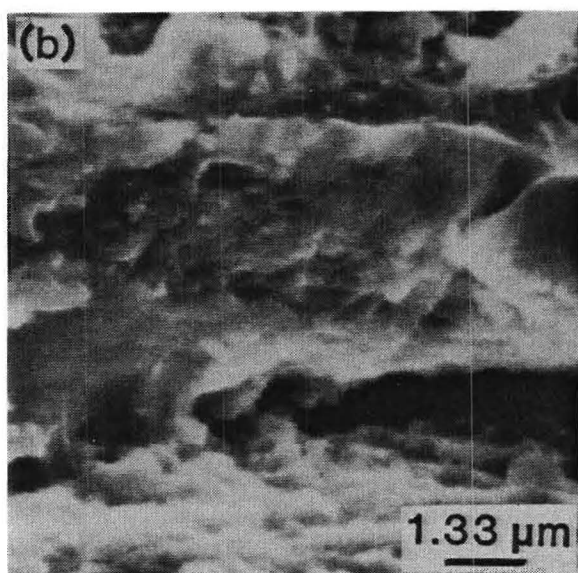
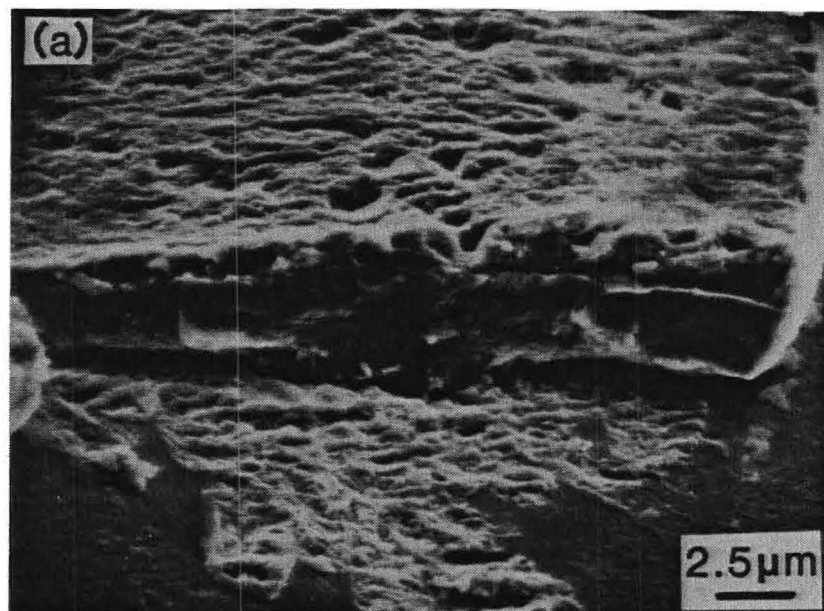


Figure 23. SEM fractographs showing features of the aluminum bonded wire fatigued to failure in laboratory air while carrying 10 mA d.c. current.

- (a) fracture surface at the first bond heel
- (b) high magnification of the bond-pad interface
- (c) features of the mating wire surface

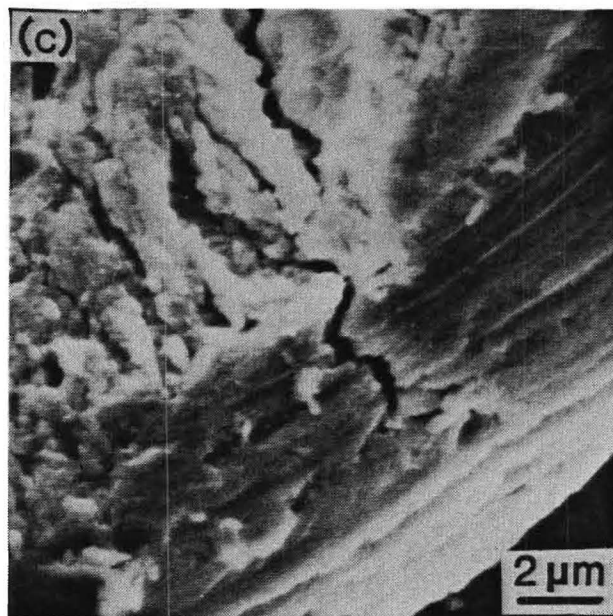
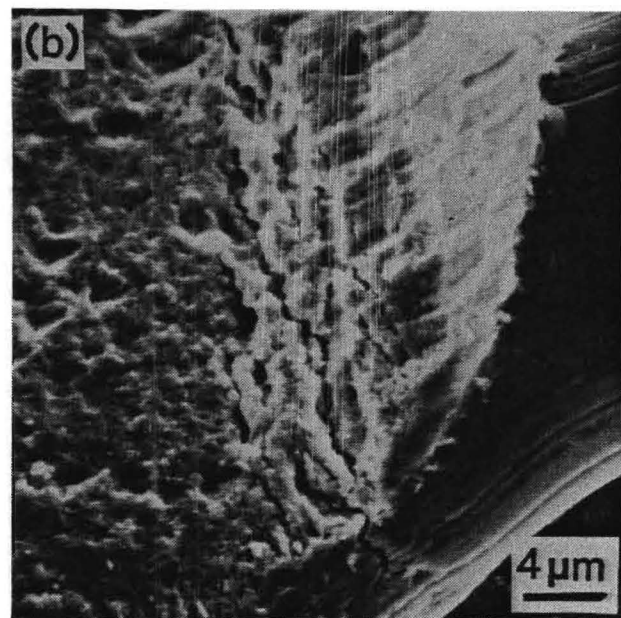
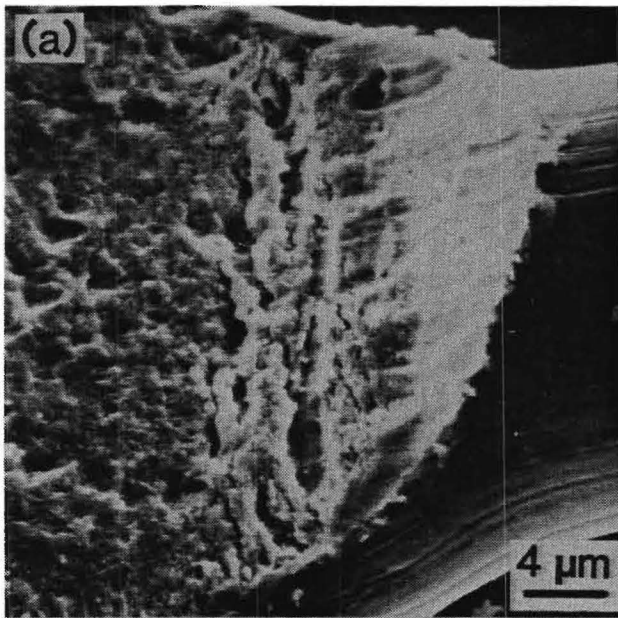


Figure 24. SEM fractographs showing features of the aluminum bonded wire fatigued in laboratory air environment while carrying 50 mA of d.c. current  
 (a) high magnification of first bond prior to the test  
 (b) first bond after 1350 cycles  
 (c) high magnification of the fatigue crack tip

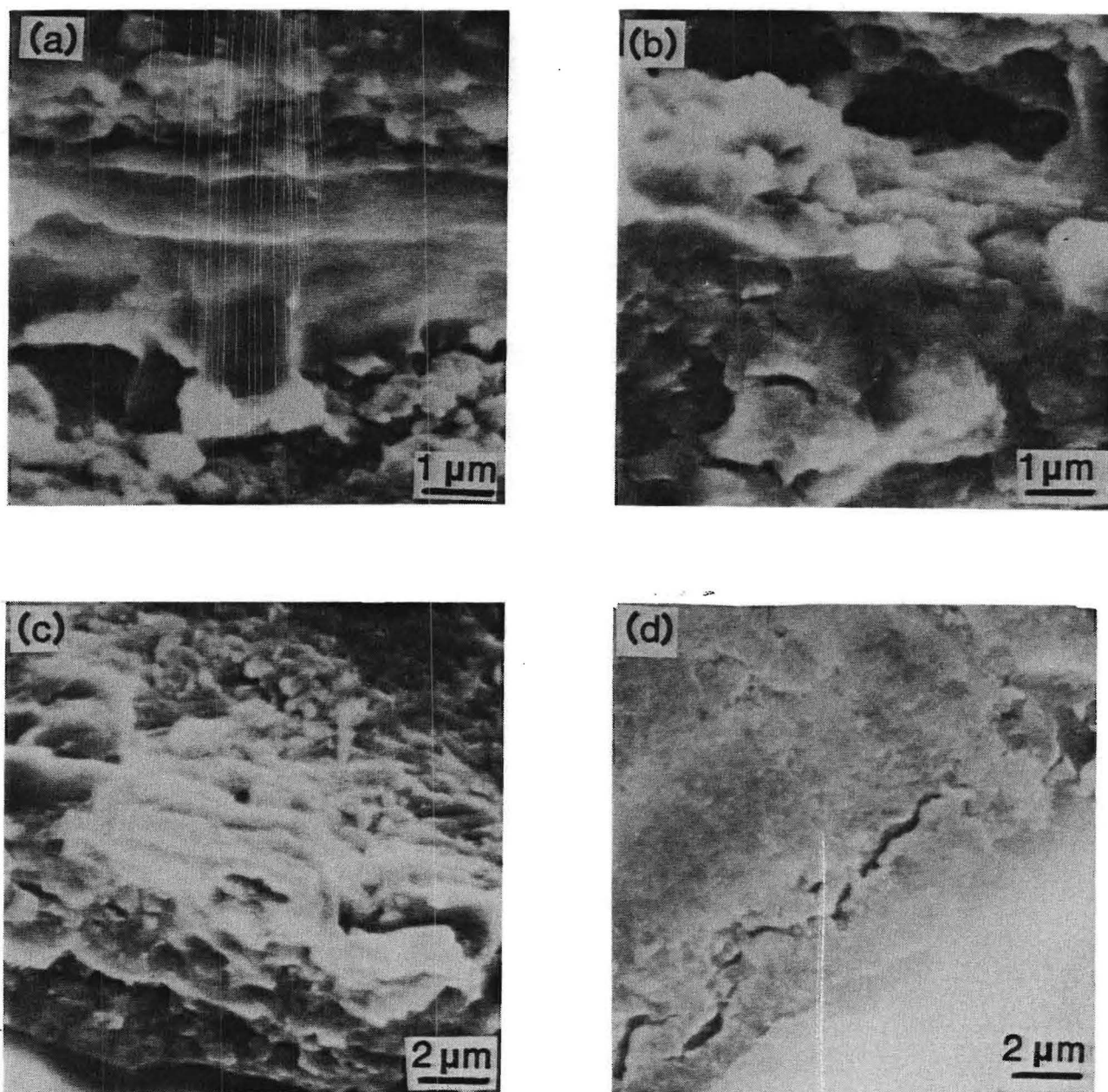


Figure 25. SEM fractographs showing features of the aluminum bonded wire fatigued in laboratory air environment while carrying 75 mA of d.c. current.

- (a) the bond-pad interface at the first bond heel,  $N_f = 403$
- (b) the bond-pad interface at the first bond heel,  $N_f = 230$
- (c) features of the wire fracture surface of (a)
- (d) features of the wire fracture surface of (b)



two wire bonds mechanically cycled while conducting a current of 75 ma. These two specimens, prepared and measured under identical conditions, behaved somewhat differently under cyclical deformation. The number of cycles to failure was 403 cycles and 230 cycles, respectively, for the two specimens. Examination of the fracture surfaces indicated that the specimen failing earlier experienced greater intergranular crack propagation in the initial stages of mechanical cycling. The micrographs indicate that for the longer lived specimen a greater degree of viscous flow took place within the aluminum bond metal. Figure 26 shows the surface geometry of an aluminum bond prior to mechanical cycling. The lower SEM micrograph shows the appearance of the second bond of this specimen after experiencing 460 mechanical cycles with a bond current of 100ma.

The observed differences in mechanical behavior here is most likely due to details concerning surface features either introduced during the bonding process or existing on the particular section of bond wire which happened to make up the heel metal. Surface scratches, inclusions or other asperities with dimensions less than a micron can easily account for the observed differences in mechanical fatigue behavior because of the importance of such features in initiating the operating degradation mechanisms. A perfectly smooth bond surface and a bond-pad interface without the surface oxide and impurity debris would result in wire bonds having consistently greater fatigue lives.

The appearance of viscous flow type deformation in the

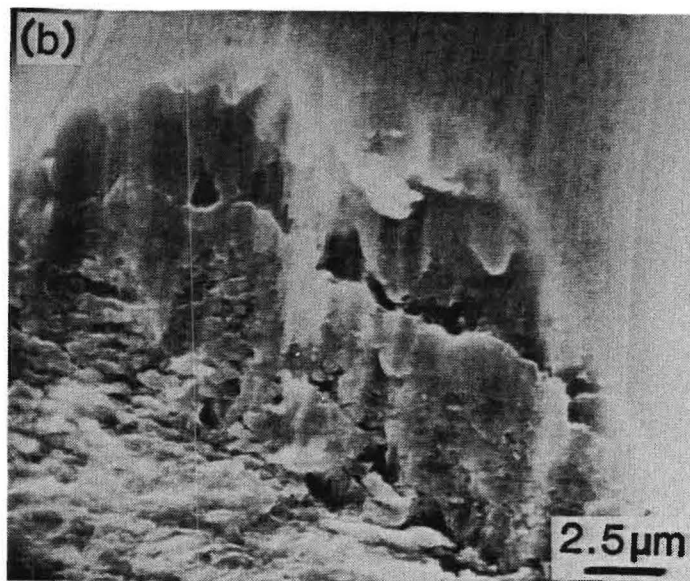
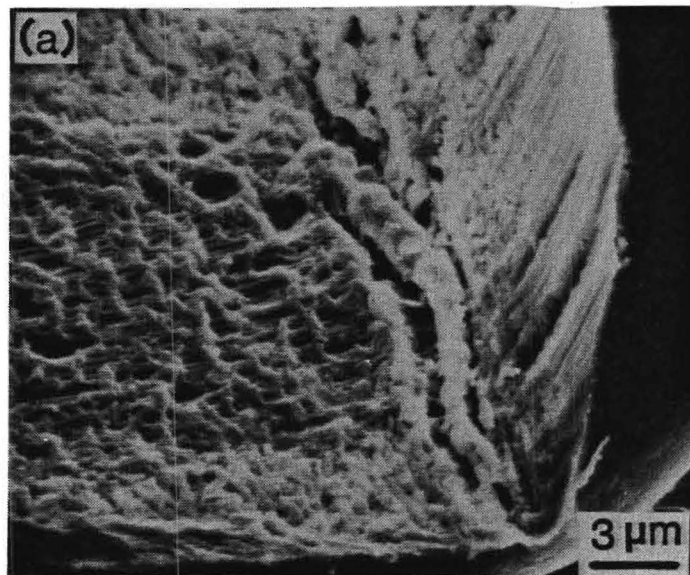


Figure 26. SEM fractographs of the aluminum bonded wire prior to fatigue with 100 mA showing  
(a) effect of bonding process on wire deformation at the first bond  
(b) the second bond after 460 cycles.

crystalline metals of microcircuit bond wire materials is illustrated in the set of SEM micrographs contained in Figure 27. This bond appears to have experienced intergranular crack growth early in the cyclical deformation which turned into significant viscous flow in the last stages of the fracture. The 100 ma bond current constricted in these final stages resulted in a high localized current density which assisted chaotic plastic flow through both a current excited dislocation motion and through the normal thermally activated mechanisms enhancing dislocation motion over pinning features. Figures 28 and 29 contain SEM micrographs of aluminum bonds mechanically cycled at successively higher bond current values, enhancing the area of the bond metal involved with viscous flow mechanisms.

Micrographs of the fracture surfaces of several aluminum wire bonds cycled in an environment maintained very close to a humidity of 100 % are shown in Figures 30 - 33. The fracture surfaces of these specimens appear in the SEM to correspond closely to the characteristics of bonds fatigued in air. In addition, a couple of micrographs of a bad bond produced with the bonding machine parameters off optimum values are shown in Figure 34. Manufacturing mistakes of this magnitude should be discovered in the standard environmental stress screening sequences involving thermal mechanical cycling since these stress levels will probably accelerate the growth mechanisms of the large initial crack to failure.



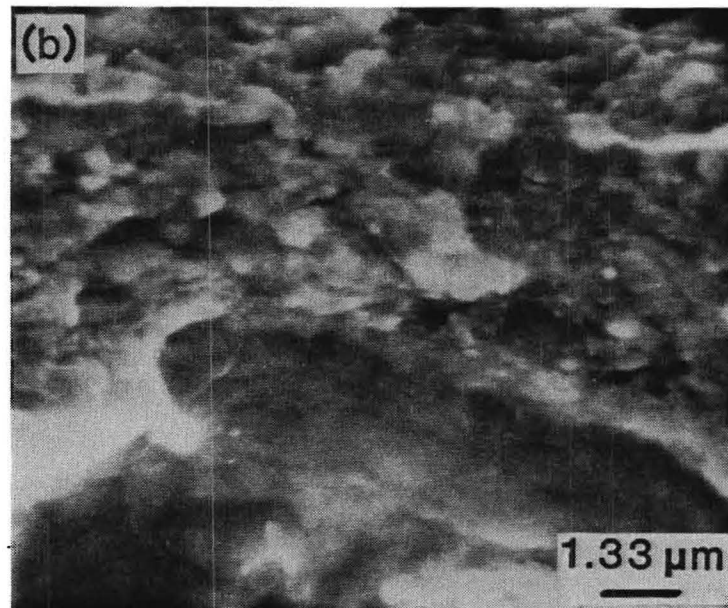
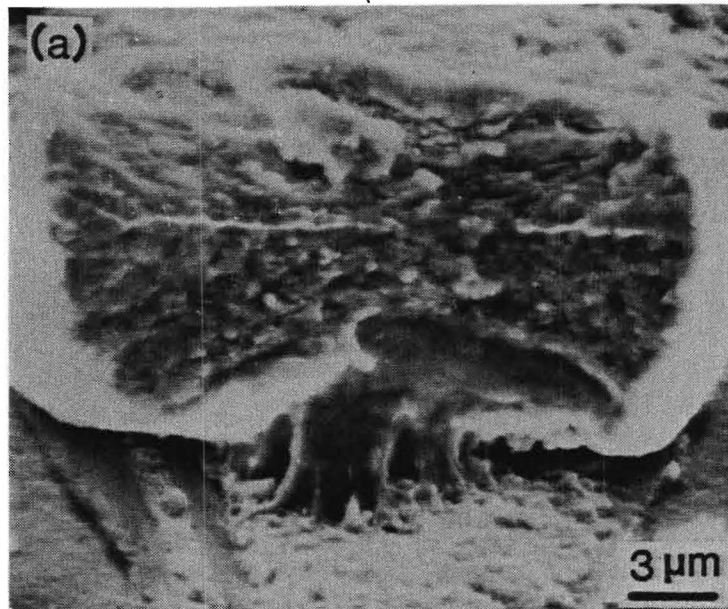


Figure 27. SEM fractographs showing features of the aluminum bonded wire fatigued in laboratory air environment while carrying 100 mA of d.c. current  
 (a) bond heel fracture surface at the pad;  $N_f = 170$  cycles  
 (b) high magnification of the surface features of (a)

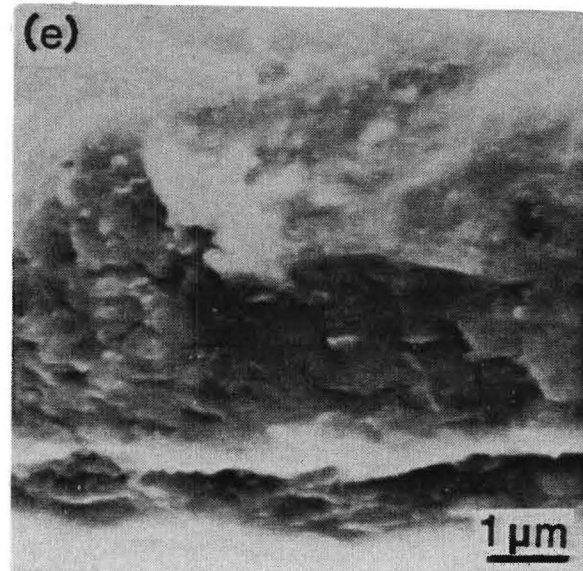
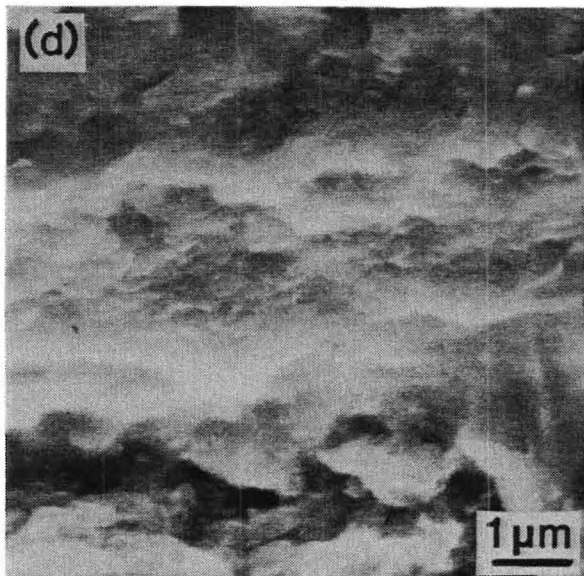
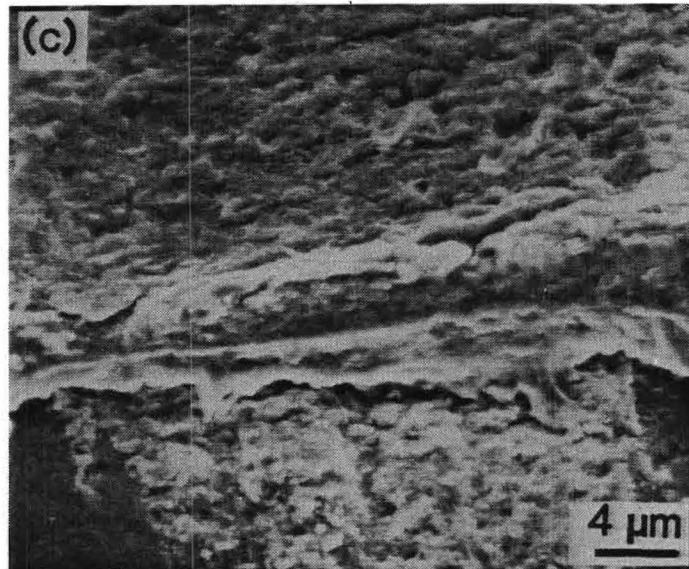


Figure 27.(Cont.)

- (c) bond-heel fracture features at the region of the bond-pad interface
- (d) high magnification of the bond-pad interface of (c)
- (e) high magnification showing features on the mating wire fracture surface.

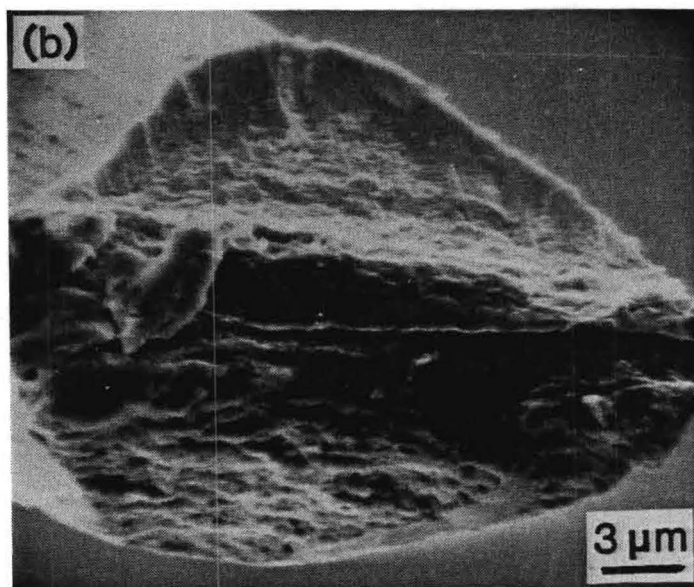
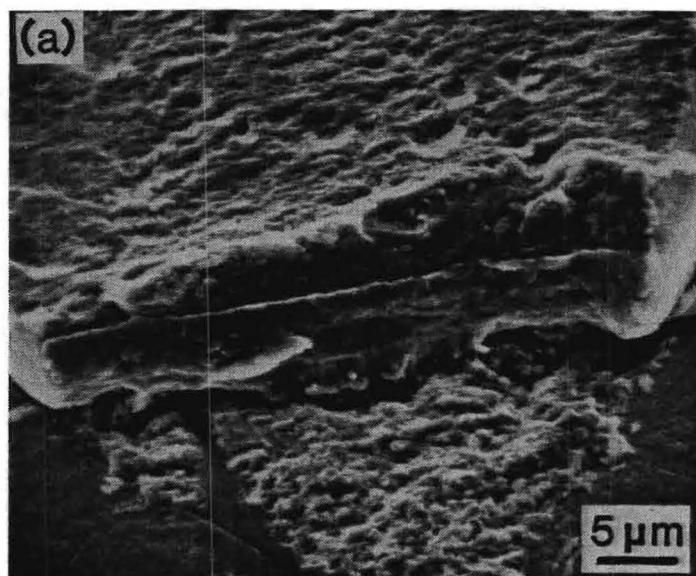


Figure 28. SEM fractographs of the aluminum bonded wire fatigued in laboratory air environment while carrying 150 mA of d.c. current  
(a) first bond heel at pad-bond interface  
(b) mating wire fracture surface

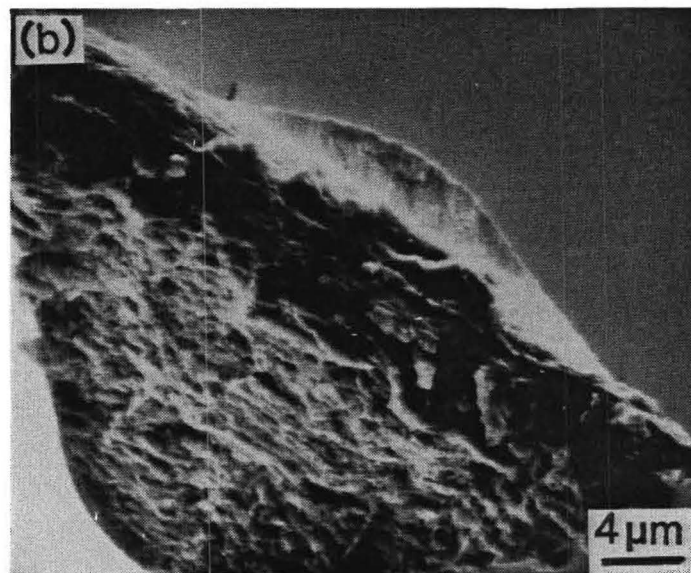
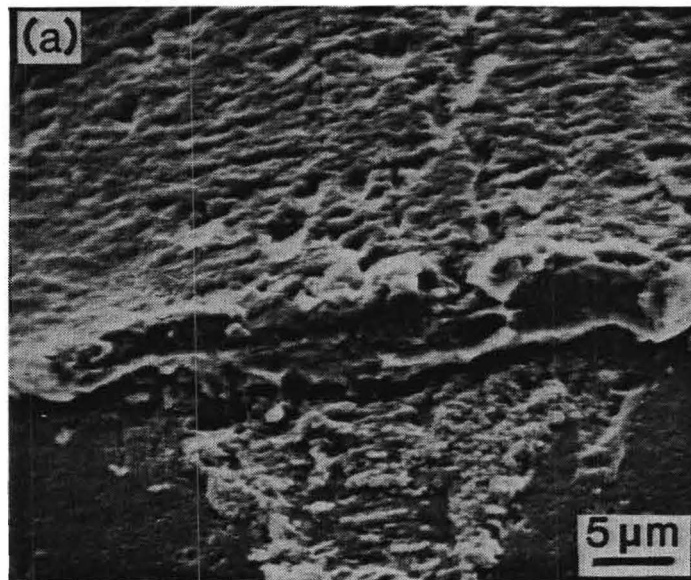


Figure 29. SEM fractographs showing features of the aluminum bonded wire fatigued in laboratory air environment while carrying 200 mA of d.c. current  
(a) first bond-heel fracture surface at the pad  
(b) features of the mating wire surface

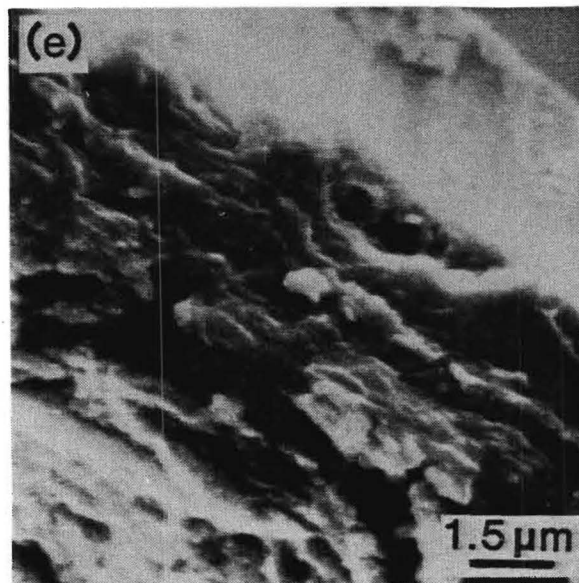
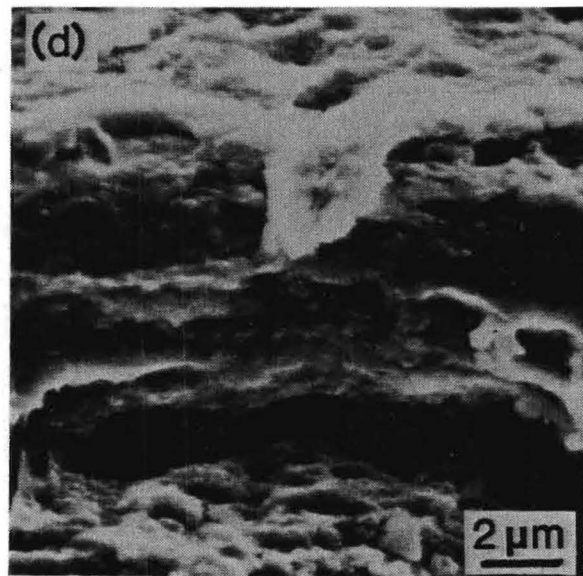
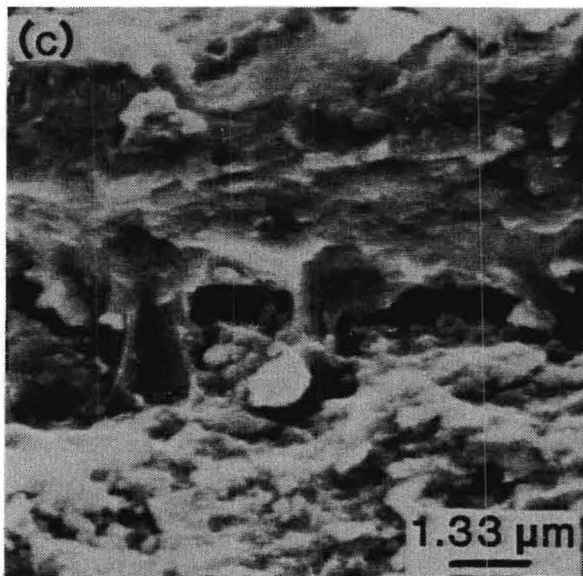


Figure 29 (Cont.)  
(c) high magnification of (a)  
(d) high magnification of bond-pad interface  
(e) high magnification of (b)



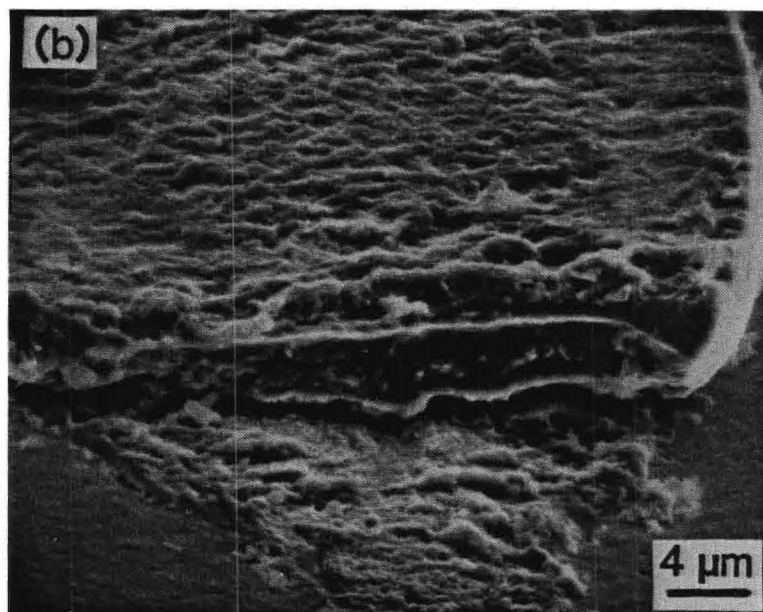
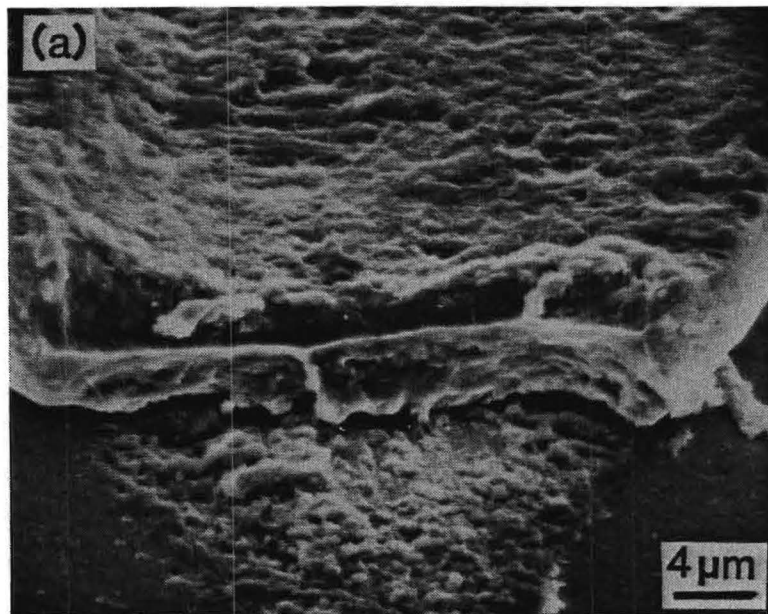


Figure 30. SEM fractographs of an aluminum bonded wire fatigued in humid environment  
(a) typical heel fracture surface at first bond to pad after 327 cycles  
(b) heel fracture surface at first bond after 140 cycles

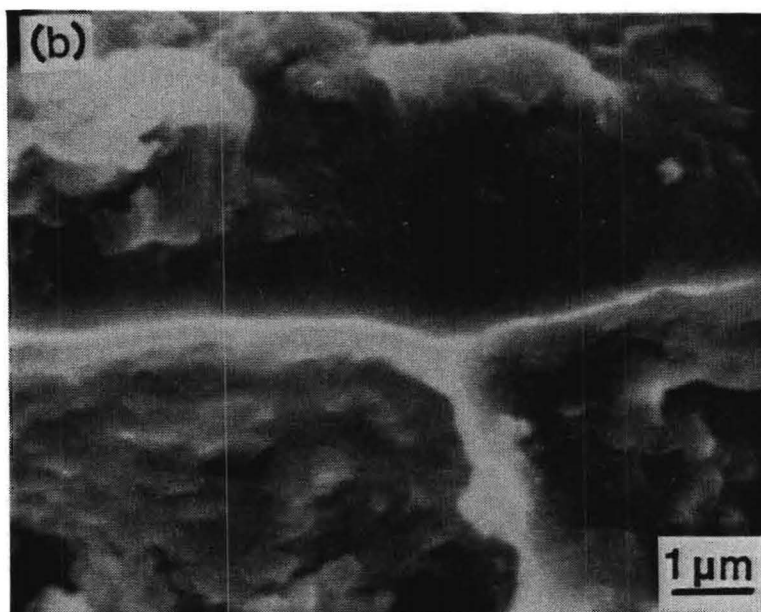
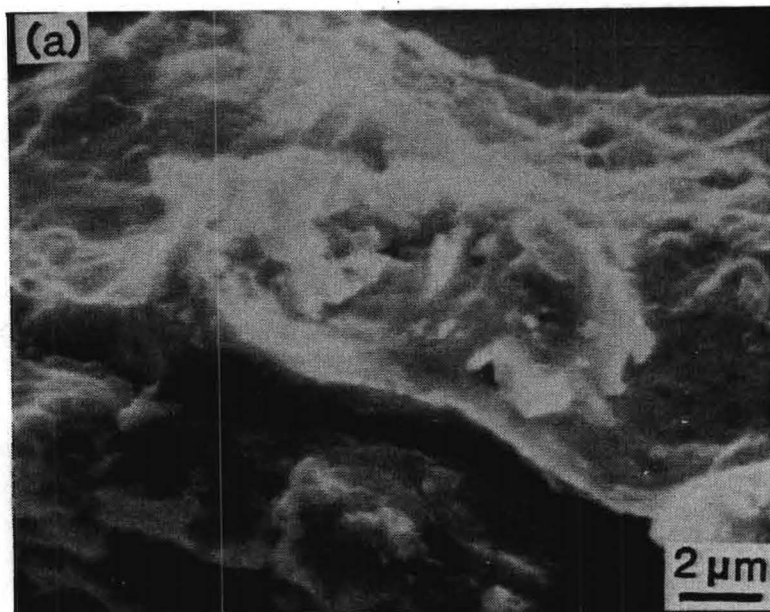


Figure 31. SEM fractographs of an aluminum bonded wire fatigued in humid environment.

- (a) wire fracture surface
- (b) bond-pad interface

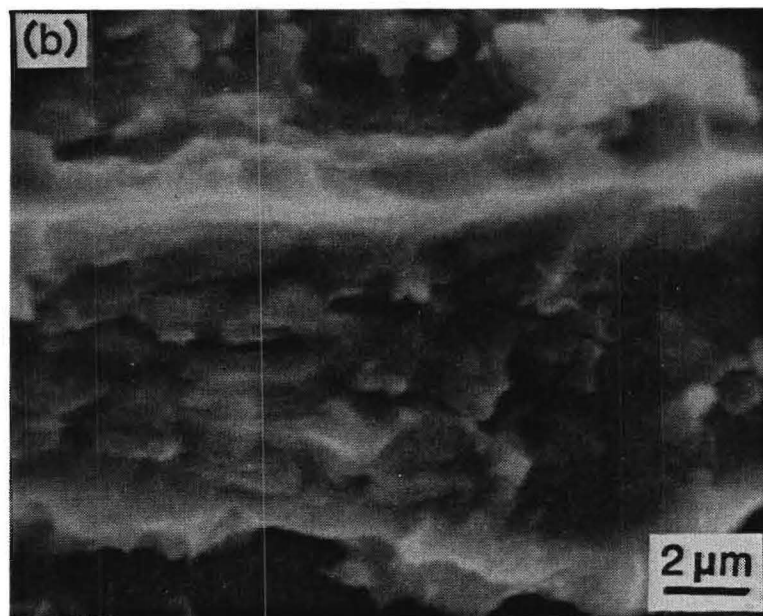
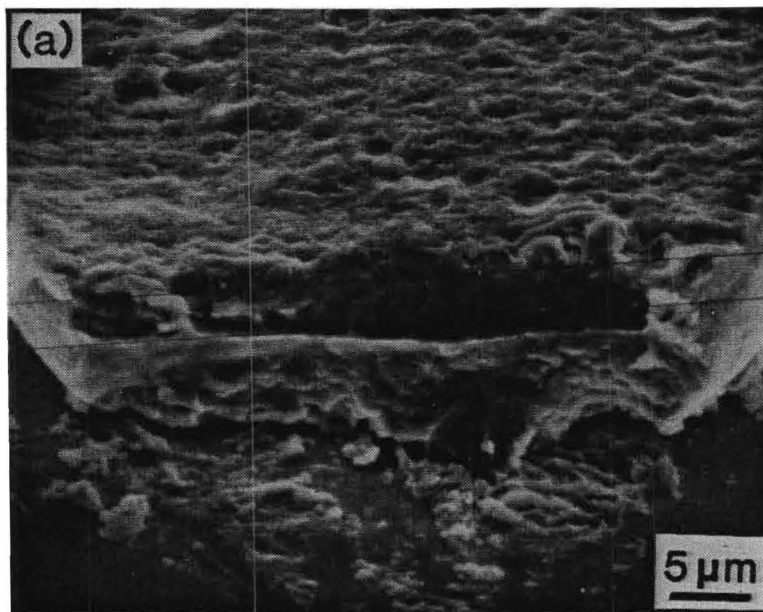


Figure 32. SEM fractographs of an aluminum bonded wire fatigued in humid environment showing features at the bond-pad interface.



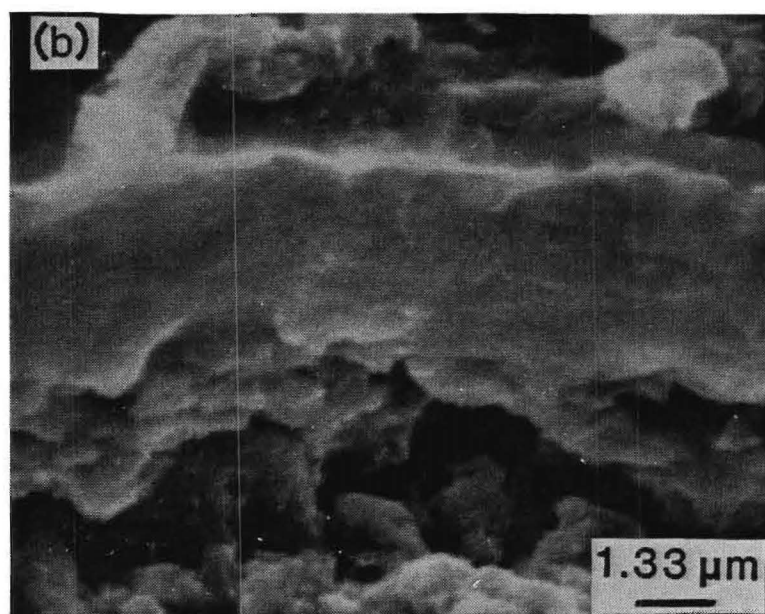
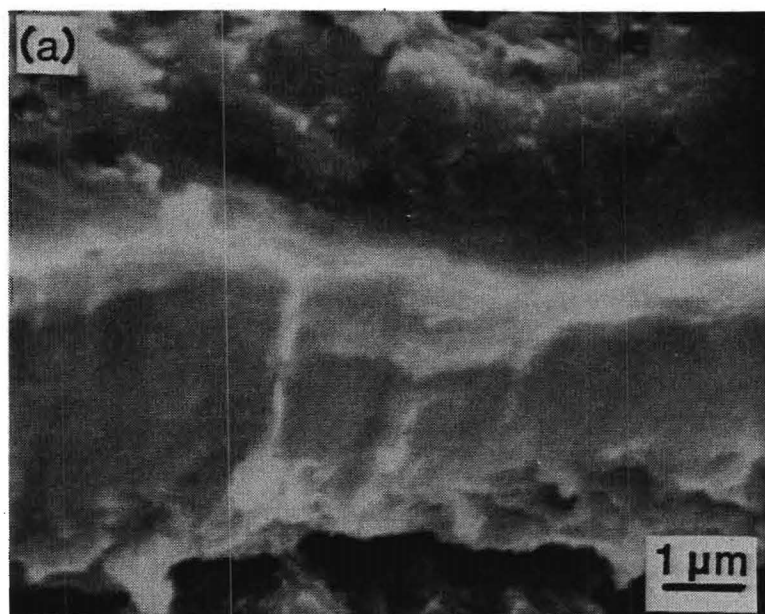


Figure 33. SEM fractographs of aluminum bonded wire fatigued in humid environment showing features at the bond pad interface. Cycles to failure: 227

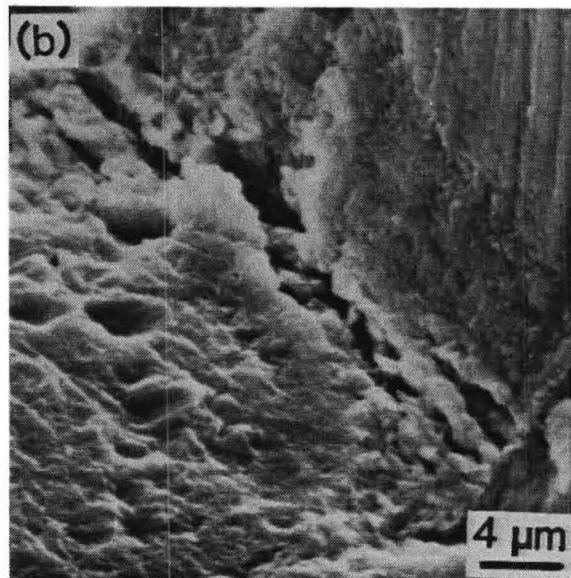
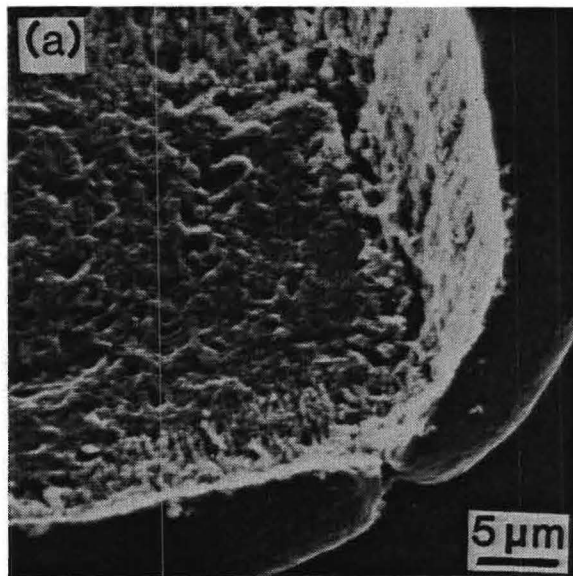


Figure 34. SEM fractographs of the aluminum bonded wire showing deformation induced due to the bonding process.

## MECHANICAL AND METALLURGICAL FACTORS AFFECTING WIRE BOND BEHAVIOR

As part of supporting investigations, various metallurgical and mechanical studies are being conducted on the wire materials and their bonds. These investigations include studies of thermal aging effects on the mechanical behavior of aluminum alloy wires, shear strength measurements on wire bonds, studies of mechanical creep phenomena in the bonds and examinations of electrical current effects on bond interfaces.

The doping and thermal mechanical history of stock aluminum bond wire has a significant effect on both the ability to produce good bonds from the material and the subsequent mechanical performance of the wire bond. The 1% silicon in aluminum provides added tensile strengthening and a saturated silicon content, which some feel inhibits certain diffusion degradation mechanisms at the chip. The metallurgical state of the 1% Si-Al alloy as employed in bond wires is not stable. These wires thus have mechanical properties highly sensitive to time-temperature exposure.

Mechanical property measurements are being conducted on bond wire materials obtained from a number of different suppliers. Tensile stress-strain measurements have been made on specimens of these wires as received and as a function of a series of accelerated aging environments. A number of wire segments were taken from the material provided by each supplier. Portions of

these segment lots were stored in a furnace held successively at several temperatures ranging up to 150 C. Five or six specimens from each supplier were removed from the furnace at selected time periods and then mounted on tabs for tensile measurements. Tensile data taken for wire materials aged at 150 C from three of the suppliers are summarized in Figures 35-37. The curves in Figure 35 show the tensile fracture strength following storage at 150 C as a function of the number of hours in storage. Figures 36 and 37 show how the tensile yield point and the elongation to fracture vary with storage time. The data for wires from the several other suppliers provided curves which were similar to the behavior shown in Figures 35-37, indicating a degree of industry wide consistency in this area.

Temperatures up to 150 C were selected for the aging experiments since this corresponds to the temperature range normally employed for environmental stress screening of microcircuits. Longer storage times at temperature are required at lower temperatures to have corresponding effects on mechanical performance. This behavior is consistent with the extensive age hardening data available from studies of corresponding aluminum structural alloys. The major property changes introduced by aging the 1% Si-Al bond wires at 150 C occur within about 15 hours.

The Al-Si phase diagram shows that silicon is not metallurgical stable as a solid solution with aluminum at the temperatures of concern here. Given time at temperature, the silicon thus precipitates from the solid solution, initially, in

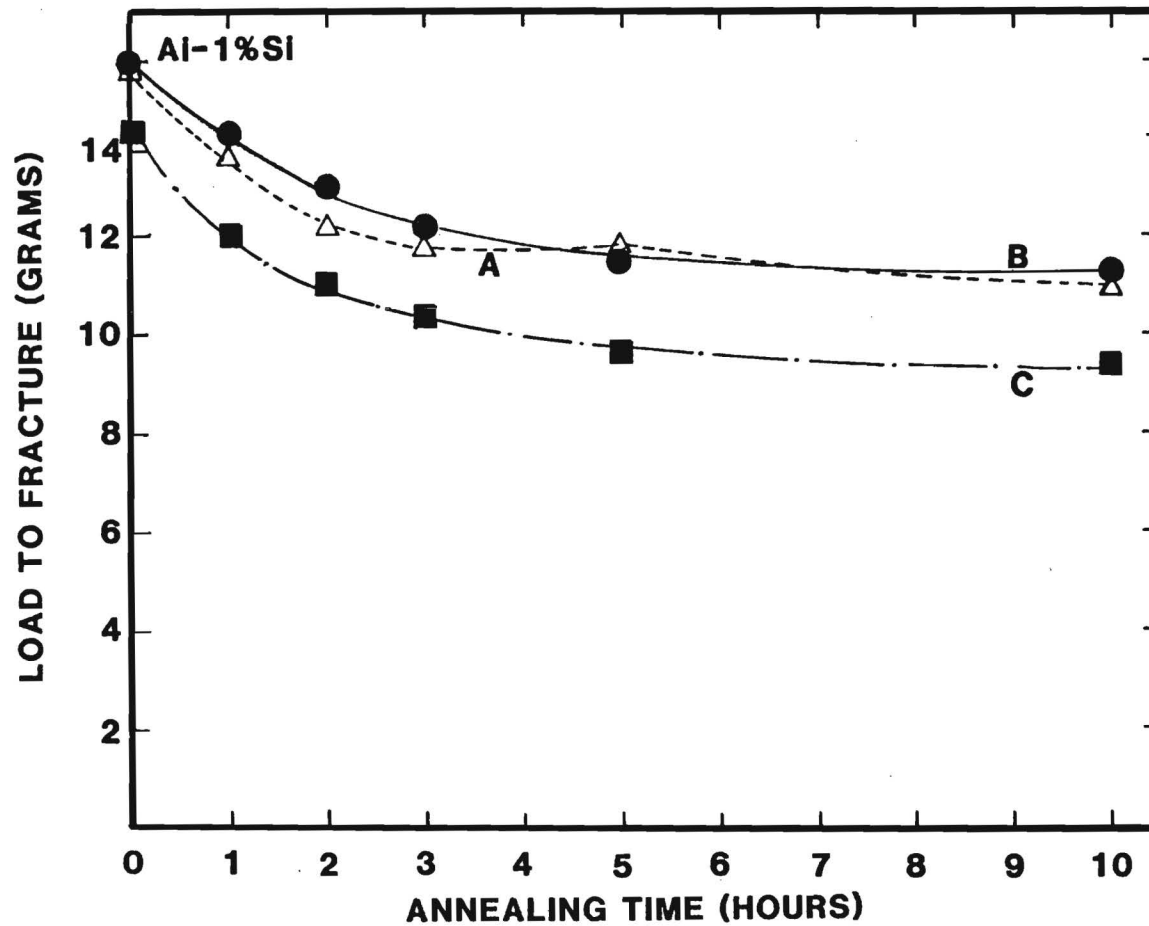


Figure 35. Plots of load to fracture as a function of annealing time for Al-1%Si bond wires from three different suppliers. Anneal temperature was 150°C and the wire diameter is 0.001 in. The measurements were made at room temperature.

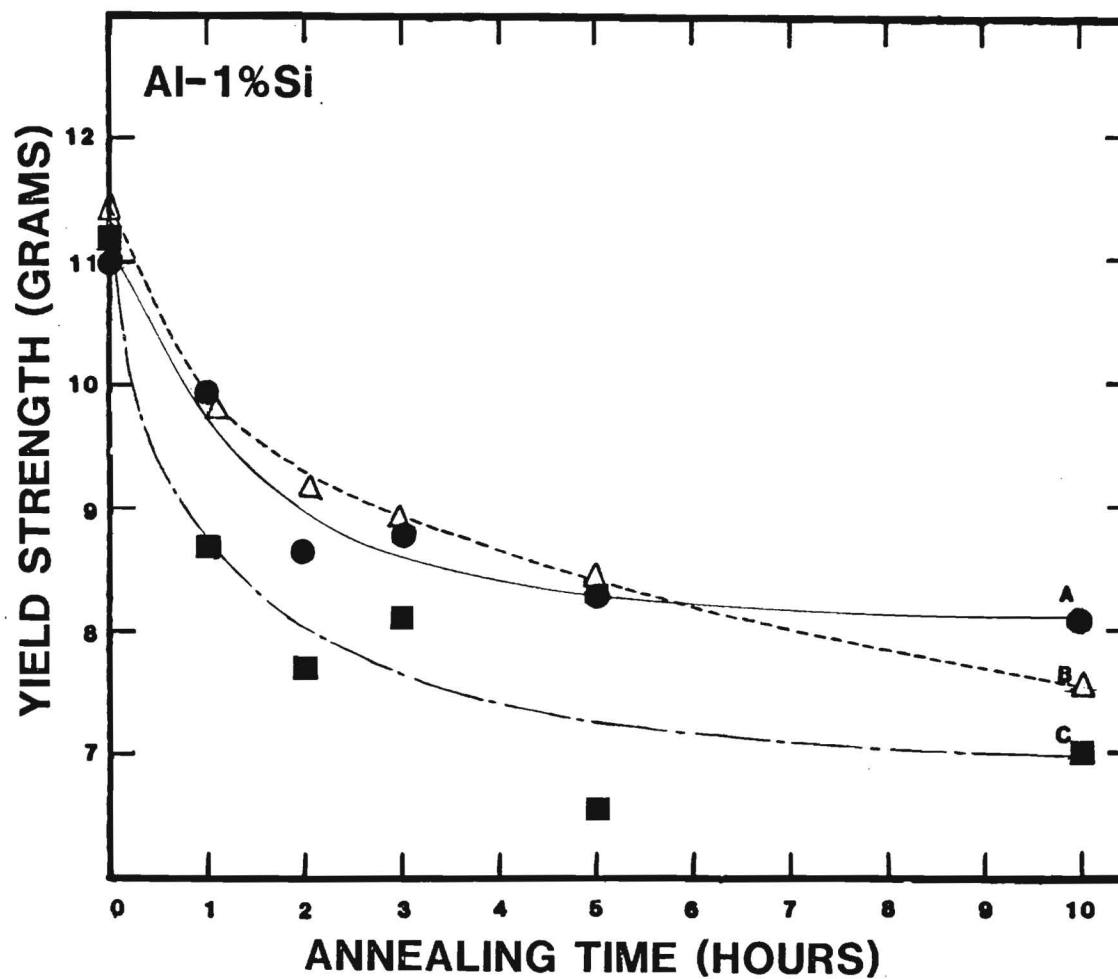


Figure 36. Plots of the tensile yield strengths as a function of annealing time for 0.001 in. diameter Al-1%Si bond wire from three different suppliers. The annealing temperature was 150°C while the measurements were made at room temperature.

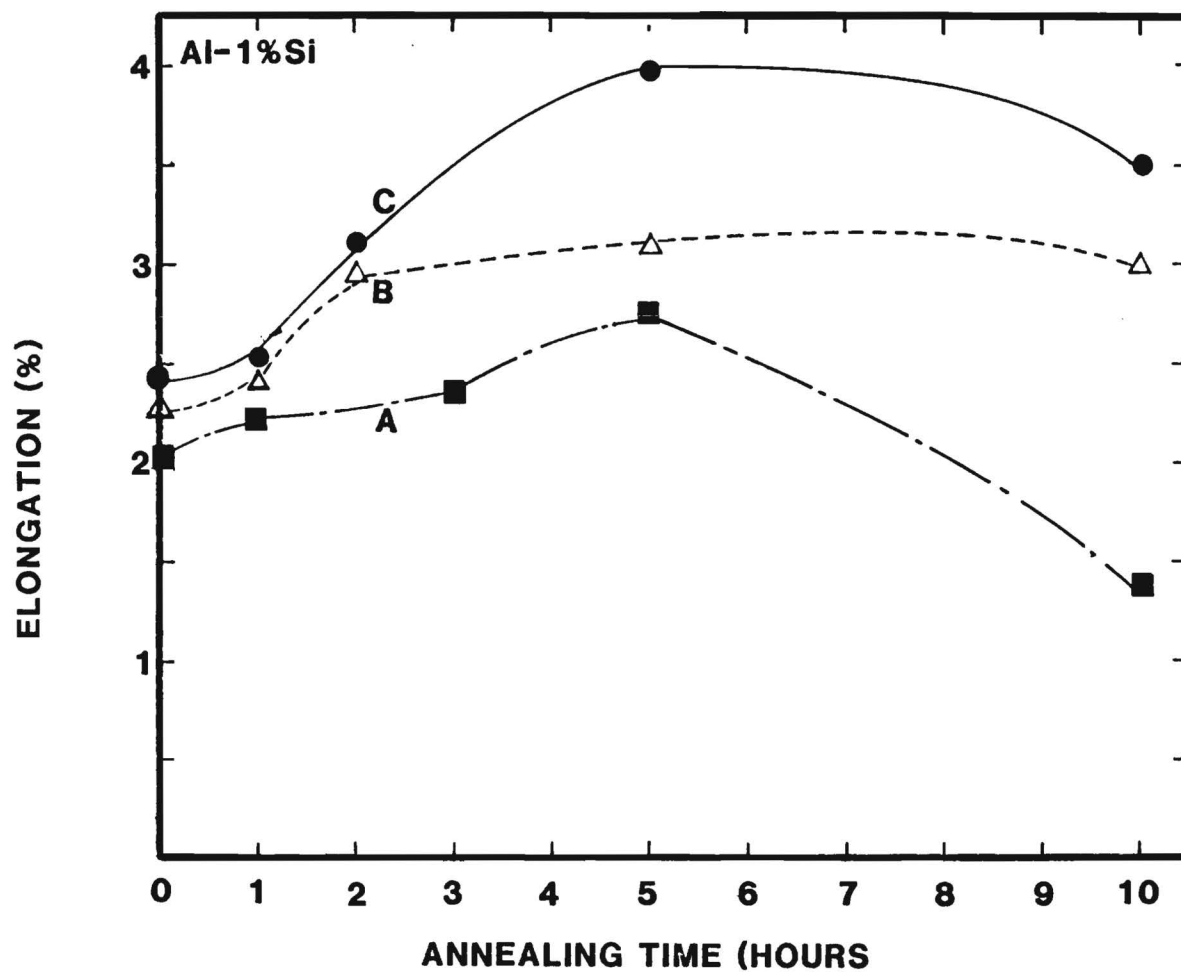


Figure 37. Plots of elongation to failure as a function of annealing time for 0.001 in. diameter Al-1%Si bonding wire from three different suppliers. The annealing temperature was 150°C while measurements were made at room temperature.

the form of tiny particles (G.P. zones). These zones often exhibit a coherency between the crystal lattice structure of the precipitate and that of the aluminum matrix. The long ranged stress fields of dislocations interact with these coherent particles in a manner which impeades dislocation glide and thus provides the desired strengthening effect. The whole point to age hardening is to choose the right temperature-time values to achieve optimum coherent precipitate sizes, in order to provide strengthening.

If the wires are properly aged as received, then all of the thermal processes normally experienced by a microcircuit will effectively serve to overage the material. Overaging, microstructurally, involves the continued growth of the silicon precipitates to particle sizes in which coherency is lost. Thus, the environmental stress screens and the normal operational temperatures of a aluminum bond wire result in the wire material experiencing a decrease in tensile strength. This loss in strength may not be particularly detrimental unless the device is subjected to strong mechanical shock or vibration levels during it's operating life. However, the same metallurgical mechanisms responsible for overaging modify the microstructures in a manner which makes the alloy more susceptible to fatigue damage. This comment applies both to the wire and to aluminum alloy film conductors deposited on the chip. Within the past two years, metallization fractures initiated by the precipitation of enlarged silicon particles have created enormously expensive



reliability problems for certain memory chips.

## **CREEP EXPERIMENTS**

A simple sample mounting technique was developed to make possible the study of mechanical properties of wire bonds stressed in shear while supporting currents and at elevated temperatures. The first and second ultrasonic bonds are made on separate chips which are then cemented to tabs for mounting on a microtensile apparatus. Segments of either another bond wire or a gold ribbon are also bonded to the chip so that electrical connections can be made to each end of the test wire with negligible mechanical loading due to the electrical contacts. Stress-controlled microtensile instrumentation in the Micromechanics Laboratory has proved ideally suited for these measurements. This combination of bond wire sample mounting technique and the microtensile instrumentation makes it possible to carry out a number of highly useful stressed electrode experiments for investigating material degradation processes in interconnections. A photograph of the apparatus showing the stressed electrode fixtures is provided in Figure 38.

The shear testing of single bonds is done by making the bond to a chip with the other end of the wire segment cemented to a tab. This particular test is also used here to check that the bonding machine parameters are consistent. As a set of specimens is prepared for the fatigue measurements, several single bonds are made for shear strength testing. Optimum settings yield first

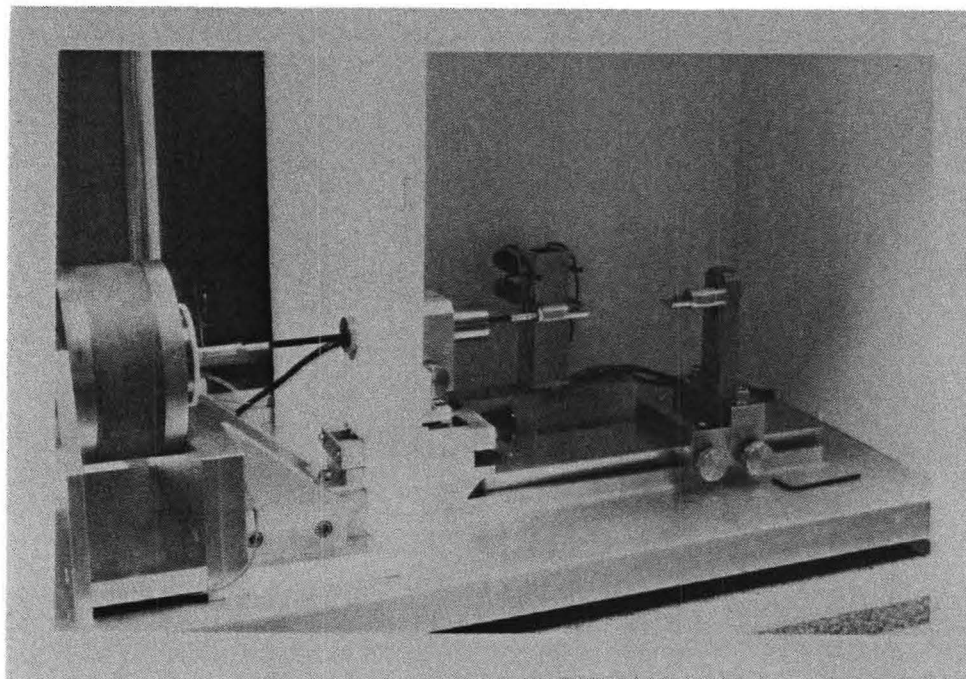
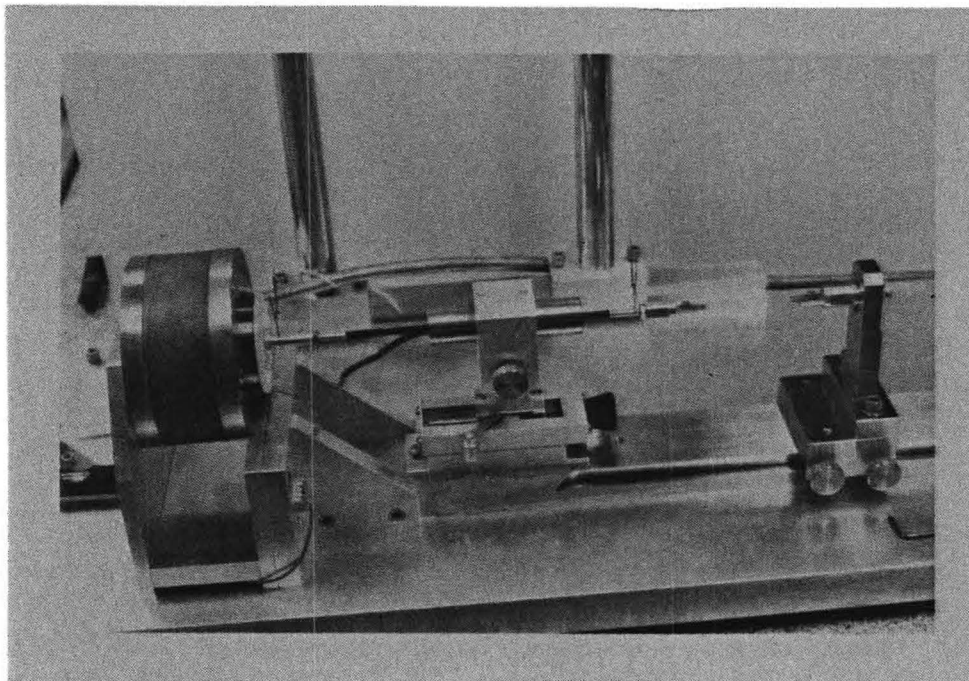


Figure 38. Stress controlled micromechanics apparatus shown in configuration for stress-strain and tensile creep measurements on wire bond.

bond shear strengths about 9.2 gram with second bonds at about 12.0 grams. The bond strength test for good bonds is less a shear test than tensile test of the heel region of the bond. For the bond interface to actually fail in shear, the bonding parameters must be far off, the wire or pad have contamination problems, etc. The almost 3 gram average difference between first and second bond strengths is probably associated with the bonding machine imposing a higher bend angle on the wire after making the first bond. The bending and tensile stresses thus applied to the narrow bond heel and wire-pad interface region is sufficient to introduce crack initiating mechanisms in the soft metal.

We had anticipated that mechanisms normally associated with mechanical creep would play a role in the elevated temperature and electric current conducting bond wire fatigue processes. Accordingly, a series of experiments was planned for studying how the creep mechanisms operate in the very special configuration of a microcircuit wire bond. The bonds are stressed in "shear" at constant load with the creep characteristics of wire bonds examined as influenced by an electrical current in the bond and by externally applied heating. The electromagnetically activated stress-controlled microtensile apparatus accommodates wire bond creep measurements with greater precision than any other known apparatus. As these measurements progressed, it was realized that a mechanical creep behavior occurs even at room temperature in the ultrasonic aluminum wire bonds. Bonds loaded to about 70% of their "normal" strength ultimately fail under constant load with

measured times to failure ranging from a few minutes to six hours.

Two of the room temperature creep curves for Al-Al wire bonds are shown in Figures 39 and 40. These curves have linear strain regions characteristic of quasi-viscous creep mechanisms. The data are presented as "elongation" vs. time rather than strain vs. time since it is practically impossible to determine with any precision the length of the region within the bond heel where the strain actually occurs. Most, but not all, specimens have a linear strain rate region as shown in these two figures with the linear rates ranging from about 4 microns per hour to about 15 microns per hour. Both the initial creep rate which occurs upon loading the specimen and the tertiary creep rate just prior to fracture have much higher values.

The discovery that these creep processes exist in microcircuit bond wire systems has wide ranging implications. Creep rates increase with current and/or temperature with values measured between 25 and over 100 microns/hour at 100ma. The bond region is a complex combination of highly deformed metal, precipitates, hard (oxide) interface inclusions and numerous surface and interface stress concentrators. Some bond specimens have creep behavior controlled by mechanisms best described by generalized Nabarro creep where the self diffusion of vacancies within the bond metal is greatly enhanced because of the very high defect density within the aluminum. These self diffusion processes promote dislocation climb mechanisms and thus a

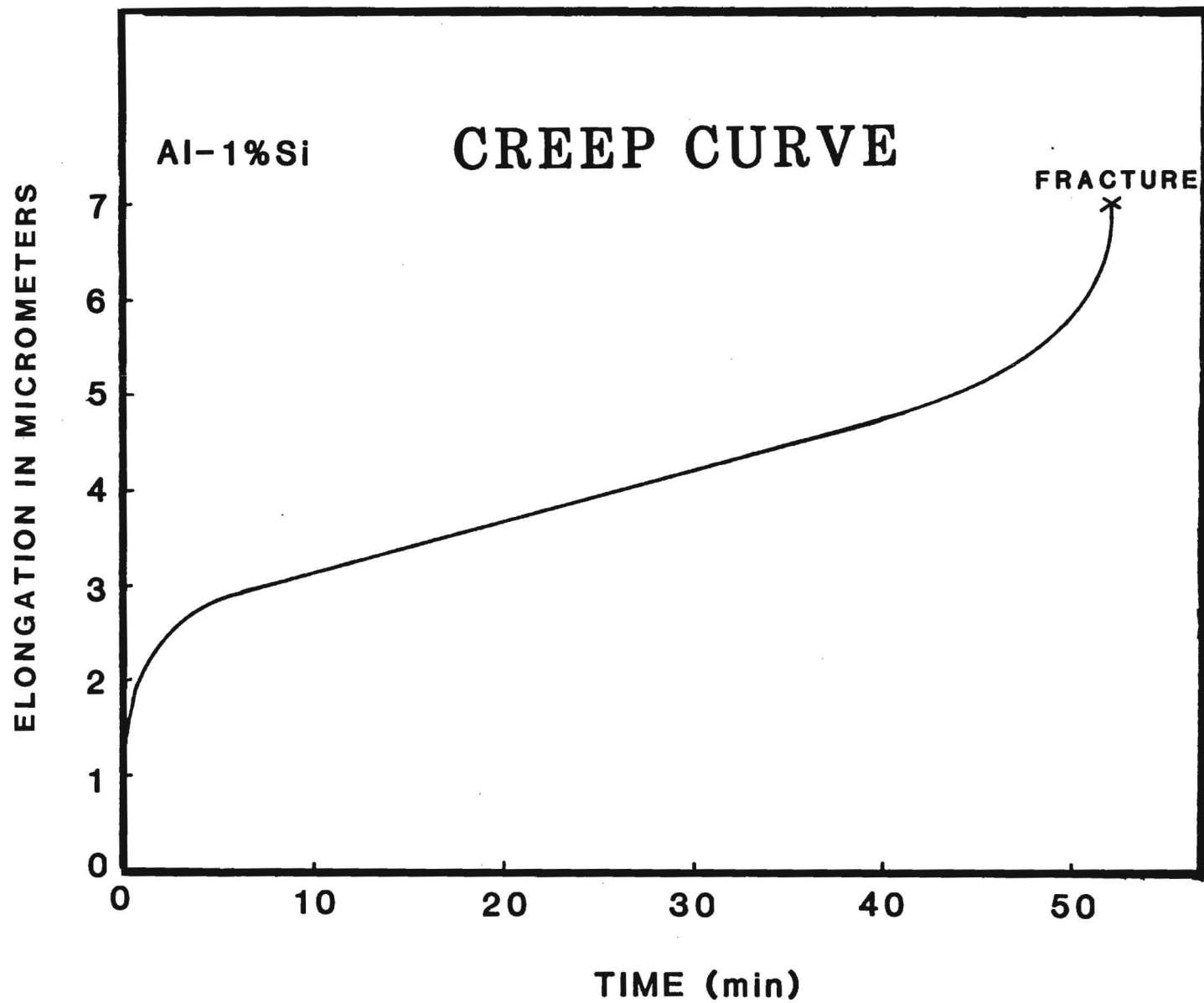


Figure 39. Mechanical creep of an Al-Al wire bond at room temperature with a constant applied load of 6.8 gramsforce.

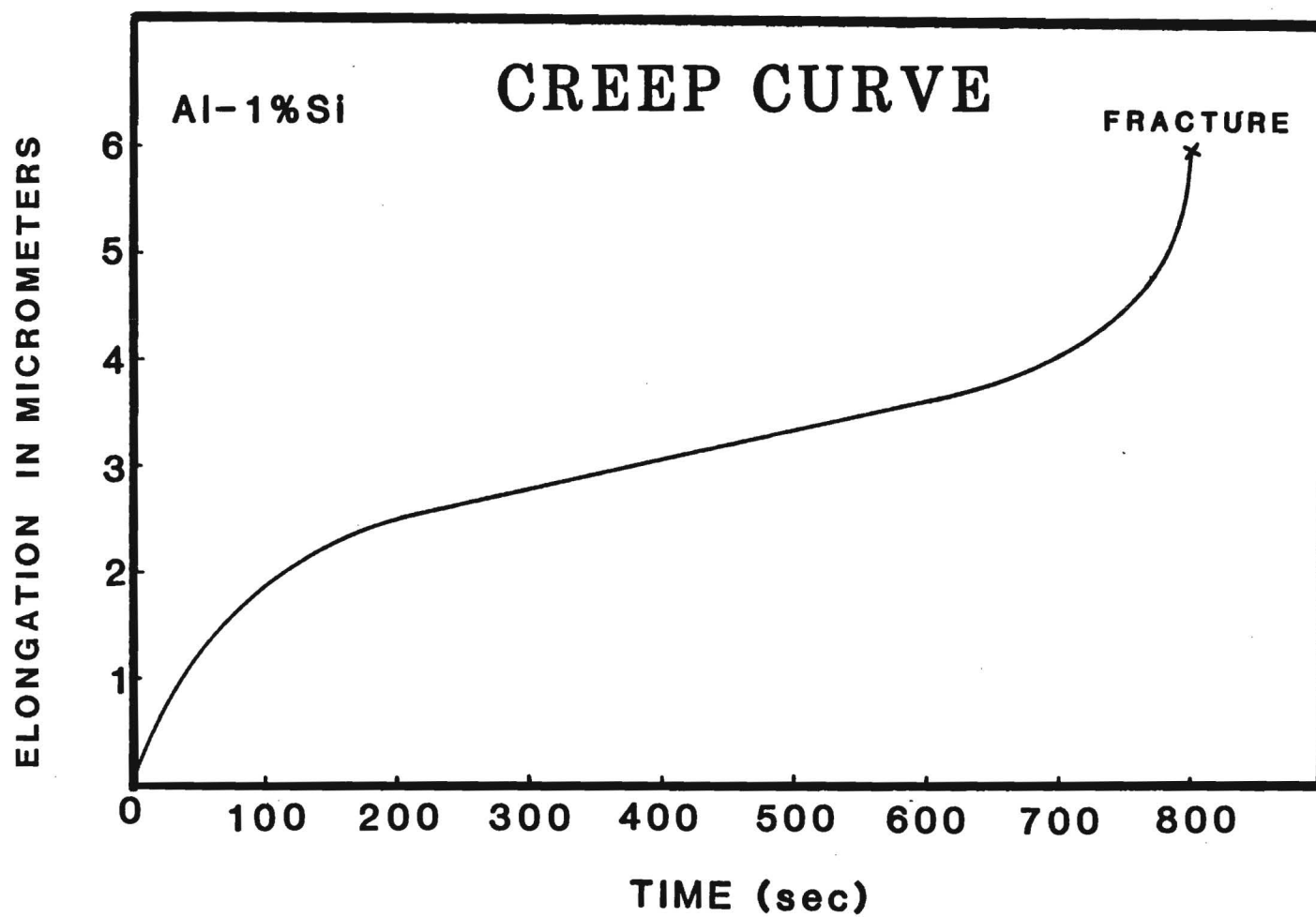


Figure 40. Mechanical creep of an Al-Al wire bond at room temperature with a constant applied load of 6.8 gramsforce.

relatively slow rate of plastic deformation without increasing the applied stress.

The heterogenous bond interface and surface nonuniformities on the wedge bonds also result in localized regions of the metal being subjected to much higher stress values than would be the case if the material were uniform. The bond therefore presents conditions which would support both the thermally activated and the stress activated viscous flow of dislocations. Very recent theoretical treatments of these mechanisms appear applicable to analysis of these experiments. The experiments are thus being modified to explore these important phenomena in much greater detail.

The mechanical creep phenomena had not previously been noticed, to our knowledge, by other investigators of microcircuit materials. However, the observations have similarities to some recently reported investigations of creep phenomena in fcc metals for purposes other than microelectronics. The important point is to determine how these mechanisms operate in the particular materials configurations employed in the fabrication of microcircuits. As described elsewhere, the freshly made wire bond and a metallization conductor, are unstable metallurgical structures which initially have high residual mechanical stresses. These stresses may be partially relieved during either a high temperature storage screen or later during operation at elevated temperatures. This stress relief should occur via the same dislocation mechanisms which are involved with creep.



The wire bond creep data have demonstrated that normal microcircuit operating stresses (temperature, current) introduce conditions which activate creep mechanisms. The mechanical fatigue degradation of wire bonds is therefore influenced by the dislocation mechanisms normally associated with creep phenomena. The critically important crack initiation and initial growth processes causing fatigue failures in wire bonds clearly occur through mechanisms which combine interactions of mechanisms associated with creep phenomena with those employed in the analysis of normal fatigue models.

## TECHNICAL DISCUSSIONS

The dimensionality of microcircuit wire bonds is shown in these investigations to have a major effect on the mechanical durability of microcircuit structures. The operation of a microcircuit involves cyclical thermal mechanical stresses in the wire bond metal leading to mechanisms normally associated with low cycle fatigue. The instrumentation of the Micromechanics Laboratory has been well suited for making the measurements needed to investigate the manner in which these mechanisms operate in specimens of the sizes of wire bonds. The special fixtures and techniques developed for this work have made it possible to measure cyclical mechanical hysteresis curves for tiny wire bond specimens. These cyclical mechanical hysteresis data are being analyzed along with studies of SEM micrographs to obtain a better understanding of the fatigue degradation mechanisms in these materials.

The wire bond mechanical hysteresis curves exhibit unique characteristics when related to the corresponding types of data normally obtained for structural alloy specimens. In the first place, the bond hysteresis curves are distinctly asymmetrical in shape. In one half of a cycle, the wire-pad interface is in compression while the upper surface of the bond is flexed in tension. The other half of the cycle then places the top surface of the bond in compression while the material joining the wire to the pad experiences tensile stresses. It is generally recognized

that the major strains causing fatigue damage in metals occur as a result of tensile stresses in the surface material.

The amplitudes of the cyclical stresses imposed in the wire bond metal induce the movement of large numbers of dislocations. Specimens showing work hardening indicate that dislocation densities are being multiplied, forming complex tangles whereby further slip is inhibited by interactions between the large numbers of dislocations. These dislocation interactions with each other, of course, account for the work hardening phenomena in all metals. An unusual aspect of the wire bond data is that a specimen can exhibit cyclical hardening in the compressive half of the flexure cycle while cyclical softening occurs in the tensile half, and conversely. Cyclical softening is generally associated with orientation of the dislocation debris into cell structures, the formation of dislocation dipoles, etc. as a result of stresses causing the reverse movement of dislocations.

The explanation for these differences is partially found in the very different types of interfaces existing at the upper and lower surfaces of a wedge bond. A wedge bond is clearly seen in the SEM micrographs to involve highly deformed metal with the upper surface of the wire roughened due to the action of the bonding tool. The lower side of the wire, which is bonded to the pad, involves the bond interface which includes impurities and other surface debris which one would prefer to not have there. Thus the detailed features of both the upper and lower sides of a normal bonded wire contain numerous sites which may act as

potential stress concentrators for nucleating mechanical degradation mechanisms. Considering the impossibility of precisely duplicating interface features of this nature from bond to bond in addition to the very deep deformation of the wire metal during bonding, it is not surprising that very different characteristics are often measured here in the sensitive hysteresis data for supposedly identical wire bond specimens.

The lower side of the wire of a wedge bond involves large numbers of microbonds between the wire and pad metals, with the original oxides and possible surface impurities interspersed. These intermittent sites of metal bonding are loaded during the tensile stress cycle with localized stress values considerably in excess of those calculated from an averaged load distribution. The highly localized stresses produce extensive plastic deformation in these regions, nucleating and propagating dislocations into neighboring regions of the metal as well.

The upper surface of the bonded wire, characterized by the highly roughened surface seen in micrographs, also is an example of the type of surface one would rather not have in order to achieve optimum fatigue strength in a metal couple. The forces between the soft wire material and the bonding tool deform the wire metal with scratches and depressions determined by surface asperities on the bonding tool. In addition, the rubbing of two metal surfaces is generally found to generate prow formation, which consists of small quantities of the softer metal being transferred to asperities on the surfaces of the harder metal.

These prows may subsequently be transferred back to the wire surface and be pressed into the wire during the application of force for bonding. Detailed features on the micrographs indicate that this process indeed does occur. A prow of aluminum would likely be a mixture of tiny oxidized films and the metal. Each of these potential causes for roughness contributes to a resulting surface having an extensive collection of features to nucleate fatigue cracks.

The entire thickness of a microcircuit bond region corresponds to the dimensions normally involved with nucleation and Stage I crack growth mechanisms as designated for bulk structural alloys. The operation of cyclical degradation within a microcircuit bond material is therefore a very special case of material fatigue with the crack nucleation and initial growth of a bond metal. Slip bands initiating near one surface are directly influenced by factors affecting mechanical stresses near the opposite surface of the bond.

A dislocation mechanism for the development of surface extrusions and intrusions at the surfaces of bond metals with cyclical plastic deformation is illustrated in Figure 41. The stress in one direction produces slip on a suitably oriented plane, resulting in the slip step in (b). The stress reversal creates a similar step at some angle to the initial slip plane. Subsequent repeated stress cycles activate dislocation motion on neighboring slip planes to generate the intrusions and extrusions illustrated in (d) and (e).

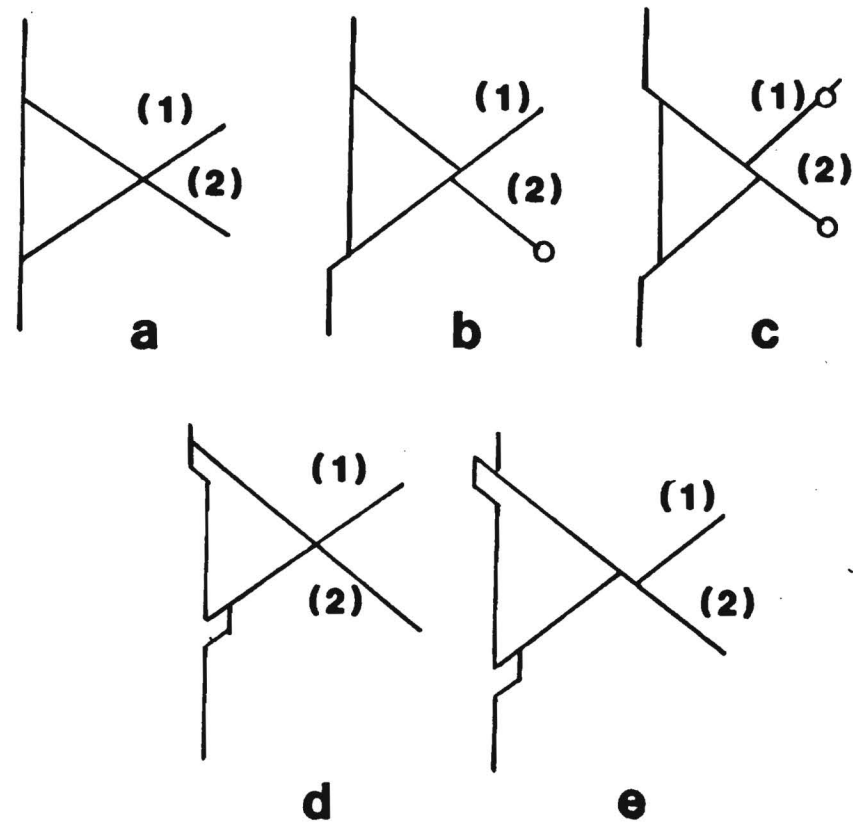


Figure 41. Operation of two intersecting slip bands in sequence resulting in the formation of intrusions and extrusions. The forward cycle is represented by (b) and (c) and, the reverse cycle by (d) and (e).

As discussed earlier, the surfaces of aluminum are never free of oxides. We carried out calculations of the interface interaction forces for dislocations in geometries of concern here for natural aluminum oxide films of various thicknesses on pure aluminum metal and plotted some of these in Figure 6. Close to the oxide coating, the dislocation is effectively repelled by the interface due to stress field energy considerations. However, real metals never present single dislocation interactions and one is really concerned with the forces acting on large assemblies of dislocations. This situation is schematically represented in Figure 42 where dislocation "pile-ups" are shown to develop on active slip planes. When the numbers of dislocations increase such that the shear stress at the leading dislocation exceeds the fracture stress of the oxide, the oxide surface fractures permitting the egress of dislocations and formation of a surface slip step. The mechanisms described in Figure 41 then proceed.

It was pointed out earlier that the surface strengthening due to oxide and dielectric films are critically important to the stability of a microcircuit. Thus, anything that changes the properties of the surface coating material, potentially, may have a deteriorating effect on the durability of the metal member. For example, moisture and other chemical agents are known to reduce parameters such as the elastic modulus of thin natural oxide coatings on aluminum, or even to dissolve them. The environment thus weakens the surface strengthening mechanisms operating in the microcircuit materials resulting effectively in corrosion

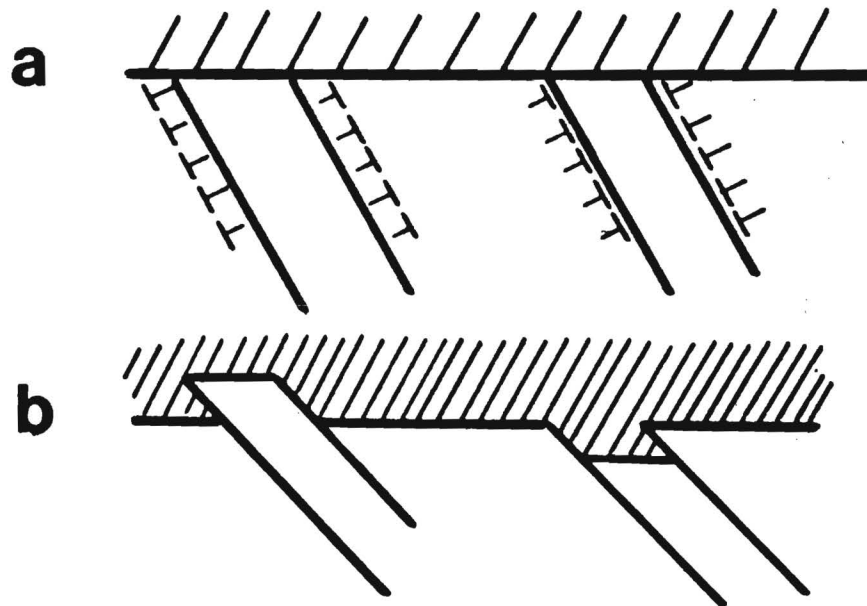


Figure 42. Schematic showing dislocation pile-ups due to cyclic straining.



fatigue degradation under cyclical loading. Figure 43 illustrates another model for environmentally assisted crack growth with cyclical loading of the aluminum surfaces.

A model developed and verified by researchers of low cycle fatigue mechanisms in bulk structural alloys to describe the growth of fatigue cracks in metals is illustrated and described in Figure 44. The asperities existing at both bond surfaces provide precisely the conditions for operation of this mechanism in the "bulk" of the bond wire metal in the region of the heel.

The 1% Si typically employed in aluminum bond wires will precipitate with time-temperature aging and form rigid particles which may also serve as stress concentrators for nucleating tiny fatigue cracks. This mechanism for crack nucleation is well documented in the literature for the fatigue degradation of structural aluminum alloys. Aluminum oxides which happen to exist within the bond heel region will similarly serve as stress concentrators.

The cyclical fatigue experiments and related investigations conducted during the course of this program have shed considerable light concerning the operation of fatigue degradation mechanisms in wire bond metals. They have also raised many questions which need to be explored. For example, experiments using wire bond specimens taken from a set made under identical conditions often had considerable variations in the various fatigue parameters measured. However, monotonically stressed specimens from the same group yield bond pull test

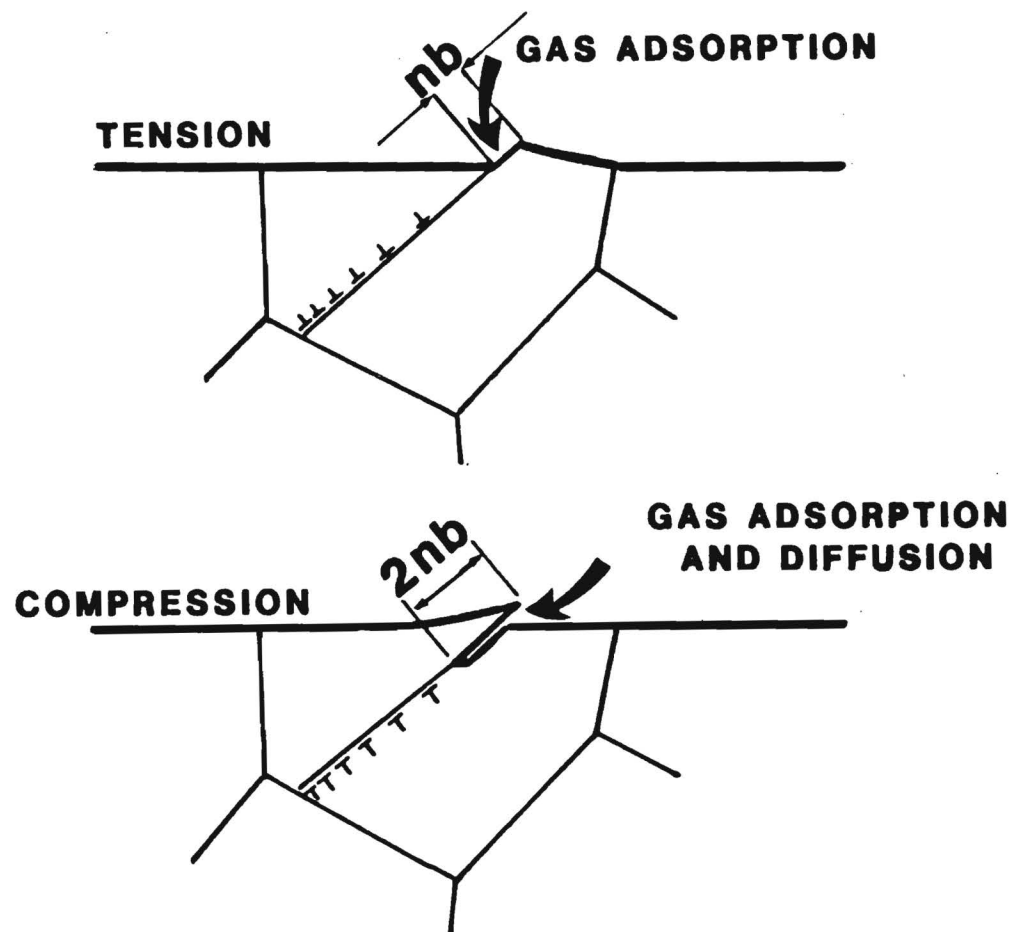


Figure 43. Schematic showing environmentally assisted cyclic slip-band cracking.

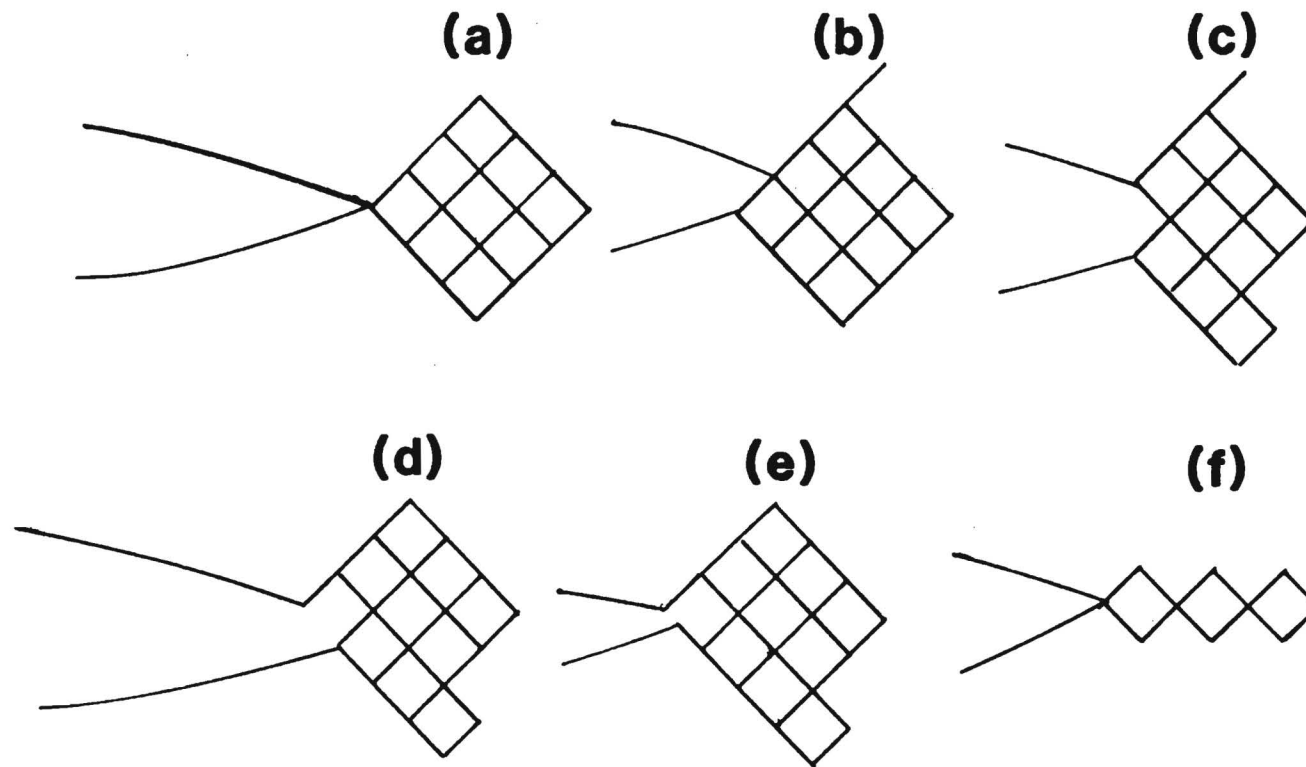


Figure 44. Schematic representation of a model for fatigue crack growth by shear sliding. (a) initial configuration, (b) crack opened in tension with shear sliding along a slip plane above the crack plane, (c) shear sliding along a slip plane below the crack plane, (d) crack unloaded with reverse shear sliding on slip plane of (b), (e) crack tip sharpening and crack advance, (f) repetitions of the mechanism.

values with comparatively small scatter. There clearly are particular metallurgical features which have a greater effect on fatigue characteristics than on the monotonic tensile strengths (pull tests) of wire bonds.

All microcircuit bonds involve highly deformed metal, where high dislocation densities were necessary in order to make the bond. It might therefore be anticipated that only cyclical work softening would occur with mechanical cycling. In fact, the hysteresis loops of wire bond specimens go either way. Apparently the dislocation arrays generated during the bonding process do not cause the heel region of the bond to be in the highest work hardened state. This point is supported by the shapes of monotonic stress-strain curves taken for single bonds stressed in tension.

The hysteresis loop energies are found to vary somewhat during the cyclical life of a wire bond specimen. Over a number of years, workers in the area of cyclical fatigue in bulk, structural alloys have been able to establish correlations between the total energy to fracture and number of cycles to fracture and stress amplitude. We have not yet been able to make these particular correlations from the data obtained for the wire bond materials. This may be due to the extraordinary softness of the metals used for electronic applications as compared to the high strength metal alloys employed in larger structures. However, the variations in energy absorbed per cycle reflect the mechanisms operating during the cyclical plastic deformation. The

dislocation--lattice interactions occurring with plastic flow convert mechanical energy into heat, with very little of the cyclical energy stored in the metal as residual elastic stress energy. If dislocation movements were completely arrested via strong pinning points, one would expect narrow hysteresis loops. There is also evidence for energy dissipation due to what may be frictional processes occurring within multiple microcracks as the stress alternates in sign. This latter mechanism likely occurs in some structural alloys, but it would be more significant in the soft aluminum and gold of wire bonds.

The energy per loop data show different trends for bond specimens cycled in dry air, in the several types of moist environments and for electrical currents in the bonds. The humidity level, with and without NaCl, tends to reduce the loop areas, and reduce the number of cycles to failure.

In air, a freshly created aluminum surface will immediately grow an aluminum oxide surface film. Friction measurements were made using aluminum film and wire surfaces as the rubbing pair at very small loads (using another instrument of the Micromechanics Laboratory) involve essentially single asperity contact. The friction at normal forces below a few dynes has little or no stick-slip character and low friction coefficients. Increasing the normal force slightly begins to introduce fractures in the oxide coating such that metal-to-metal bonds are made, resulting in a distinct stick-slip character and significant energy dissipation. The microbonds typically produce tiny prows. The

reduced energy per cycle for bond specimens in the moist environments may be associated with the migration of water and perhaps Cl and Na ions into the microcracks to reduce the capacity of the metal to reform microbonds in successive deformation cycles.

The hysteresis loop energies recorded for bonds cycled with currents through the bonds generally exhibit a peak in the energy absorbed per cycle shortly before fracture. There are probably several factors simultaneously operating here. As the conducting material is reduced by crack propagation, the current is constricted, resulting in localized areas of higher current densities. These higher current densities produce Joule heating and also directly enhance dislocation motion through the electroplastic effect. Both the electroplastic mechanism and the thermal activation serve to assist dislocation motion through the resistance of dislocation cell structures and lattice pinning points. Another factor is that even small electric potentials can break down the electrical resistance of the freshly created aluminum oxide films of a few molecular layers, thus aiding in the process of making new microbonds. For example, the loop energy per cycle for two aluminum-aluminum bonds having about 300 cycles to failure life times at a current of 350 ma, exhibited peaks of, respectively, 0.694 erg and 0.398 erg a few cycles prior to fracture. This is to be compared with the respective energy per cycle values of 0.668 erg and 0.338 erg within the first few cycles of the specimen life.

The features of "high ductility" were first observed in micrographs of the early specimens fatigued with current and was initially assumed to be local melting of the bond metal as the bond fractured. However, spherically shaped features were not seen in the micrographs, as would be expected from surface tension effects with molten aluminum. The high ductility characteristics were also found to occur in very small regions of wire bond specimens cycled without conducting current. The tensile experiments on wire bonds led to the realization that mechanical creep mechanisms operate in the wire bond metal at room temperature and at loads well removed from the normal fast fracture strengths of the bond. It was then recognized that this high ductility type of deformation, or viscous behavior, occurs because of high localized stresses due to a number of factors characteristic of the way wire bonds are made. Work done elsewhere was recently published, providing a theoretical treatment proposing the viscous type of plastic flow to explain high local stress deformation phenomena in copper, which also has a fcc crystal structure.

Large numbers of dislocations are induced to flow in a pattern which takes on a highly chaotic situation when compared to the normal dislocation motion on slip planes in crystalline metals. The viscous flow appears to be important for both interconnections and other metal features in microcircuits.

Facilities are currently being placed into operation at Georgia Tech which greatly enhance our capabilities to interpret

the various mechanisms investigated in the environmental fatigue studies. Both the scanning AES and the ESCA instruments will be useful for resolving the trace contaminants which migrate into the bond interfaces during mechanical cycling. In order to avoid contaminating the surfaces of specimens after fracture has occurred in the environment, experiments will be performed where specimens are mechanically cycled in the relevant environment and the cyclical deformation then stopped at a desired stage of the fatigue life. The bond wire specimens will later be fractured in a clean environment so that the pattern of impurity migration in the cracks can be traced. The AES and ESCA data should be a valuable method to evaluate how the contaminants move relative to the progression of fatigue crack nucleation and growth mechanisms.

The oscillatory variations recorded for both stress amplitudes and loop energies as the number of cycles increased in a number of wire bond specimens is a curious phenomena which needs further exploration. This behavior is clearly not an artifact in that it is measured repeatedly and precisely. Several models have been discussed involving the creation of sufficient dislocation debris to work harden one region of the bond heel (which would reduce the energy per cycle and increase the stress amplitude) followed by the activation of viscous deformation in a different region of the bond heel metal due to the high localized stresses created by this blocking. The viscous deformation would increase energy dissipation.



The static creep experiments also will be extended to include moist environments and NaCl with fracture and prefracture surfaces studied in the AES and ESCA. ESCA is expected to provide data concerning the nature of the oxide which grows within the metal during both the creep and cyclical stressing experiments.

As these experimental interpretation techniques are worked out, the effective cyclical fatigue methods developed here will be applied to evaluate the effects of other impurities introduced in microcircuits, either through the outgassing of die attach epoxies or from other likely package contaminants. The simple bond pull technique is clearly not a conclusive test to ensure the long term durability of every one of the large number of wire interconnections in a VLSI circuit. As noted repeatedly above, identically made bonds with highly uniform monotonic pull test values can exhibit very different environmental fatigue behavior dictated by a number of detailed metallurgical factors.

A-3509

# **FINAL REPORT**

## **INVESTIGATIONS OF MECHANICAL-ENVIRONMENTAL INTERACTIONS IN VLSI BOND INTERFACES**

**A-3509**

**PREPARED FOR**

**THE SEMICONDUCTOR RESEARCH CORPORATION**

**300 PARK DRIVE, P.O. BOX 12053**

**RESEARCH TRIANGLE PARK**

**NORTH CAROLINA 27709**

**By**

**B. R. LIVESAY**

**GEORGIA INSTITUTE OF TECHNOLOGY**

**MICROELECTRONICS RESEARCH CENTER**

**ATLANTA, GEORGIA 30332**

**December 1985**

# **FINAL REPORT**

## **INVESTIGATIONS OF MECHANICAL-ENVIRONMENTAL INTERACTIONS IN VLSI BOND INTERFACES**

**A-3509**

**PREPARED FOR**

**THE SEMICONDUCTOR RESEARCH CORPORATION**

**300 PARK DRIVE, P.O. BOX 12053**

**RESEARCH TRIANGLE PARK**

**NORTH CAROLINA 27709**

**By**

**B. R. LIVESAY**

**GEORGIA INSTITUTE OF TECHNOLOGY**

**MICROELECTRONICS RESEARCH CENTER**

**ATLANTA, GEORGIA 30332**

**December 1985**

**FINAL REPORT**

**INVESTIGATIONS OF MECHANICAL-ENVIRONMENTAL  
INTERACTIONS IN VLSI BOND INTERFACES**

**A-3509**

Prepared for  
The Semiconductor Research Corporation  
300 Park Drive, P.O. Box 12053  
Research Triangle Park  
North Carolina 27709

By  
B. R. Livesay  
Georgia Institute of Technology  
Microelectronics Research Center  
Atlanta, Georgia 30332

December 1985

## TABLE OF CONTENTS

Chapter	Page
I. Introduction.....	1
II. Nature of Microcircuit Wire Bonds.....	4
III. Interface Mechanics.....	11
IV. Environmental Fatigue Investigations.....	24
4.1 Introduction.....	24
4.2 Bond Fatigue.....	33
4.3 Single Bond Fatigue Studies.....	67
V. Supporting Investigations.....	81
5.1 Introduction .....	81
5.2 Studies of Thermal Annealing Effects on the Tensile Properties of Bond Wires....	81
5.3 Mechanical Creep Experiments.....	87
5.4 Microfriction Measurements.....	96
5.5 Fracture Surface Analysis Using SAM.....	100
VI. Technical Discussion.....	105
VII. References.....	119

## LIST OF FIGURES

Figure	Page
1. Interface Dislocation Network.....	15
2. Array of Misfit Accommodating Dislocations at Interface.....	16
3. Dislocation and Image Near Interface.....	18
4. Dislocation Pile-Ups at Barrier Interface.....	19
5. Dislocation Near Interface of Surface Coating.....	20
6. Force on a Dislocation as a Function of Distance from Interface.....	22
7. Hook Attachment to Bond Wire for Fatigue Test.....	25
8. Fatigue Apparatus.....	26
9. Series of Low Cycle Fatigue Hysteresis Loops.....	29
10. Measurement of Hysteresis Loop.....	34
11. Response Curves for Al-1% Si Bonds Fatigue in Lab Air.....	36
12. Work Hardening in Al Bond Fatigued in Lab Air.....	37
13. Work Softening in Al Bond Fatigued in Lab Air.....	38
14. Response Curves for Al-1% Si Bonds Fatigued in Humidity.....	40
15. Response Curves for Al-1% Si Bonds Fatigued While Conducting d.c. Current.....	41
16. Work Softening in Al bond Fatigued While Conducting 200 mA.....	42
17. Peak Stress Behavior for Cyclic Fatigue of Al Bond Conducting 300 mA.....	43
18. Peak Stress Behavior for Cyclic Fatigue of Al Bond Conducting 350 mA.....	44
19. Hysteresis Loop Energy vs. Fatigue Cycle for Al Bond Conducting 50 mA.....	46

Figure	Page
20. Hysteresis Loop Energy vs. Fatigue Cycle for Al Bonds Conducting d.c. Current.....	47
21. Peak Stress Behavior for Cyclic Fatigue of a Gold Ball Bond.....	48
22. Hysteresis Loop Energy vs. Cycle for the Gold Ball Bond.....	49
23. SEM Fractographs of Al Bond Fatigued While Conducting 10 mA.....	50
24. SEM Fractographs of Al Bond Fatigued While Conducting 50 mA.....	52
25. SEM Fractographs of Al Bond Fatigued While Conducting 75 mA.....	53
26. Deformation Induced During Ultrasonic Bonding.....	54
27. SEM Fractograph of Al Bond Fatigued While Conducting 100 mA.....	56
28. SEM Fractographs of Al Bond Fatigued While Conducting 150 mA.....	58
29. SEM Fractographs of Al Bond Fatigued While Conducting 200 mA.....	59
30. SEM Fractographs of Al Bond Fatigued in Humid Environment.....	61
31. SEM Fractographs of Al Bond Fatigued in Humid Environment.....	62
32. SEM Fractographs of Al Bond Fatigued in Humid Environment.....	63
33. SEM Fractograph Showing Features of Bond-Pad Interface.....	64
34. Deformation Induced During Bonding Process.....	65
35. Cyclic Stress Response Curves for Post and Pad Single Bonds in Air.....	69

Figure	Page
36. Cyclic Stress Response Curves For Post and Pad Single Bonds in a Saline Environment.....	70
37. Cyclic Stress Response Curves for Al-Al Single Bonds at Low Stress Amplitude in Air.....	71
38. Cyclic Stress Response Curves for Al-AL Single Bonds at Low Stress Amplitude in Pure H <sub>2</sub> O.....	72
39. Cyclic Stress Response Curves for Al-Al Single Bonds at Low Stress in Saline Solution.....	73
40. Comparison of Single Bond Cyclic Force Amplitudes at Low Stress in Three Environments.....	74
41. SEM Micrographs of Single Bonds Cycled in H <sub>2</sub> O.....	76
42. SEM Fractographs of Single Bonds Cycled in H <sub>2</sub> O.....	77
43. SEM Fractographs of Single Bonds Cycled in NaCl.....	78
44. SEM Fractographs of Single Bonds Cycled in NaCl.....	79
45. SEM Micrograph Showing Al Pad For Bond Lifted in NaCl.	80
46. Load to Fracture vs. Annealing Time for Al-1% Si Bond Wires.....	83
47. Yield Strength vs. Annealing Time for Al-1% Si Bond Wires.....	84
48. Percent Elongation vs. Annealing Time for Al-1% Si Bond Wires.....	85
49. Stress Controlled Micromechanics Apparatus.....	88
50. Mechanical Creep of Al-Al Bond.....	91
51. Mechanical Creep of Al-Al Bond.....	92
52. SEM Micrographs of Creep Fracture.....	94
53. Microfriction Forces Between Two Al Bond Wires At 1.1 Dyne N.F. ....	97
54. Microfriction of Al Wires at 1.7 Dyne N.F. ....	98
55. Microfriction of Al Wires at 2.3 Dyne N.F. ....	99
56. SEM Micrographs of Al-Al Surfaces Fatigued in NaCl But Fractured in UHV of SAM.....	102



Figure	Page
57. SAM Spectrum Showing Cl ions in Fracture.....	103
58. Intersecting Slip Bands.....	109
59. Dislocation Pile-Ups Due to Cyclic Straining.....	110
60. Environmentally Assisted Cyclic Slip Band Cracking.....	112
61. Model of Fatigue Crack Growth by Shear Sliding.....	113

## I. INTRODUCTION

Investigations have been conducted at the Georgia Institute of Technology to study fatigue degradation mechanisms operating in microcircuit wire bonds. The wire bonding techniques developed by the microelectronics industry account for approximately  $10^9$  chip-to-package interconnections each year. To perform their electrical interconnection function, the bond metals must remain structurally sound over the desired lifetime of the device. Mechanical, chemical and electrical stresses associated with the storage and operating environments of a microcircuit can induce degradation processes in the wire bond metals.

The pure and lightly doped aluminum and pure gold wires normally employed for bond wires and pads definitely are not high tensile strength metals and are not noted for good fatigue durability. In addition, structural modifications made to the wire and pad metals during the bonding processes introduce microstructural features which normally accelerate fatigue damage. However, use of these metals is highly preferred because of factors associated with their electrical conductivity and mechanical ductility, as discussed later.

This report describes investigations concerned with gaining a deeper understanding of the degradation mechanisms operating in the bonded interconnections of microcircuits. Experimental methods were developed for the cyclic stressing of wire bond specimens using micromechanics instrumentation which makes it possible to continuously record details of the stress-strain characteristics. Suitable stress-strain parameters were worked out for these studies so that the fatigue degradation mechanisms induced in the wire bond specimens would correlate with those activated in microcircuit materials during normal operations. Low cycle mechanical hysteresis loop data were recorded for a

number of wire bond specimens over a range of environmental stresses which included laboratory air, pure humidity and saline moisture, and a range of electrical currents through the bonds. The hysteresis data from these experiments are analyzed and correlated with SEM microstructural examinations of the wire bonds in order to aid in the interpretation of degradation mechanisms. Scanning AES analysis of trace quantities of impurities was used to track the penetration of active impurity ions into fatigue crack growth regions of the wires. The AES studies proved particularly valuable for gaining an understanding of how ions such as Cl accelerate crack growth.

Related studies have also shed considerable light on the mechanical degradation mechanisms in the wire bonds. Calculations were made of interface strengthening effects based on dislocation image force interactions for the aluminum-aluminum oxide film interface at the surfaces of both wires and thin film conductors. The effects of various time-temperature exposures on the mechanical behavior of bond wires obtained from a number of standard suppliers of these materials were also experimentally evaluated.

Tensile measurements at constant loads, with and without electric current, revealed that microcircuit wire bonds exhibit mechanical creep phenomena, even at room temperature. The discovery of this effect demonstrated that an important mechanism of viscous plastic flow could affect the cyclic degradation of wire bond specimens.

The subsequent chapters discuss important aspects pertaining to microcircuit wire bonds which make them a special class of materials for performing low cycle fatigue investigations. A primary aspect of this study has been the exploration of interface strengthening processes in terms of their importance concerning the small dimensions involved with

both the wire interconnections and with metallization layers on the chips of microcircuits. Results from the several different types of mechanical investigations are presented and interpretations of the operating degradation mechanisms in the bond metals are rationalized.

The contributions of the following individuals to various aspects of these investigations are gratefully acknowledged:

#### STUDENTS

David J. Locker, Jr. Graduate Student in Electrical Engineering.

Dawn L. Maguire Graduate Student in Physics.

John W. Vidic Student in Chemical Engineering, now graduated.

Elaine A. Webb Student in Chemical Engineering, now graduated.

#### POSTDOCTORAL FELLOW

Dr. Tirumalai S. Srivatsan

#### PROFESSIONAL STAFF

Dr. W. B. Carter

Mr. H. M. Harris

Mr. J. L. Larsen

Dr. J. T. Sparrow

In addition, the industrial mentor, Mr. Charles Hewitt of Harris Corporation, visited with us and provided a number of specimen packages which greatly aided the investigations.

## II. THE NATURE OF MICROCIRCUIT WIRE BONDS

The standard wire bonding processes employed by the microelectronics industry are extraordinary in that both identical and dissimilar metal pairs are reliably joined without their surfaces being made molten, without a flux and without an interconnecting solder or weld alloy. The techniques for both thermocompression and ultrasonic wire bonding of microcircuits as well as various characteristics of these bonds are well documented in the technical literature [1-8]. Our principal concern here is with the effects these bonding techniques have on bonded metal members and with the interface(s) created by the bond. The mechanisms required to make intermetallic joints result in highly altered microstructures in the metal pairs in the immediate neighborhood of the bond. The resulting physical state of the deformed bonded metal and the geometrical aspects of the bond shape are critical to the performance and ultimate durability of the bond interconnection under operational and other stresses imposed on the circuit.

The wire and pad of either a thermocompression or an ultrasonic bond are highly deformed during bonding, but by very different mechanisms. Aluminum, gold and other proposed metals for bond wires have the face centered cubic crystal structure with twelve slip systems [9], which promotes easy deformation within randomly oriented individual grains. Pure thermocompression bonds are heated to facilitate plastic flow under mechanical pressure. The plastic flow creates new, atomically clean, metal surfaces of the wire and pad materials at their interface as they are compressed together. Creation of the new surfaces at the wire-pad interface enhances interfacial diffusion and thus establishes the intimate metallic contact essential for making the conducting bond. In the case of

thermocompression bonding, thermally activated mechanisms greatly enhance dislocation dynamics to provide for extensive plastic deformation under moderately applied mechanical pressure. It is crucial for making conducting wire bonds that the wire and pad metals have high ductility in order to facilitate the necessary plastic flow required to create the new surfaces, as mentioned above. The ductility of the bond wire metal also disperses the mechanical forces of bonding which minimizes stress concentration, and potential damage, to the brittle chip material.

In contrast, ultrasonic bonding processes employ intense ultrasonic energy to facilitate easy dislocation glide without appreciably increasing the temperature of the bonding members. The intense ultrasonic energy is absorbed by the crystal lattice and is concentrated on lattice defects in a manner which enhances dislocation glide past normal pinning features without appreciably raising the temperature of the bonding metal. One can make correspondence between the experimental tensile curves for pure aluminum stressed at various elevated temperatures and similar curves of aluminum exposed to progressively elevated ultrasonic energy densities, but with the aluminum held at a low temperature [10]. The yield point of aluminum is decreased significantly as the temperature is raised [11-13] and, correspondingly, as the ultrasonic energy density is increased. The extensive plastic flow with coincidental exposure to intense ultrasonic energy and mechanical pressure brings freshly created metal surfaces into immediate contact. Intermetallic bonding at the interface requires sufficient interatomic diffusion between the wire and pad metals to establish the bond interface. During the last few years, thermosonic ball bonders have been available which simultaneously take advantage of both thermal and ultrasonic enhancement of plastic flow.

A microcircuit wire bond is normally a complex metallurgical

structure. The bonding mechanisms involve extensive deformation of the wire and pad, as mentioned above. In addition, surface oxides and other surface impurities remain in the resulting bond interface. The fact that gold does not form a surface oxide at room temperature has been a characteristic of immense value for making electrical contacts, including microcircuit wire bonds. However, even gold-to-gold bonds are found to have interface impurities due to residual processing materials, improper handling and atmospheric impurities, including moisture, which may exist in process areas.

A gold-aluminum bond thus has the potential for establishing an array of intermetallic compounds with consequent multiple interfaces. The formation of these intermetallic compounds is critically sensitive to the combination of time and temperature exposure, either during the bonding process or with subsequent exposure to elevated temperatures. Certain of the interfaces which develop in the Al-Au system after elevated temperature exposure are so brittle that bonds lift at zero force levels from the bond pads. Bond failures involving Al-Au intermetallic compound interfaces have resulted in some well known catastrophic system failures. There have been a number of investigations concerning the materials and processing parameters which lead to the excessive growth of the Au-Al intermetallic compounds and their effects on the mechanical behavior of wire bond systems. The gold-aluminum phase diagram has five intermetallic compounds,  $\text{Au}_4\text{Al}$ ,  $\text{Au}_5\text{Al}_2$ ,  $\text{Au}_2\text{Al}$ ,  $\text{AuAl}$  and  $\text{AuAl}_2$ . The important point is that an aluminum-gold bond is metallurgically unstable. Either mistakes during manufacture or subsequent exposure to elevated temperatures during testing, storage or operation can provide the thermal environment which supports the growth of one or more of the intermetallic compounds in the bond interface. The electronics industry has carefully learned to handle the Au-Al

intermetallic compound problem by essentially trying to avoid the relevant circumstances.

The Al-Al ultrasonic bond has become increasingly more important in recent years for microcircuit interconnections for several reasons. Aluminum metallization is now used in most microcircuits and it is therefore advantageous to use aluminum wires in order to avoid the intermetallic compounds discussed above. In addition, gold wires have significantly greater mass and are subject to correspondingly greater mechanical acceleration problems. Radiation damage is also a major problem with gold. The technology for making aluminum ball bonds has been developed during the last several years and should have a favorable impact for greater aluminum wire usage in the future.

Fragments from the natural oxide of aluminum remain conspicuously within the interface of all aluminum wire bonds. Sectioned Al-Al wire bonds clearly show that patches of aluminum oxide are distributed throughout the central plane of the bond interface. During the ultrasonic bonding process, the oxide is fractured into many tiny segments as the bonding surface effectively expands during compressive deformation. The effective electrical and mechanical bond is provided by numerous tiny intermetallic bonds made by atomic contact between the newly created, and protected, surfaces.

Ultrasonic bonds are employed in enormous quantities to provide interconnections between chip and package terminals and also between adjacent chips within a package. Early generations of monolithic devices generally required 10-30 wire interconnections from chip pads to package posts. Complex hybrid microcircuits have long involved hundreds of wire bonds. During the last few years the development of high density VLSI chips has greatly multiplied the number of chip-to-package interconnections in monolithic circuits. Some VLSI devices now



require over 300 I/O terminals and the numbers are increasing.

The large numbers of bonds involved with individual microcircuits has greatly emphasized the importance of the reliability statistics for making good wire bonds. In addition, the bond structure must be durable under the operational and environmental stresses it is required to handle within a microcircuit package. If the statistical reliability for making good bonds were 99%, there clearly would be a major concern with production yields for microcircuits having a hundred or more bonds. This concern led to the early development of "non-destructive" bond pull tests for hybrids where large bond counts made it statistically probable to have one or more bad bonds within each package. Hybrids with an investment of a number of chips and an expensive package cannot be simply discarded because of a single bad bond, as is the case for simpler ICs. A "non-destructive" bond pull test consisting of a low force tug on each bond essentially determines that the bond adheres to the pad. The magnitude of this low force tug introduces mechanical deformation within the bond wire material which may, or may not, be of truly non-destructive nature.

The wire bond is subject to combinations of mechanical, chemical and electrical stresses during testing, storage and operation of the circuit. The response of the wire bond material structure to these stresses is an important factor in the overall durability of a microcircuit. Mechanical stresses are generated within the wire bond during thermal excursions due to differential thermal expansion coefficients of circuit materials and due to thermal gradients associated with rapid thermal excursions. Temperature cycling occurs during normal operation, in various environments while the circuit may even be electrically dormant and during environmental stress screening. In addition, microcircuit fabrication processes always leave

residual mechanical stresses within the wire bond materials. The chemical stresses are associated with tiny quantities of residual process chemicals, moisture, impurities introduced during fabrication and packaging and chemical agents which come out of packaging materials such as epoxies used for die bonding, etc. All of these chemical agents make up the microenvironment of a package cavity. Electrical stress occurs with high currents in certain bond wires to a circuit.

The metal in the bond region is highly deformed and contains a high density of defects as well as trapped debris consisting of oxides and other impurities originally on the wire and pad surfaces. The highly deformed region where the wire is flattened against the bond pad to form the bond is mechanically supported by the bond interface. The geometrical configuration of the heel region, which bridges the flattened wire with the undeformed wire, serves as a microscopic stress concentrator. Movement of the wire loop due to thermal expansion and contraction or due to mechanical vibrations will accordingly induce the greatest mechanical stress in the metal of the heel region of the bond. Mechanically induced bond failures of "good" bonds generally occur at the heel.

The heel region of the wire contains a high defect density induced during bonding deformation and generally has a roughened surface caused by abrasive interaction with the bonding tool. The defects include an extensive dislocation debris and voids. The nature of the deformation also induces residual mechanical stresses in the bond metals. The high dislocation density at the heel junction effectively work hardens the metal. The dislocation networks will concentrate voiding resulting in the formation of incipient microcracks in the aluminum during mechanical cycling. These and other factors emphasize the

susceptibility of the heel region of a wire bond to fatigue damage.

### III. INTERFACE MECHANICS

The close proximity of surfaces and other interfaces profoundly affect the mechanical behavior of metal structures. The thin planar configuration of microcircuits makes all metal features on a chip subject to strong interface interactions. For example, yield strength measurements for bulk aluminum single crystals are normally on the order of  $1 \times 10^7$  dyne/cm<sup>2</sup>, or less. According to this value, an aluminum crystal only one micron thick by ten microns wide would thus yield with a tensile load of about one dyne. If the aluminum interfaces of this thin strip were only with vacuum (i.e., an unsupported aluminum film with no oxide or other coating), then the surface energy of aluminum, 860 dyne/cm, would itself support a load of about 1.9 dynes.

The metal interfaces existing in a microcircuit are much more complex. Rather than pure aluminum-vacuum interfaces, there are interfaces between aluminum and its oxide, aluminum and another metal, aluminum and the silicon chip and aluminum and a dielectric. A similar statement can be made for gold metallization as well, except for the fact that gold does not have a stable oxide under these conditions. Pure gold and pure aluminum are face-centered-cubic metals whose mechanical properties are very well characterized from large numbers of investigations on bulk specimens [9,14]. The mechanical durability exhibited by thin film structures of these metals deposited on chips with respect to the stresses to which they are exposed to during normal operational cycles, cannot be attributed to lattice strength factors intrinsic to these metals alone. Both surface and interface parameters are critically important to the mechanical integrity of a microcircuit.

In order to account for the structural integrity of a microcircuit, one must examine other relevant factors. Important

mechanical strengthening factors for a microcircuit structure are associated with the discontinuities bridged by the interfaces between the metal film and its neighboring layers.

A deposited fcc film is normally polycrystalline with columnar grains having a close-packed plane parallel to the substrate. Developing a fine grain structure in bulk metals is important for mechanical strengthening [15-18]. However, the dimensions of strip lines and other metal features in VLSI devices are comparable with the grain sizes. This results in a "bamboo" appearance in an etched thin circuit conductor thereby demonstrating that the conductor becomes a string of tiny single crystals connected together in a line. Similarly, one also sees bamboo structures in bond wires where they have been exposed to elevated temperatures for times sufficient for the growth of large grains.

The annealing which takes place in a microcircuit during either the high temperature bake, burn-in or with time in normal operation would result in weak mechanical structures based on the intrinsic lattice strengths of gold and aluminum. If only lattice strengthening processes were available in these thin structures, one would reasonably expect the gold or aluminum films to be catastrophically distorted under the imposed thermal mechanical stresses during operation of microcircuit. The complex interface structures created in microcircuit designs in order to accomplish their electronic functions turn out to be critically important for mechanical durability as well.

The deformation characteristics of all fcc metals, including gold and aluminum, are associated with dislocation dynamics. The strength of these metals is thus determined by the effectiveness of barriers to dislocation motion within the metal lattice. High strength is achieved in structural alloys through careful alloying and heat treatment schedules to control grain structures

[14,19-21]. Only limited alloying is used in microcircuit metallic conductors and the thermal treatments normally involved here lead to mechanical softening rather than strengthening.

Dislocation stress fields extend over distances comparable to one or more dimensions of microcircuit features [9,22,23]. Interfaces may present material discontinuities which distort dislocation stress fields to effectively either attract or repel the dislocation from the interface. For example, an aluminum-vacuum interface energetically favors dislocation glide towards surfaces and out of the metal, or a softening effect. However, an aluminum interface with either its own oxide, with silicon or with most dielectric materials will provide a barrier to the egress of dislocations, and thus strengthen the metal layer [24].

The barrier effects created by dislocation interactions with normal microcircuit interfaces are primary strengthening mechanisms in microcircuit metals. In general, interface strengthening factors are important for metal members having dimensions typical of microcircuit bond wires as well as the thin metallization layers discussed earlier [22,24,25]. The interfaces within a microcircuit bridge differences in such parameters as elastic modulus, lattice constants, crystal structures, crystallographic orientation and chemical properties. In addition to the surface tension effects mentioned earlier, interfacial energies play an important role in the formation and strength of an interface. A detailed analysis is necessary to evaluate the effect of particular interface configurations on the strength and durability of a metallic structure.

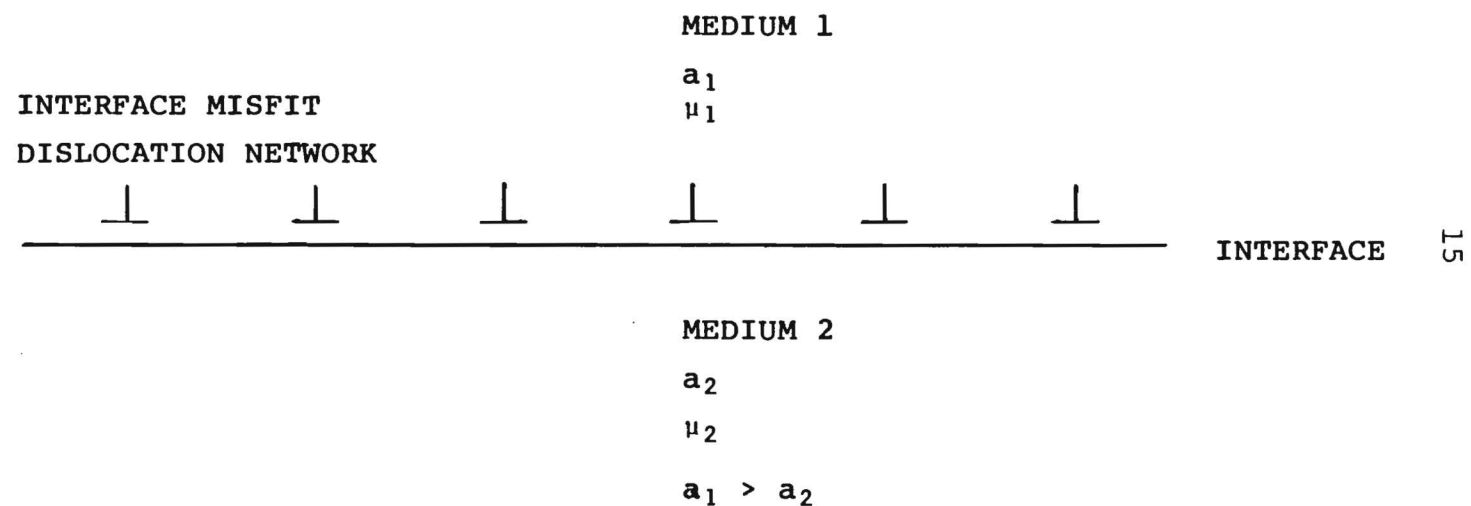
The following describes several of the interface strengthening mechanisms of importance to VLSI materials.

Differences in lattice constants across an interface introduce large elastic strain components at a coherent interface. The lattice misfit would generate local mechanical

stresses well beyond the strength of the material extended over a few lattice spacings. In order to successfully accommodate this misfit, metals are found to generate arrays of dislocations which essentially serve to relax the accumulated stress built up after several lattice spacings[26,27]. These periodic arrays of dislocations, shown schematically in Figures 1 and 2, are called accommodating dislocation networks and they are critically important for being able to produce a good interface between two materials [28]. The creation of this network depends upon the existence of a suitable dislocation generation and glide mechanism within the crystal structure of the metal. If the crystallographic natures of a particular pair of materials is such that they cannot generate a suitable accommodating dislocation network, one usually finds extensive cracking or separation in the surface coating.

The important point concerning these accommodating networks here is that glide dislocations must traverse the network in the interface during plastic deformation. The stress field of the fixed accommodating network inhibits dislocation glide towards and through the interface, with a net strengthening contribution. Another factor associated with lattice misfit is that the Burgers vectors are different in the two materials bridged by an interface. Under mechanical stress, the transport of dislocations through an interface generates a lattice displacement debris corresponding to the Burgers vector difference and the accumulated number of transmitted dislocations. The displacement debris at an interface is accompanied by a lattice stress field effectively repelling successive glide dislocations.

The effect of elastic modulus difference on dislocation glide towards an interface is briefly outlined in the following model.



$a$  - LATTICE PARAMETER OF MATERIALS  
 $\mu$  - SHEAR MODULUS OF ELASTICITY

Figure 1. INTERFACE DISLOCATION NETWORK



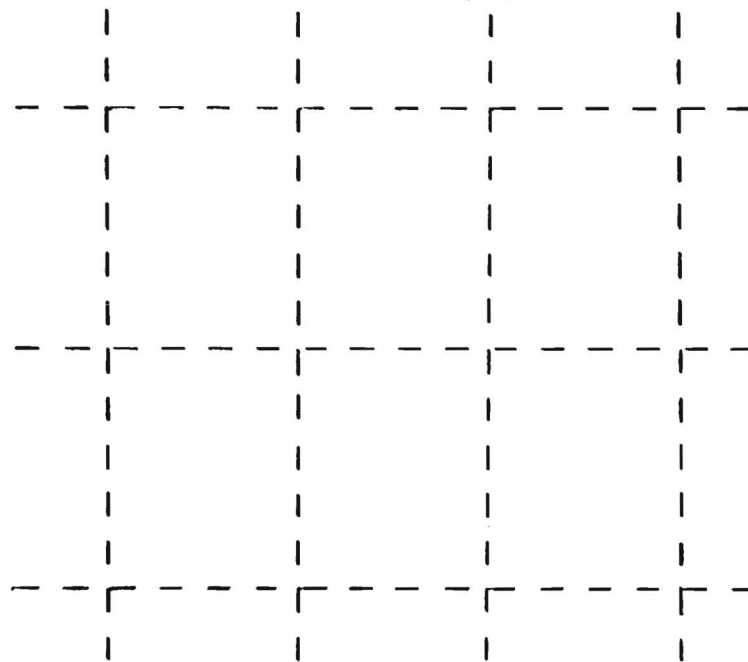


Figure 2. ARRAY OF MISFIT ACCOMMODATING DISLOCATIONS AT INTERFACE

The stress field of a dislocation in a solid is long ranged, having an inverse distance dependence. A dislocation located at distance,  $a$ , from an interface (see Figure 3) thus experiences an effective force of interaction,  $F_x$ , due to the interface according to expressions of the form

$$F_x = \left( \frac{\mu_2 - \mu_1}{\mu_2 + \mu_1} \right) \mu_1 \frac{b^2}{4\pi a} \quad (1)$$

where  $\mu_1$  and  $\mu_2$  are the elastic moduli of the two materials and  $\vec{b}$  is the Burgers vector of the dislocation [25].

It is seen from equation (1) that for a metal-vacuum interface, i.e.,  $\mu_2 = 0$ , the elastic stress field in the medium exerts a force on the dislocation towards the interface. Thus dislocations are energetically prone to exit at the free surface of crystals where they have sufficient mobility. However, if  $\mu_2 > \mu_1$ , then the image dislocation effectively repels the real dislocation. Thus there exists an effective barrier to dislocation transport across the interface. This situation is exemplified in Figure 4 wherein a dislocation pile-up is shown schematically on a slip plane oriented at an angle to the interface. Such dislocation pile-ups are observed in transmission electron microscopy investigations of dislocations.

The interface configuration relevant to a surface coating (which may be a thin deposited film, a thermal oxide, etc.) of thickness,  $t$ , is shown schematically in Figure 5. The theoretical calculations for this configuration are made by considering individual interactions of the single real dislocation with an infinite series of image dislocations. The expression used to carry out computer calculations for the net force acting on a dislocation at any site due to the proximity of

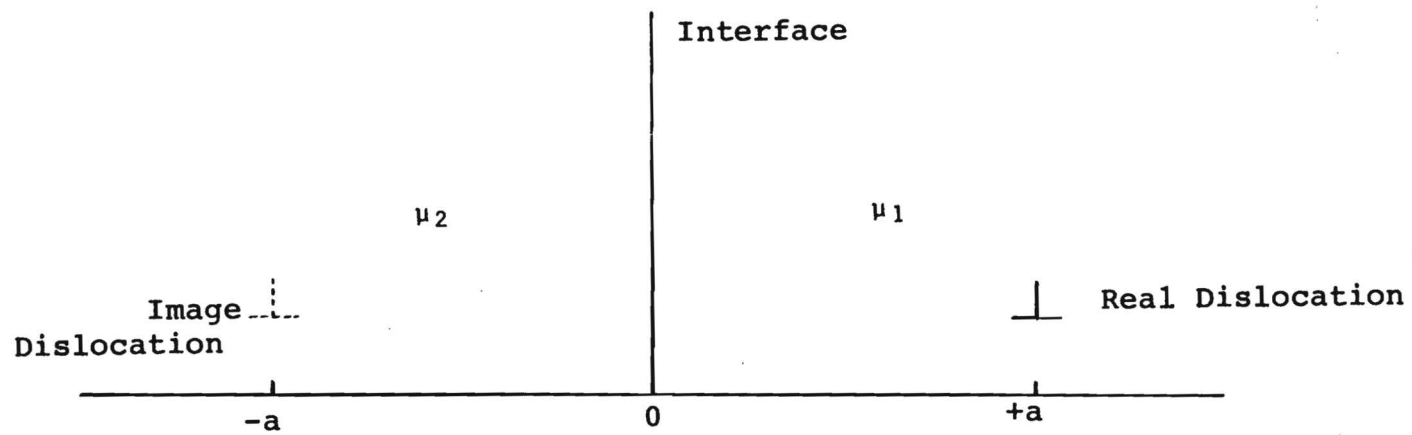


Figure 3. Dislocation and Image Near Interface  
of Two Semi-Infinite Solids

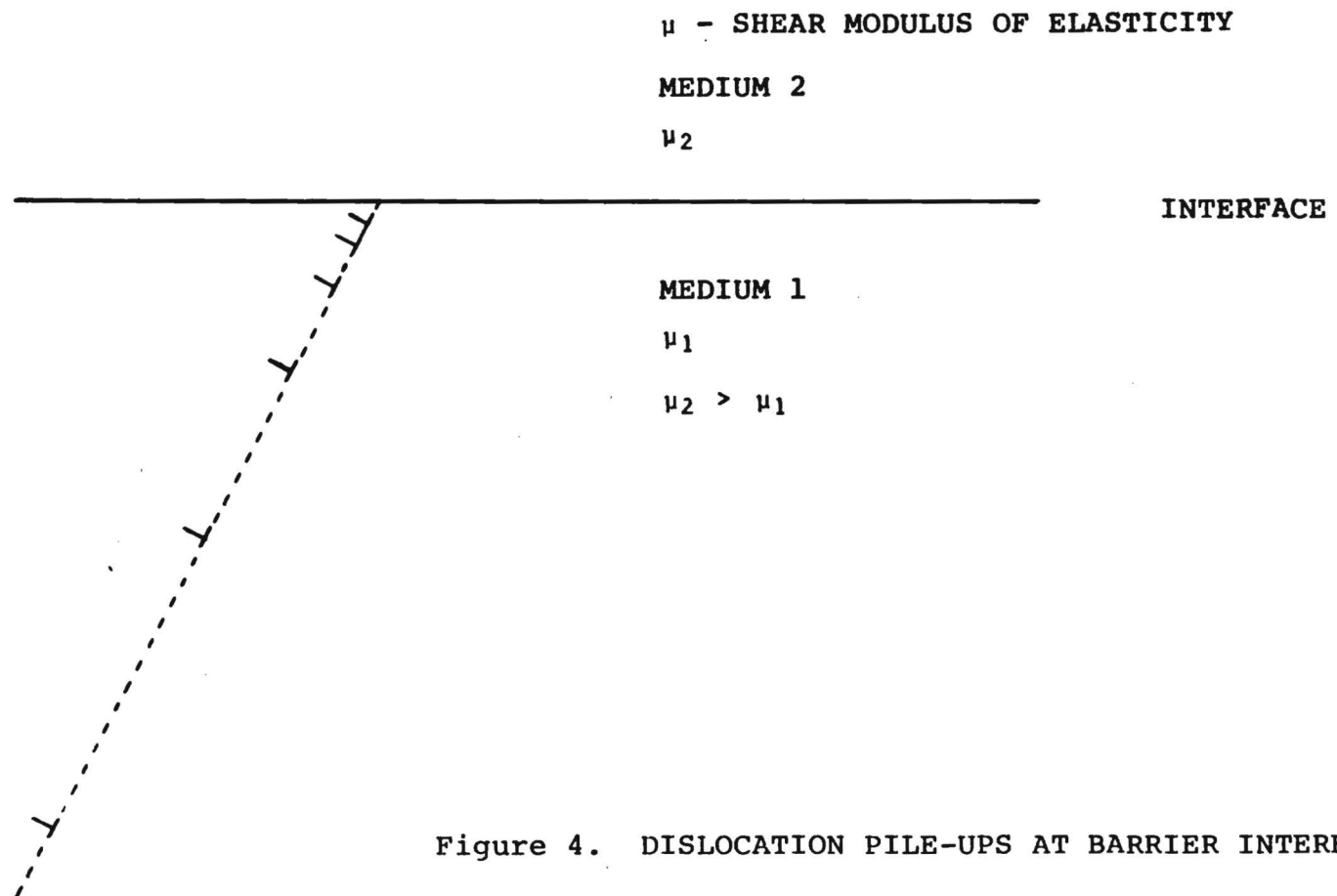


Figure 4. DISLOCATION PILE-UPS AT BARRIER INTERFACE

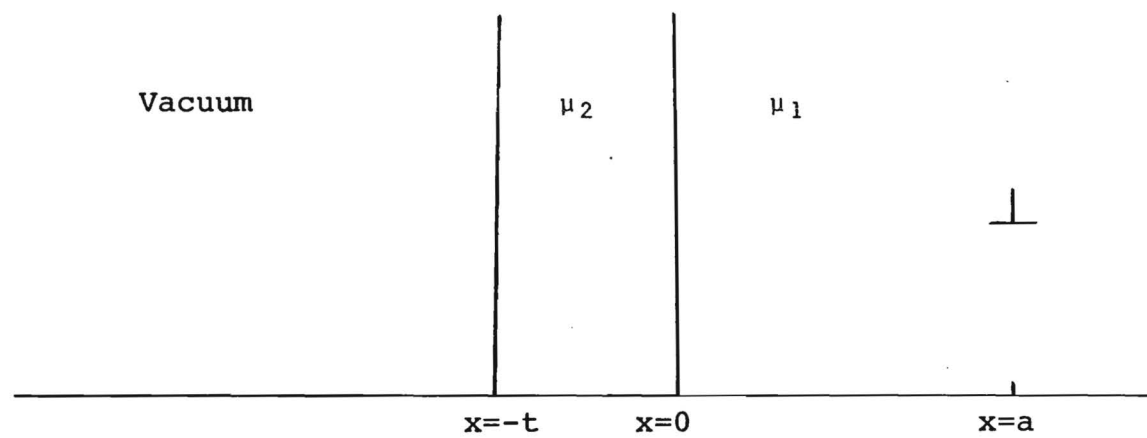


Figure 5. Schematic of Dislocation Near Interface of Surface Coating

a surface having a finite coating is

$$F = \frac{\mu_1 b^2}{4\pi a} \left[ \kappa - (1 - \kappa^2) \sum_{n=1}^{\infty} \frac{\kappa^{n-1}}{1+nr} \right] \quad (2)$$

where  $r = t/a$  and  $\kappa = (\mu_2 - \mu_1)/(\mu_2 + \mu_1)$  [25].

Assuming an aluminum-aluminum oxide interface, interaction forces were calculated for dislocations approaching the oxide from within the metal and are shown in Figure 6. At large distances from the interface, the dislocation is attracted towards the interface as it would be if the interface were a free surface. As a dislocation approaches the interface, the attractive force decreases, which is the opposite situation to that for a free surface. At a particular distance from the surface, based on substrate and coating material characteristics, the dislocation is in equilibrium and the force on the dislocation then becomes repulsive as the dislocation approaches an interface from that point. Calculations for smaller coating thicknesses indicate that the equilibrium distance decreases linearly with film thickness. The maximum repulsive force is determined by factors associated with the region of highly displaced crystal within the dislocation core. The effective shear stress,  $\tau$ , imposed by the interface is given by the

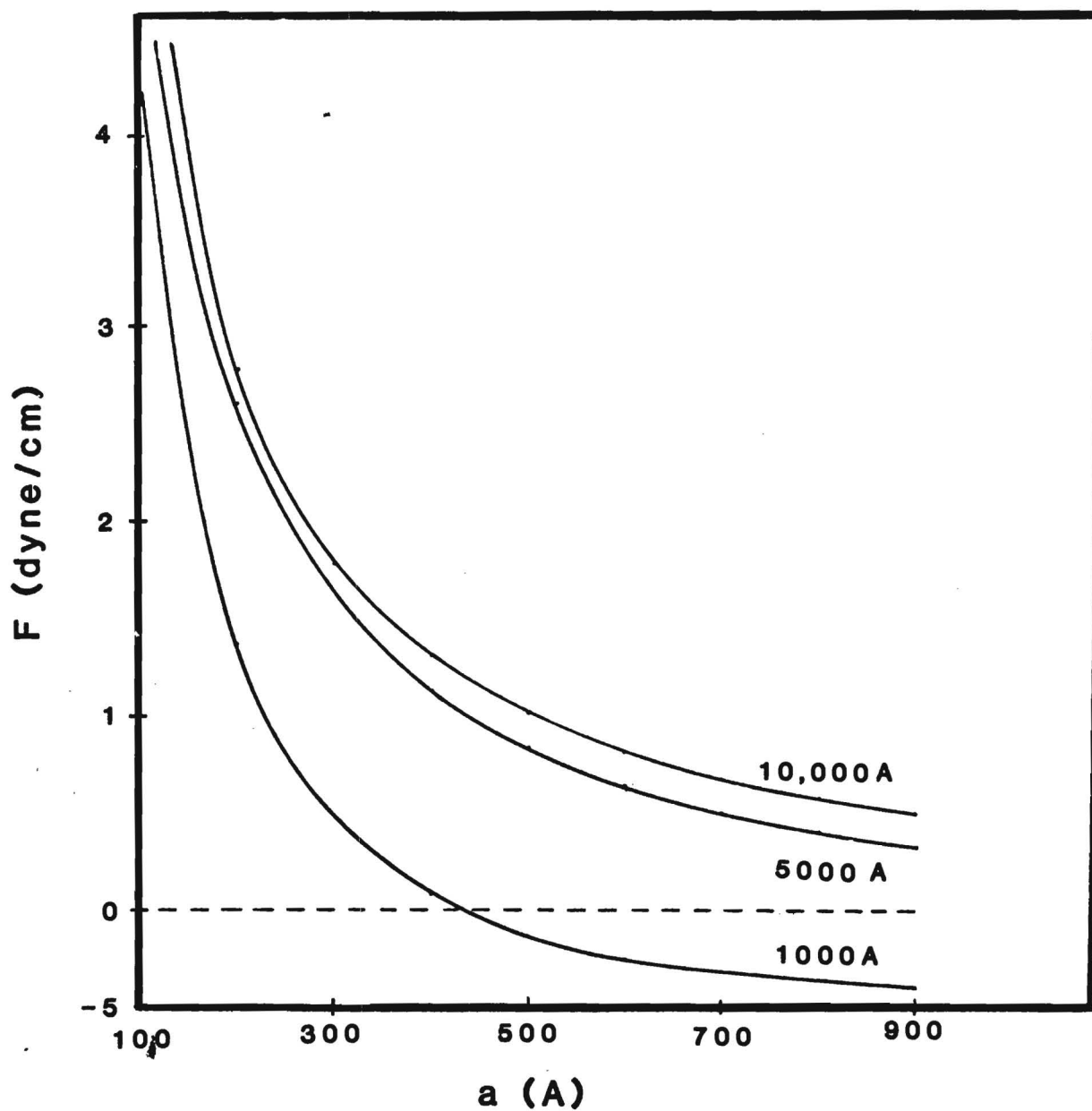


Figure 6. Curves of calculated forces acting on a dislocation in aluminum as a function of the dislocation distance,  $a$ , from the metal-oxide interface. Curves for several oxide thicknesses are shown here. Note the force equilibrium at about 450 Å for the 1000 Å film thickness curve. Similar calculations for thinner oxides show that the equilibrium distance decreases linearly with the film thickness below 1000 Å.

expression [22]

$$\tau = F/b \quad (3)$$

In real metal members, multiple dislocation interactions occur simultaneously. In addition, brittle metal oxide layers at the surfaces of bond wires fracture with the egress of slip bands, thereby modifying the interfacial configuration. The new surfaces created by the egress of slip bands provide significant interfacial energy changes which contribute to the mechanical strengthening in these thin members. Certainly it is not possible to represent a bond or a strip line with a single dislocation model, any more than one represents electrical conductivity with single electron transport models. However, the dislocation interface interaction calculations do provide an order of magnitude estimate of these effects. Further, a more detailed representation of the microcircuit interface configurations will help increase the precision of theoretical results. The mechanisms considered here, indeed, do control the strengthening processes in the various thin metal features employed in microelectronic structural devices.



## IV. ENVIRONMENTAL FATIGUE INVESTIGATIONS

### 4.1 INTRODUCTION

Bonded wire interconnects were cyclically stressed under selected environmental conditions. Configurations involving both dual bonds with the associated wire loop and single bonds were studied. The primary emphasis has been to apply strain-controlled flexures of bond wire loops to accelerate the stresses typically experienced by microcircuit wire bonds during temperature cycling associated with operating or other temperature variations. A major concern in the design of these experiments was properly representing the physical stress configurations generated with wire loop flexures while employing a fatigue test geometry which could be applied as consistently as possible with successive wire bond specimens.

The simple experimental arrangement shown in Figure 7 was adapted to the strain-controlled microtensile apparatus shown in Figure 8 for dual bond wire loop measurements. The microcircuit package is cyclically displaced via a micrometer screw drive mechanism. The fixture used to clasp the bond wire consists of a slot with an opening slightly larger than the diameter of the bond wire. The slot had been machined into the side of a stainless steel wire. The precision slot proved effective for clasping the bond wire without damaging it in order to apply and measure both compressive and tensile flexure forces at the apex of the wire loop. Small wire hooks with various adhesives were employed for a number of the early bond fatigue measurements. However, the adhesives were sometimes found to progressively degrade with either exposure to the environment or during mechanical cycling, particularly with current being conducted in the wire loop.

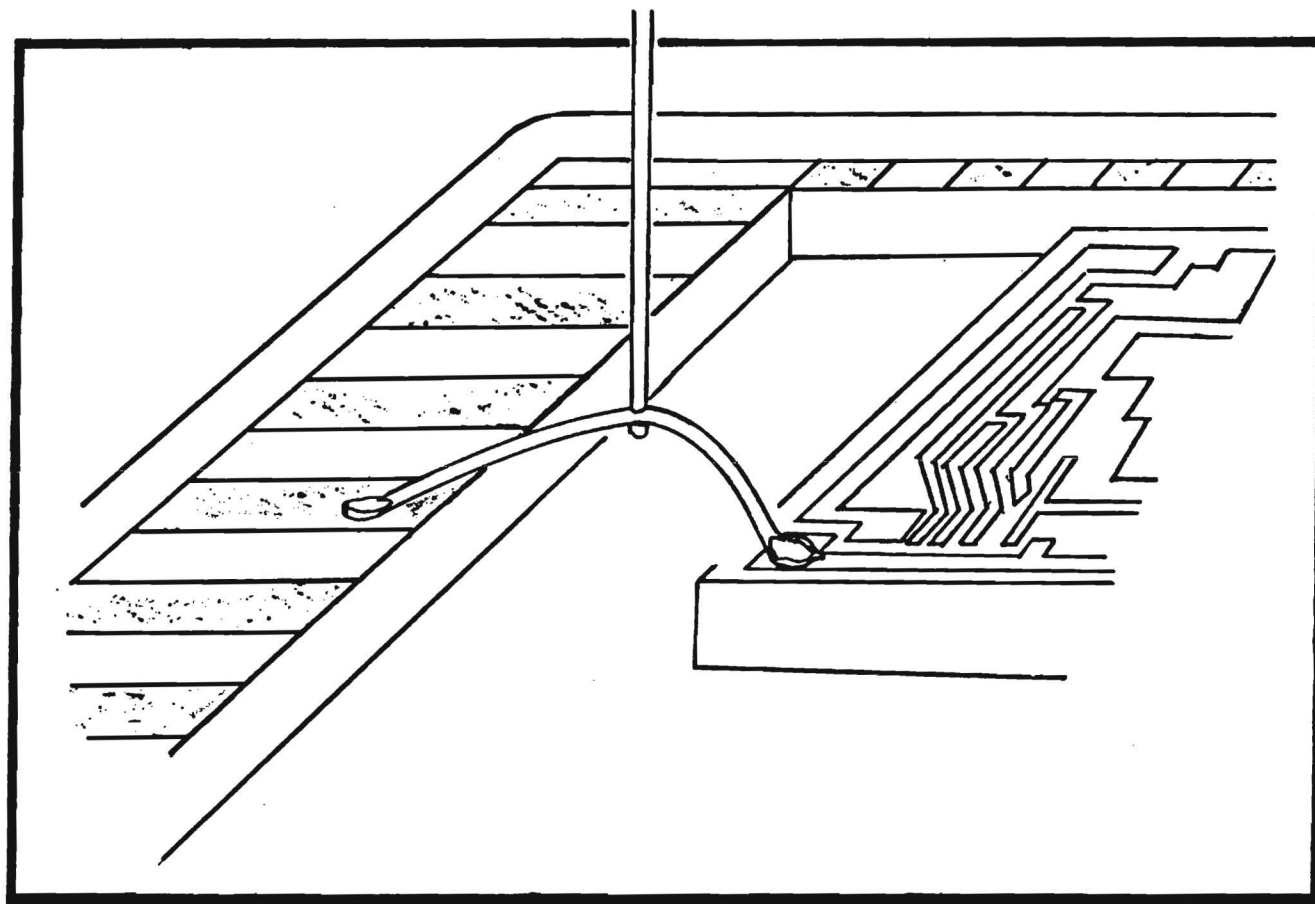


Figure 7. Schematic of the notched hook as it grasps the aluminum wire during a low cycle fatigue experiment. The wire is bonded in a standard DIP package.

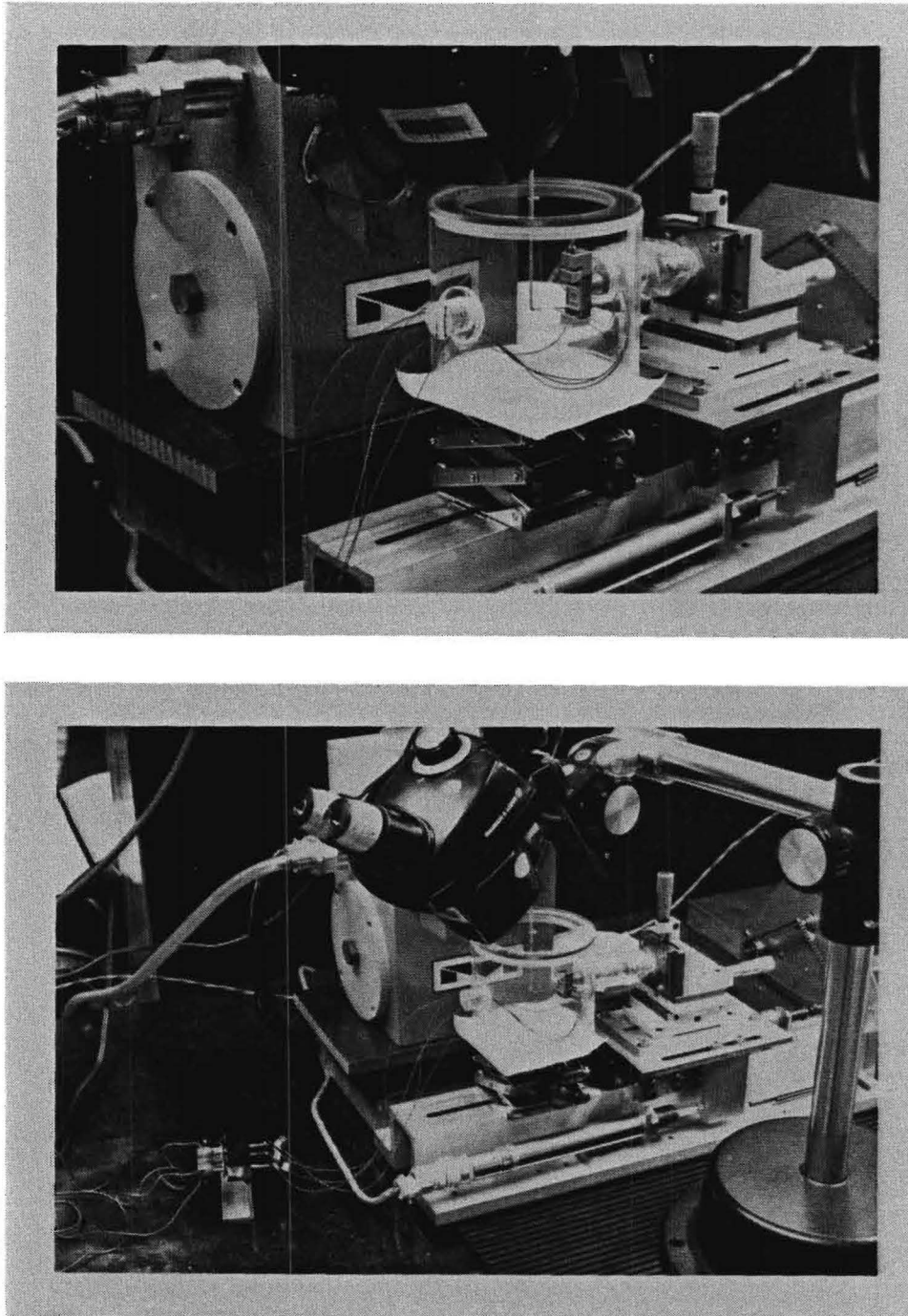


Figure 8. Strain controlled micromechanics apparatus shown in configuration for low cycle fatigue measurements on microcircuit wire bonds.

An automatic mechanism drives the package with a preselected cycling amplitude and strain rate. The flexure force is measured using a torque dynamometer having an air bearing to which a fine tube is attached as a lever arm. At the other end of this lever arm, attachment is made to a fine wire or tube having either a hook or the above described slot to clasp the bond wire. The package is supported by a mounting fixture attached to a three stage micropositioner. The micropositioner is used to bring the wire, viewed through a microscope, precisely to the location of the hook or slot without introducing any mechanical deformation to the very soft bond wire metal. The three dimension micropositioner is mounted on the micrometer screw driven slide stage of the micromechanics apparatus. Loop displacements are measured with a differential transformer transducer. Analog outputs for the flexure force and displacement are supplied to an X-Y recorder to display and record low-cycle mechanical hysteresis loops. The chamber shown in Figure 8 allows the necessary attachments to the wire and package while providing a means to expose specimens to a range of gaseous environments and vapors at atmospheric pressure. The chamber is transparent since the ability to continuously observe specimens through a microscope is important. Arrangements are also made for bringing electrical conductors into the chamber for applying current to the bond wire and for resistance measurements.

The number of cycles to failure for microcircuit wire bonds varies with cyclic stress amplitude, and is sometimes of the order of thousands of cycles. Consequently, this results in a large number of hysteresis loops being recorded for each specimen. Procedures were therefore evolved for selecting particular cycles for recording the hysteresis loops.

Selected mechanical hysteresis curves taken in sequence while cyclically stressing an aluminum ultrasonic wedge wire bond

are shown in Figure 9. These curves, which are reduced from 11x14 inch X-Y recorder plots, illustrate the typical recorded stress vs. strain behavior of the asymmetrical configuration where a bond wire loop is stressed in compression and tension with the attachment made at the apex of the wire loop and with the line of displacement approximately perpendicular to the wire.

A central problem associated with conducting an experimental fatigue investigation is in selecting the appropriate stress (or strain) amplitude and cyclical rate such that the experiments can be completed in a reasonable amount of time. The cyclic stress and time rate values normally associated with actual microcircuit environments, of course, involve fatigue time-to-failure periods which would be entirely impractical for experimental investigations. The purpose of these investigations was to contribute to the understanding of the degradation mechanisms involved in mechanical fatigue processes of the wire bonds in microelectronic devices. It was therefore desirable to accelerate the mechanical damage processes in a manner which did not appreciably alter the operation of the basic mechanisms within the materials. The concern here is with mechanisms of environmentally assisted fatigue which involve important time dependent environmental interactions in synergism with the mechanical stress field. Therefore, the accelerated fatigue cycling rates need to be as slow as practical for accumulating reliable experimental data on the operating mechanisms.

There have been a few experimental investigations reported in the technical literature of mechanical and thermal mechanical fatigue phenomena in microcircuit bond wires. However, none of the previous experiments have involved the necessary instrumentation to provide quantitative stress-strain data, as needed for evaluating low-cycle fatigue mechanisms. Earlier studies provided little information in terms of quantitative data

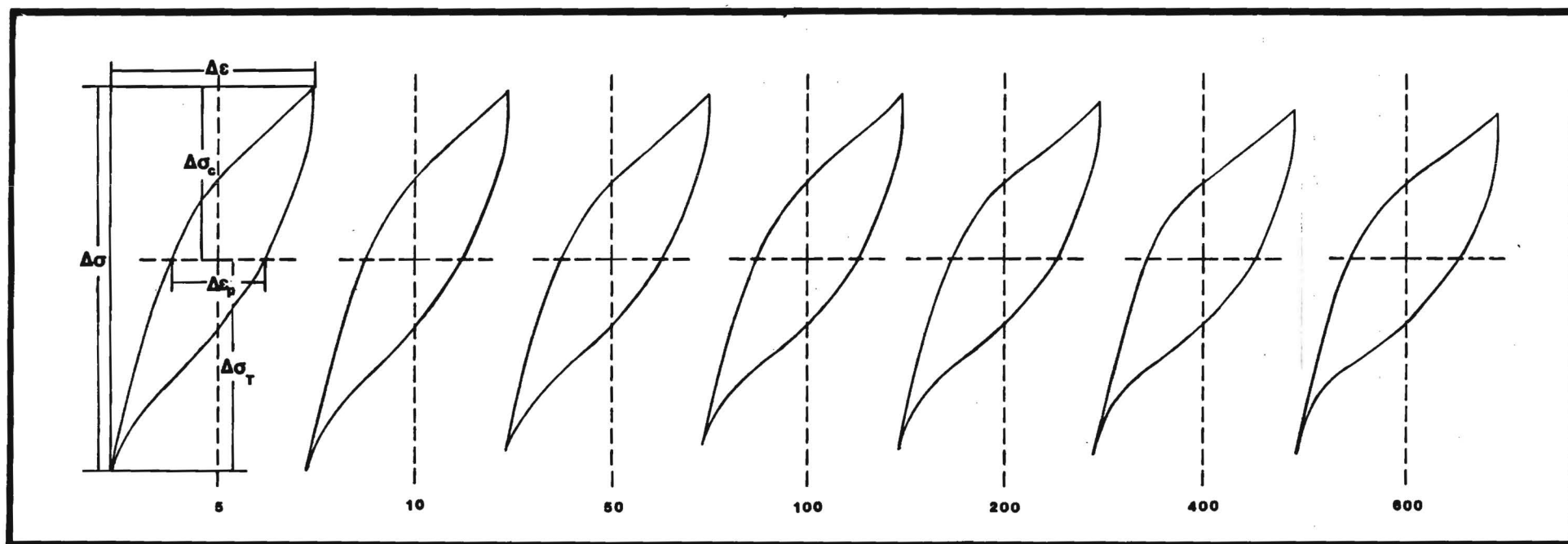


Figure 9. Reduced graphs of mechanical hysteresis loops for an aluminum wire bond recorded at indicated cyclical intervals in the fatigue life of the bond. The vertical axis is mechanical stress and the horizontal axis is strain. The stress and strain amplitudes, the instantaneous slopes of stress-strain behavior and the loop areas (hysteresis energy) are valuable parameters for interpreting damage mechanisms.

to design the experiments necessary to achieve the goals of the program. It therefore was required for us to empirically determine the optimum stress and strain amplitudes and cyclical rates which would be most appropriate for environmental fatigue investigations on VLSI wire bond interconnections.

Thermal cycling studies conducted by Fitch [4] on large numbers of packaged integrated circuits (ICs) showed significant wire bond fatigue failure occurring after 1,000 to 4,000 temperature cycles. He noted that microstructural damage occurred in wire bonds after only a few cycles. Fitch also found that the circuits having longer bond wires experienced enhanced failure rates.

The bond wires involved with VLSI devices are generally longer than those in the LSI circuits studied by Fitch. The temperature coefficient of expansion for aluminum,  $25 \times 10^{-6}/\text{C}$  degree, is considerably larger than that of most of the other materials used in the fabrication of microcircuits. For example, the thermal expansion coefficient of aluminum is about ten times the value,  $3 \times 10^{-6}/\text{C}$  degree, for silicon. Thermal excursions in wire interconnects of over  $100^\circ\text{C}$  are quite common. Depending upon details of particular VLSI loop geometries, the thermal expansion induced deflection of a bond wire loop normal to and at the apex of the loop would be 50 to 300 microns. Our empirical fatigue tests on wire bonds at various strain levels in the relatively innocuous laboratory air environment indicated that the amplitude range provided mechanical failure time or fatigue lives ranging from a few hundred to several thousand cycles, depending upon bonding parameters. These values correspond well with the IC wire bond wear-out temperature cycling data of Fitch. Our calculations of thermal mechanical induced stresses based on his temperature excursions and assumed bond wire geometries are in reasonable agreement with the conditions used in this study. It



was accordingly concluded that the bond stress and strain levels which result from direct mechanical displacement of the wire apex in this range, would be appropriate for the quantitative wire bond fatigue studies. Most of our environmental wire bond fatigue life experiments were therefore conducted employing strain displacement amplitudes of between 50-150 microns and with 50 second cycle durations.

Single bond fatigue experiments were also conducted using the apparatus shown in Figure 8. Bonds to the chip pad and to the package post were individually subjected to cyclical stressing and the resulting hysteresis loops recorded to evaluate the low cycle fatigue parameters for this configuration. This set of single bond fatigue measurements was primarily a study of annealing effects, with the bonds aged in an oven at 110 C for selected time intervals prior to mechanical cycling. Annealing was expected to mechanically soften the material while accelerating the growth of silicon precipitates in the wire and pad metals and promoting interdiffusion at the Al-Au interface on the post. The single bond fatigue geometry also presented a different stress arrangement from that of a wire loop bonded at each end.

A series of single bond fatigue experiments was carried out at very small stress amplitudes in order to investigate the effects of environmental conditions at these stress levels. A special apparatus was required to conduct the small force mechanical measurements involved here. Whereas the wire loop experiments with standard dual bonds involved force amplitudes up to about 1,000 dynes, and the single bond forces discussed in the previous paragraph were about 1/5 of those with dual bonds, the small stress experiments involve amplitudes on the order of 15 dynes. The ultimate sensitivity of the micromechanics apparatus adapted for these measurements was about  $1 \times 10^{-3}$  dyne, thus



providing the desired small force capability needed here. A small d'Arsonval galvanometer is employed as the force transducer. An electro-optical system detects orientation of the galvanometer coil and an operational amplifier is employed to automatically balance the applied mechanical torque resulting from bond stresses by supplying an appropriate current to the coil. A special low noise drive mechanism was designed and fabricated to accomplish the cyclical translation needed for the small amplitude fatigue measurements. The sensitivity of these experiments proved sufficient to be able to follow the progression of chlorine attack on cycled single bonds. Cyclic deformation could thus be arrested so that bonds could subsequently be fractured within the ultra high vacuum of the scanning AES for the detailed analysis of fracture surfaces.

## 4.2 BOND FATIGUE

A typical mechanical hysteresis loop measured for an aluminum wedge bond is shown in Figure 10 with the stress and strain amplitudes for compression and tension modes as indicated. This particular curve is an actual loop taken for the 5th cycle of an Al-Al wedge bond. The area of the curve represents the mechanical energy absorbed by the wire interconnection during a single complete cycle. The absorbed energy is dissipated in plastic deformation processes occurring within the overall bond wire loop material. However, microscopic observation of the flexure motions in different regions of a wire loop and studies of fatigue degradation in numerous wire bonds reveal that most of this energy is absorbed either within or in the neighborhood of the heel region of the bonds located at the two ends of the wire loop. In contrast, the corresponding stress-strain behavior for a similar wire loop stressed only in the elastic region would yield an essentially closed hysteresis loop. Nearly closed hysteresis loops were obtained for very small stress studies carried out on single Al-Al bonds, where most of the strain was elastic.

The cyclic stress-response data from aluminum and gold wire bond materials clearly demonstrate that significant plastic deformation is occurring with the strain amplitudes employed in this study and that finite hysteresis occurs even with considerably smaller strain amplitudes. Low cycle fatigue damage mechanisms are thus operative in the wire bond during each power (temperature) excursion greater than some small increment. In addition to the loop parameters mentioned above, the slopes of the individual stress-response curves provide data which are useful for evaluating the work-hardening, or softening, occurring in the bond regions during the course of a fatigue cycle.

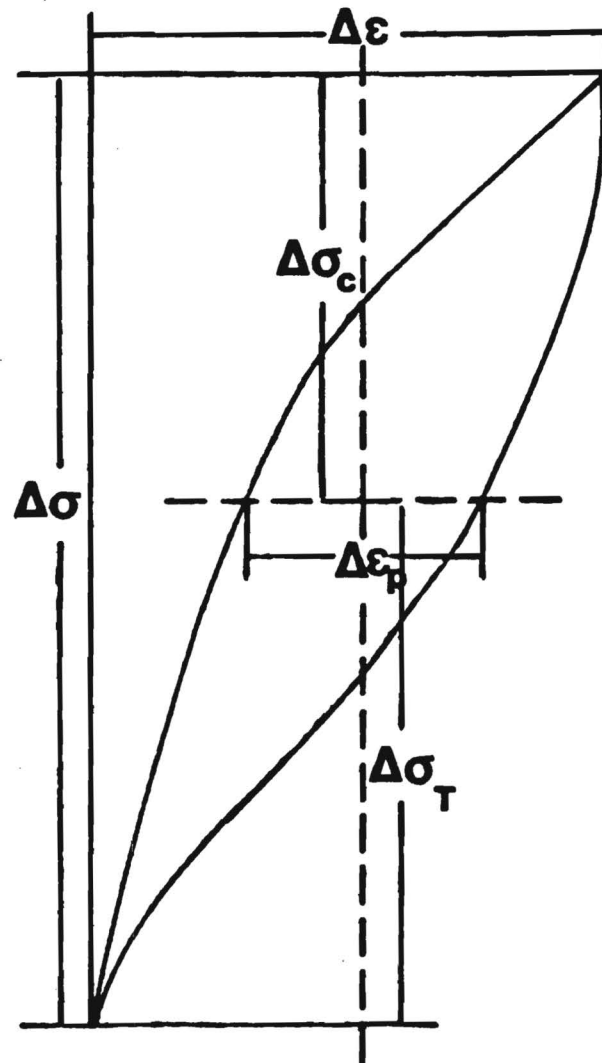


Figure 10. Shows a hysteresis loop as it is measured for plastic strain and peak tensile and compressive stresses.

Cyclic response curves for three bond wires mechanically cycled in the laboratory air (relative humidity ~50 %) environment are shown in Figure 11. The stress amplitudes taken from hysteresis curves during the fatigue life of a bond are plotted as a function of the cycle number. The plastic strain amplitude reflects cyclical "strengthening" or "weakening" effects which occur in the heel region of the bond as cycling progresses. Figures 12 and 13 show the manner in which the measured peak stress varies as a function of the cycle number over the fatigue lives in laboratory air of two supposedly identical aluminum-aluminum ultrasonically bonded wires. In each figure, the upper curve represents the maximum stress on the hysteresis loop in the tension (pulling) mode while the lower curves are for the compression mode. The mechanisms responsible for this behavior are determined by microstructural modifications induced in the bonded metals during mechanical cycling and are discussed in greater detail later.

The cross section of a wire bond is both very small and non-uniform such that it is very difficult to obtain meaningful values for cross sectional areas under these conditions. In addition, the mechanical stress distribution within the material of a flexed wire bond is quite complex. For these reasons, precise calculations of relevant engineering stress values are not feasible in flexed microcircuit wire bonds even though the force measurements are relatively precise. However, highly approximate estimates of the effective mechanical stresses are attempted in some of our data in order to make comparisons with corresponding data on bulk metals. The key factor for these studies was maintaining consistency in bonding parameters and bond geometry in order to allow direct comparisons of performance under the various environmental conditions.

The cyclic response curves taken for a set of similar

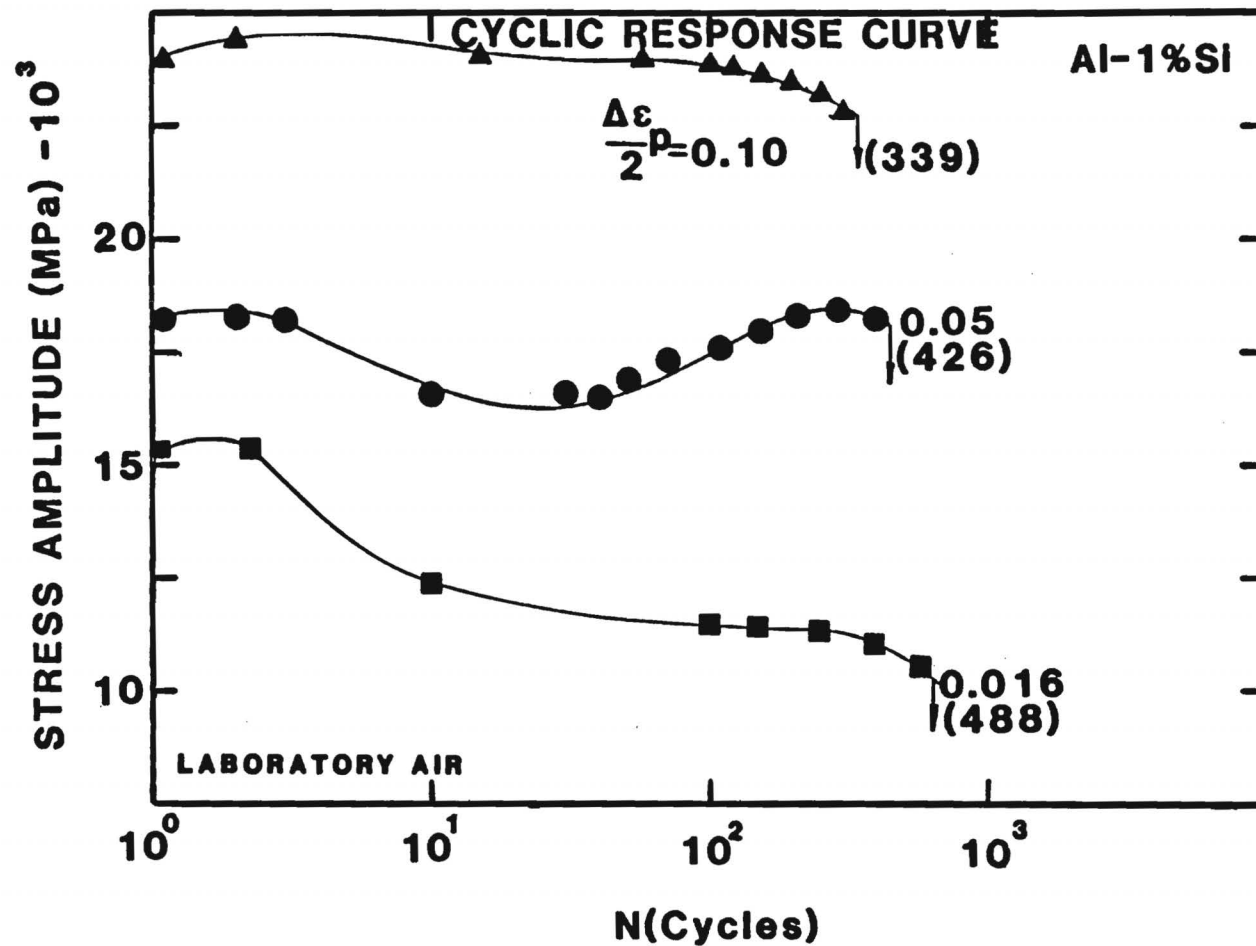


Figure 11. Cyclic response curve for the Al-1%Si bond wire fatigued in laboratory air at different plastic strain amplitudes. Number in parenthesis denotes cycles to failure ( $N_f$ ).

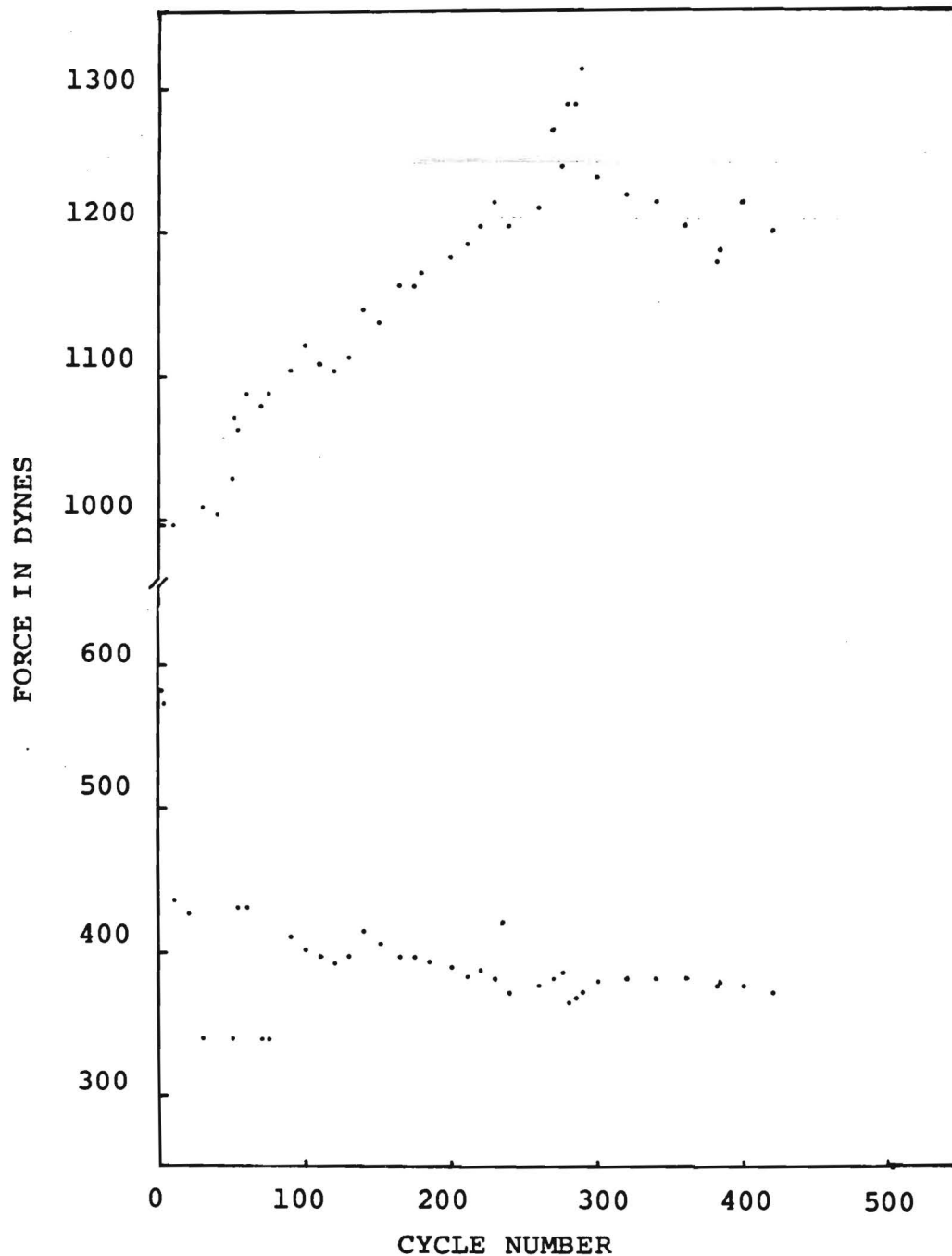


Figure 12. Peak stresses measured as a function of the cycle number of an Al-Al wire bond specimen fatigued in air. The upper curve is for tension (pulling) and the lower curve compression. The bond is found to cyclically work-harden in the tension mode for the first 300 cycles, followed by gradual work softening to failure at about 400 cycles. The compression mode shows only work softening.

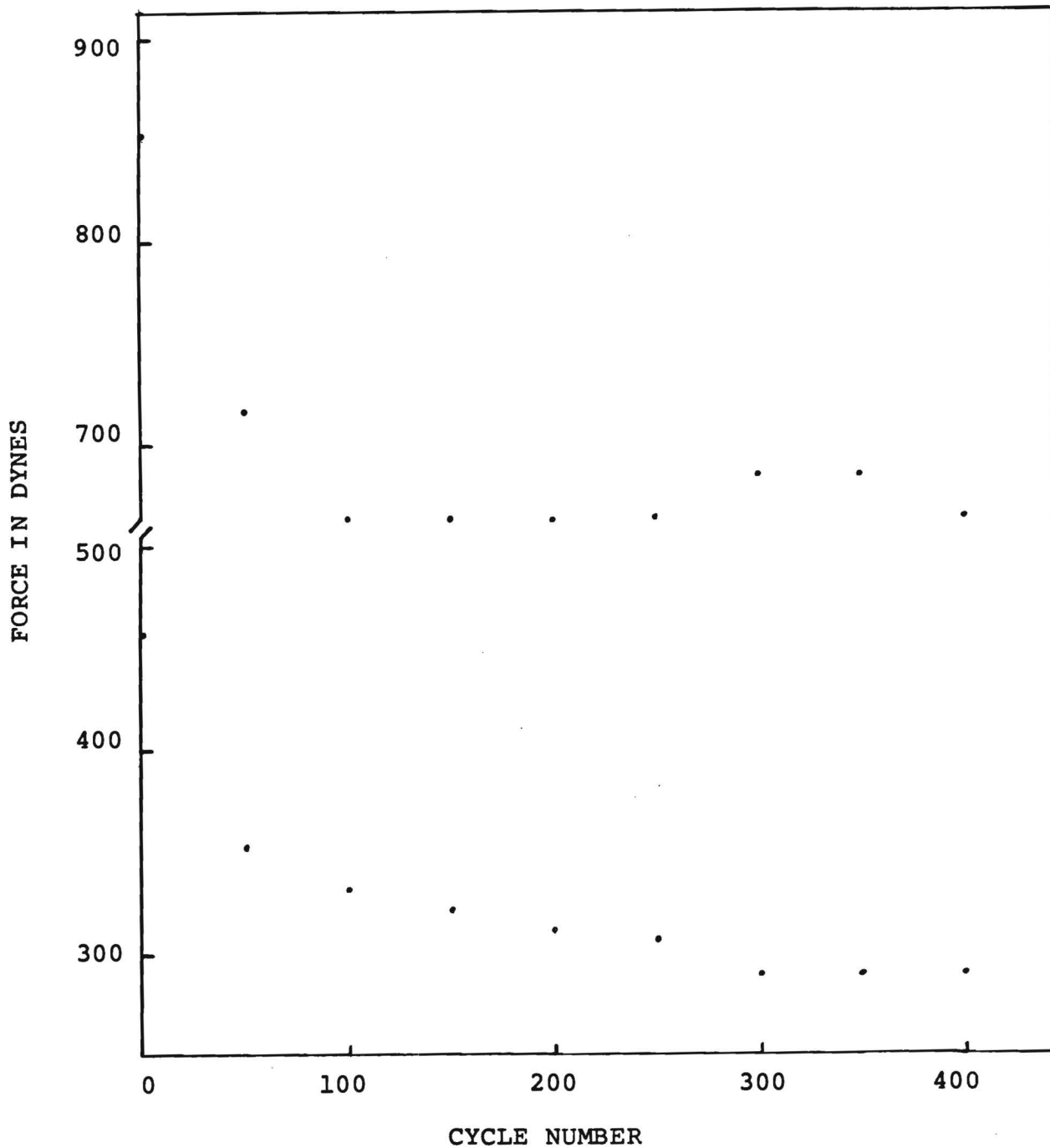


Figure 13. Peak stresses measured as a function of the cycle number of an Al-Al wire bond specimen fatigued in air. The upper curve is from the tension (pulling) mode and the lower curve is from the compression mode. The measurements show significant cyclical work softening occurring during the first 100 cycles in both the tension and compression modes. The bond subsequently hardens in tension until just prior to fracture.

aluminum wire bonds fatigued-to-failure at the same rate and wire loop displacement amplitude in an environment very close to 100 % relative humidity, are shown in Figure 14. The bonds cycled in the high humidity environment have generally failed earlier than those under otherwise identical circumstances. Extensive scatter was observed in the fatigue data for different bonds such that some wire bonds cycled in an environment having high humidity exhibited fatigue life times somewhat longer (over 400 cycles) than those indicated above. However, comparative data for the two sets of wire bonds shown in Figure 14 are representative of the overall trend observed in these environments at various strain levels. The rapid rate of cyclic softening is characteristic of the aluminum bonds fatigued in the humid environment. It was also observed that the mechanical hysteresis loop areas for bonds cycled in the humid environment were generally smaller than those cycled in the seemingly inert dry air.

A third set of cyclic response curves is shown in Figure 15 for wires fatigued under mechanical conditions identical to those discussed previously, except that d.c. currents at the indicated levels were conducted through the bonds as they were mechanically cycled. Progressive cyclic softening occurred from the onset of fatigue deformation. Bonds cycled at higher current levels, showed evidence of rapid cyclic degradation, as anticipated. However, significant variations in behavior were also observed. Figures 16-18 highlight the comparison of peak stresses taken from the low-cycle hysteresis data for three aluminum-aluminum wire bond specimens fatigued, respectively, with bond currents of 20 ma, 300 ma and 350 ma. The particular bond cycled to failure with a current of 200 ma demonstrated increased softening resulting, as a consequence, in early failure. The specimen of Figure 18 cycled with a current of 350 ma exhibited uniform work



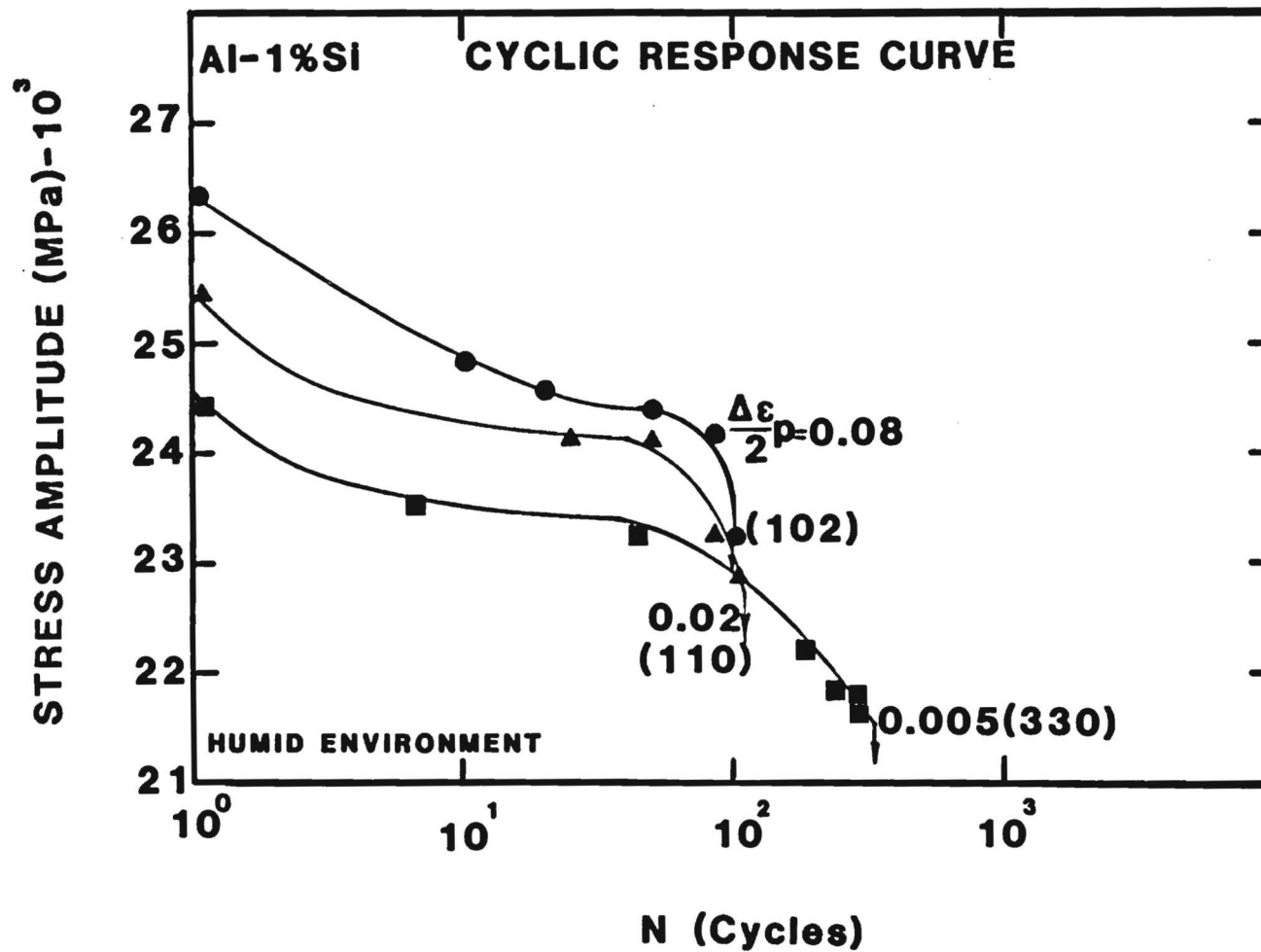


Figure 14. Cyclic response curve for the Al-1%Si bond wire showing progressive softening to failure at all plastic strain amplitudes in the humid environment. Number in parenthesis denotes cycles to failure ( $N_f$ ).

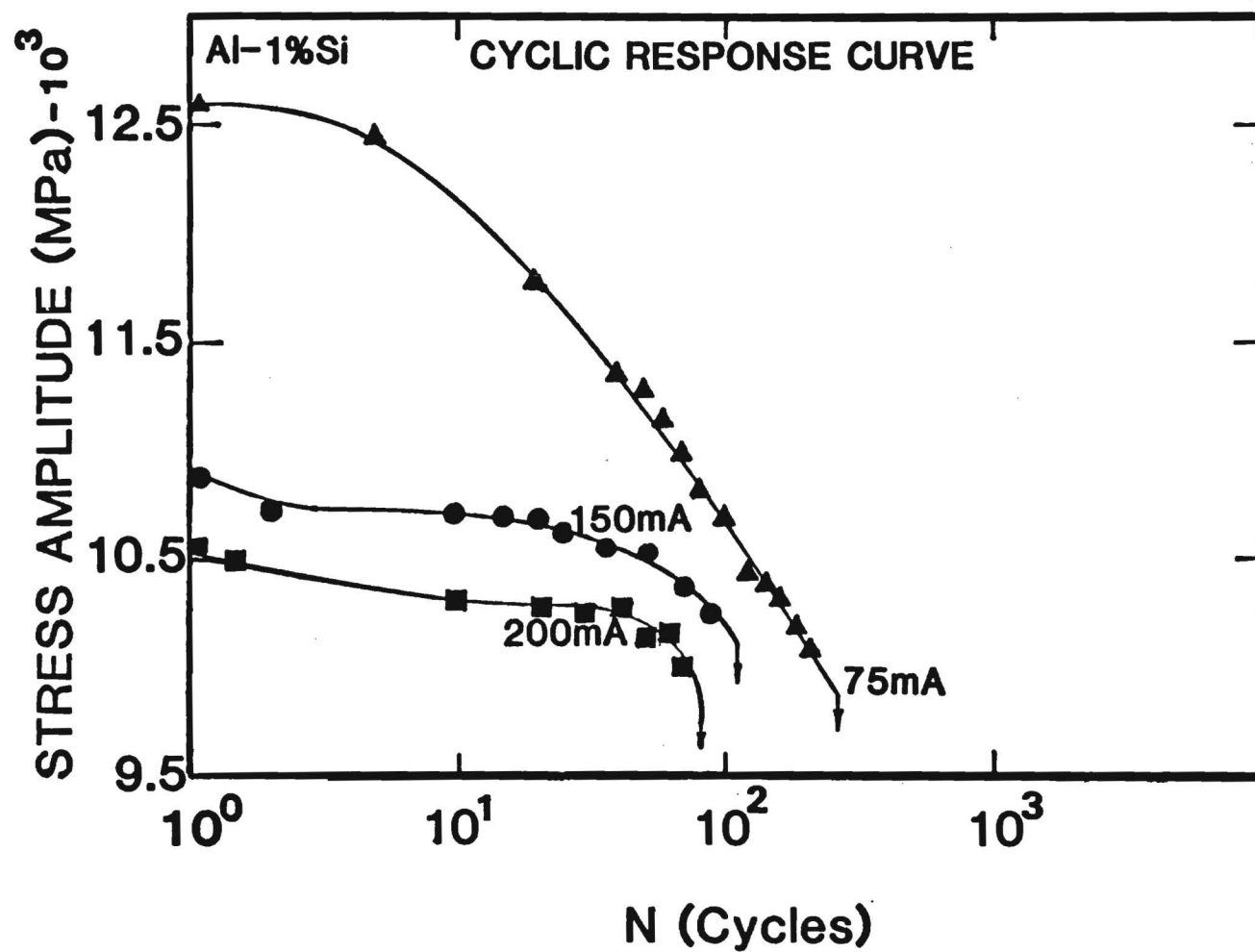


Figure 15. Cyclic response curve for the Al-1%Si bond wire showing cyclic softening to failure for the different values of electric current.

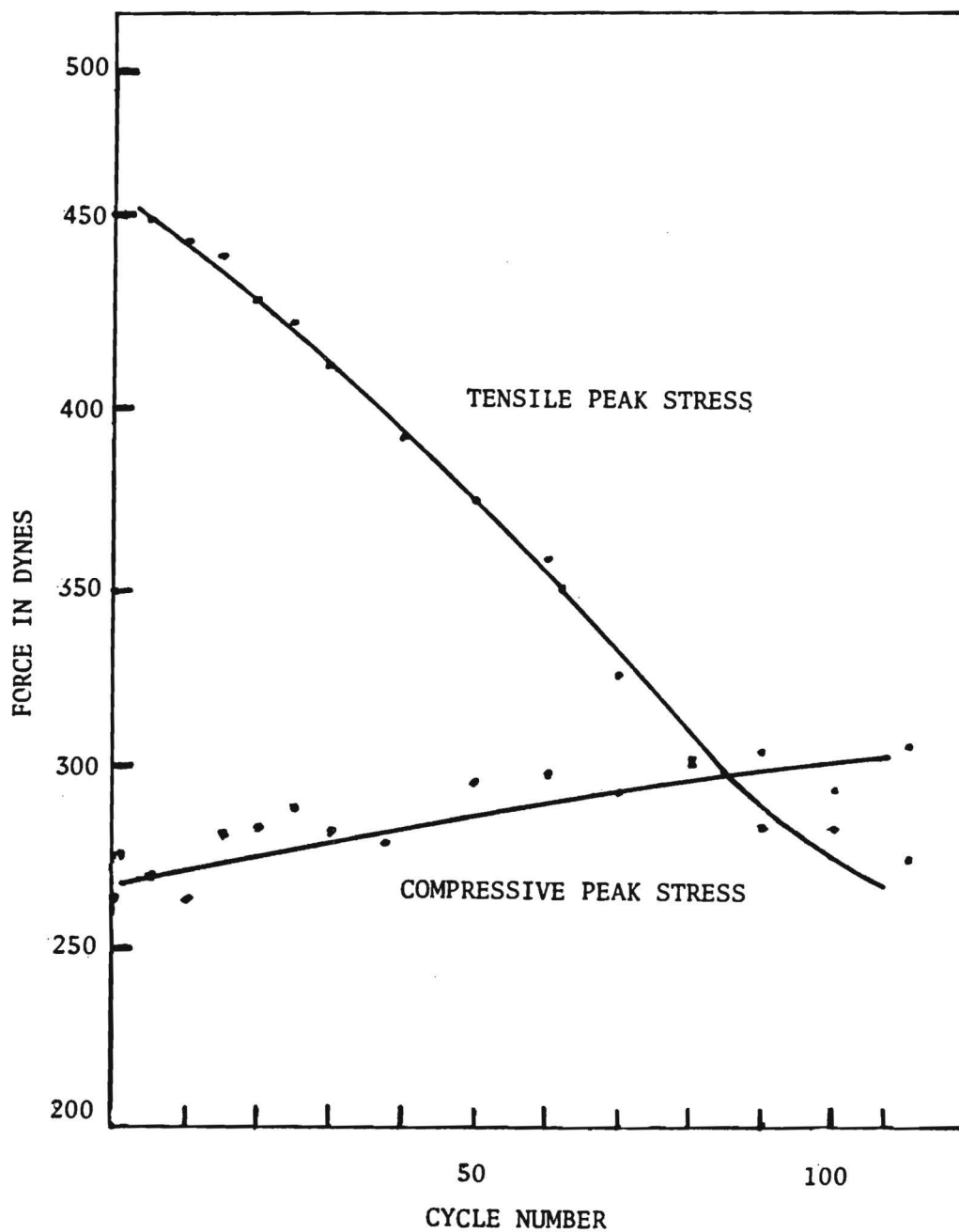


Figure 16. Peak cyclical force values measured versus cycle number for an aluminum-aluminum bond conducting 200mA current. The tensile peak rapidly softens to early failure.

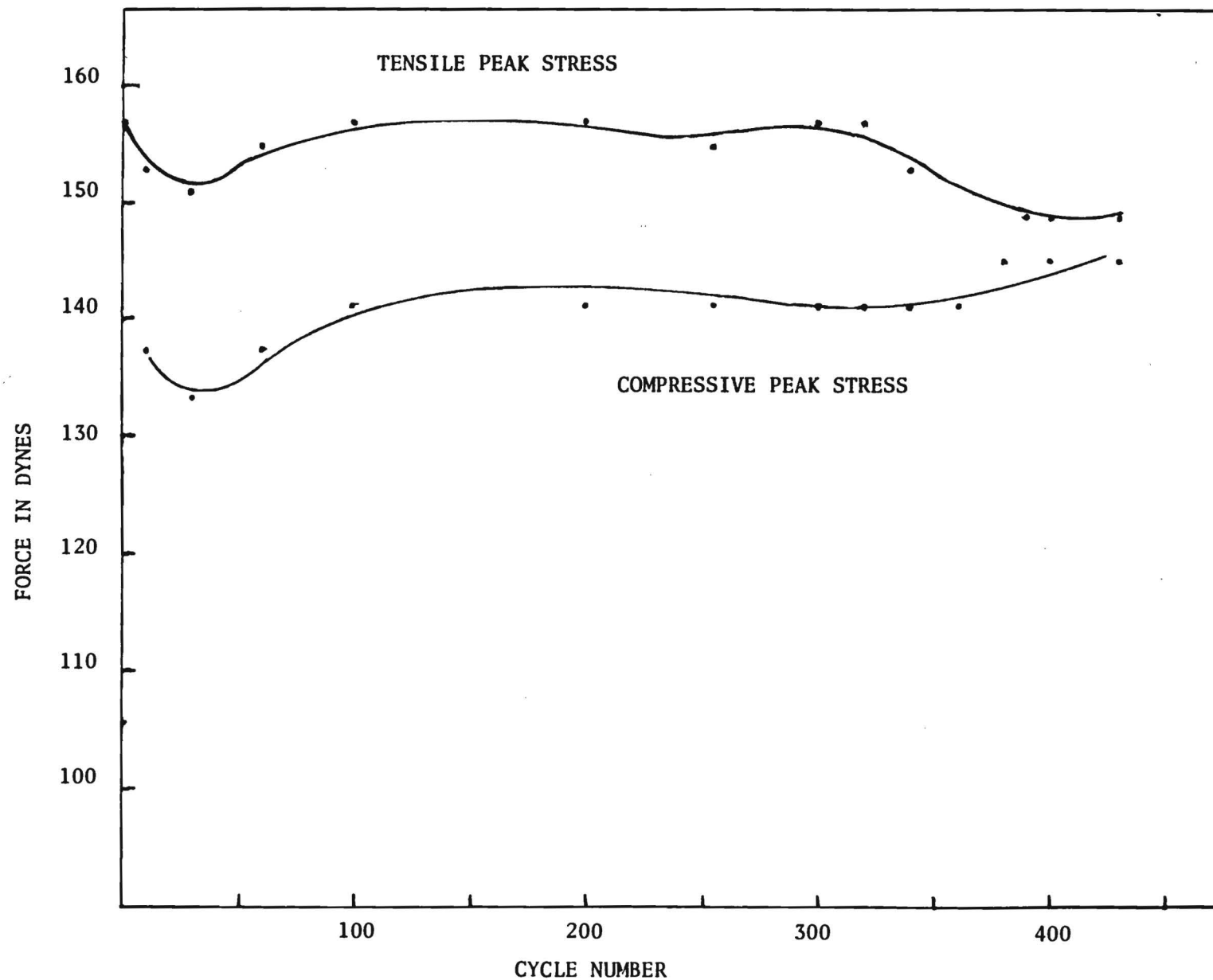


Figure 17. Plots of tensile and compressive peak stresses as a function of cycle number for an aluminum bond conducting 300mA current.

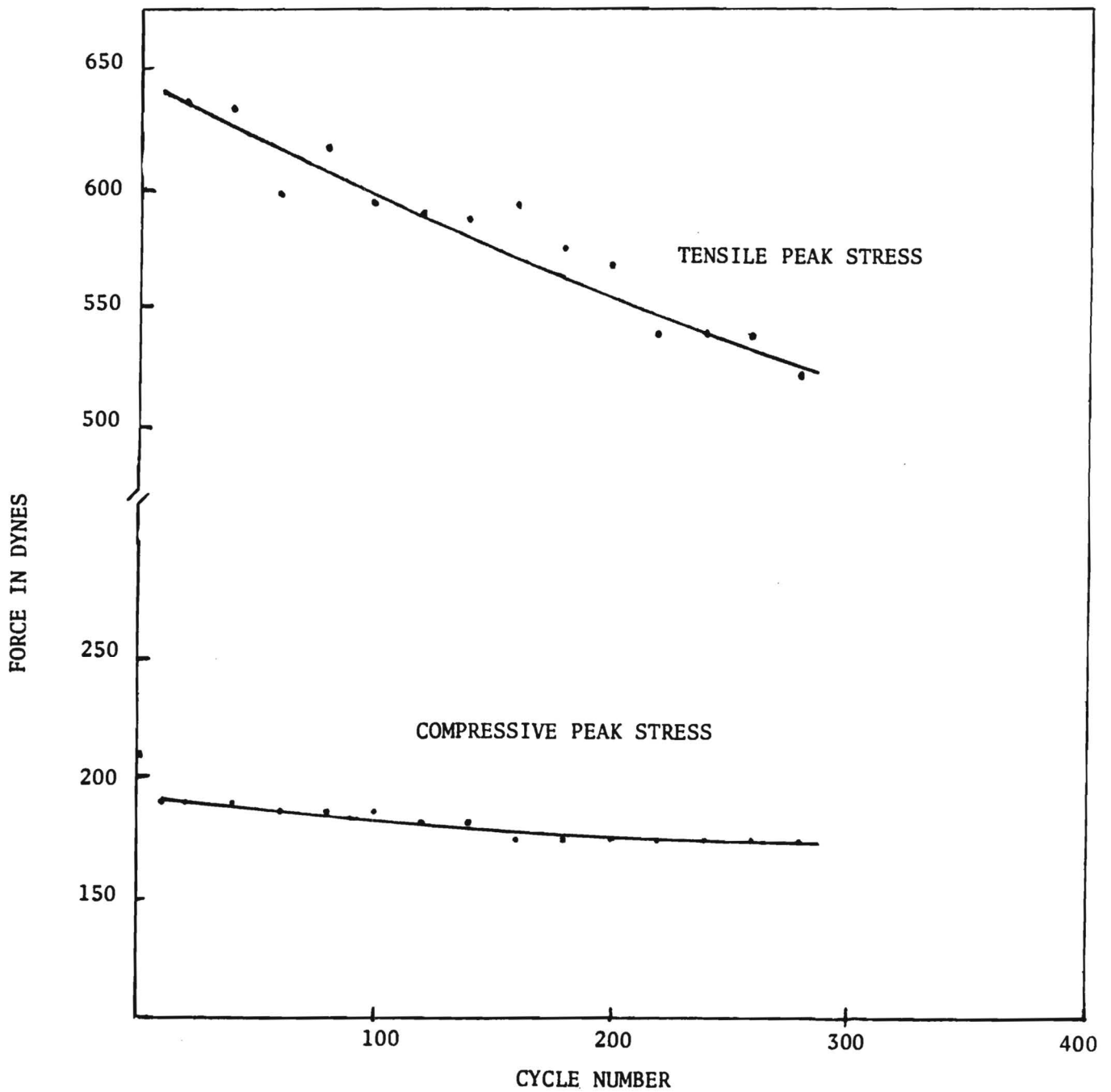


Figure 18. Tensile and compressive peak stresses plotted as a function of cycle number for an aluminum-aluminum bond conducting a 350mA current.

softening in both compressive and tensile modes. Figure 18 elucidates the behavior of the aluminum-aluminum bond at 300 ma, showing regions of work hardening and progressive softening in both compression and tension. The force levels were also observed to be much smaller than normal. However, the bond remained "good" for over 400 cycles. A plot of the hysteresis loop energy per cycle as a function of the cycle number for an aluminum wedge bond fatigued with 50 ma is shown in Figure 19. The loop energy is seen to decrease during the early phases of the bond life, but subsequently increases to an elevated value prior to final failure. Hysteresis loop energies measured for three specimens cycled at currents of 300 ma and greater are shown in Figure 20. Small differences seen between successive loops taken every 20-30 cycles have been consistently observed in wire bond data and are attributed to microstructural modifications in the bond region. Corresponding peak stresses and hysteresis energies for a thermosonically ball bonded gold (to aluminum) wire are shown for comparison in Figures 21 and 22.

Scanning electron micrographs shown in Figure 23 reveal the fracture surface features of an aluminum wire bond mechanically cycled to failure while conducting a small current. The fracture occurred at the thin heel region of the bond. The 10 ma. current through the wire bond during fatigue cycling did not appreciably affect the fatigue degradation process. The current was used to monitor changes in electrical resistance of the bond through a four point probe arrangement, as the cyclic degradation progressed. Traces of intergranular crack propagation were evident from the fracture surfaces. In addition, regions indicating a viscous flow behavior were also observed. The cracks responsible for inducing a failure appear to have been initiated at the surface, propagating intergranularly to failure. During the latter stages of cyclic deformation, the central

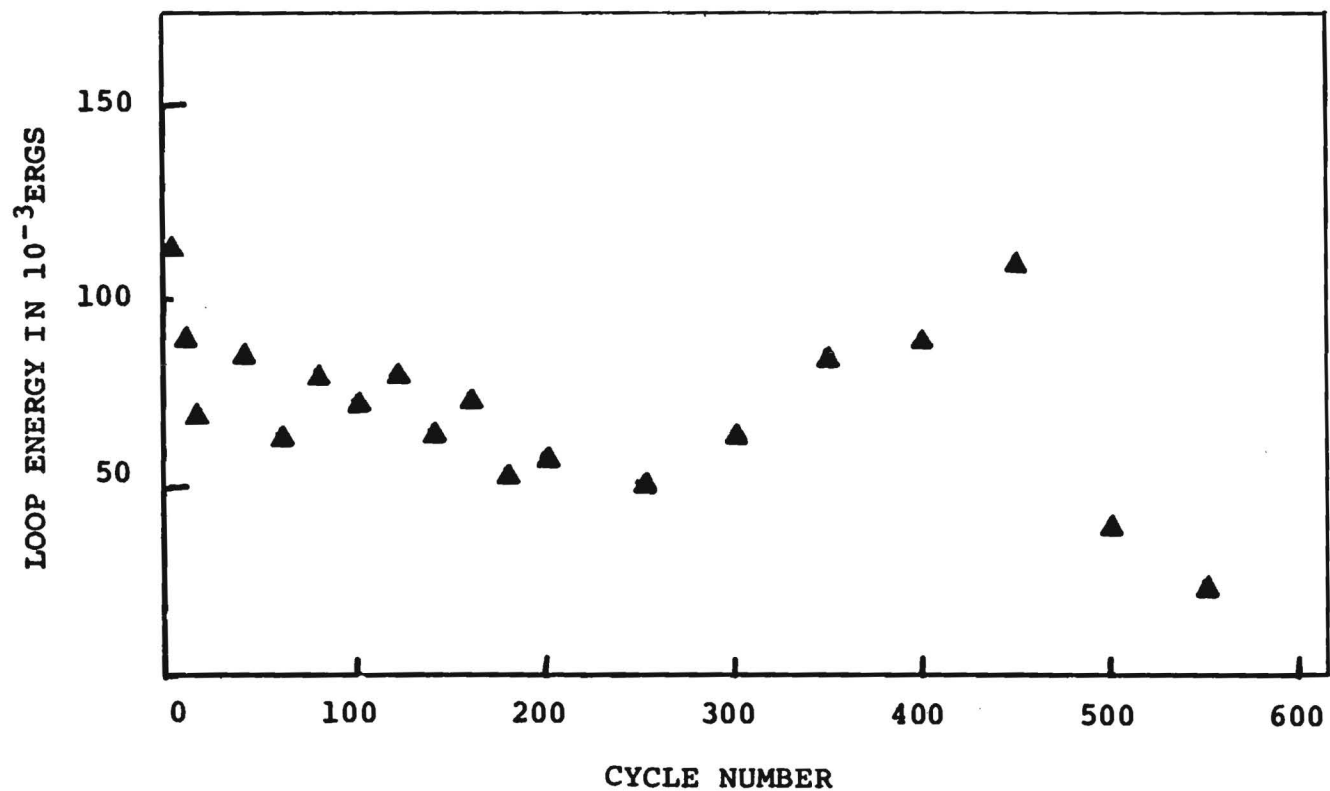


Figure 19. Hysteresis loop energy for an aluminum-aluminum wire bond cycled with 50mA d.c. current.

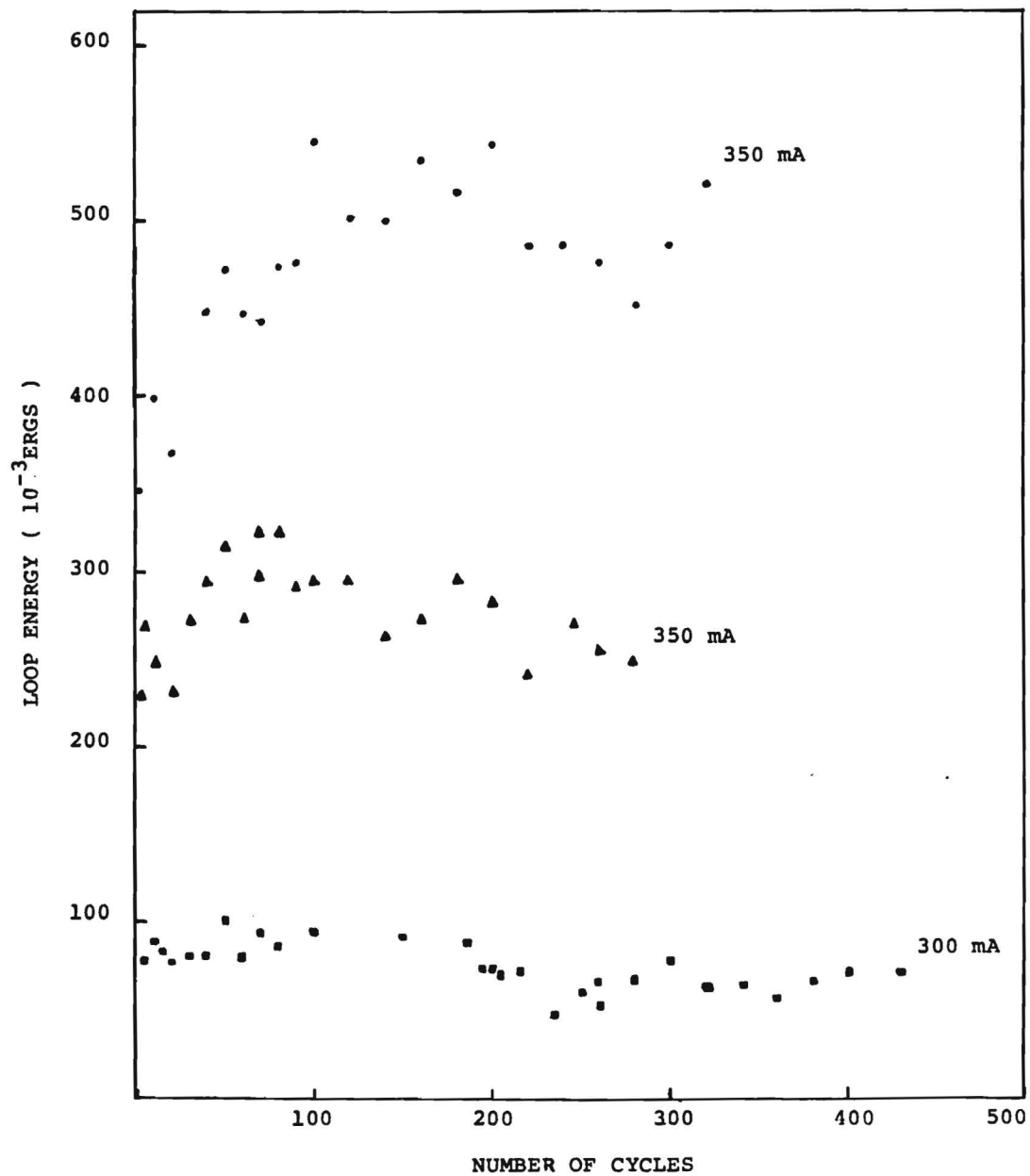


Figure 20. Low cycle fatigue hysteresis loop energies measured as a function of cycle number for three aluminum-aluminum wire bonds mechanically cycled while conducting currents at the indicated level.



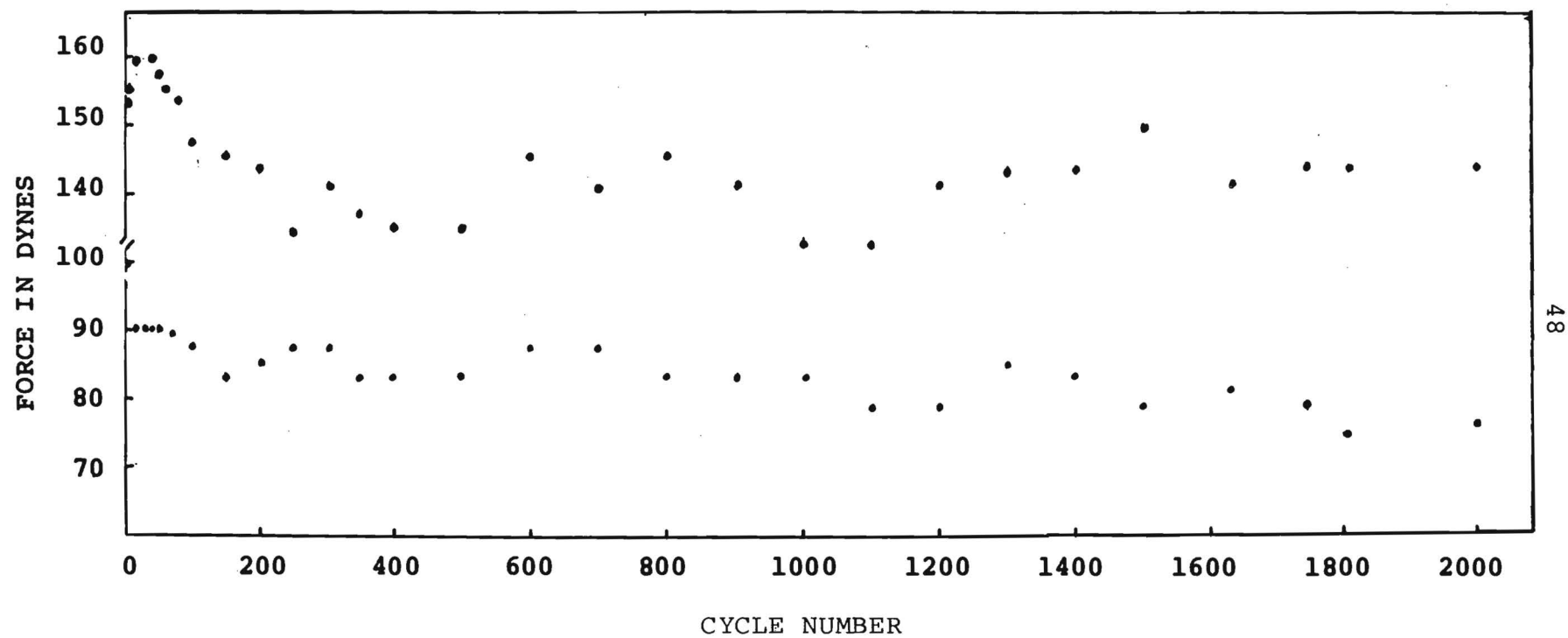


Figure 21. Peak force values measured for a gold ball bond (to aluminum.)

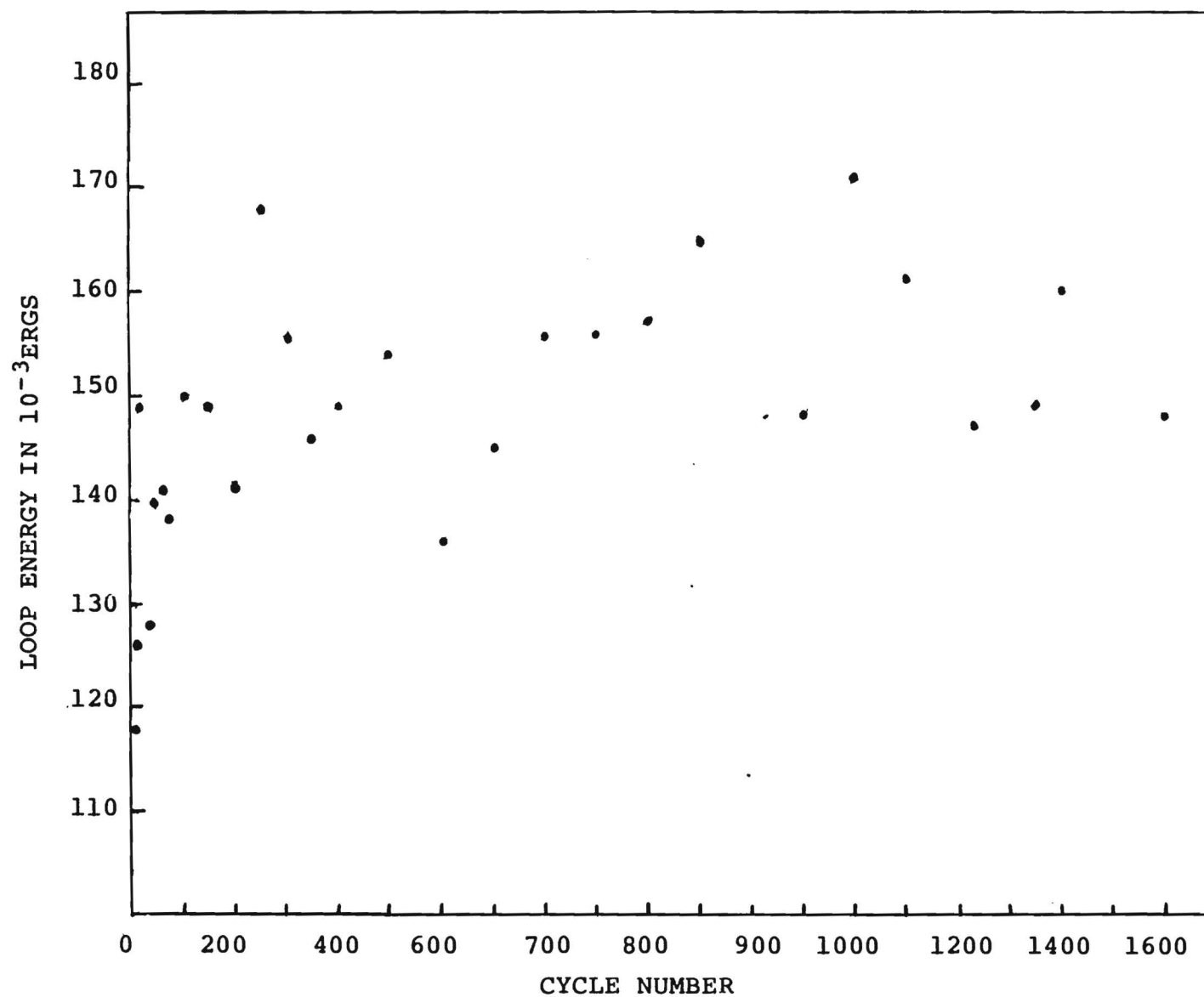


Figure 22. Hysteresis loop energies measured for a gold ball bond that was mechanically cycled in air.

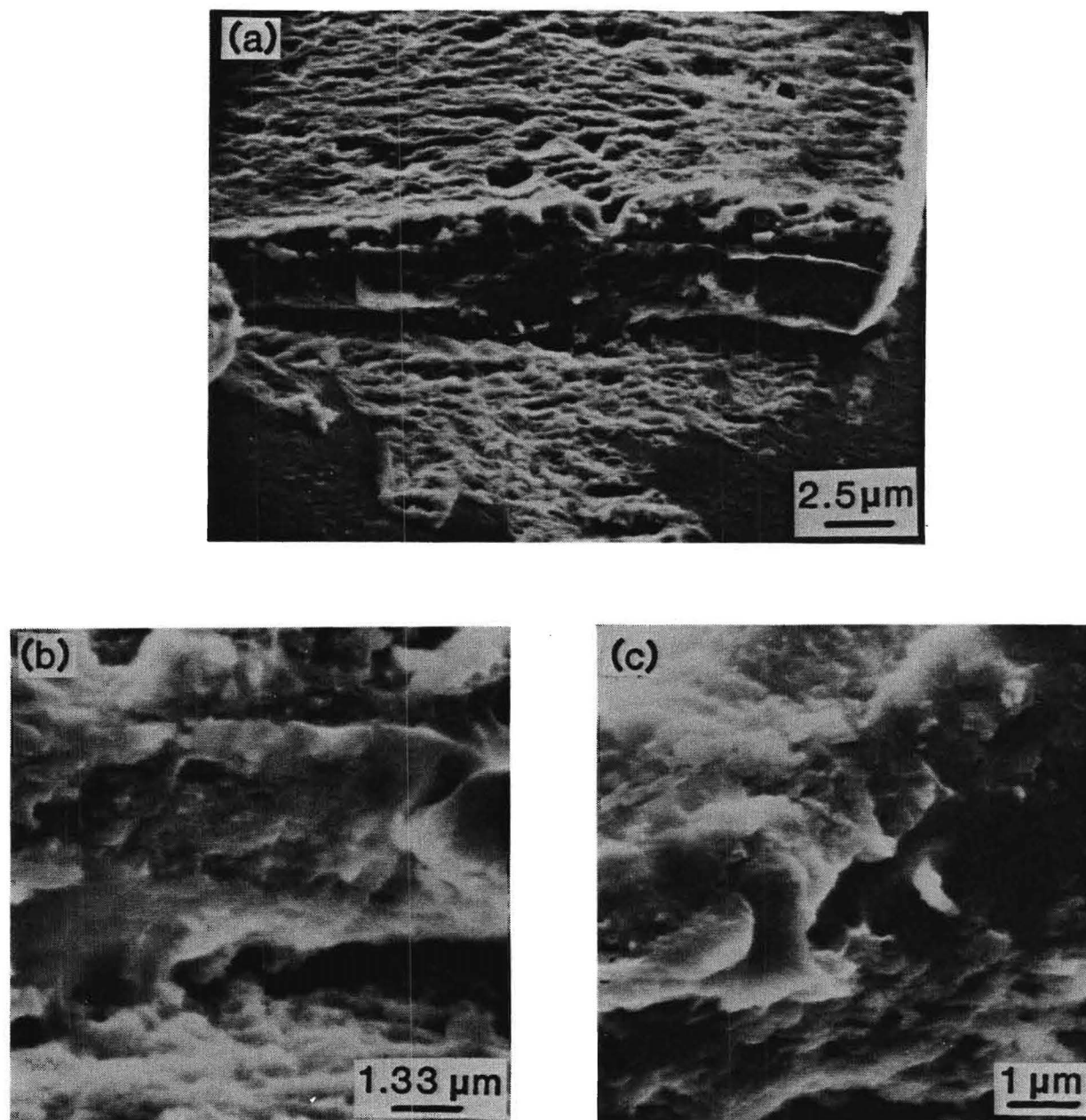


Figure 23. SEM fractographs showing features of the aluminum bonded wire fatigued to failure in laboratory air while carrying 10 mA d.c. current.  
(a) fracture surface at the first bond heel  
(b) high magnification of the bond-pad interface  
(c) features of the mating wire surface

region of the wire undergoes a highly ductile monotonic type fracture, with a viscous flow appearance. The initial surface oxides appear as debris at the wire-pad bond interface.

Figure 24 highlights the heel of an aluminum bond after 1350 cycles, but prior to complete fracture. Figure 24a shows the surface configuration of the bond prior to the specimen being installed on the micromechanics testing machine. By carefully monitoring the mechanical hysteresis loops, the specimen was removed from the testing apparatus prior to failure and observed in an SEM for structural studies. The remaining two micrographs in Figure 24b&c show the arrested growth of a crack from the upper surface of the heel into the central region of the bond wire.

Figure 25 reveals that the fracture surface features of two wire bonds mechanically cycled to failure while conducting a current of 75 ma. These two specimens, prepared and measured under identical conditions, behaved somewhat differently during cyclic deformation. The number of cycles to failure was 403 cycles and 230 cycles, respectively, for the two specimens. Examination of the fracture surfaces revealed that the specimen failing earlier experienced greater intergranular crack propagation in the initial stages of fatigue cycling. The SEM micrographs reveal that for the longer lived specimen, a greater degree of viscous flow occurred within the aluminum bond metal as evident from Figure 24a. Figure 26a shows the surface geometry of an aluminum bond prior to mechanical cycling. Figure 26b shows the appearance of the second bond after 460 cycles with a bond current of 100 ma.

The differences in mechanical behavior observed are most likely due to details concerning surface features either introduced during the bonding process or existing on the particular section of the bond wire which happened to make up the

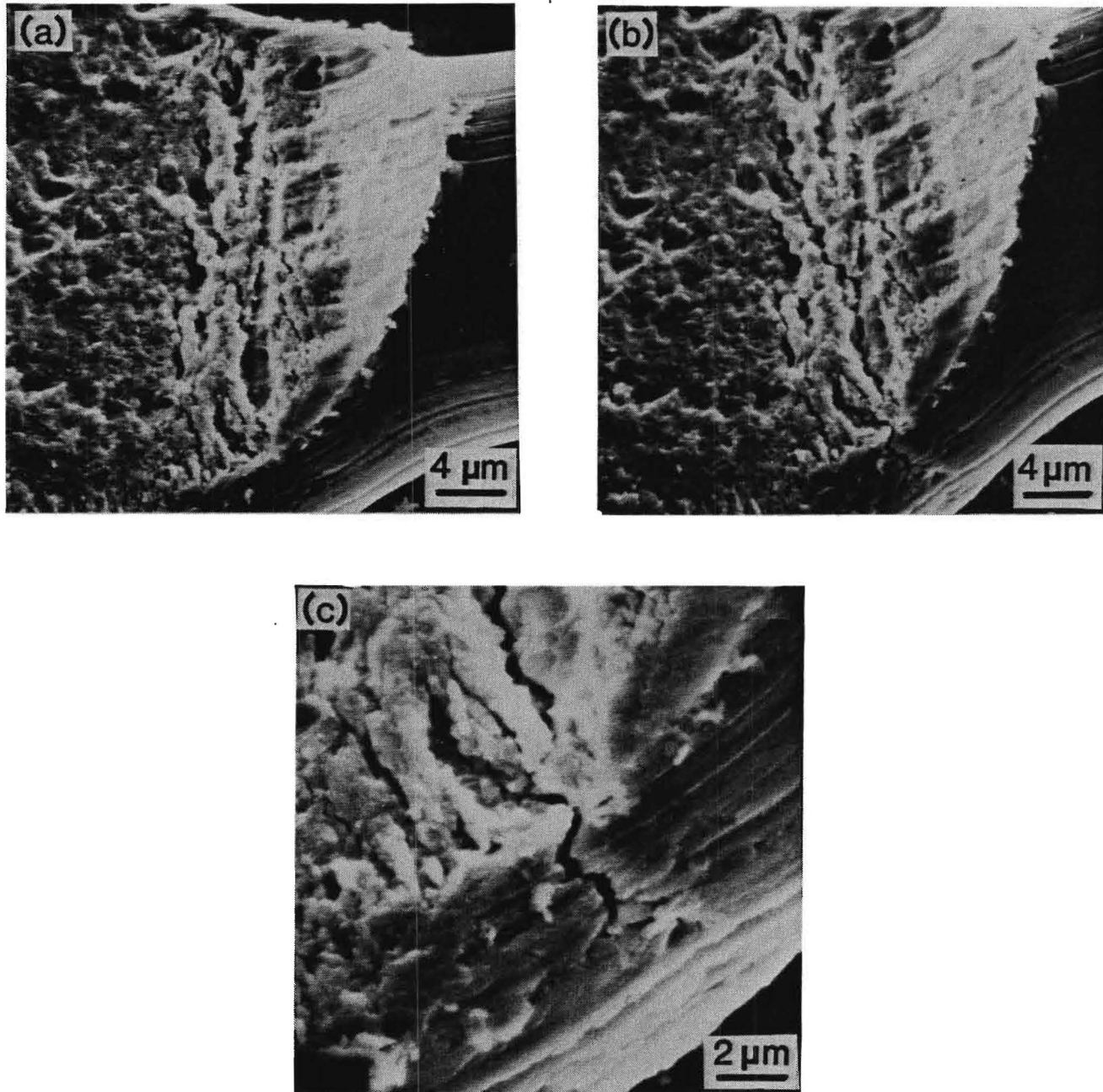


Figure 24. SEM fractographs showing features of the aluminum bonded wire fatigued in laboratory air environment while carrying 50 mA of d.c. current  
(a) high magnification of first bond prior to the test  
(b) first bond after 1350 cycles  
(c) high magnification of the fatigue crack tip

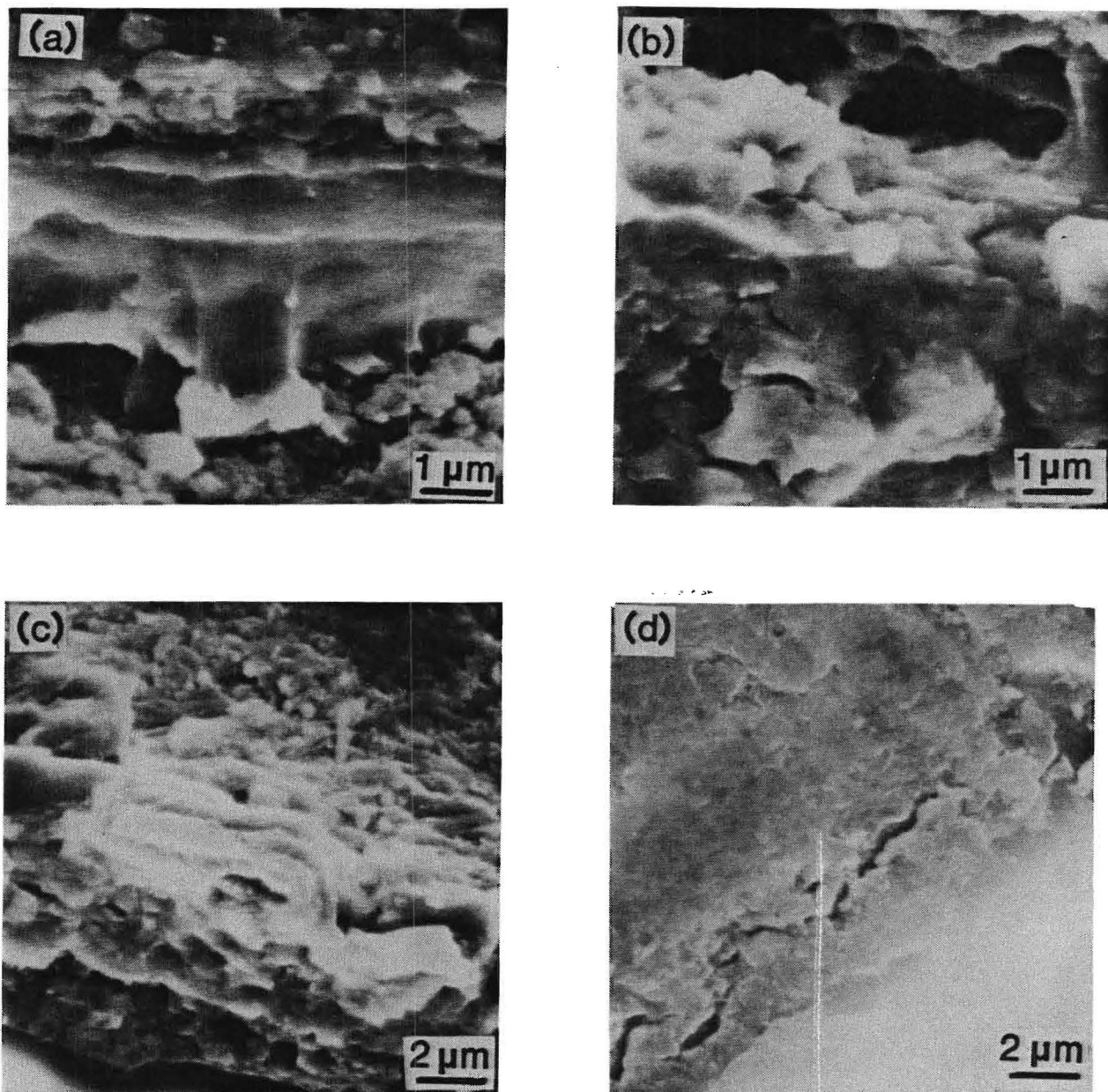


Figure 25. SEM fractographs showing features of the aluminum bonded wire fatigued in laboratory air environment while carrying 75 mA of d.c. current.

- (a) the bond-pad interface at the first bond heel,  $N_f = 403$
- (b) the bond-pad interface at the first bond heel,  $N_f = 230$
- (c) features of the wire fracture surface of (a)
- (d) features of the wire fracture surface of (b)



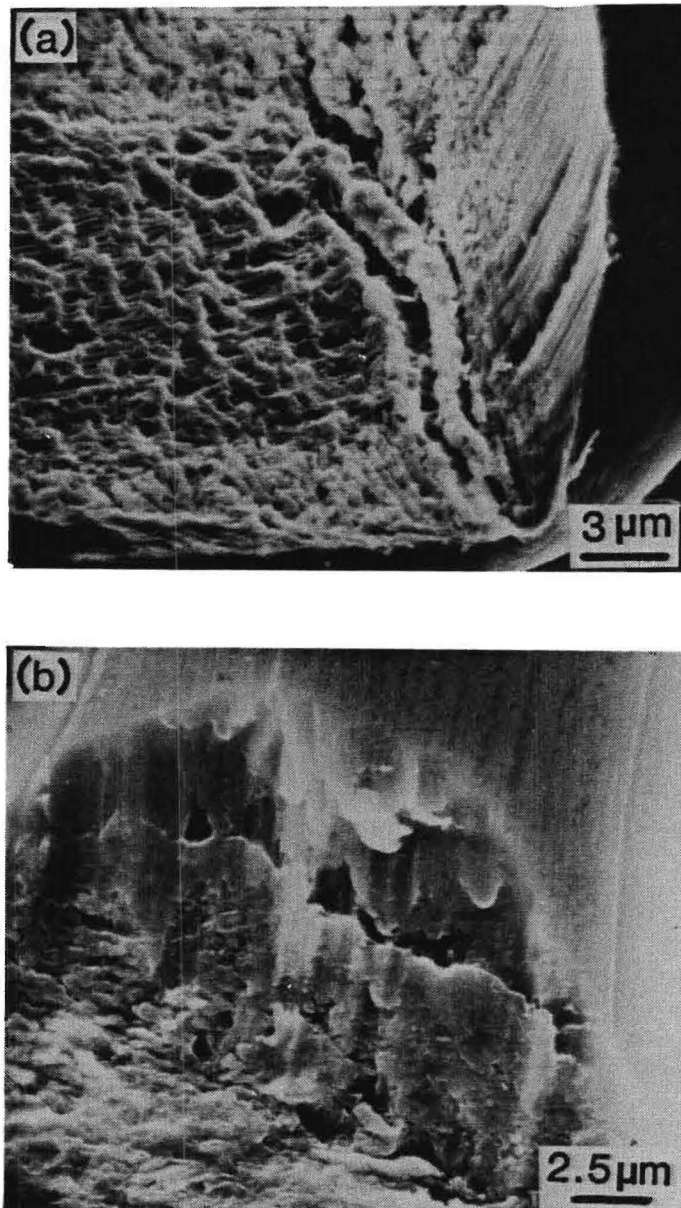


Figure 26. SEM fractographs of the aluminum bonded wire prior to fatigue with 100 mA showing  
(a) effect of bonding process on wire deformation at the first bond  
(b) the second bond after 460 cycles.

heel metal. Surface scratches, inclusions or other asperities with dimensions less than a micron can also account for the observed differences in cyclic deformation characteristics and fatigue life because of the importance of such features in controlling degradation mechanisms. A perfectly smooth bond surface and a bond-pad interface without the surface oxide and impurity debris could potentially result in wire bonds having consistently greater fatigue lives.

The appearance of a viscous flow type deformation in the crystalline metals of microcircuit bond wire materials is illustrated in the SEM micrographs contained in Figure 27. This wire bond appears to show evidence of intergranular crack growth during the early stages of deformation which converted into significant viscous flow in the later stages prior to fracture. The 100 ma bond current constricted in these final stages results in a high localized current density which assists chaotic plastic flow through both a current excited dislocation motion and through the normal thermally activated mechanisms enhancing dislocation motion over pinning features. The SEM micrographs of Figures 28 and 29 show features of aluminum bonds mechanically cycled while carrying higher bond current values, thereby, enhancing the area of the bond metal involved with viscous flow mechanisms.

Micrographs of the fracture surfaces of several aluminum wire bonds cycled in an environment maintained very close to a humidity of 100% are shown in Figures 30-33. The fracture surfaces of these specimens appear in the SEM to correspond closely to the characteristics of bonds fatigued in the seemingly innocuous laboratory air. In addition, SEM micrographs of a bad bond produced with the bonding machine parameters off optimum values are shown in Figure 34. Manufacturing mistakes of this magnitude should be discovered in the standard environmental



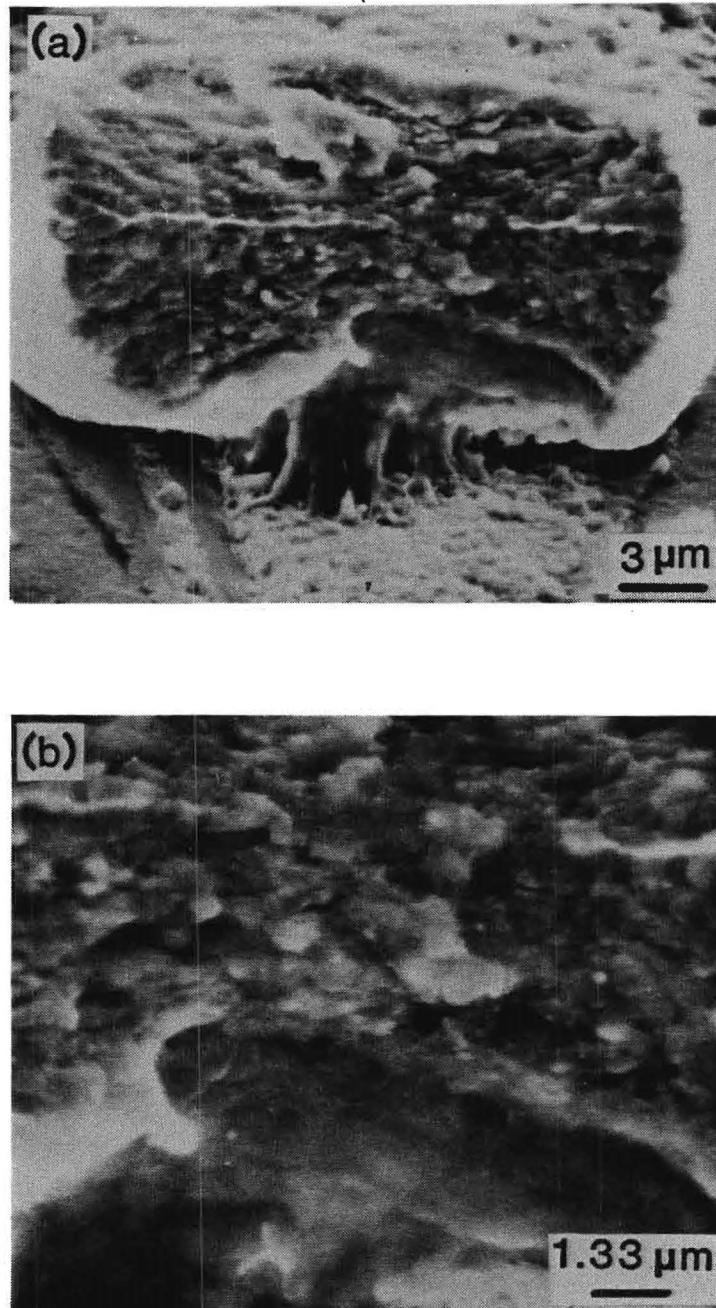


Figure 27. SEM fractographs showing features of the aluminum bonded wire fatigued in laboratory air environment while carrying 100 mA of d.c. current  
(a) bond heel fracture surface at the pad;  $N_f = 170$  cycles  
(b) high magnification of the surface features of (a)

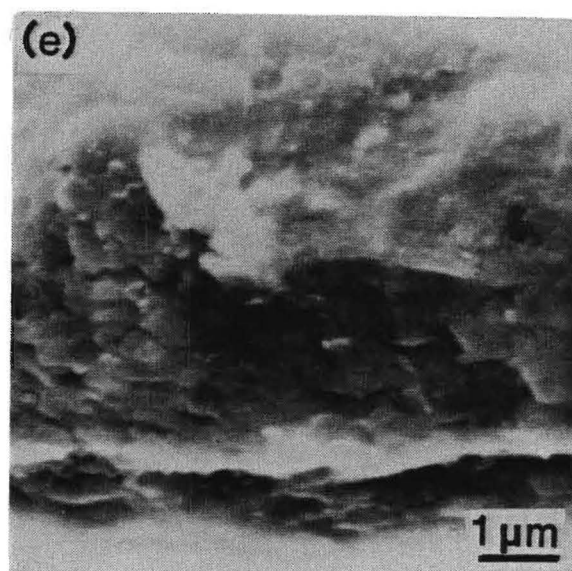
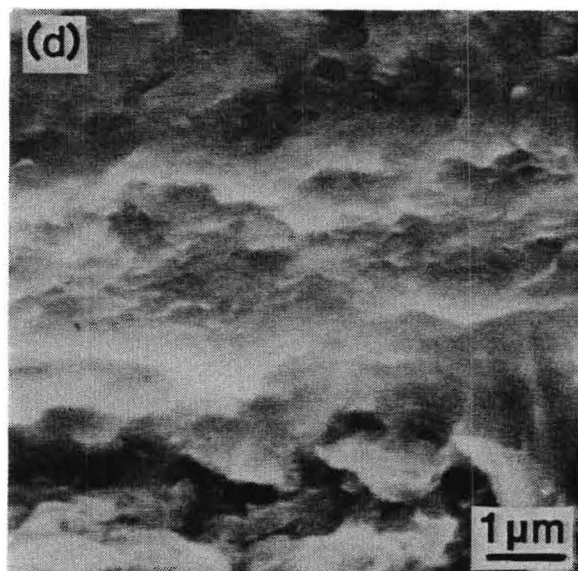
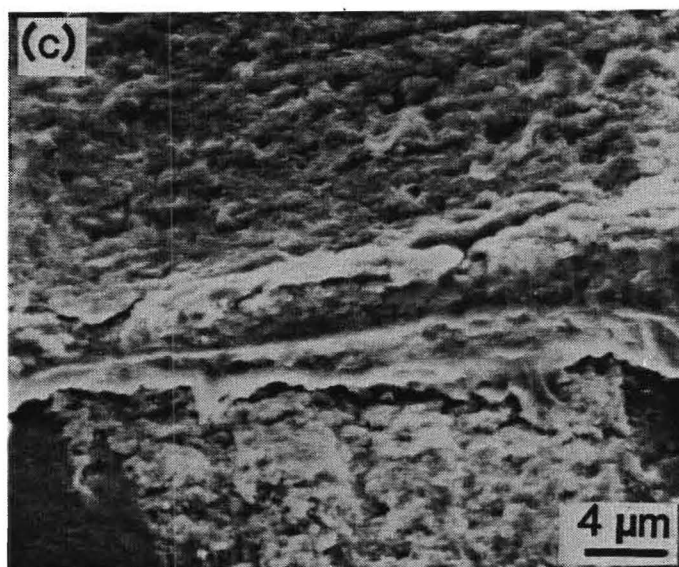


Figure 27.(Cont.)

- (c) bond-heel fracture features at the region of the bond-pad interface
- (d) high magnification of the bond-pad interface of (c)
- (e) high magnification showing features on the mating wire fracture surface.

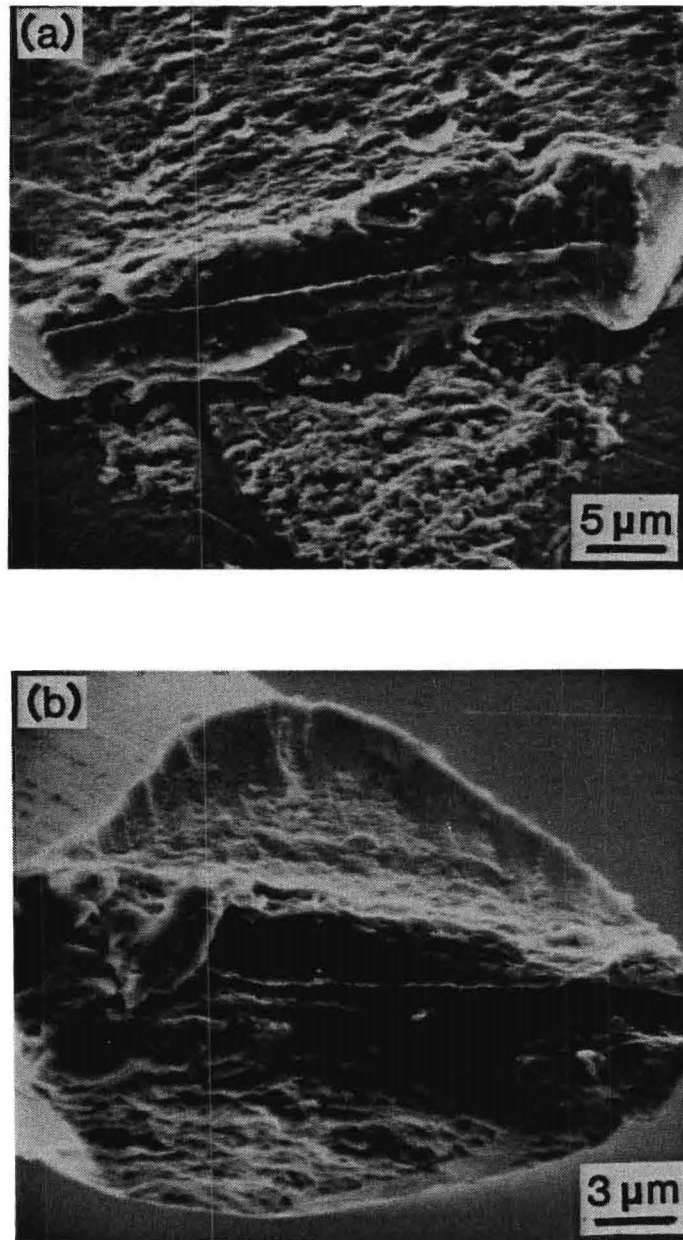


Figure 28. SEM fractographs of the aluminum bonded wire fatigued in laboratory air environment while carrying 150 mA of d.c. current

(a) first bond heel at pad-bond interface

(b) mating wire fracture surface

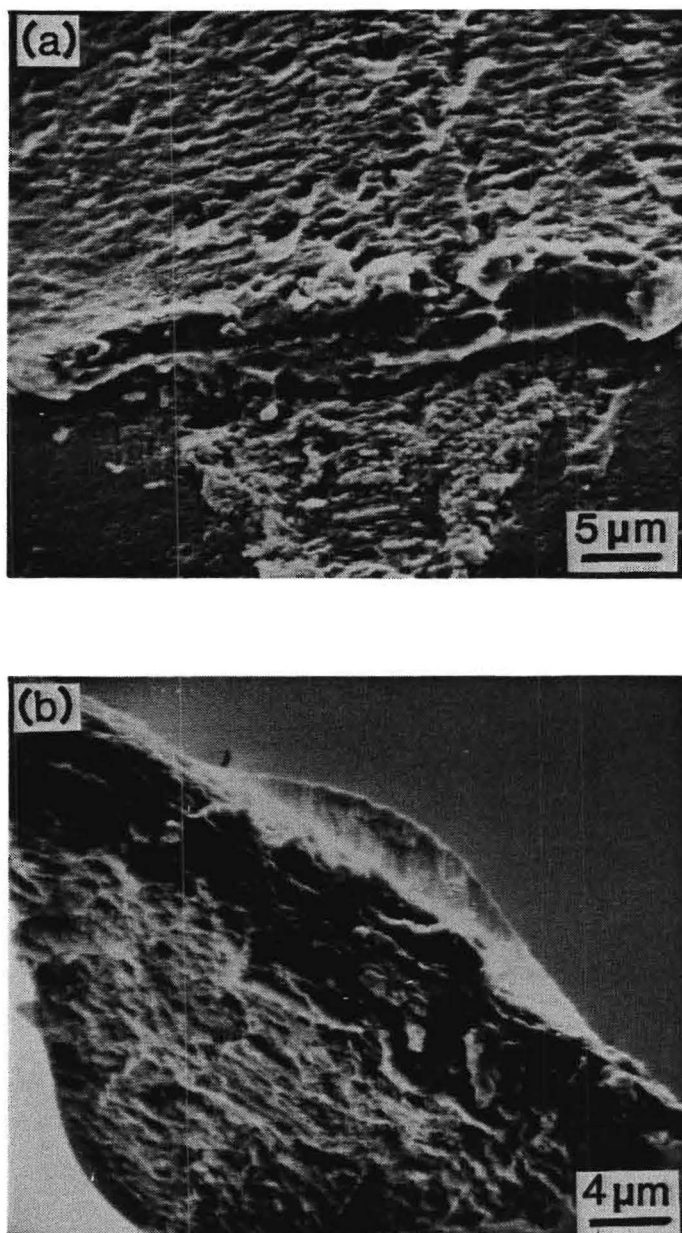


Figure 29. SEM fractographs showing features of the aluminum bonded wire fatigued in laboratory air environment while carrying 200 mA of d.c. current  
(a) first bond-heel fracture surface at the pad  
(b) features of the mating wire surface

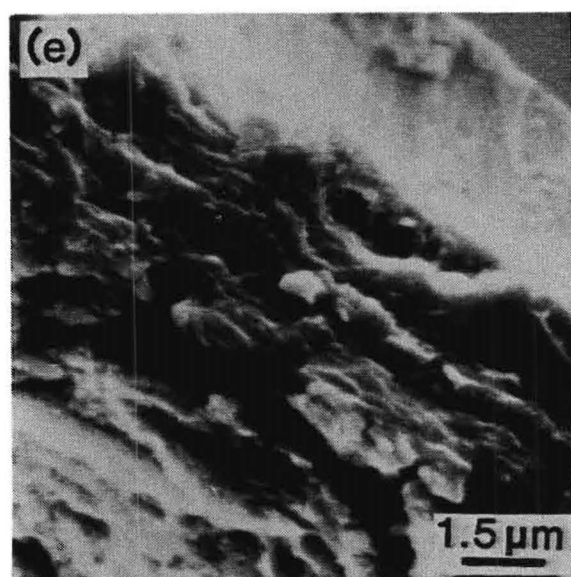
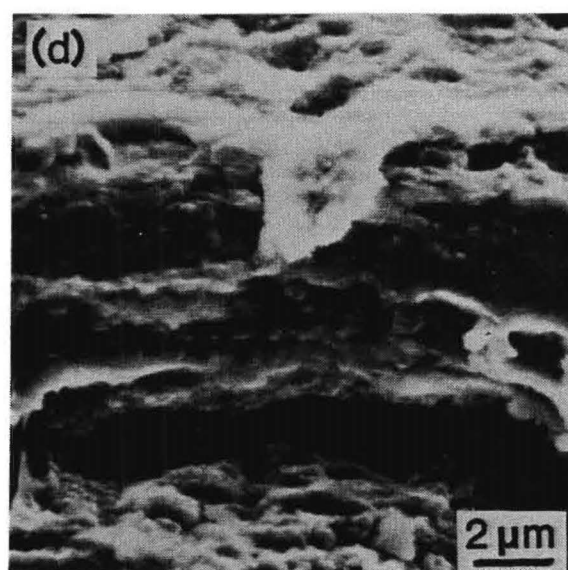
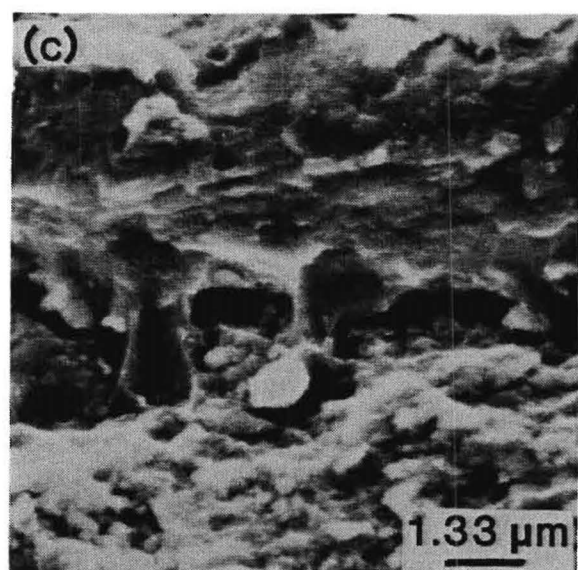


Figure 29 (Cont.)

- (c) high magnification of (a)
- (d) high magnification of bond-pad interface
- (e) high magnification of (b)

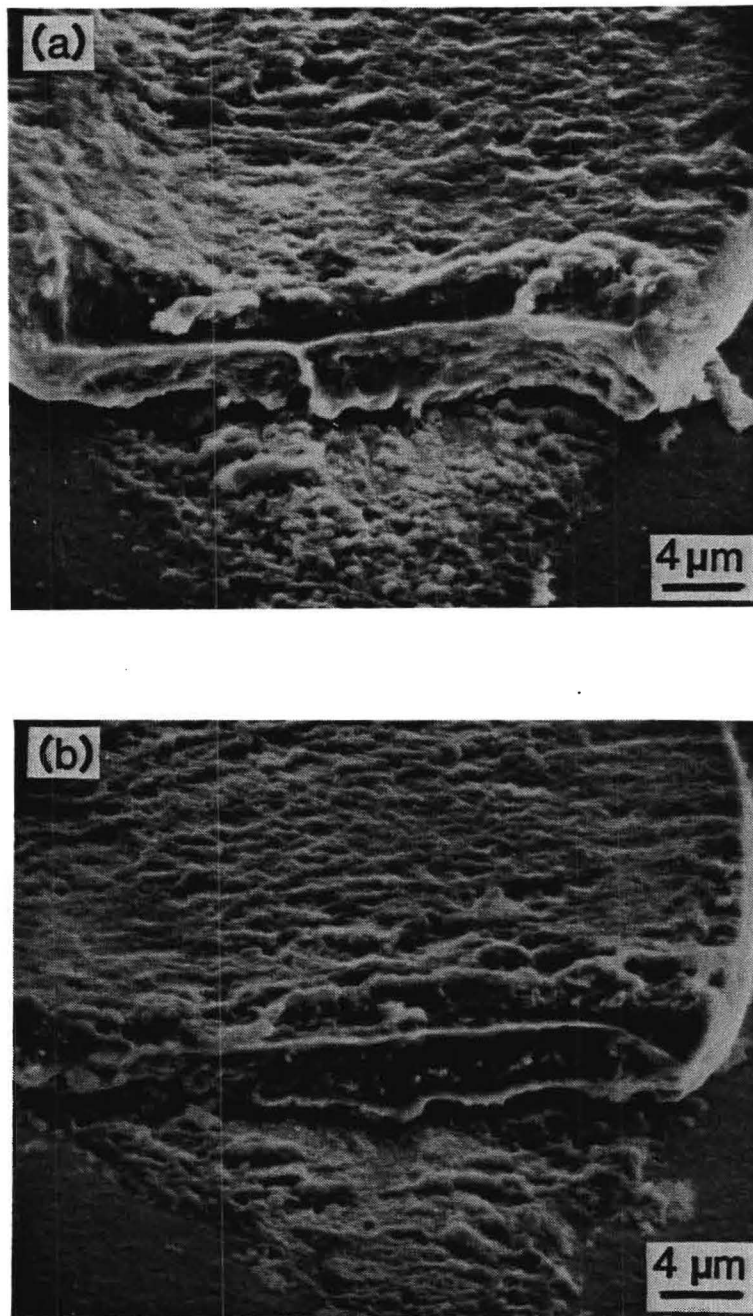


Figure 30. SEM fractographs of an aluminum bonded wire fatigued in humid environment  
(a) typical heel fracture surface at first bond to pad after 327 cycles  
(b) heel fracture surface at first bond after 140 cycles



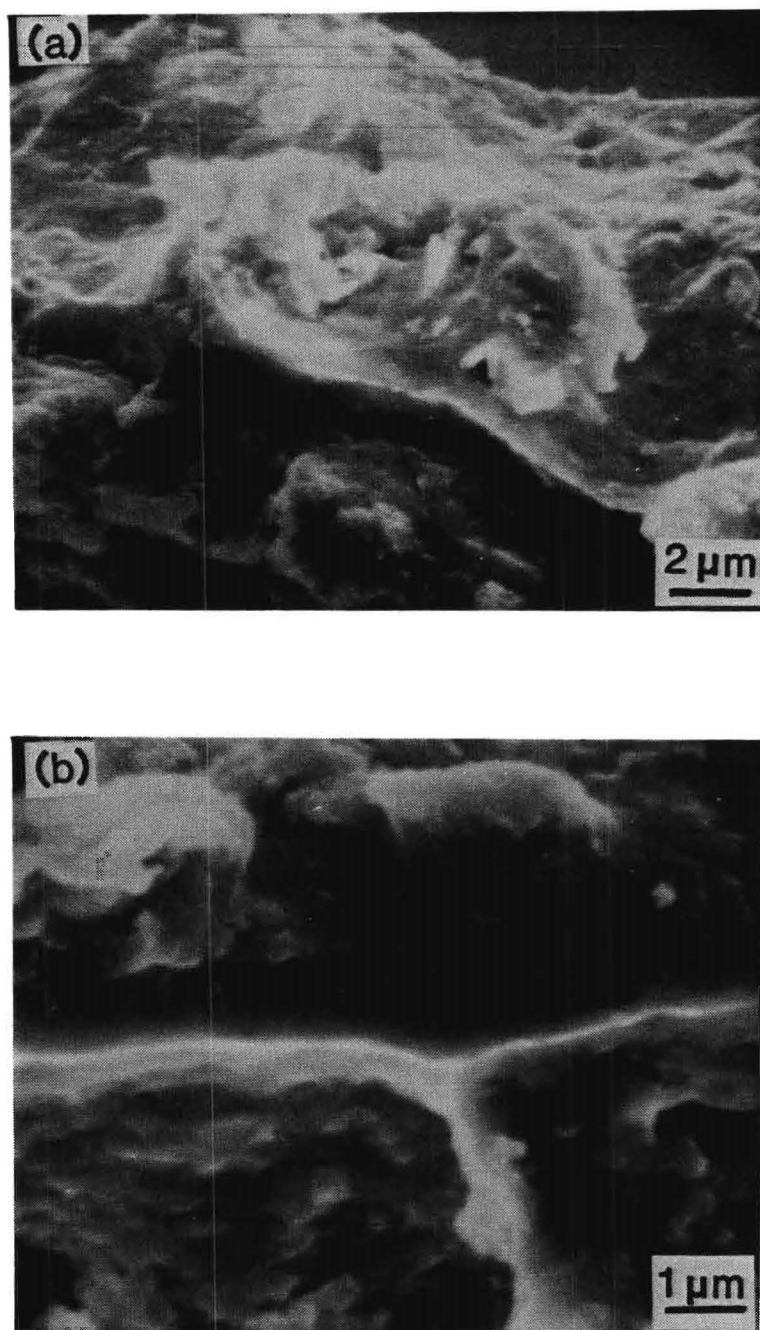


Figure 31. SEM fractographs of an aluminum bonded wire fatigued in humid environment.

- (a) wire fracture surface
- (b) bond-pad interface

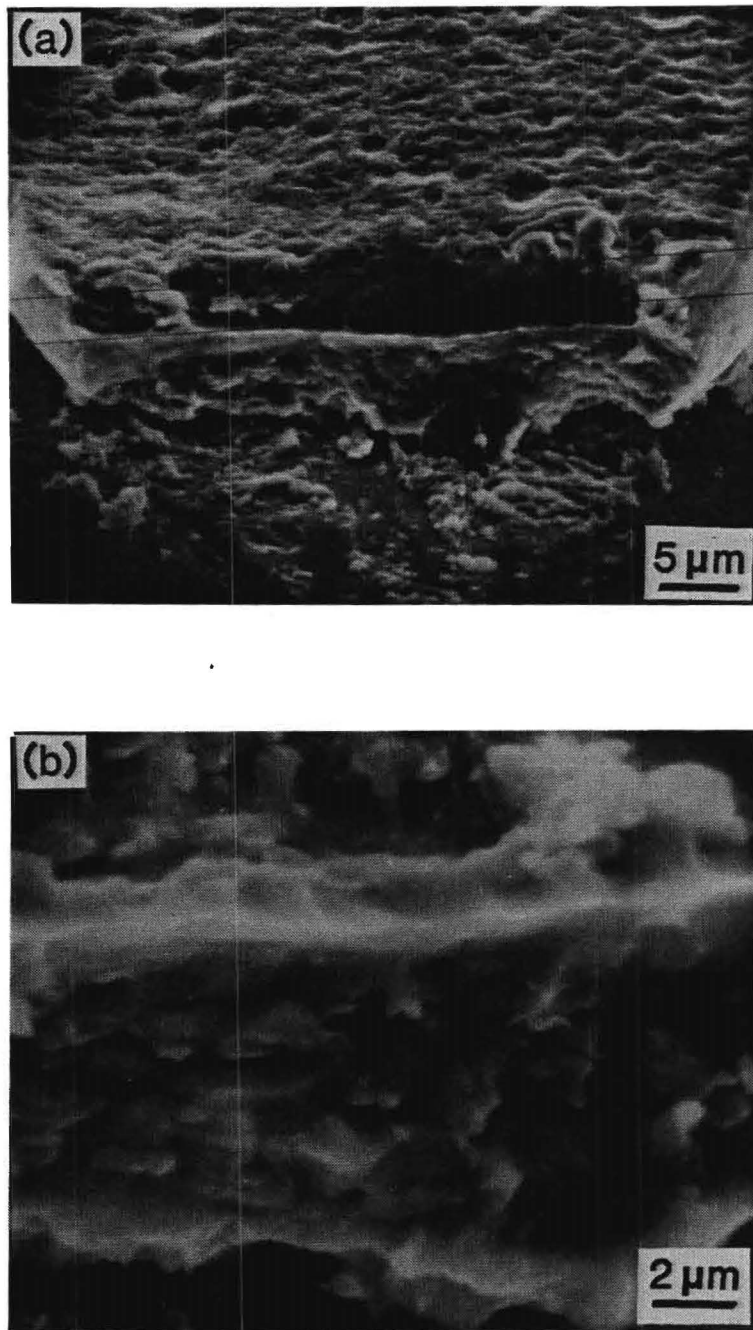


Figure 32. SEM fractographs of an aluminum bonded wire fatigued in humid environment showing features at the bond-pad interface.



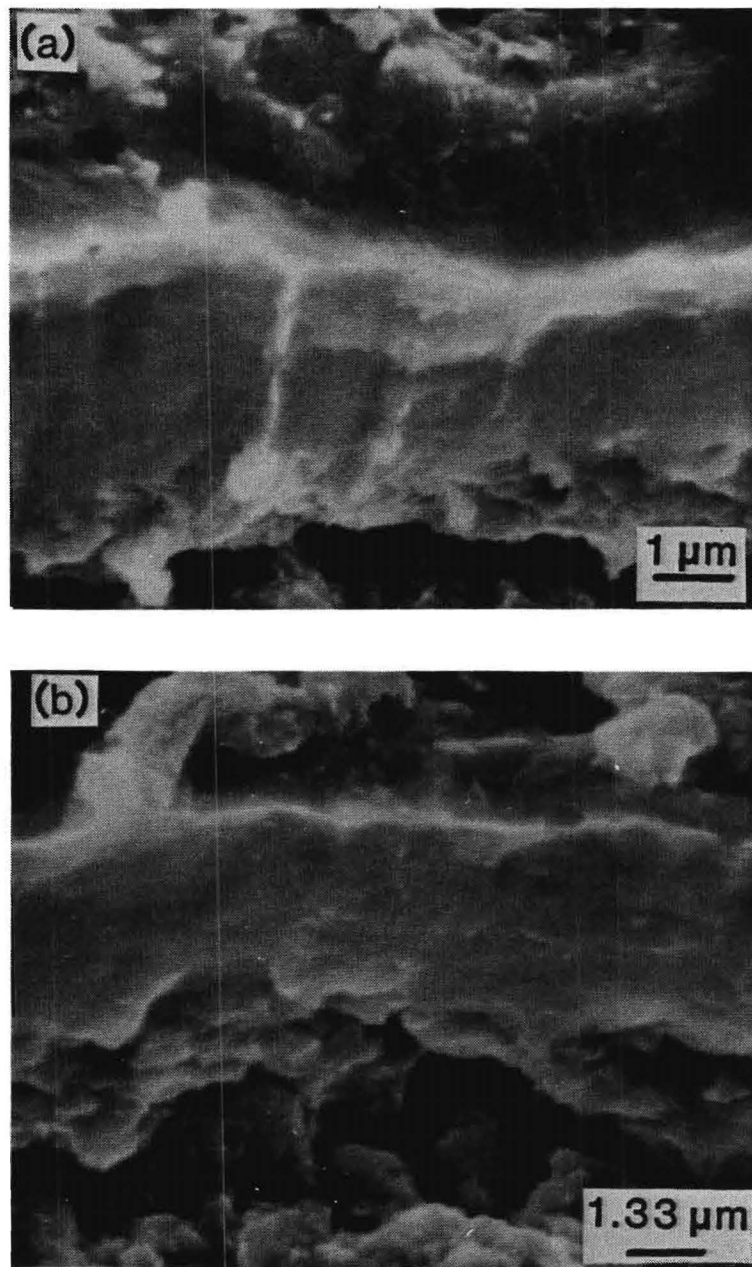


Figure 33. SEM fractographs of aluminum bonded wire fatigued in humid environment showing features at the bond pad interface. Cycles to failure: 227

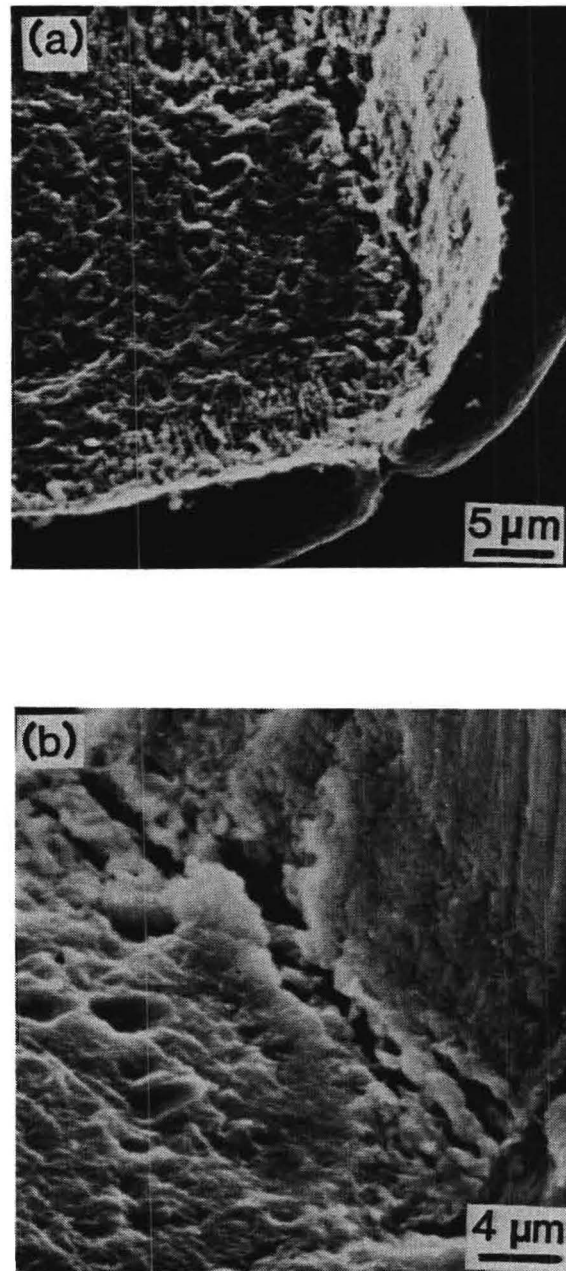


Figure 34. SEM fractographs of the aluminum bonded wire showing deformation induced due to the bonding process.

stress screening sequences involving thermal mechanical cycling since these stress levels will probably accelerate growth mechanisms leading to premature failure.

#### 4.3 SINGLE BOND FATIGUE EXPERIMENTS

The stresses generated within the loop of a normal microcircuit bond wire interconnection are quite complex. As described earlier, the experimental technique of force application and measurement by firmly clasp the wire at the loop apex was considered to provide a realistic approximation of the cyclical stresses induced in such loops during thermal excursions. However, it was felt that other configurations might provide additional insight on the fatigue degradation mechanisms operating in the bonded wires. Two sets of single bond fatigue experiments were conducted involving bonding parameters identical to those employed in the dual bond measurements. The bonds were made in standard DIPs to aluminumized silicon chip pads and Au package posts using an ultrasonic wedge bonding machine. Prior to making either the post or pad bond, as desired, the ultrasonic power of the bonding machine was reduced to zero. This bond could thus be easily lifted without doing mechanical damage to the good bond.

For the two single bond experiment sets, widely different stress levels were employed. The first set involved the application of strain amplitudes which were approximately those imposed at each bond during the dual bond measurements, and the second involved strain levels which resulted in stresses less than 1/10 of those values. The micromechanics instrumentation employed with the dual bond fatigue measurements was also suitable for the high stress single bond measurements. However, the low stress experiments required modification of another strain controlled micromechanics apparatus, as described in the introduction of this chapter, to achieve the greater sensitivity needed for precise force measurements of considerably less than one dyne.

Cyclic stress response curves for single bonds at the larger strain amplitude level in laboratory air are shown in Figure 35. These four bonds had been annealed at 110 C for 48 and 72 hours, as indicated, prior to mechanical cycling. Stress amplitudes for post bonds after both 48 and 72 hour anneal times are considerably greater than the corresponding cyclic stress amplitudes for the chip pad bonds. However, the fatigue lifetimes are not significantly different for either the two different bond types or for the two anneal times with each. Stress amplitudes in the saline environment were surprisingly independent of the anneal times, as illustrated in Figure 36. The mechanical hysteresis loops for single bonds stressed at the higher levels showed large energy losses in each cycle, as was the case with most dual bonds.

The low stress, single wire bond experiments yielded fatigue lifetimes as high as 20,000 to 30,000 cycles. All of the single bond, low stress fatigue measurements have been conducted on the bonds made to the chip pad. Nearly lossless mechanical hysteresis curves were typical of the first 90 - 95 % of a bond's fatigue life such that measurable energy losses provided a good indication for the initiation of significant cyclic mechanical degradation. Cyclic response curves for three pad bonds in laboratory air are shown in Figure 37. Similar curves for bonds cycled with a carefully imposed moist environment derived from distilled water demonstrated corresponding long fatigue lifetimes as illustrated in the data shown in Figure 38. Care was exercised to not introduce ionic impurities with the moisture in these specimens. However, the introduction of even small quantities of NaCl with moisture derived from a saline solution had a marked effect on the low stress fatigue lifetimes and hysteresis loop parameters of similarly cycled bonds, as shown in Figures 39 and 40.

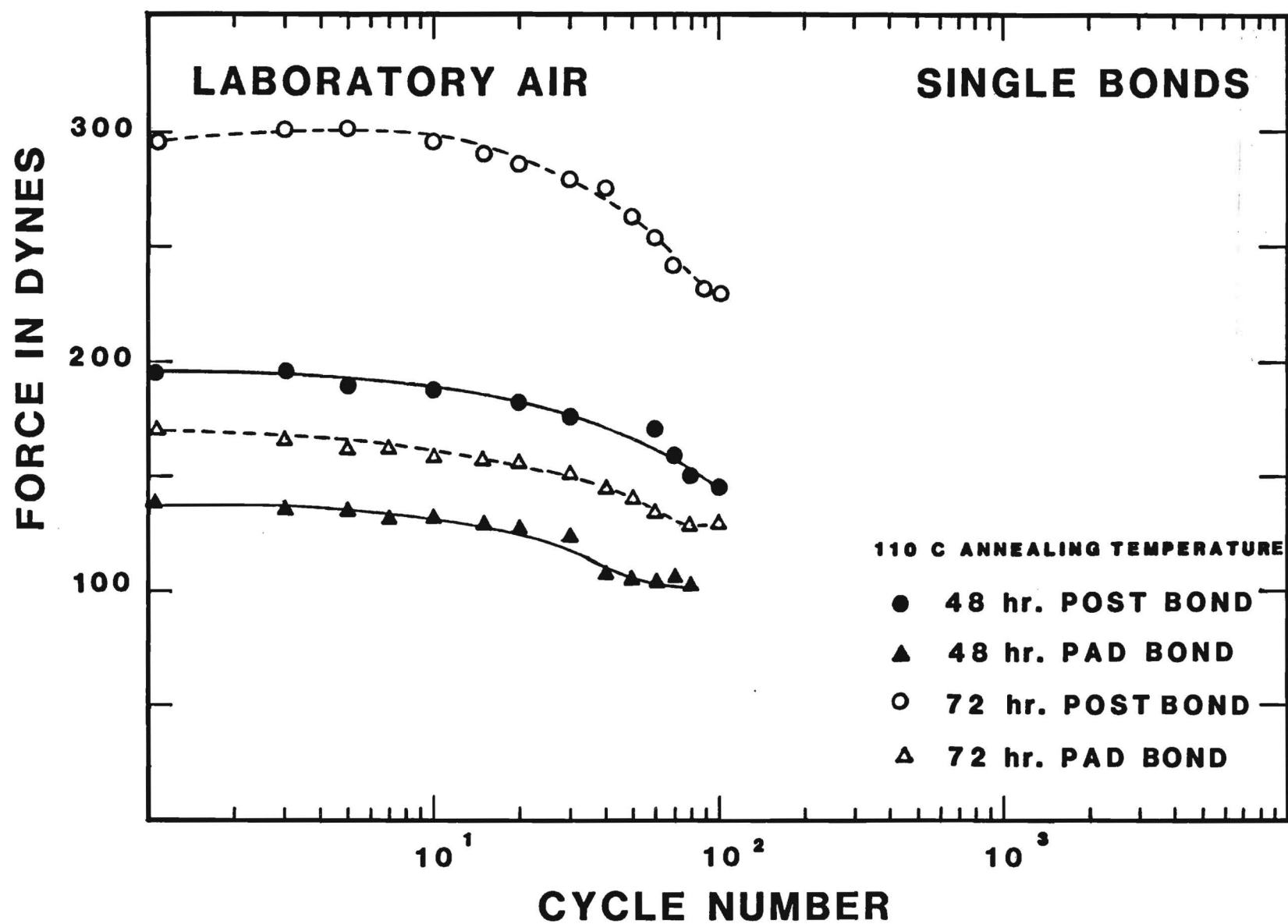


Figure 35. Cyclic stress response curves of post and pad bonds showing effects of aging time and type of bond cycled in laboratory air.

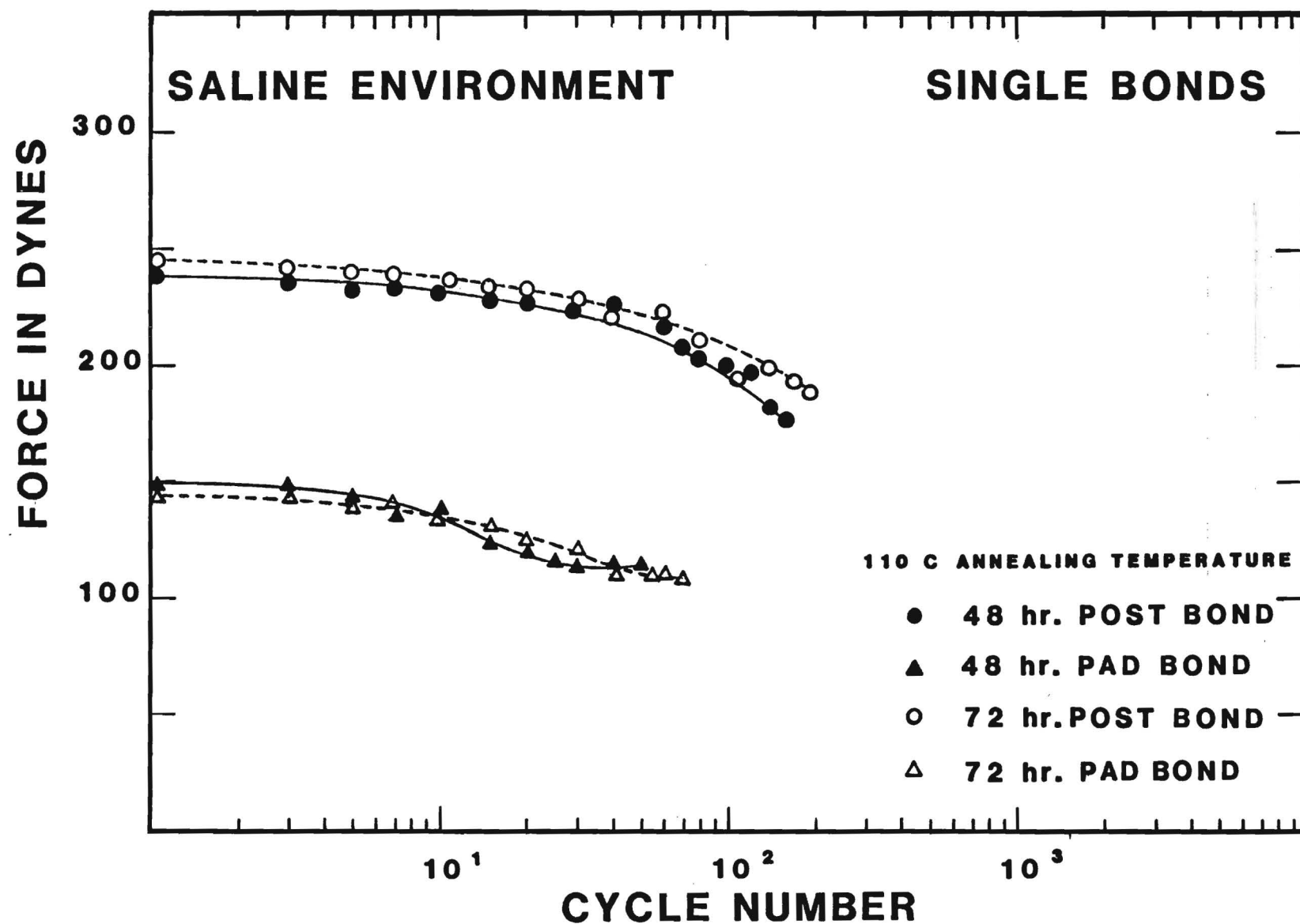


Figure 36. Cyclic stress response curves with indicated aging times for single bonds cyclically stressed in a moist saline environment.

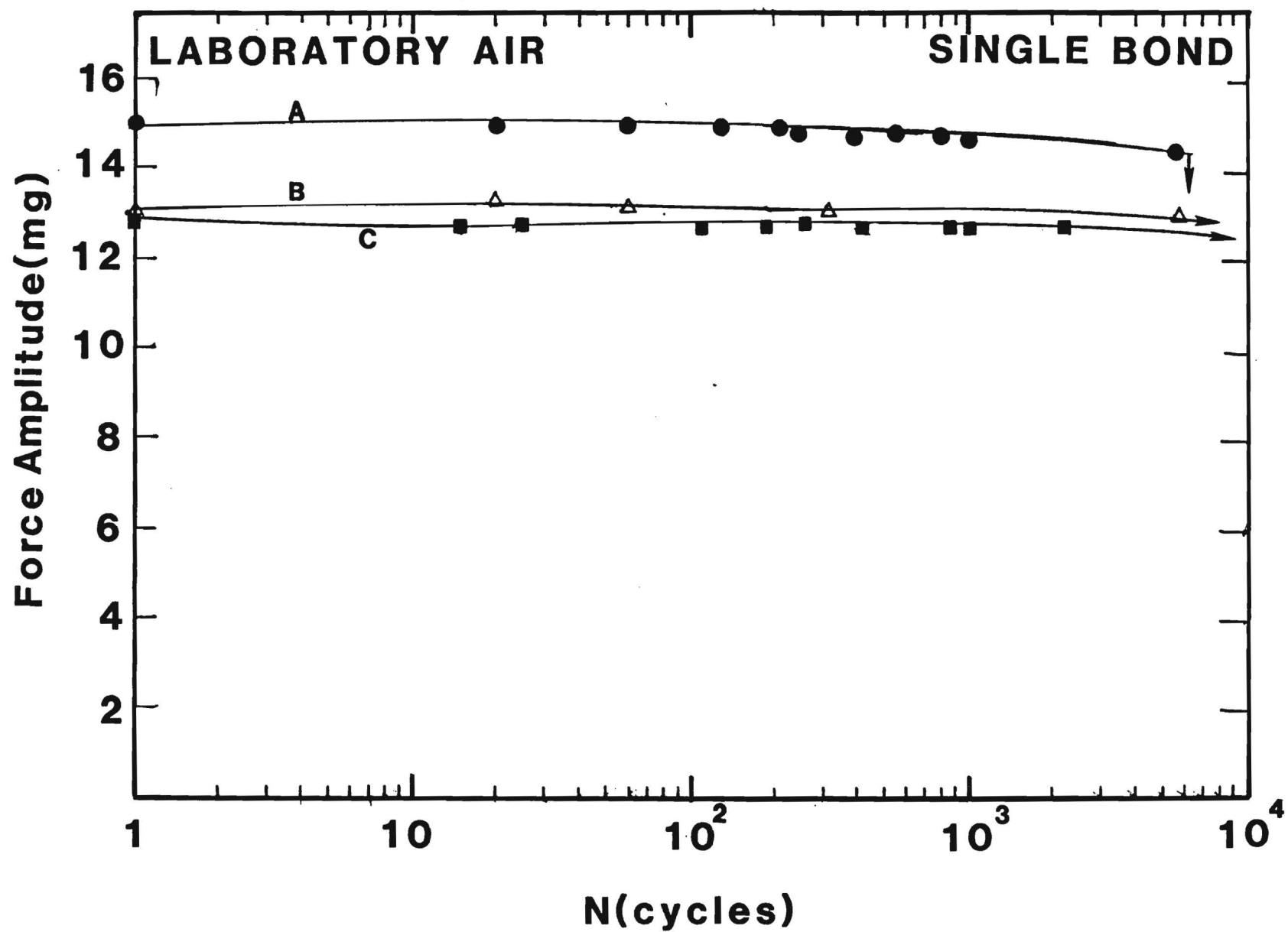


Figure 37. Cyclic stress response curves for Al-Al single bonds cycled at very low force amplitudes in laboratory air.



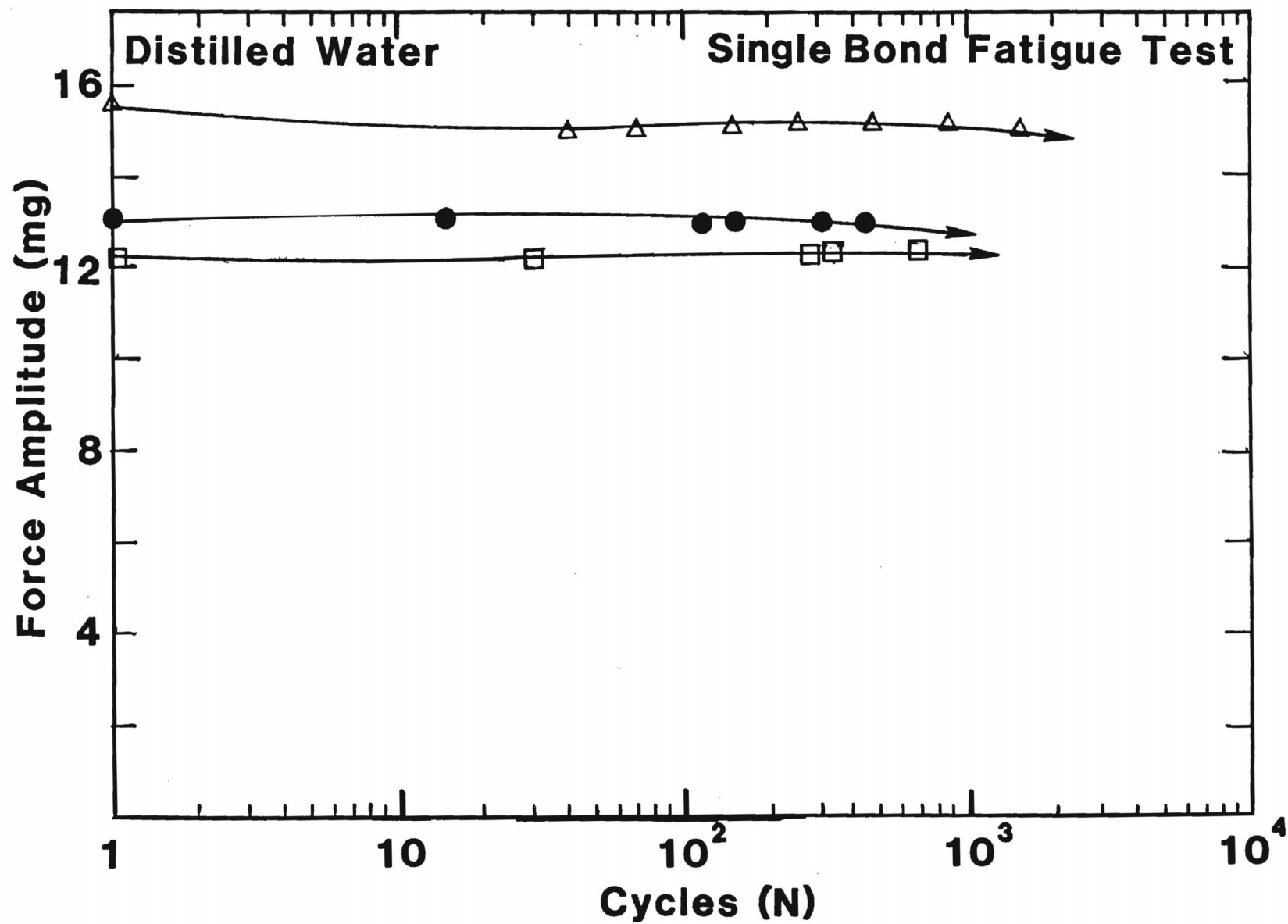


Figure 38. Cyclic stress response curves for Al-Al single bonds cycled at very low force amplitudes in high purity moisture.

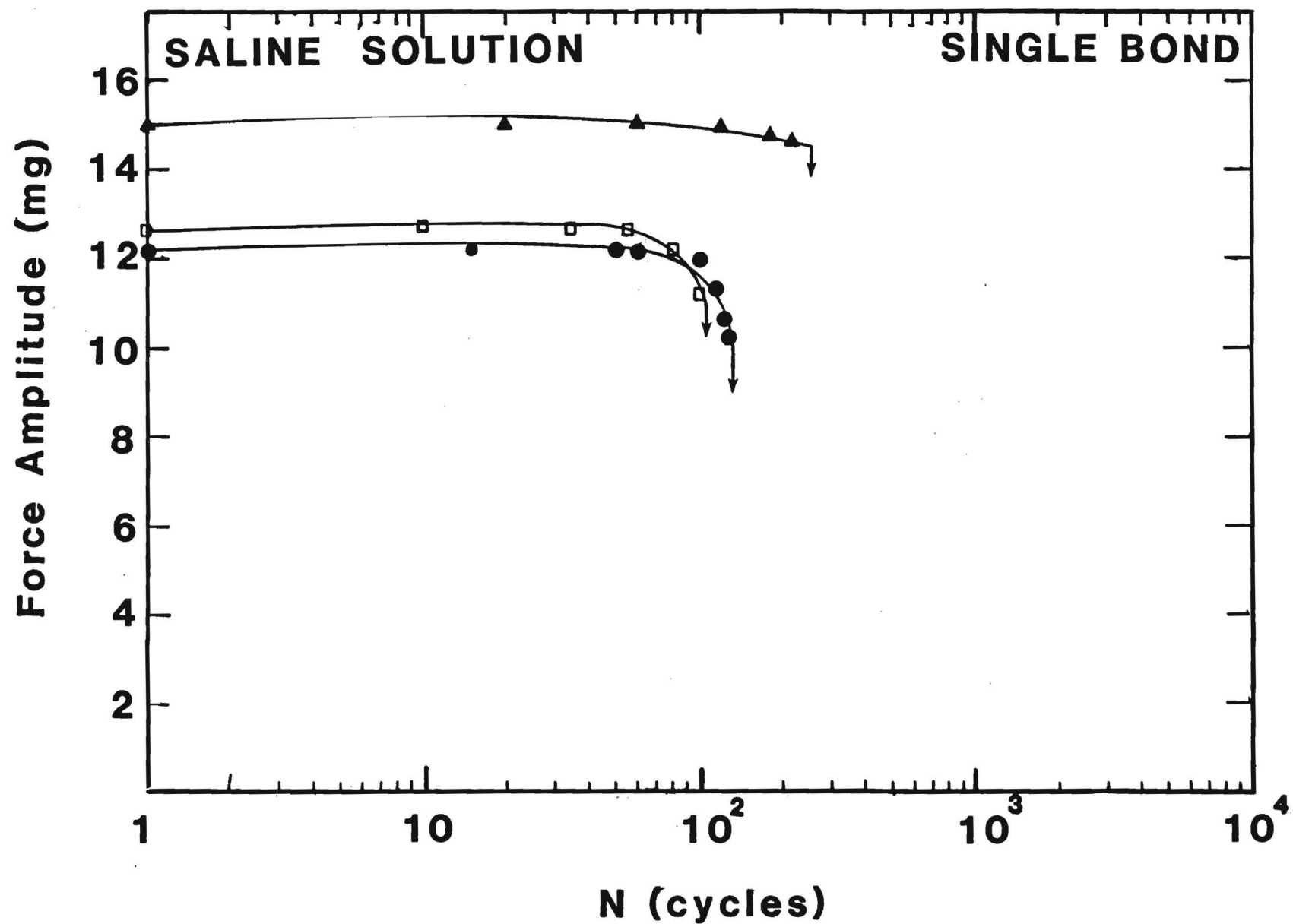


Figure 39. Cyclic stress response curves for Al-Al single bonds cycled at very low force amplitudes in moisture derived from a saline solution.

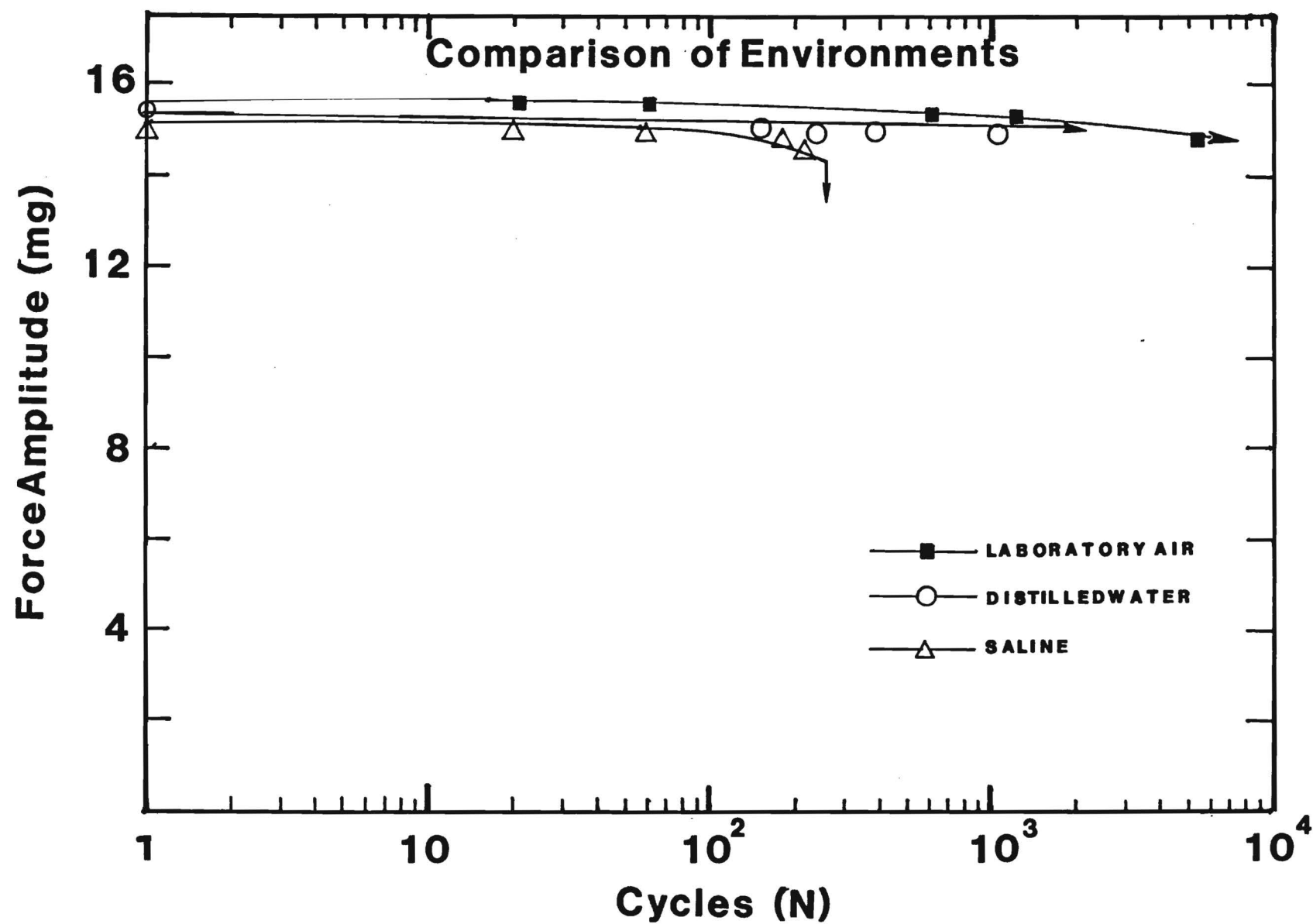


Figure 40. Comparison of cyclic force amplitudes for three single Al-Al wire bonds mechanically cycled at low force amplitudes in the indicated environments.

Micrographs of fracture surfaces of single Al-Al wire bonds mechanically cycled in moist environments derived from distilled water or from a saline solution are shown in Figures 41 - 45. There clearly is extensive plastic deformation in the bonds cycled in the pure H<sub>2</sub>O moisture environment, (see Figures 41 and 42) indicative of the operation of viscous flow mechanisms noted earlier in the fatigue degradation of dual bonds. The SEM micrographs from aluminum bonds cycled in the saline environments (Figures 43 and 44) show apparent intergranular crack growth which advanced rapidly through the bond heel as noted by the mechanical fatigue data. Figure 45 shows a region of an aluminum bond pad where the wire had lifted while being mechanically cycled in a saline environment.

The granular appearance of the fracture surfaces in the saline environment strongly indicate the participation of corrosion-fatigue crack growth mechanisms due to Cl or Na ions derived from the saline solution. Attempts were made to detect the presence of these, or other, ions using the X-ray capabilities of the SEM. However, the detection sensitivity is not sufficient in an SEM for the small quantities involved here. Indeed, subsequent efforts were quite successful in tracing the migration of Cl ions into the crack growth region of the bond heel using very careful experimental techniques which took advantage of the recently installed scanning AES facilities in the Microelectronics Research Center at Georgia Tech. These experiments are described in section 5.5 of the next chapter. The combination of the mechanical hysteresis behavior, the SEM fractographs and the special AES analysis of wire materials has clearly identified the critical participation of chlorine ions in greatly accelerating mechanical degradation of stressed aluminum wires and metallization layers.

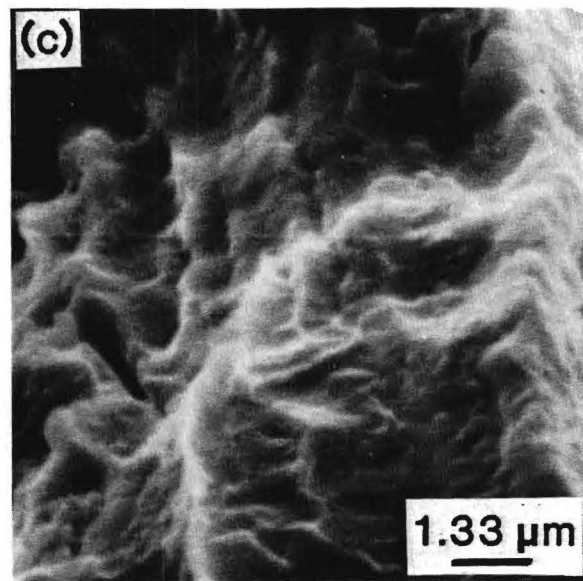
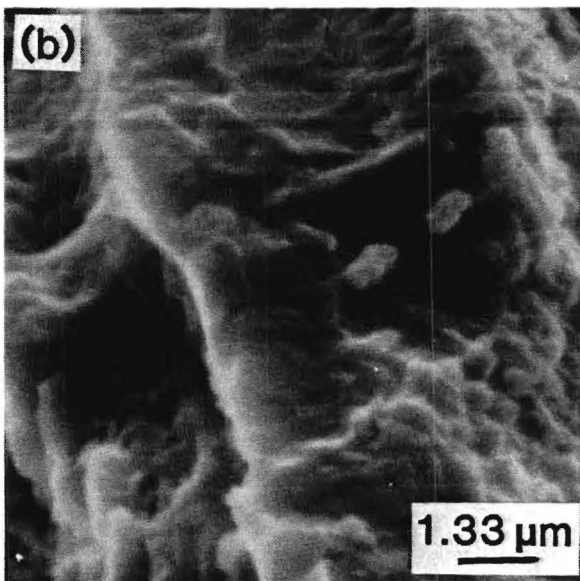
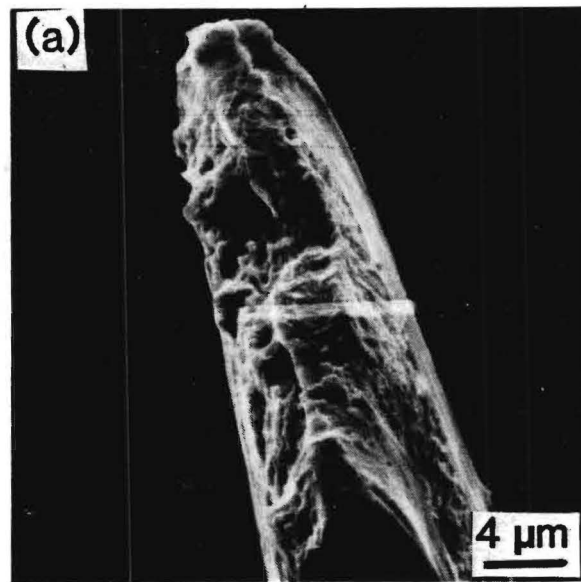


Figure 41. SEM fractographs of an aluminum wire bond (single bond) fatigued in the distilled water environment, showing features of the wire surface.

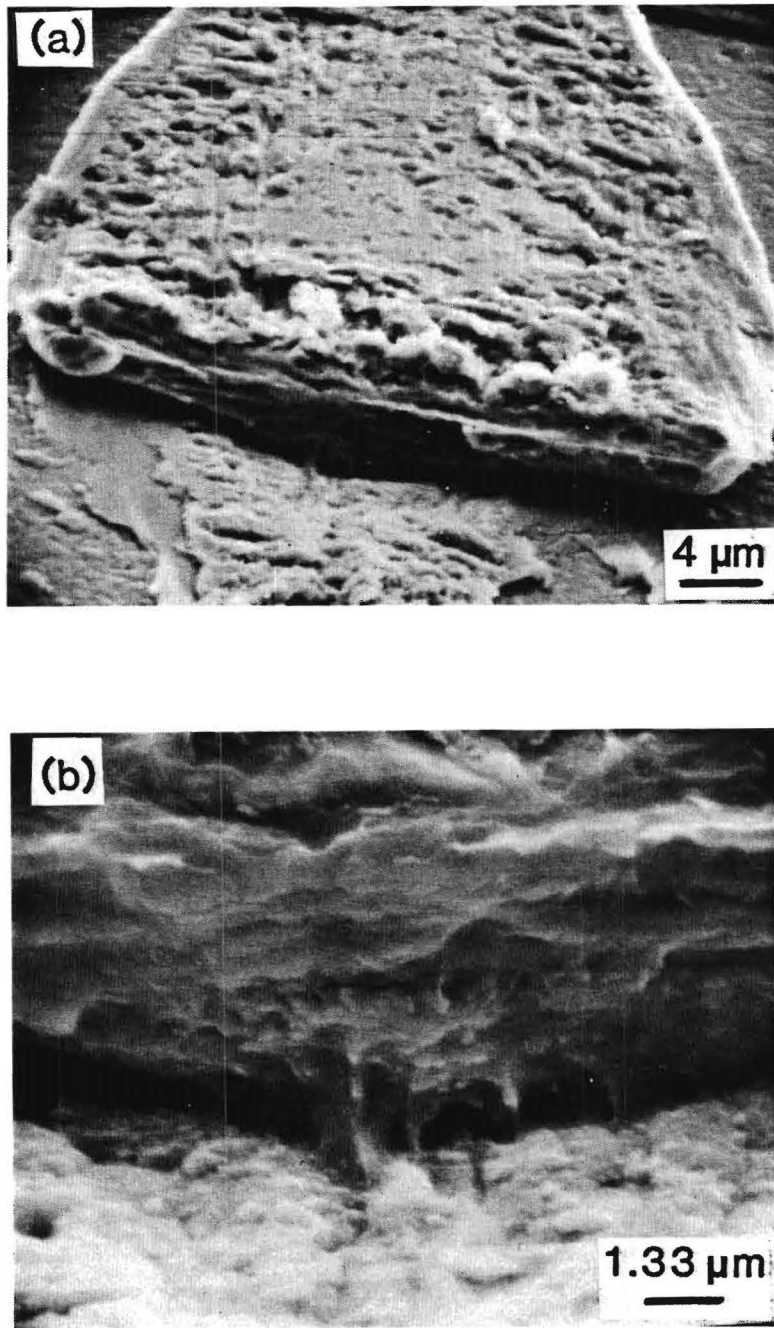


Figure 42. SEM fractographs of an aluminum wire bond (single bond) fatigued to failure in the distilled water environment, showing features at the bond-pad interface.

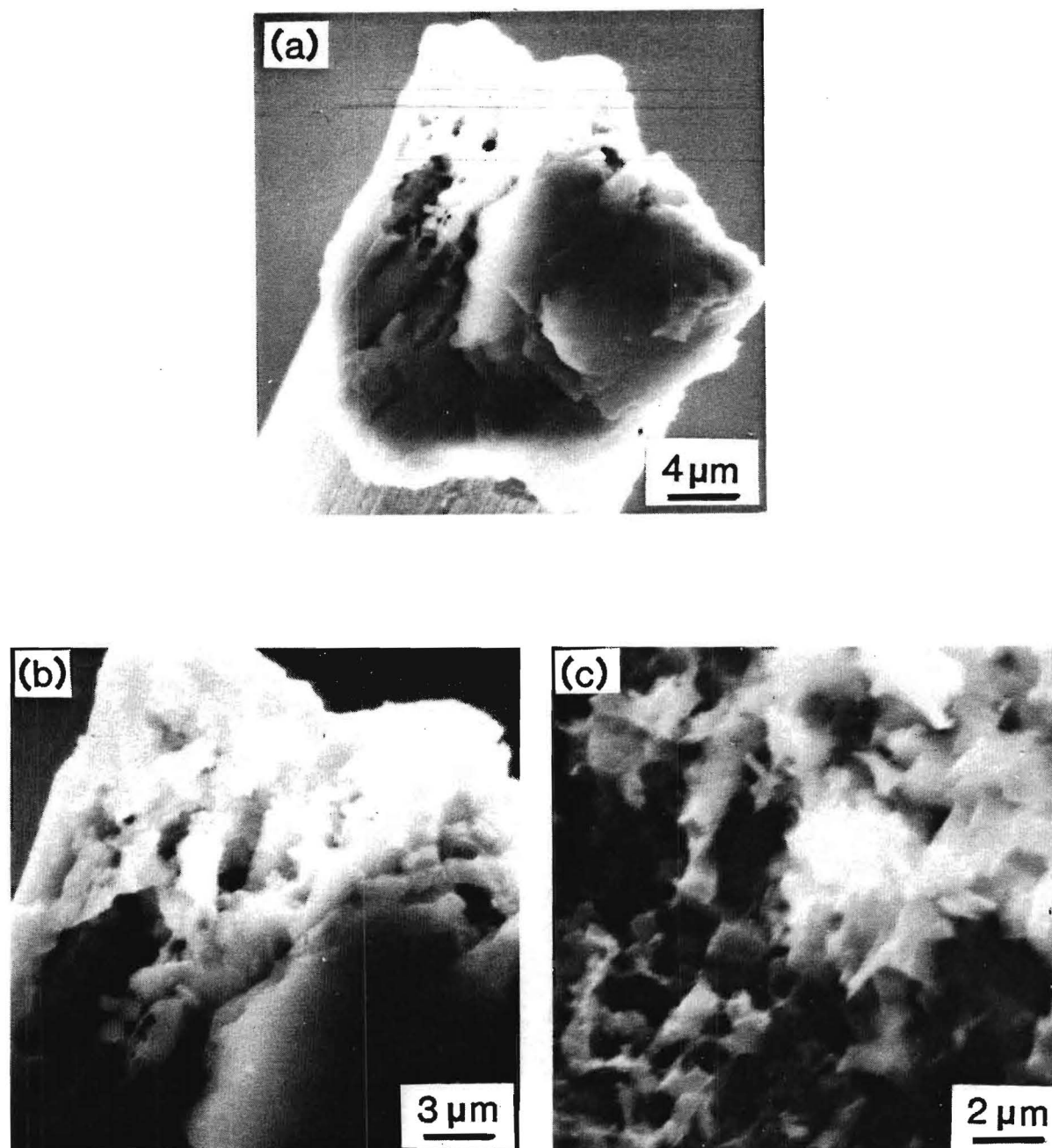


Figure 43. SEM fractographs showing features of an aluminum wire bond (single bond) fatigued in a saline environment. The features are typical of wire bonds fatigued in the hostile NaCl environment.

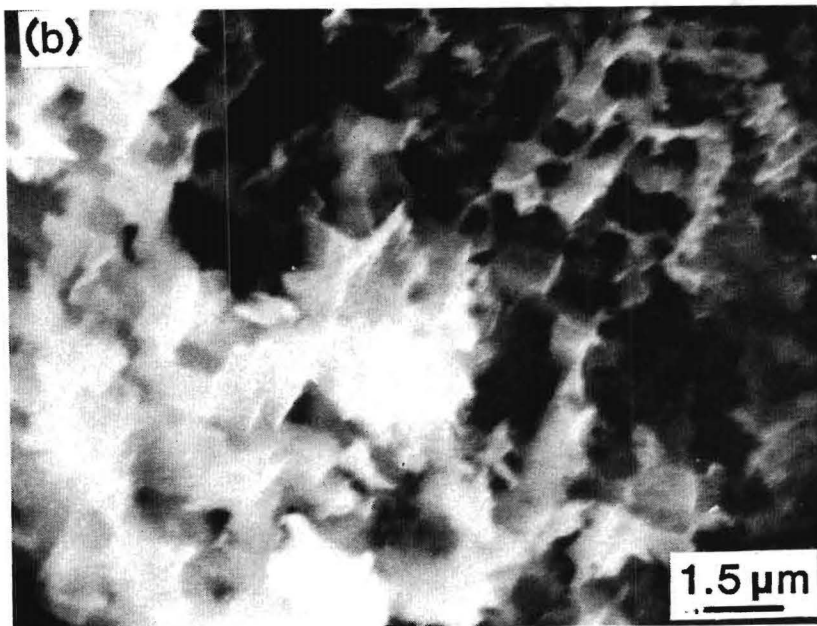


Figure 44. SEM fractographs of an aluminum wire bond (single bond) fatigued to failure in the hostile NaCl environment showing features of the heel region of the bond at the pad.



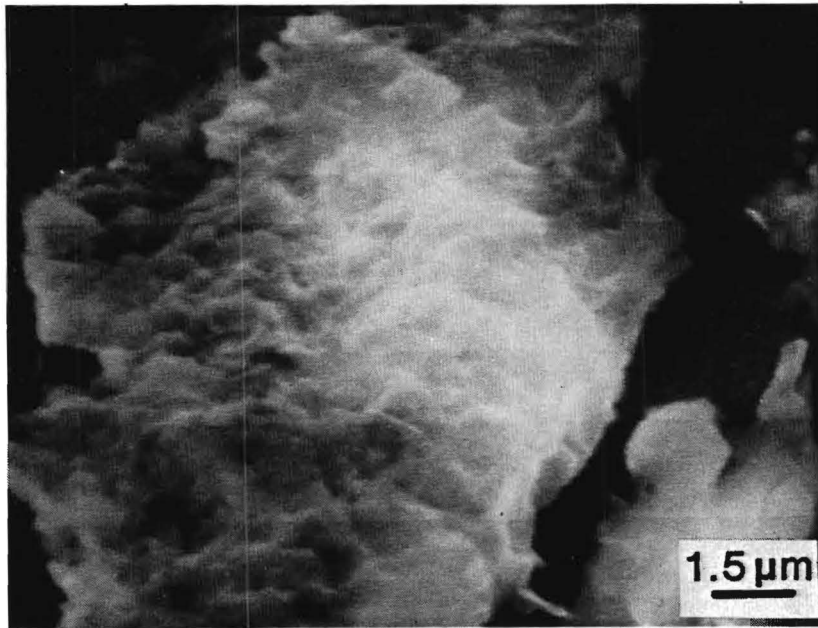


Figure 45. SEM fractograph of a region on an aluminum chip pad where an Al-Al bond had lifted during mechanical cycling in a moist saline environment.

## V. SUPPORTING INVESTIGATIONS

### 5.1 INTRODUCTION

As part of supporting investigations, various metallurgical and mechanical studies were conducted on wire materials and their bonds. These investigations include studies of thermal aging effects on the mechanical behavior of aluminum alloy wires, shear strength measurements on wire bonds, studies of mechanical creep phenomena of the wire bond, examinations of electrical current effects on bond interfaces and microfriction measurements between bond wire surfaces.

### 5.2 STUDIES OF THERMAL ANNEALING EFFECTS ON THE TENSILE PROPERTIES OF BOND WIRES

The doping and thermal mechanical history of stock aluminum bond wire has a significant effect on the ability to produce good bonds from the material and on the subsequent mechanical performance of the wire bond. The 1 percent silicon content in aluminum provides strength through dispersion strengthening. In addition, the saturated silicon content inhibits diffusion degradation mechanisms at the chip. The metallurgical structure of the 1% Si-Al alloy wire used in microcircuits is not thermodynamically stable. These wires have mechanical properties which are highly sensitive to time-temperature exposure.

Mechanical property measurements were conducted on bond wire materials obtained from a number of different suppliers. Tensile stress-strain measurements were made on the as received specimens of these wires as a function of a series of accelerated aging environments. A number of wire segments were taken from the material provided by each supplier. Portions of these segment

lots were stored in a furnace held successively at several temperatures ranging from ambient to 150°C. The specimens were removed from the furnace at selected time intervals and then mounted on tabs for measurement of tensile properties. Tensile data taken for wire materials aged at 150°C are summarized in Figures 46-48. The curves in Figure 46 reveal how the tensile fracture strength of 1% Si-Al bond wires decreases following storage at 150°C as a function of the number of hours in storage. Figures 47 and 48 show how the tensile yield point and elongation to fracture vary with storage time. The wires from several other suppliers provided data which were similar to the behavior shown in Figures 46-48, indicating a degree of industry wide consistency.

Temperatures up to 150°C were selected for the aging experiments since this corresponds to the temperature range normally employed for environmental stress screening of microcircuits. Longer storage times at lower temperatures are necessary in order to have corresponding effects on mechanical performance. This behavior is consistent with the extensive data available from studies of strengthening in corresponding structural aluminum alloys. The major property changes induced by aging the 1 percent Si-Al bond wire at 150 °C occur within about 15 hours.

The Al-Si phase diagram shows that silicon is not metallurgically stable as a solid solution with aluminum at the temperatures of interest in this study. Given time at temperature, the silicon precipitates from the solid solution, initially, in the form of tiny particles. These particles are incoherent with the aluminum matrix and are favored to fracture during cyclic deformation. The long range stress field of dislocations interacts with these incoherent particles in a manner which inhibits dislocation penetration of the particle but

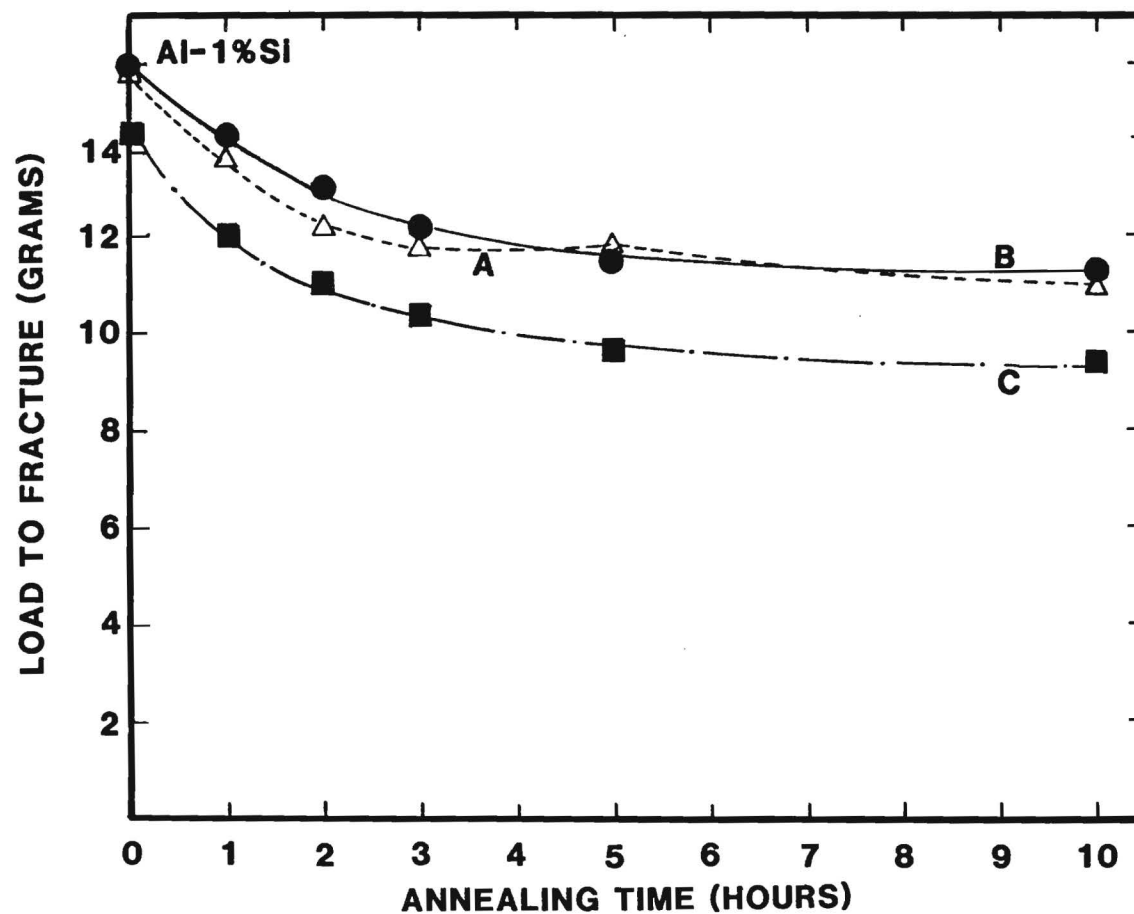


Figure 46 . Plots of load to fracture as a function of annealing time for Al-1%Si bond wires from three different suppliers. Anneal temperature was 150°C and the wire diameter is 0.001 in. The measurements were made at room temperature.

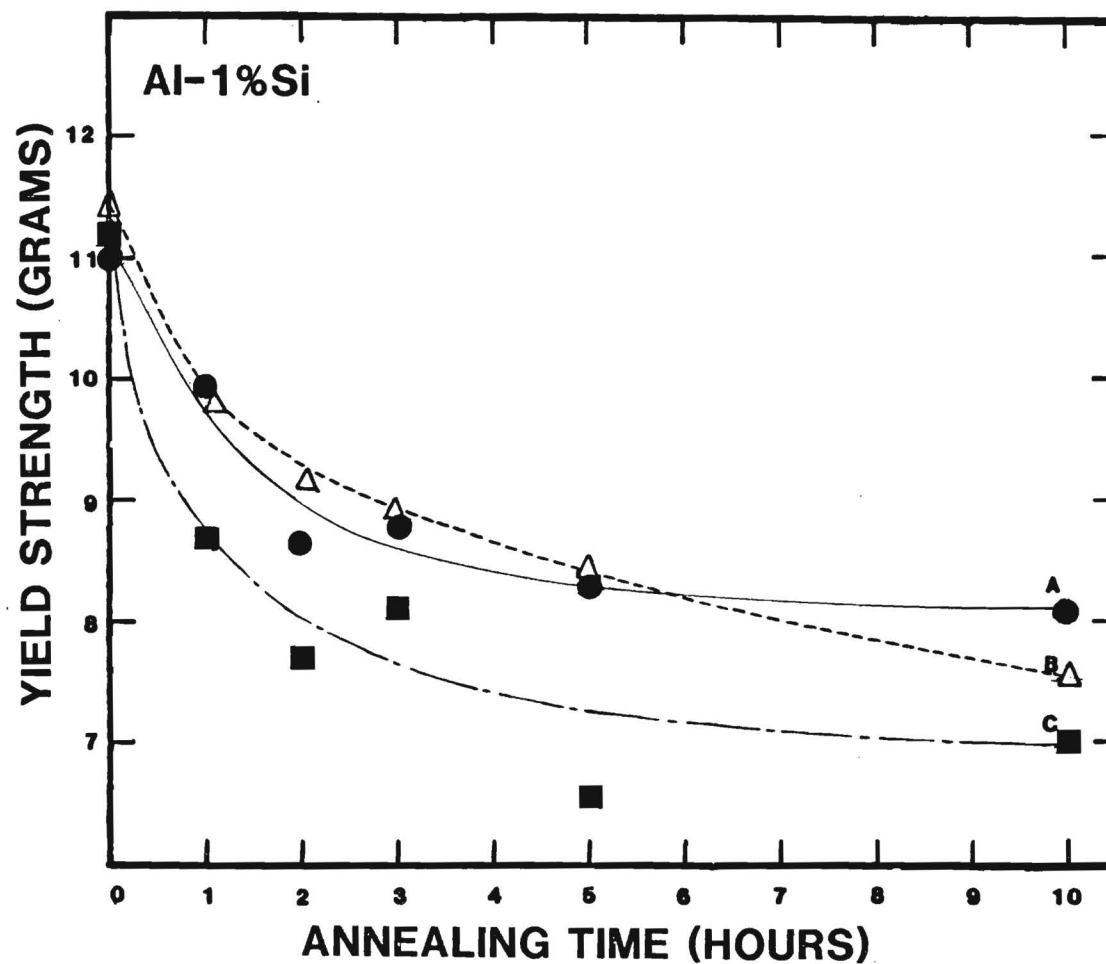


Figure 47. Plots of the tensile yield strengths as a function of annealing time for 0.001 in. diameter Al-1%Si bond wire from three different suppliers. The annealing temperature was 150°C while the measurements were made at room temperature.

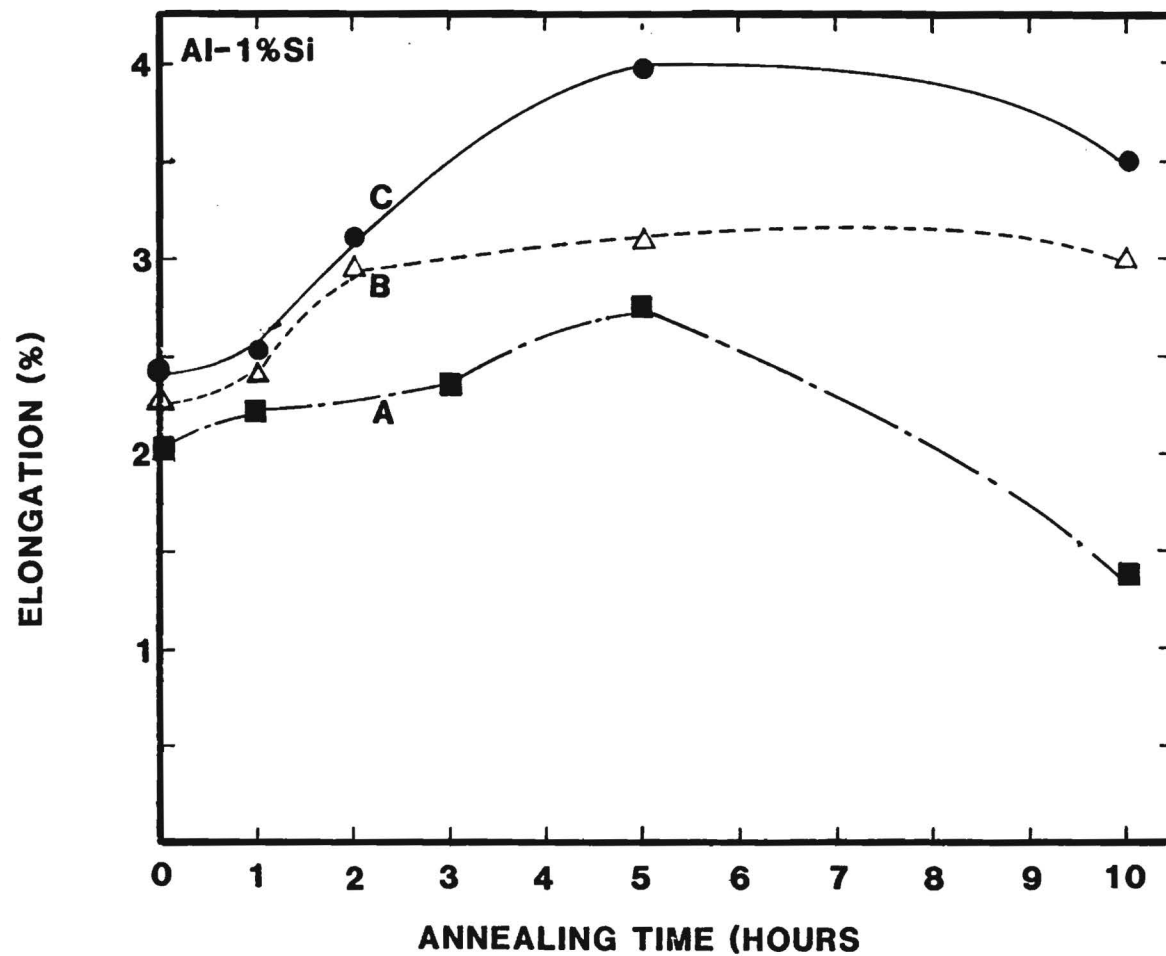


Figure 48 . Plots of elongation to failure as a function of annealing time for 0.001 in. diameter Al-1%Si bonding wire from three different suppliers. The annealing temperature was 150°C while measurements were made at room temperature.

promotes dislocation looping.

If the as-received wires have the proper thermal-mechanical treatment, then the thermal processes normally experienced by a microcircuit will effectively serve to anneal the material. Thermal excursions will promote the silicon particles to coalesce and spheroidize. The environmental stress screens and the normal operational temperatures of an aluminum bond wire result in the wire material experiencing a loss in tensile strength. This loss in strength may not be particularly detrimental unless the device is subjected to strong mechanical shock or vibration levels during its operating life. However, metallurgical changes concomitant with dislocation-particle interactions make the alloy more susceptible to fatigue damage. This mechanism applies both to the wire and to aluminum alloy film conductors deposited on the chip. Recently, metallization fractures initiated by the precipitation of enlarged silicon particles have created enormously expensive reliability problems for certain memory chips.

### 5.3 MECHANICAL CREEP EXPERIMENTS

A simple sample mounting technique was developed to make possible the study of mechanical properties of wire bonds stressed in shear while supporting currents and at elevated temperatures. The first and second ultrasonic bonds are made on separate chips which are then cemented to tabs for mounting on a microtensile apparatus. Segments of either another bond wire or a gold ribbon are also bonded to the chip so that electrical connections can be made to each end of the test wire with negligible mechanical loading due to the electrical contacts. Stress-controlled microtensile instrumentation in the Micromechanics Laboratory has proved to be ideally suited for these measurements. The combination of bond wire sample mounting technique and microtensile instrumentation makes it possible to carry out a number of highly useful stressed electrode experiments for investigating material degradation processes in interconnections. A photograph of the test apparatus showing the stressed electrode fixtures is provided in Figure 49.

Shear testing of single bonds is done by making the bond to a chip and with the other end of the wire segment cemented to a tab. This particular test is also used to ensure that the bonding machine parameters are consistent. As a set of specimens is prepared for fatigue measurements, several single bonds are made for shear strength testing. Optimum settings yield the first bond shear strength to be about 9.2 gram with the second bond at about 12.0 grams. The bond strength test for good bonds is less a shear test than it is a tensile test of the heel region of the bond. For the bond interface to actually fail in shear, either the bonding parameters must be far off or else the wire or pad surfaces are contaminated. The average three gram difference observed between the first and second bond strengths is probably



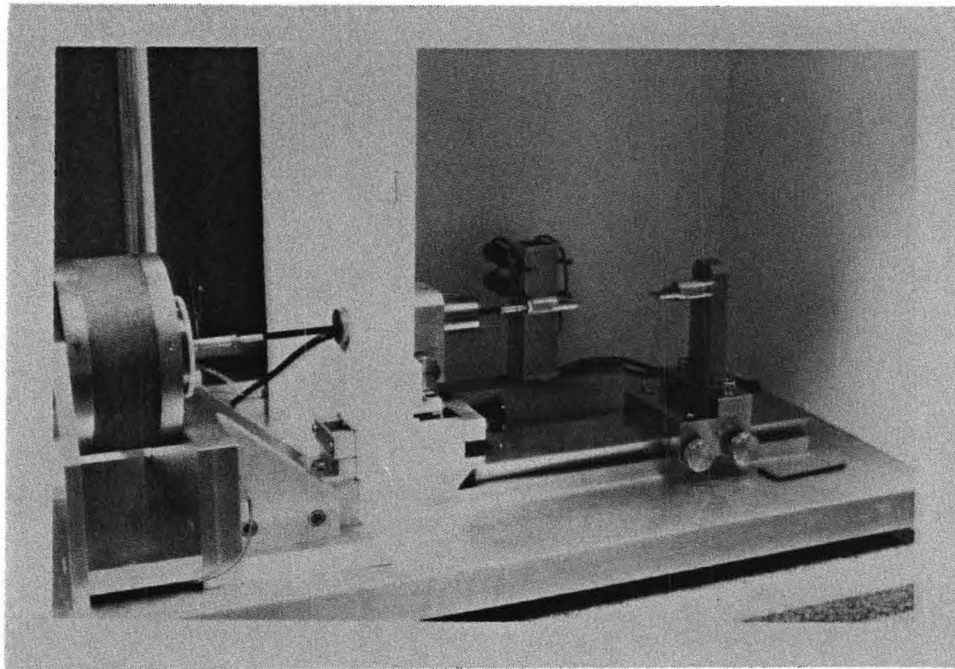
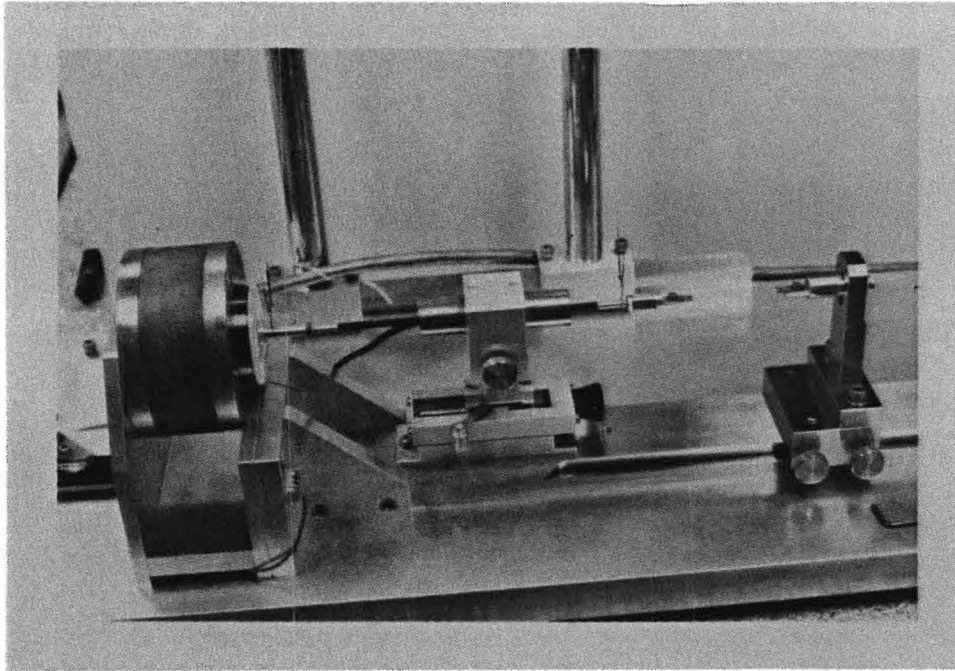


Figure 49 . Stress controlled micromechanics appratus shown in configuration for stress-strain and tensile creep measurements on wire bond.

due to the bonding machine imposing a higher bend angle on the wire after making the first bond. The bending and tensile stresses applied to the narrow bond heel and wire-pad interface region are sufficient to introduce crack initiating mechanisms in the soft metal. However, the post bond involves an aluminum-gold interface which might make a stronger bond under these conditions. There was one case where the post bond lifted for an unfatigued dual bond wire loop pulled in the scanning AES system. A careful survey of the fracture surfaces showed that aluminum was distributed fairly uniformly over the gold post surface but no gold could be found on the mated aluminum wire bond surface. Thus one might conclude that the Al-Au interface was itself strong, but undetermined factors resulted in the separation occurring a few atomic layers within the aluminum wire material. There were also a few patches of much thicker aluminum left on the post.

It had been anticipated that mechanisms normally associated with mechanical creep would play a significant role at elevated temperature and while conducting electric current through the bond wire during the fatigue process. Accordingly, a series of experiments was planned to study the creep mechanisms that operate in the very special configuration of a microcircuit wire bond. The bonds were stressed in "shear" at constant load and the creep characteristics of wire bonds examined as influenced by an electrical current through the bond and externally applied heating. The electromagnetically activated stress-controlled microtensile apparatus accommodates wire bond creep measurements with greater precision than any other known apparatus. As mechanical measurements progressed, it was discovered that creep behavior occurs even at the ambient temperature (298 K) in ultrasonic aluminum wire bonds. Bonds loaded to about 70% of their "normal" strength ultimately failed under constant load

with measured times to failure ranging from a few minutes to six hours. There apparently is a creep threshold for the Al-Al bonds. Low stresses produced no measurable creep over several days. (In these cases, thermal expansion of the wire is measured as room temperature varies from day to night.) Moderate stresses produced creep failures after 18 - 24 hours.

Two very representative ambient temperature creep curves for Al-Al wire bonds are shown in Figures 50 and 51. These curves have linear strain regions characteristic of quasi-viscous creep mechanisms. The data are presented as "elongation" vs. time rather than strain vs. time since it is practically impossible, using normal transducer technologies, to estimate with any precision the length of the tiny region within the bond heel where the strain is suspected to occur. Creep has also been measured in the wire itself by reinforcing both ends with a high strength adhesive. However, the wire creep rates are very small for the force values providing high bond creep rates. Most, but not all, specimens have a linear strain rate region as shown in these two figures with the linear rates ranging from less than 2 microns per hour to about 15 microns per hour. However, it is always observed that the initial creep rate, which occurs upon loading the specimen, and the tertiary creep rate just prior to fracture have much higher values.

The discovery that creep processes exist in microcircuit wire bonds has wide ranging implications. Creep rates were found to increase with current and/or temperature with values ranging from 25 and over 100 microns/hour at 100ma. As discussed earlier, the bond region is a complex combination of highly deformed metal, particles, oxide interface inclusions and numerous surface and interface stress concentrators. Some bond specimens exhibited creep behavior controlled by mechanisms that can be best described by the generalized Nabarro creep phenomenon

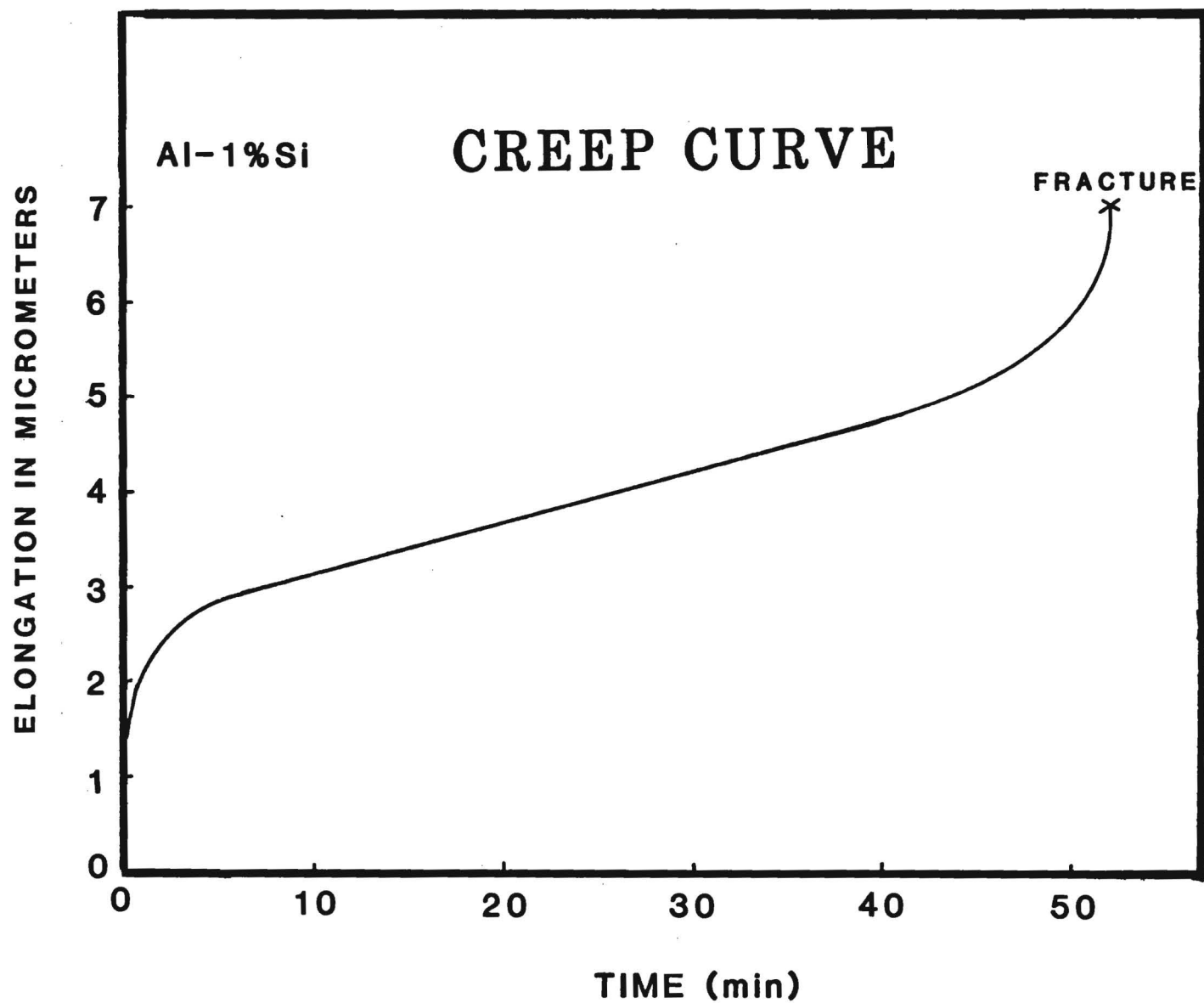


Figure 50. Mechanical creep of an Al-Al wire bond at room temperature with a constant applied load of 6.8 gramsforce.

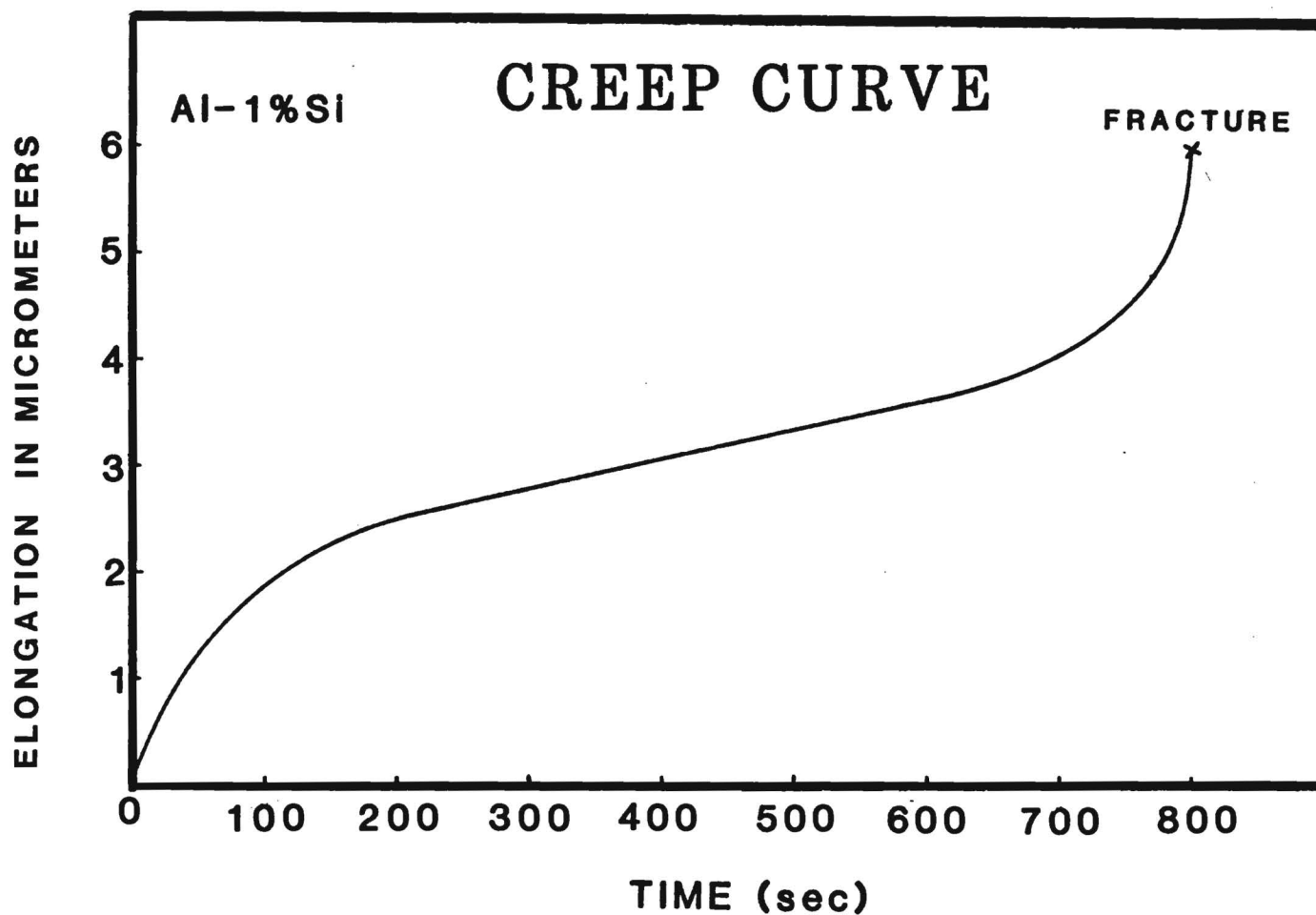


Figure 51. Mechanical creep of an Al-Al wire bond at room temperature with a constant applied load of 6.8 gramsforce.

wherein the self diffusion of vacancies within the bond metal is greatly enhanced due to the high defect density within the aluminum. The self diffusion processes promote dislocation climb mechanisms and thereby a relatively slow rate of plastic deformation.

The heterogenous bond-pad interface, coupled with surface nonuniformities on the wedge bonds, results in localized regions of the metal being subjected to much higher stresses than would be the case if the material were uniform. SEM micrographs of an aluminum wire fractured during a mechanical creep measurement are shown in Figure 52. The plastic deformation indicated by creep fracture surfaces is always much more extensive than that of mechanically cycled fractures. A bond presents conditions which promote both thermally activated and stress activated viscous flow of dislocations. Recent theoretical treatments of these mechanisms appear applicable to analysis of these experiments [29]. Consequently, the experiments have been modified in order to explore these important phenomena in greater detail.

To the author's knowledge, the mechanical creep phenomena had not been previously observed directly by other investigators of microcircuit materials. However, a review of the microelectronics reliability literature has provided several examples where creep mechanisms were apparently active in influencing the reported materials behavior.

The present observations show similarities to recently reported investigations on creep phenomena in fcc metals for purposes other than microelectronics[30]. The important point is to rationalize how these different mechanisms operate in configurations used in the fabrication of microcircuits. As outlined elsewhere, the freshly made wire bond and a metallization conductor are unstable metallurgical structures which initially have high residual mechanical stresses. These

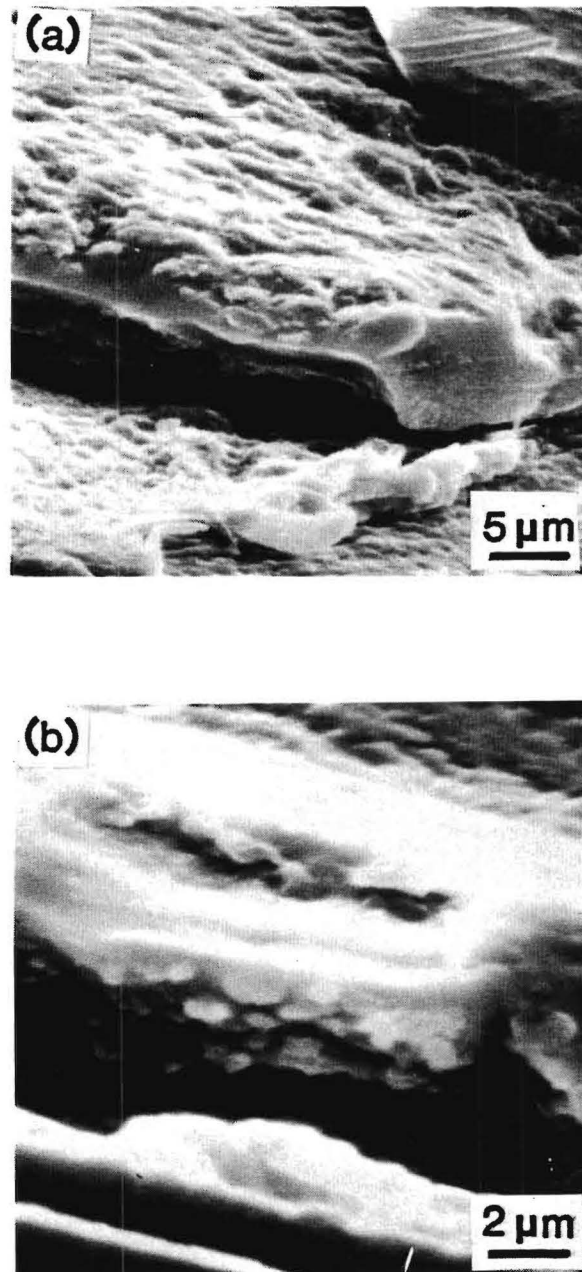


Figure 52. Scanning Electron Micrographs showing typical features observed in the Al-1wt pct. Si microcircuit wire subjected to creep at ambient temperature.

stresses may be partially relieved during either a high temperature storage screen or later during operation at elevated temperatures. This stress relief probably occurs via the same mechanisms which are involved in creep.

The wire bond creep data have convincingly demonstrated that normal microcircuit operating stresses (temperature, current) introduce conditions which activate mechanical creep mechanisms. The mechanical fatigue degradation of wire bonds is therefore influenced by atomic diffusion and dislocation mechanisms which normally are associated with creep phenomena. The critically important crack initiation and initial crack growth processes that cause fatigue failure in wire bonds evidently occur through synergistic interactions of various micromechanisms associated with creep phenomena and those employed in the analysis of cyclic fatigue models.



#### 5.4 MICROFRICTION MEASUREMENTS

Relationships have been proposed between friction characteristics and intermetallic bonding phenomena. While the previously reported quantitative relationships are primarily empirical, there is a strong fundamental materials basis for such relationships since solid-solid friction involves the repeated making and breaking of microscopic adhesive bonds. The opening and closing action within a growing fatigue crack presents similar behavior.

In order to illustrate the stick-slip interactions occurring between two aluminum surfaces at low contact forces, friction forces were measured between two 1 % Si-Al bond wires. Curves from measurements made on aluminum bond wire specimens at three values of normal force appropriate to those anticipated in a fatigue crack are shown in Figures 53 - 55. The bond wires were suspended under tension by bows and oriented at right angles with each other. The normal forces of 1.1, 1.7 and 2.3 mg are indicated on the data. The upper curve represents the sliding of one wire over the other in one direction with the lower curve in the reverse direction. The forces for the two curves have opposite signs as indicated. The fine structure of the stick-slip friction characteristics indicates the mechanisms likely to be active within a fatigue crack. The individual force peaks, indicative of the making and breaking of microbonds, may be either greater or less within a fatigue crack, depending upon both the environmental penetration and time scale. Other curves have illustrated the fracturing of relatively loose surface oxide coatings on aluminum and the lubricating effect of moisture or other impurities on the surfaces.

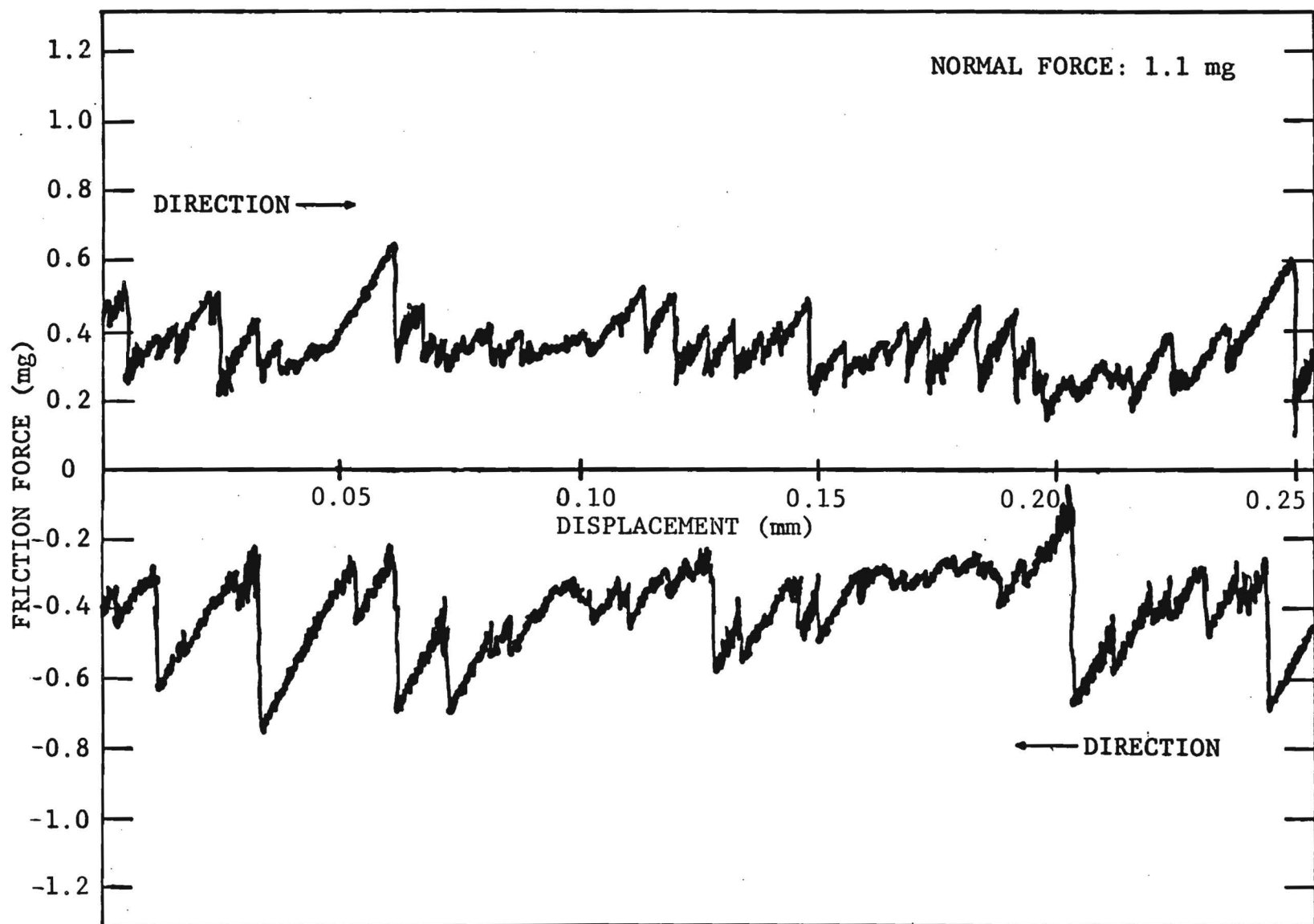


Figure 53 . Microfriction forces for two aluminum bond wires with 1.1 dyne normal force.

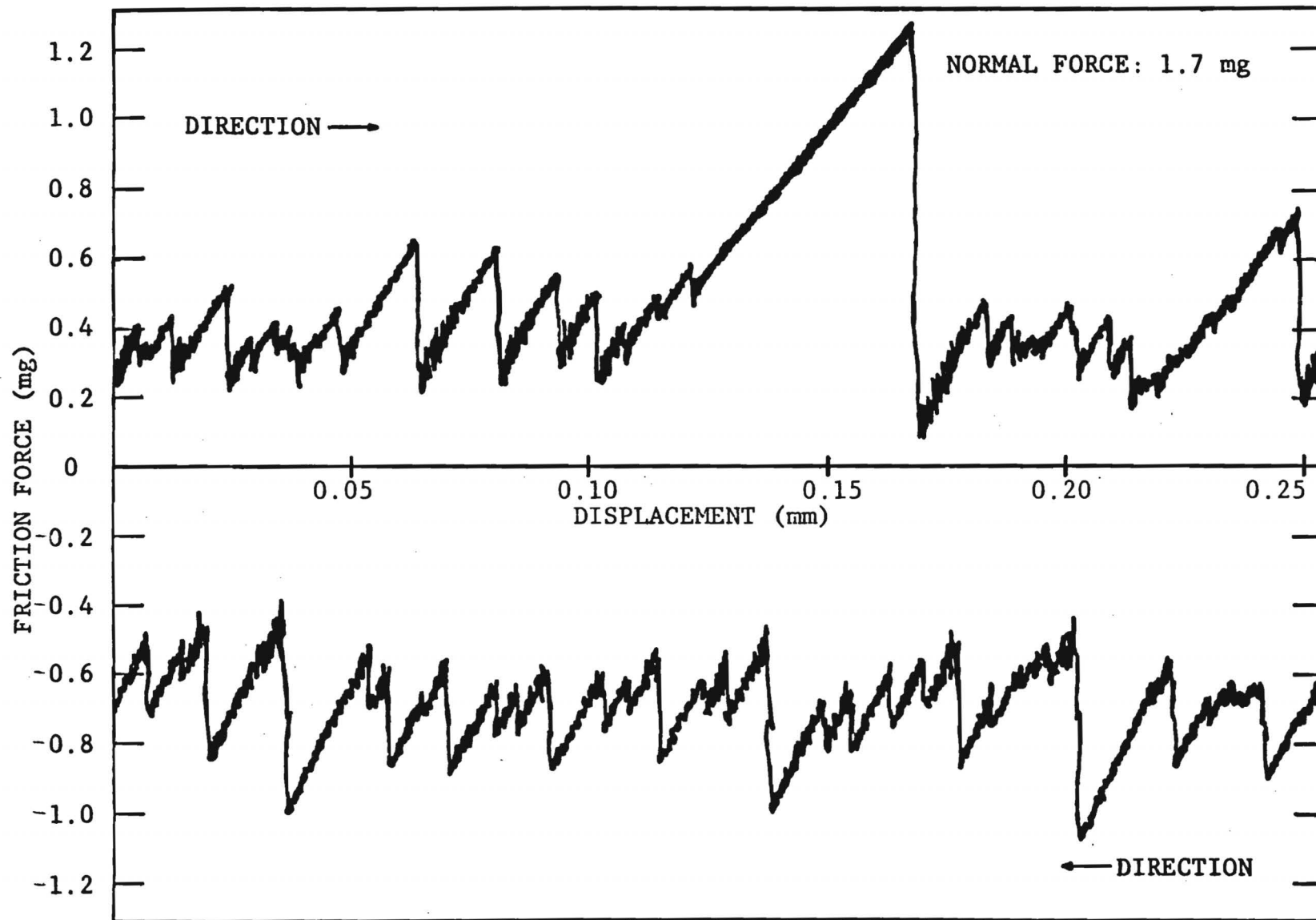


Figure 54 . Microfriction forces for two aluminum bond wires with 1.7 dyne normal force.

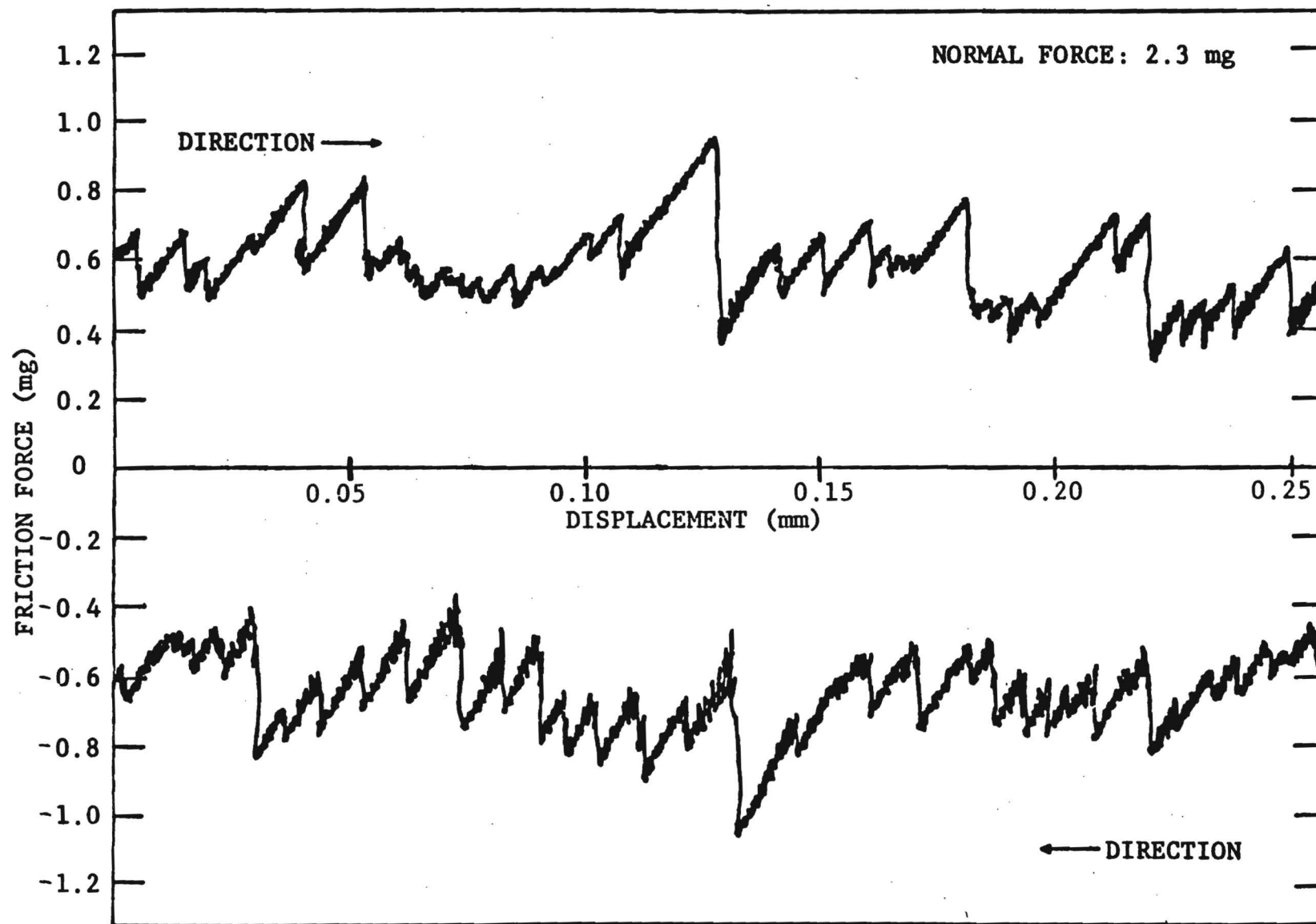


Figure 55. Microfriction forces for two aluminum wire bonds with 2.3 dyne normal force.

## 5.5 FRACTURE SURFACE ANALYSIS OF ALUMINUM BONDS USING SCANNING AES TECHNIQUES

Very small quantities of impurities can have a profound effect on the mechanical, chemical and electrical integrity of materials. This is particularly true for the small and delicate structures involved in various microelectronic devices. Consequently, considerable care has been exercised in keeping bond test materials as clean as possible for these studies.

Extensive studies of stress corrosion cracking and corrosion fatigue in structural metals have demonstrated that active ions of certain chemical agents are able to penetrate the materials through mechanical stress activated mechanisms which greatly accelerate mechanical degradation. It was accordingly desired here to determine if it would be possible to detect the projection of the chemical ions producing environmental fatigue degradation in the Al-Al wire bonds. Attempts had earlier been made in our experiments to detect the presence on bond fracture surfaces of ions such as Cl and Na from the saline environments using the X-ray analysis capabilities of the SEM. However, the detection sensitivity of the SEM proved inadequate for the small quantities of these chemicals responsible for crack growth in wire bonds.

The recent installation of new state-of-the-art surface analysis facilities at Georgia Tech made it possible to design a set of experiments to detect the possible penetration of ions from stress activated chemical agents in microcircuit materials. The detection sensitivity of the scanning AES, or SAM, is quite sufficient for these needs but special procedures are required for these measurements to have meaning. A primary problem is that bond surfaces, subsequent to fatigue fracture in a particular environment, may become completely coated by the

chemical after the metal fails.

Techniques accordingly were developed for arresting the environment assisted fatigue crack growth prior to complete fracture. The wire bond specimens were subsequently fractured within the ultra high vacuum chamber of the SAM and their freshly exposed surfaces immediately subjected to composition analysis.

The low stress single bonds mechanically cycled in the NaCl environment proved to be well suited for this type of experiment due to the relatively simple configuration of a single bond. The hysteresis loops were carefully monitored and compared to those which progressed to fracture under similar circumstances. In this manner, it was possible to arrest the mechanical fatigue damage process at approximately desired states of progression. The specimen was then carefully rinsed with distilled water to remove the salt from all exposed surfaces. The free end of the bond wire was then carefully cemented to a post so that the wire formed a loop to facilitate later fracture in the SAM chamber.

The SEM micrographs shown in Figure 56 were made in the SAM of an aluminum bond for which fracture was completed in the SAM chamber. High chlorine levels were measured in the granular regions seen in the higher magnification micrographs. Na has not been detected on any fracture surfaces, indicating that Cl is, indeed, the ion responsible for the relatively rapid progression of mechanical degradation for the bonds mechanically cycled at low stress amplitudes while exposed to saline moisture. A SAM spectrum showing the Cl is provided in Figure 57. Bonds fractured in air after similarly being partially fatigued did not reveal Cl on fracture surfaces when subsequently analyzed in the SAM. Apparently, the chlorine ions are able to escape from fractured aluminum surfaces either due to the atmospheric exposure or else during the pump-down in the SAM chamber.

Traces of copper and sulfur were found on some of the

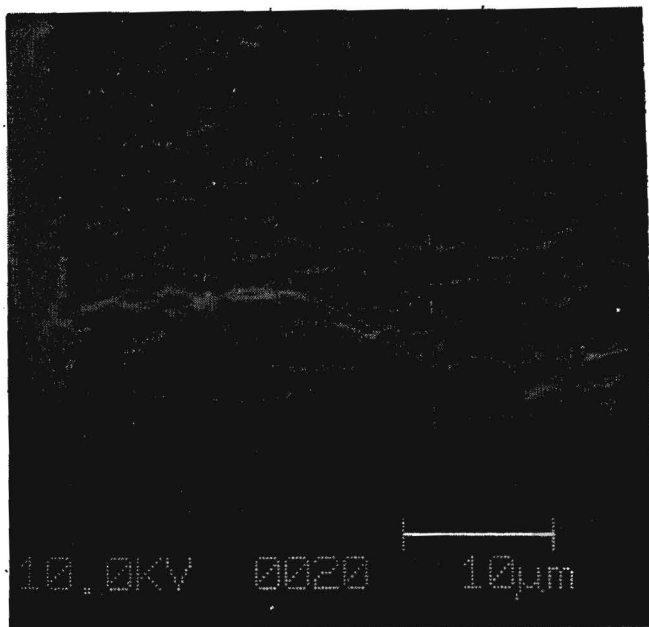
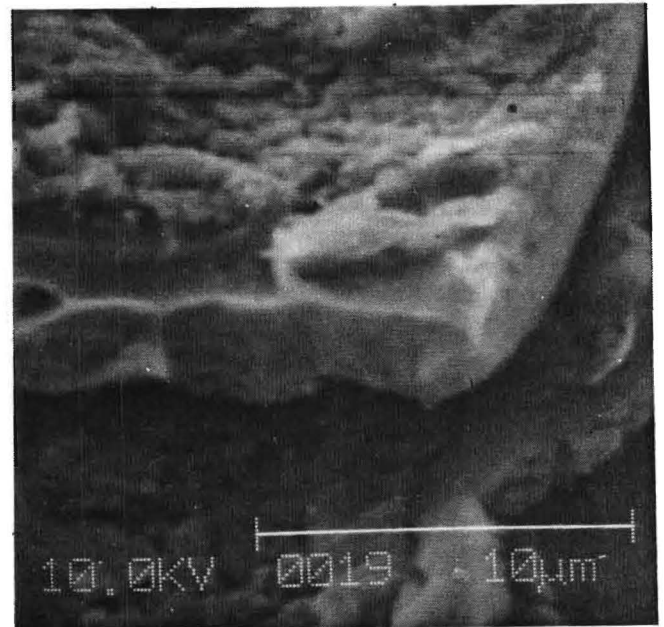
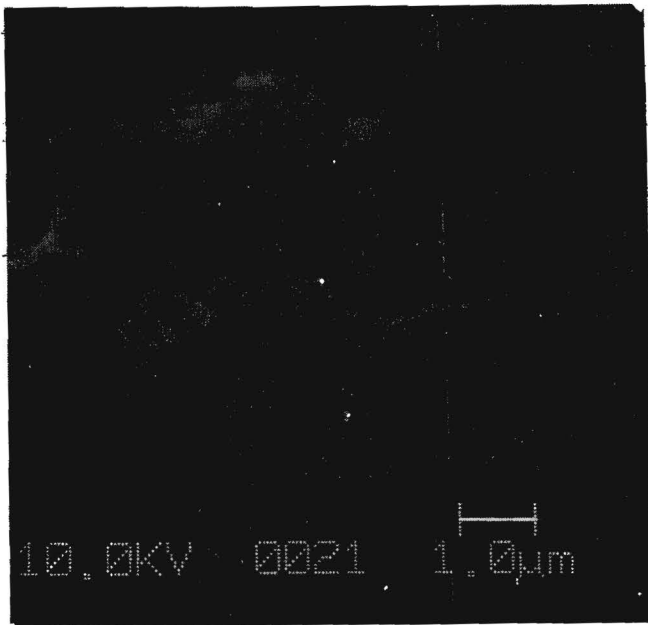
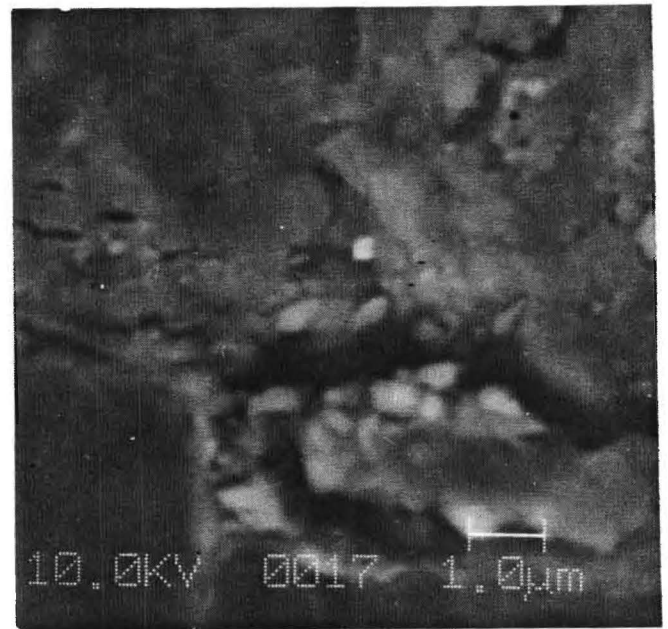
**(a)****(b)****(c)****(d)**

Figure 56. SEM fractographs taken in the SAM showing regions surveyed for the presence of chlorine.

- (a) Pad foot and fracture surface.
- (b) Region on the right side of the pad foot fracture surface.
- (c) High magnification of features on the pad foot fracture surface.
- (d) High magnification of region on the mating wire fracture surface showing corrosive attack of Al by chlorine.

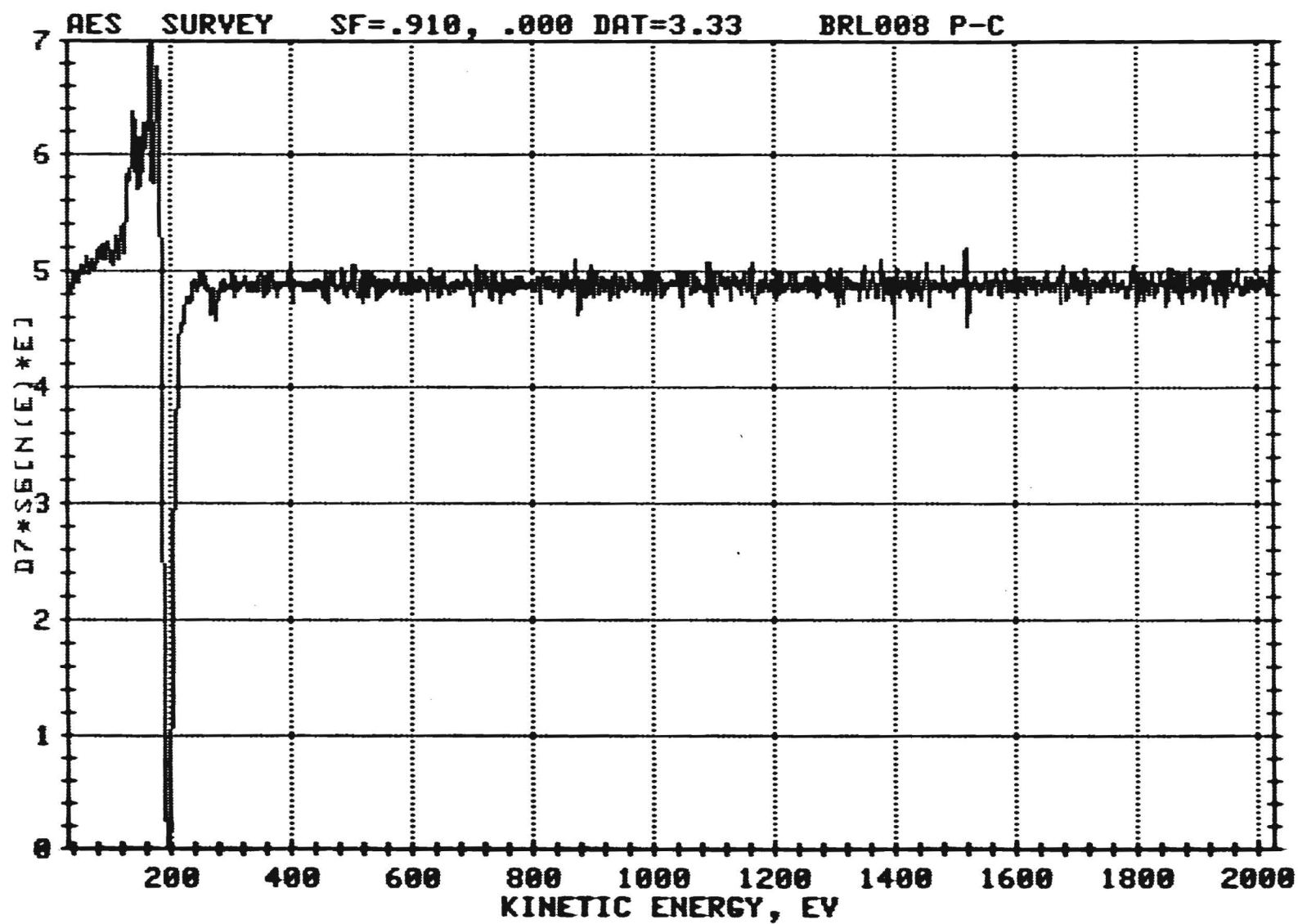


Figure 57. AES survey of region on wire fracture surface in figure 56d showing presence of a chlorine peak at 190 eV.



package post pad surfaces along with the gold metallization. Carbon appears in some degree on all surfaces, apparently as an artifact of the system. Post bonds were found to be generally stronger than chip pad bonds during these investigations. Accordingly, when the normal double bonds were fractured in the SAM chamber, chip bond failures were expected. However, one post bond lifted in the SAM as a dual bond was pulled, permitting a careful examination of the resulting fractured surfaces. It was found that traces of aluminum remained generally on most of the gold plated pad surface, with some thicker clumps of Al. Au was not detected anywhere on the mating aluminum wire surface which had been bonded to the post. Apparently the Al-Au interface fracture occurred entirely within the aluminum metal, but very close to the interface. Cl was not detected on this surface.

The SAM became available for these investigations only recently. However, the type of study represented by the relatively preliminary experiments described in this section clearly provides a powerful technique for investigating details of mechanisms involved in environmental assisted mechanical damage processes in small microcircuit materials. The Cl ion penetration should be examined in much greater detail for various bond damage configurations and for other metallurgical combinations. Studies involving other chemical agents similarly exposed to mechanically stressed microcircuit materials are also in order. Similar applications with ESCA and SIMS should prove valuable as well. These newly available surface analysis facilities have greatly enhanced the Micromechanics Laboratory's capability for determinations of operating degradation mechanisms in the small specimens typical of microelectronic members.

## VI TECHNICAL DISCUSSIONS

The dimensionality of microcircuit wire bonds is shown in these investigations to have a major effect on the mechanical durability of microcircuit structures. The operation of a microcircuit involves cyclic thermal mechanical stresses in the wire bond metal leading to mechanisms normally associated with low cycle fatigue. The instrumentation of the Micromechanics Laboratory has been well suited for making the measurements needed to investigate the manner in which these mechanisms operate in specimens of the sizes of wire bonds. Special fixtures and techniques developed made it possible to conduct extensive measurements of mechanical hysteresis phenomena in tiny wire bond specimens. These cyclic hysteresis data analyzed along with optical, SEM and AES studies of the fracture features have provided a better understanding of the degradation mechanisms in microcircuit materials.

The hysteresis curves exhibit unique characteristics when related to similar curves obtained for bulk specimens of various structural alloys. In the first place, the bond hysteresis curves are distinctly asymmetrical in shape. In one half of a fatigue cycle, the wire-pad interface is in compression while the upper surface of the bond is flexed in tension. During the other half of the cycle, the top surface of the bond is in compression while the material joining the wire to the pad experiences tensile stresses. It is generally recognized that the major strains causing fatigue damage in metals occur as a result of tensile stresses in the surface material.

The amplitudes of cyclic stresses imposed in the wire bond metal induce the movement of large numbers of dislocations. Specimens showing work hardening indicate that dislocation densities are being multiplied, forming complex tangles whereby

further slip is inhibited by interactions between the large numbers of dislocations. Dislocation-dislocation interactions account for the work hardening phenomena in all metals. An unusual aspect of the wire bond fatigue data is that a specimen can exhibit cyclical hardening in the compressive half of a flexure cycle while softening occurs during tension. Cyclic softening in aluminum alloys is generally ascribed to factors with orientation of the dislocation debris into cell structures, formation of dislocation dipoles, etc. as a result of stresses causing the reverse movement of dislocations [31-34].

An explanation for these differences is partially found in the different types of interfaces existing at the upper and lower surfaces of a wedge bond. A wedge bond is clearly seen in the Scanning Electron Microscope to be comprised of highly deformed metal with the upper surface of the wire roughened due to the action of the bonding tool. The lower side of the wire, which is bonded to the pad, involves the bond interface which includes impurities and other surface debris which one would rather not have. Thus, the intricate surface features of both the upper and lower sides of a normal bonded wire contain numerous sites which may well act as potential sites for stress concentration, thereby enhancing the activation of degradation mechanisms. Considering the difficulty involved in precisely duplicating interface features of this nature from bond to bond in addition to the very deep deformation of the wire metal during bonding, it is not surprising that different characteristics are often measured here in the sensitive hysteresis data for supposedly identical wire bond specimens.

The lower side of the wire of a wedge bond involves large numbers of microbonds between the wire and the pad metals, with the original oxides and possible surface impurities interspersed. These intermittent sites of metal bonding are loaded during the

tensile part of a stress cycle, with localized stress values considerably in excess of those calculated from an average load distribution. The highly localized stresses produce extensive plastic deformation in these regions, nucleating and propagating dislocations into neighboring regions of the metal as well.

The upper surface of the bonded wire, characterized by a highly roughened surface as seen in the SEM, also is an example of the type of surface one would rather not have in order to achieve optimum fatigue strength in a metal couple. The forces between the soft wire material and the bonding tool deform the wire metal with scratches and depressions determined by surface asperities on the bonding tool. In addition, rubbing of two metal surfaces is generally found to cause prow formation, which consists of small quantities of the softer metal being transferred to asperities on the surface of the harder metal. The prows may subsequently be transferred back to the wire surface and pressed into the wire during the application of force for bonding. Exhaustive SEM observations of different bonds indicate that this process indeed does occur. A prow of aluminum would likely be a mixture of tiny oxidized film fragments and the metal. Each of these potential sites for roughness results in a surface having an extensive collection of features to nucleate fatigue cracks.

The entire thickness of a microcircuit bond region corresponds to the dimensions normally involved with crack nucleation and Stage I crack growth mechanisms as designated for bulk structural alloys. The operation of cyclic degradation within a microcircuit bond material is therefore a very special case of material fatigue. Slip bands initiating near the surface are directly influenced by factors affecting mechanical stresses at the opposite surface of the bond.

A dislocation mechanism for the development of surface

extrusions and intrusions at the surfaces of bond metals with cyclical plastic deformation is illustrated in Figure 58. The stress in one direction produces slip on a suitably oriented plane, resulting in the slip step in (b). The stress reversal creates a similar step at some angle to the initial slip plane. Subsequent repeated stress cycles activate dislocation motion on neighboring slip planes to generate the intrusions and extrusions illustrated in (d) and (e) [35].

As discussed earlier, the surfaces of aluminum are never free of oxides. Calculations of the interface interaction forces of dislocations in geometries of concern here for natural aluminum oxide films of various thicknesses on pure aluminum metal are plotted in Figure 6. Close to the oxide coating, the dislocation is effectively repelled by the interface due to stress field energy considerations. However, real metals never present single dislocation interactions and one is really concerned with the forces acting on large assemblies of dislocations [36]. This situation is schematically represented in figure 59 where dislocation "pile-ups" are shown to develop on active slip planes. When the numbers of dislocations increase such that the shear stress at the leading dislocation exceeds the fracture stress of the oxide, the oxide surface fractures permitting the egress of dislocations and formation of a surface slip step. The mechanisms described in Figure 58 then proceed.

It was pointed out earlier that the surface strengthening due to oxide and dielectric films are critically important to the stability of a microcircuit. Thus, anything that changes the properties of the surface coating material, potentially, may have a deteriorating effect on the durability of the metal member. For example, moisture and other chemical agents are known to reduce parameters such as the elastic modulus of thin natural oxide coatings of aluminum or even to dissolve them. The

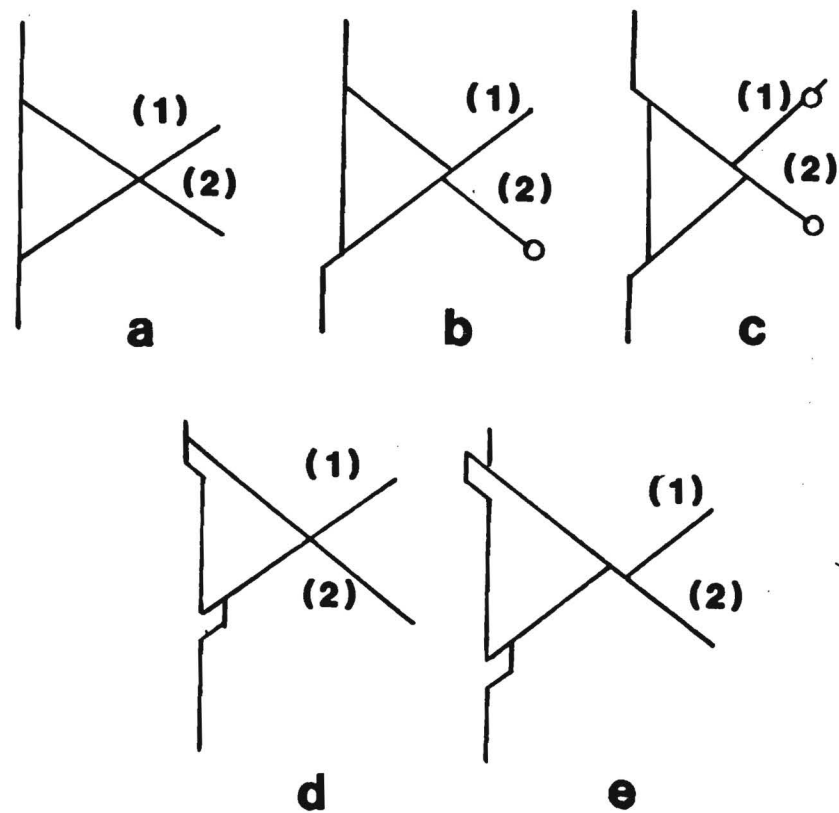


Figure 58 . Operation of two intersecting slip bands in sequence resulting in the formation of intrusions and extrusions. The forward cycle is represented by (b) and (c) and, the reverse cycle by (d) and (e).

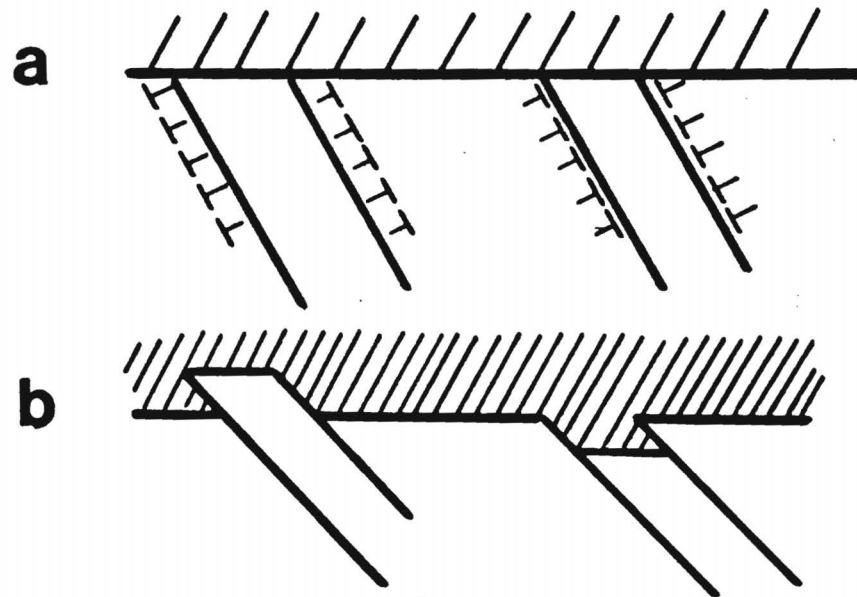


Figure 59 . Schematic showing dislocation pile-ups due to cyclic straining.

environment thus weakens the surface strengthening mechanisms operating in the microcircuit materials resulting effectively in corrosion fatigue degradation under cyclical loading. Figure 60 illustrates another model for environmentally assisted crack growth [41] with cyclical loading of the aluminum surfaces.

A model developed to describe the growth of low cycle fatigue in bulk structural alloys is illustrated in Figure 61 [37]. The asperities existing at both bond surfaces provide precisely the conditions necessary for operation of this mechanism in the "bulk" of the bond wire metal at the region of the heel.

The 1 %Si alloying typically employed in aluminum bond wires will precipitate hard particles which serve as sites for stress concentration and consequently the nucleation of fatigue cracks. This mechanism of crack nucleation is well documented in the literature and is largely responsible for fatigue degradation in structural aluminum alloys. Aluminum oxides which exist within the bond heel region will similarly serve as sites for stress concentration during cyclic deformation.

The fatigue experiments and related investigations conducted during the course of this program have shed considerable light concerning the operation of fatigue degradation mechanisms in wire bond metals. They have also raised many questions which need to be explored. For example, experiments using wire bond specimens taken from a set made under identical conditions often exhibited considerable variation in the fatigue parameters measured. However, monotonically stressed specimens from the same group yield bond pull test values with comparatively small scatter. Thus, there clearly exists metallurgical features which have a greater influence on fatigue characteristics than on the monotonic tensile strengths (pull tests) of wire bonds.

All microcircuit bonds involve highly deformed metal, which



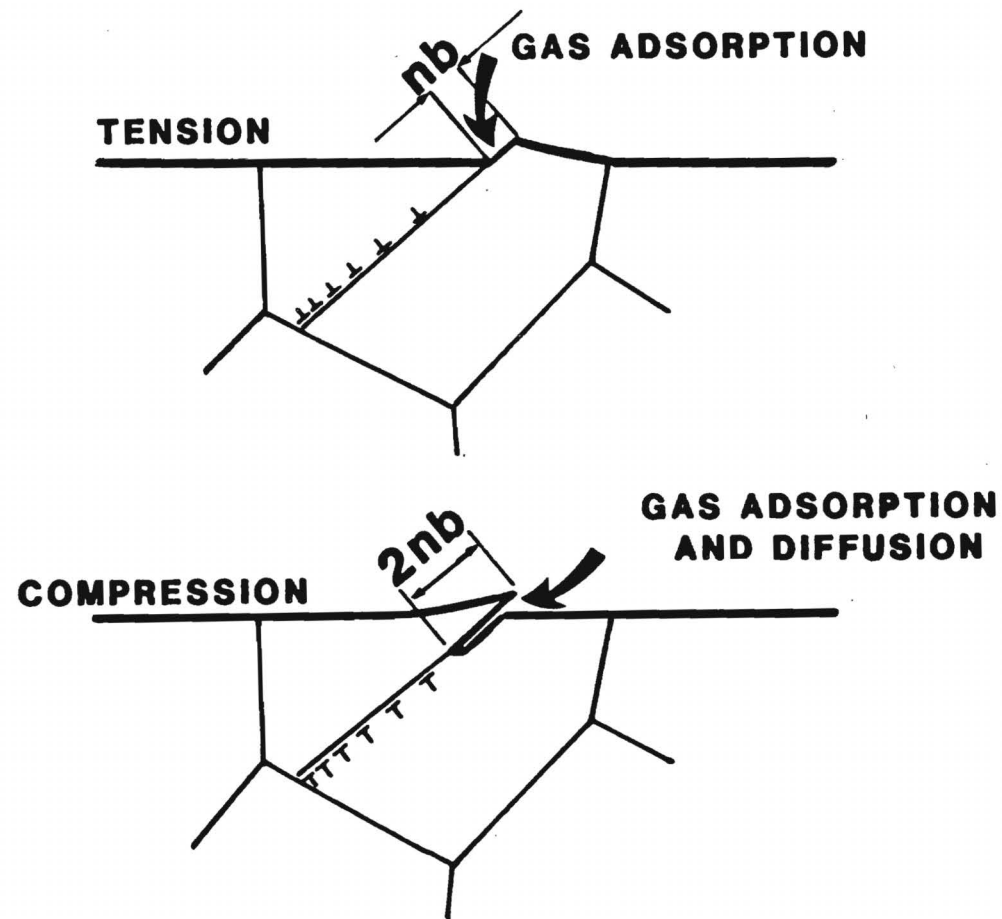


Figure 60 Schematic showing environmentally assisted cyclic slip-band cracking.

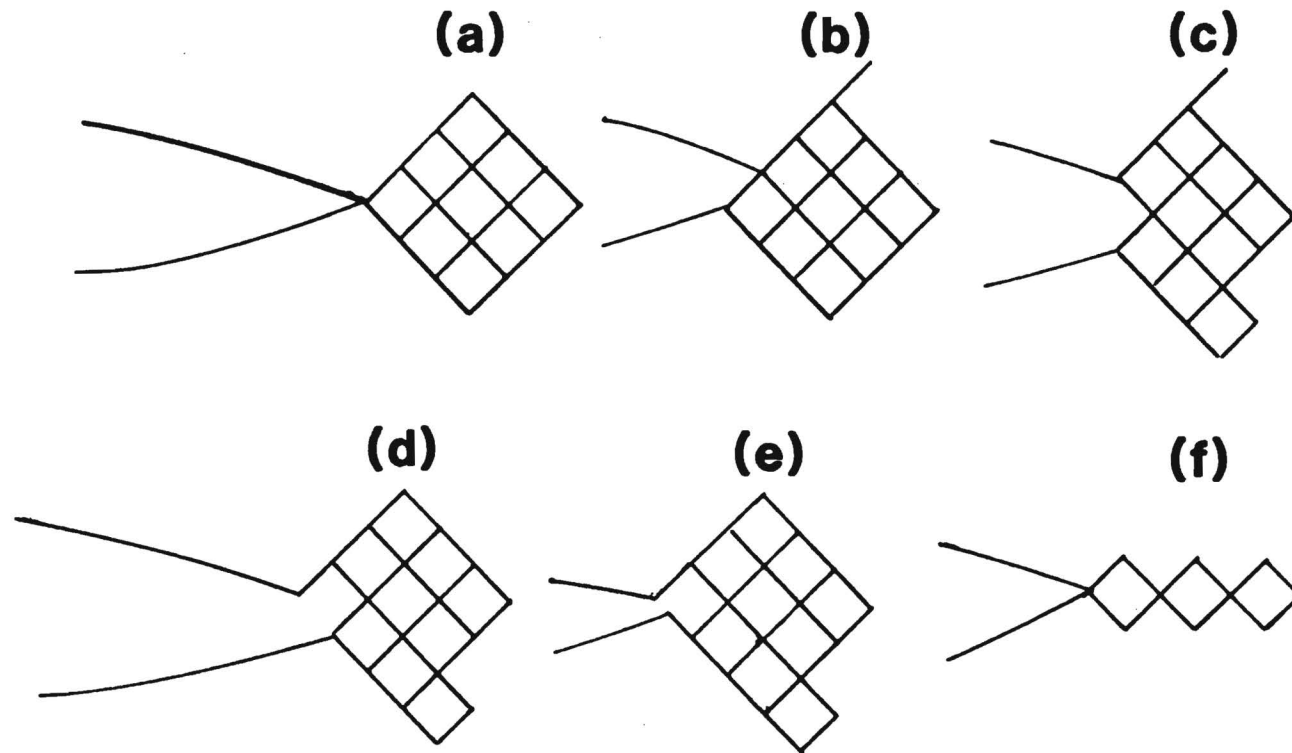


Figure 61. Schematic representation of a model for fatigue crack growth by shear sliding. (a) initial configuration, (b) crack opened in tension with shear sliding along a slip plane above the crack plane, (c) shear sliding along a slip plane below the crack plane, (d) crack unloaded with reverse shear sliding on slip plane of (b), (e) crack tip sharpening and crack advance, (f) repetitions of the mechanism.

induces high dislocation debris and, consequently, hardening due to dislocation-dislocation and dislocation-particle interactions. It might therefore be anticipated that only softening would occur during fatigue cycling. In fact, the hysteresis loops of wire bond specimens go either way. Apparently, the dislocation arrays generated during the bonding process fail to cause the heel region of the bond to be in a fully work hardened state. This point is supported by the shapes of monotonic stress-strain curves taken for single bonds stressed in tension.

The hysteresis loop energies were found to vary during fatigue cycling of a wire bond specimen. Over a number of years, several extensive investigations of cyclic fatigue characteristics in bulk structural alloys have been able to establish correlations between the total energy to fracture and number of cycles to fracture and stress amplitude [32, 38, 39]. However, the data do not support similar types of correlations for the wire bond materials of the current study. This may be attributed to the extraordinary softness of the metal used for electronic applications as compared to the high strength metal alloys employed in large aerospace structures. However, variations in energy absorbed per cycle reflect the micro-mechanisms operating during cyclic plastic deformation. The dislocation-lattice and dislocation-dislocation interactions occurring with plastic flow convert mechanical energy into heat, with very little of the cyclic energy stored in the metal as residual elastic stress energy. If dislocation movements were completely arrested via strong pinning points, one would expect very little plastic deformation. There is also evidence for energy dissipation due to what may be frictional processes occurring within multiple microcracks as the stress alternates in sign. This latter mechanism most likely occurs in some bulk structural alloys, but it would be more significant in the soft

aluminum and gold used in wire bonds.

The loop energy data show different trends for bond specimens cycled in the inert dry air environment, in the several types of moist environments and for electrical currents in the bonds. The high humidity level, with and without a saline atmosphere, tends to reduce the loop areas and the number of cycles to failure.

In the laboratory air environment, a freshly created aluminum surface will immediately grow an aluminum oxide surface film. Friction measurements made between two aluminum bond wires pressed together at loads of only a few dynes illustrate how microbonds are first established and then broken. Increasing the normal force slightly begins to induce fractures in the oxide coating such that metal-to-metal bonds are made, resulting in a distinct stick-slip character and significant energy dissipation. The microbonds typically produce tiny prows. The reduced energy per cycle for bond specimens in the moist environments may be associated with the migration of water and ions into the microcracks, thereby reducing the capacity of the metal to reform microbonds during successive deformation cycles.

The hysteresis loop energies recorded for bonds cycled with currents through the bonds exhibit a peak in the energy absorbed per cycle shortly before fracture. There are probably several factors simultaneously operating here. As the conducting material is reduced by propagation of a fatigue crack, the current is constricted, resulting in localized areas of high current density. The higher current densities produce Joule heating and also directly enhance dislocation motion through an electroplastic effect[42]. Both the electroplastic mechanism and the thermal activation serve to assist dislocation motion through the resistance of dislocation cell structures and lattice pinning points. Another factor is that even small electric potentials

can break down the electrical resistance of the freshly created aluminum oxide films of a few molecular layers. Thus aiding in the process of making new microbonds. For example, the loop energy per cycle for two aluminum-aluminum bonds having about 300 cycles to failure life times at a current of 350 ma, exhibited peaks of, respectively, 0.694 erg and 0.398 erg a few cycles prior to fracture. This is to be compared with the respective energy per cycle values of 0.668 erg and 0.338 erg within the first few cycles of the specimen life.

The features of "high ductility" were first observed in scanning electron micrographs of the specimens fatigued with current and was initially assumed to be local melting of the bond metal as the bond fractured. However, spherical shaped features were not seen in the SEM even at high magnifications, as would be expected from surface tension effects with molten aluminum. The high ductility characteristics were also found to occur in very small regions of wire bond specimens cycled without conducting current. The tensile experiments on wire bonds have led to the realization that mechanical creep mechanisms operate in the wire bond metal at ambient temperature and at loads well below the normal fast fracture strength of the bond. This high ductility type of deformation, or viscous behavior, occurs due to highly localized stresses caused by a number of factors characteristic of the manner in which wire bonds are made. Work done elsewhere and recently published [30], provided a theoretical treatment proposing the occurrence of viscous type of plastic flow to account for the high local stress deformation phenomena in copper, which also has a fcc crystal structure.

During deformation, large numbers of dislocations are induced to flow in a pattern which results in a highly chaotic situation when compared to normal dislocation motion on slip planes in crystalline metals. The viscous flow phenomenon

appears to be important for both interconnections and other metal features in microcircuits.

Facilities recently placed into operation at Georgia Tech have greatly enhanced our capabilities to interpret the various micro-mechanisms associated with environmental assisted fatigue. Both the SAM and the ESCA instruments are used for resolving trace contaminants which migrate into the bond interfaces during mechanical cycling. In order to avoid contamination of the surfaces of specimens after fracture has occurred in a specific environment, specimens are mechanically cycled in the relevant environment and the cyclic deformation then stopped at a desired stage of the fatigue life. The bond wire specimens are then fractured in the clean ultra high vacuum environment of the scanning auger electron spectrometer to trace impurity migration in cracks.

Oscillatory variations observed for both stress amplitudes and loop energies as the number of cycles increased in a number of wire bond specimens is a phenomena which needs further exploration. This behavior is clearly not an artifact in that it is measured repeatedly and precisely. Several models have been discussed involving the creation of dislocation debris to work harden one region of the bond heel (which would reduce the energy per cycle and increase the stress amplitude) followed by the activation of viscous deformation in a different region of the bond heel metal due to the high localized stresses created by this blocking. The viscous deformation would increase energy dissipation.

As these experimental interpretation techniques are refined, the effective cyclic fatigue methods developed here will be applied to quantitative evaluations of effects of other impurities introduced in microcircuits, either through the outgassing of die attach epoxies or from other likely package

contaminants. The simple bond pull technique is clearly not a conclusive test to ensure the long term durability of every one of the large number of wire interconnections in a VLSI circuit. Implications of this study will also help reveal how bonds made with highly uniform monotonic pull test values can exhibit different environmental fatigue behavior dictated by a number of intrinsic metallurgical factors.

The results of the investigations reported here provide a foundation for the examination of both other materials and range of other environments. Studies of other bonding materials, including gold and other aluminum alloys as well as various solders used for microjoints would be useful. The environmental fatigue and creep behavior of unsupported thin film structures equivalent to microcircuit metallization layers could similarly be pursued. The thin film measurements are difficult but were proved to be feasible using techniques developed here earlier for interface investigations. The creep investigations need to be extended to include various gas environments, including hydrogen, pure oxygen, chlorine, etc.

Three technical publications reporting different aspects of these investigations are either near or already completed.

## REFERENCES

1. K. V. Ravi and E. Philofsky: "The Structure and Mechanical Properties of Fine Diameter Al-1 % Si Wire," Met. Trans., 2A, 1971, pp. 711-717.
2. M. Paugh and K. Seshan: "Degradation of Mechanical Properties after 100 C to 250 C Storage of 25 um Al-1% Si Microelectronic Interconnect Wire," Met. Trans., 14A, 1983, pp. 921-924.
3. K. V. Ravi and E. M. Philofsky: "Reliability Improvement of Wire Bonds Subjected to Fatigue Stresses," 10th Annual Proceedings IEEE Reliability Physics Symposium, Las Vegas, Nevada, pp. 143-148, 1972.
4. William T. Fitch: "The Degradation of Bonding Wires and Sealing glasses with Extended Thermal Cycling," 13th Annual Proceedings IEEE Reliability Physics Symposium, Las Vegas, Nevada, pp. 58-69, 1975.
5. G. G. Harmon and K. O. Leedy: "An Experimental Model of the Microelectronic Ultrasonic Wire Bonding Mechanism," in 10 th Annual Proceedings of IEEE Reliability Physics Symposium, Las Vegas, Nevada, pp. 49-52, 1972.
6. M. R. Nowakoski and F. Villedella: "Thermal Excursion can Cause Bond Problems," 9th Annual Proceedings of IEEE Reliability Physics Symposium, Las Vegas, Nevada, pp. 143-148, 1972.
7. K. C. Joshi, "The Formation of Ultrasonic Bonds Between Metals", Welding Journal, p. 840, 1971.
8. C. W. Wirsing, Solid State Technology, Vol. 16, p48, 1973.



9. G. E. Dieter: Mechanical Metallurgy, 2nd. Edition, McGraw Hill, 1970.  
J. Friedel, Dislocations, Pergamon Press, 1964.  
J. P. Hirth and Jens Lothe, Theory of Dislocations, McGraw-Hill, New York, 1968.
10. B. Langenecker, IEEE Trans. on Sonics and Ultrasonics, SU-13, 1, 1966.
11. P. C. Varley: The Technology of Aluminum and its Alloys, Butterworths, London, 1970.
12. K. R. Van Horn (ed.): Aluminum, Volume I, Properties, Physical Metallurgy and Phase Diagrams, American Society for Metals, Metals Park, Ohio.
13. Marc Van Lancker: Metallurgy of Aluminum Alloys, Chapman & Hall, Ltd., London, 1967.
14. L. F. Mondolfo: Aluminum Alloys: Structure and Properties, Butterworths, London, 1976.
15. M. E. Fine: "Fatigue Resistance of Metals," Met. Trans., 11A, 1980, pp. 365-380.
16. N. S. Stoloff and D. J. Duquette: "Microstructural Effects on the Fatigue Behavior of Metals and Alloys," Vol. 4, pp. 615-685, CRC Press, Cleveland, Ohio.
17. D. Kalish and B. G. LeFevre: "Subgrain Strengthening of Aluminum Conductor Wires, Met. Trans., 6A, 1975, pp. 1319-1324.
18. D. Kalish, B. G. LeFevre and S. K. Varma: "Effect of Alloying and Processing on the Subgrain Strength Relationship in Aluminum Conductor Wires," Met. Trans., 8A, 1977, pp. 204-206.
19. E. H. Chia and E. A. Starke, Jr.: "Application of Subgrain Control to Aluminum Wire Products," Met. Trans., 8A, 1977, pp. 825-832.

20. R. W. Landgraf and C. E. Feltner: "Selecting Materials to Resist Low Cycle Fatigue," ASME Paper No. 69-DE 59, American Society of Mechanical Engineers, 1969.
21. C. Laird: "Effect of Dislocation Substructures on Fatigue Fracture," Met. Trans., 8A, 1977, pp. 851-860.
22. B. R. Livesay and E. A. Starke, Jr. "Interactions of Dislocations with Interfaces", Acta Met, Vol 21, p247-254, 1973.
23. F. Nabarro, Editor: Dislocations in Solids, Vols. 1 -6, North Holland Pub. Co., New York, 1980.
24. J. C. Grosskreutz: "The Effect of Oxide Films on Dislocation Surface Interactions in Aluminum," Surface Science, 8, 1967, pp. 173-190.
25. B. R. Livesay: Doctor of Philosophy Thesis, Georgia Institute of Technology, 1972.
26. J. W. Matthews, Phil. Mag., vol. 13, p. 1207, 1966.  
A. I. Fedorenko and R. Vincent, Phil. Mag., vol. 25, p. 55, 1971.
27. A. K. Head: "The Position of Dislocations in Arrays," Phil. Mag., 4, 1959, pp. 295-302.
28. R. W. Balluffi and G. B. Olson: "On the Hierarchy of Interfacial Dislocation Structure," Met. Trans., 16A, 1985, pp. 529-541.
29. T. H. Alden, "Plastic and Viscous Deformation of Metals", Met. Trans., 16A, pp. 375-390, 1985.
30. A. M. Nomine, et al., "Creep and Cyclic Tension Behavior of a Type 316 Stainless Steel at Room Temperature", ASTM-STP 770, pp.45-68, 1980.
31. C. E. Feltner and C. Laird: "Cyclic Stress Strain Response of FCC Metals and Alloys -I, Phenomenological Experiments," Acta. Met., 15, 1967, pp. 1601-1632.
32. C. Laird: "The General Cyclic Stress Strain Response of

- Aluminum Alloys," ASTM STP 637, American Society for Testing Materials, 1977, pp. 3-35.
33. C. Laird and G. C. Smith: "Initial Stages of Damage in High Stress Fatigue in Some Pure Metals," Phil. Mag., 8, 1963, pp. 1945-1964.
  34. R. C. Boettner, C. Laird and A. J. McEvily, Jr.: "Crack Nucleation and Growth in High Strain Low Cycle Fatigue," Trans. AIME, Vol. 233, 1965, pp. 379-387.
  35. C. Laird: "Mechanisms and Theories of Fatigue," in Fatigue and Microstructure, M. Meshii (ed.), ASM, 1978, pp. 149-203.
  36. C. Laird and D. J. Duquette: "Mechanisms of Fatigue Crack Nucleation," Corrosion Fatigue, NACE 2, Houston, TX, 1970, pp. 88-110.
  37. P. Neumann, Acta. Met., Vol 22, p.1167, 1974.
  38. E. A. Starke, and G. Lutjering: "Cyclic Plastic Deformation and Microstructure," in Fatigue and Microstructure, M. Meshii (ed.), 1978, pp. 205-243.
  39. R. W. Landgraf: "The Resistance of Metals to Cyclic Deformation," in the Achievement of High Fatigue Resistance in Metals and Alloys, ASTM STP, 1970.
  40. J. A. Gorman, D. S. Wood and T. Vreeland, Jr.: "Mobility of Dislocations in Aluminum," Journal of Applied Physics, 40 (No. 2), 1969, pp. 833-842.
  41. F. E. Fujita: Fracture of Solids, Vol. 20, Interscience, 1963, p. 657.
  42. K. Okazaki, M. Kagawa and H. Conrad, Materials Science and Engineering, vol 45, pp.109-116, 1980.